Hippocampal Neurophysiology During Exploratory Behaviour and Sleep in Rats Heterozygous for the Psychiatric Risk Gene *Cacna1c*

Edward Richard Morrell

A Thesis Presented for the Degree of

Doctor of Philosophy

December 2020

Word Count: 43,582

Abstract

Genome-wide association studies reveal that calcium channel gene variants confer risk for psychiatric disorders across diagnostic categories. One consistently implicated gene is *CACNA1C*, a gene encoding the α1 pore-forming subunit of the L-type calcium channel. Recent rodent research highlights an important role for *Cacna1c* in hippocampal synaptic plasticity and related cognition, yet little is known about the effects of reduced *Cacna1c* gene dosage on hippocampal neurophysiology in vivo. Using tetrodes targeted to the dorsal CA1 I recorded single unit and local field potential activity in rats heterozygous for *Cacna1c* during free exploration and rest.

Cacna1c heterozygous rats displayed enlarged place-fields and an associated reduction in place-cell spatial information content during runs on a linear track in a familiar and novel orientation, while place-cell activity during exploration of a novel open-field was intact. In addition, while 6-10Hz theta and 25-140Hz gamma rhythms were comparable in frequency and power in heterozygotes, their dependence on locomotion was compromised. Phase-amplitude coupling between theta and slow-gamma was also attenuated in *Cacna1c* heterozygous rats running on the track in a novel orientation.

Hippocampal recordings at rest revealed intact 120-250Hz sharp-wave ripple oscillations, yet an enhanced participation of individual neurons in sharp-wave ripple events in *Cacna1c* heterozygotes. Despite the elevation in ripple-associated activity, coactivity between cell pairs during sharp-wave ripple events was markedly impaired. Changes to neurophysiology during sleep-associated oscillations appeared independent of global sleep architecture, since *Cacna1c* heterozygotes showed normal circadian activity patterns.

Finally, combining genetic L-type calcium channel hypofunction with NMDA receptor blockade using systemic ketamine administration, did not exacerbate hippocampal deficits in *Cacna1c* heterozygotes, indicating a divergence of these biological pathways.

This research reveals an important role for *CACNA1C* in hippocampal neurophysiology that may contribute to cognitive deficits associated with psychiatric risk.

Acknowledgements

I would like to thank my supervisors Professor Matt Jones, Professor Lawrence Wilkinson and Professor Jeremy Hall for giving me the opportunity to undertake this research project and for their ongoing support, advice and inspiration over the last four years. Without their hard work and encouragement this would not have been possible.

I would also like to thank all members of the Jones Lab, both past and present, for their continuous technical support and assistance, intellectual stimulation, feedback and scrutiny of my research, and friendship throughout the course of my PhD. In particular: Dr Aleks Domanski, Dr Ullrich Bartsch, Dr Alice Fodder, Dr Julia Heckenast, Dr Emma Roscow, Dr Tim Howe, Dr Ross Purple, Dr Pratap Tomar, Dr Silviu Rusu, Amber Roguski, Dr Eszter Kormann, Daniel Titheradge and Luke Burguete.

I would like to thank Dr Cezar Tigaret and the rest of my collaborators in Cardiff for their insightful research that provided much of the basis for the work presented in this thesis.

Finally I would like to thank my parents and family for their support over the past four years and for providing me with a place to live and write my thesis amidst the coronavirus pandemic.

This work was funded jointly by the Wellcome Trust strategic award DEFINE, Cardiff University School of Psychology and School of Medicine, and supported by an MRC Senior Non-clinical Research Fellowship awarded to Professor Matt Jones.

Contents

List of Tables

List of Figures

List of Abbreviations

AHP ..... *Afterhyperpolarisation*
ANOVA ..... *Analysis of variance*
ASD ..... *Autism spectrum disorder*
BDNF ..... *Brain-derived neurotrophic factor*
BPD ..... *Bipolar disorder*
CA1,..,3 ..... *Cornu ammonis field 1,..,3*
CACNA1C ..... *Calcium voltage-gated channel subunit alpha1C*
Cacna1c+/-/Het ..... *Cacna1c heterozygous*
CamKII ..... *Calcium/calmodulin-dependent protein kinase II*
CaN ..... *Phosphatase calcineurin*
CNV ..... *Copy number variation*
CSD ..... *Current source density*
dCA1 ..... *Dorsal CA1*
DG ..... *Dentate gyrus*
DTI ..... *Diffusion tensor imaging*
EC ..... *Entorhinal cortex*
EEG ..... *Electroencephalography*
EI ..... *Excitatory-inhibitory*
eQTL ..... *Expression quantitative trait loci*
fMRI ..... *Functional magnetic resonance imaging*
GWAS ..... *Genome-wide association study*
IS ..... *Interdaily stability*
ISI ..... *Interspike-interval*
IV ..... *Intradaily variability*
LFP ..... *Local field potential*
LTCC ..... *L-type calcium channel*
LTD ..... *Long-term depression*
LTP ..... *Long-term potentiation*
MAM ..... *Methylazoxymethanol acetate*
MDD ..... *Major depressive disorder*

MEG ..... *Magnetoencephalography*
NFAT ..... *Nuclear factor of activated T-cells*
NIMH ..... *National institute mental health*
NMDA ..... *N-methyl D-aspartate*
NREM ..... *Non-rapid eye movement*
PAC ..... *Phase-amplitude coupling*
PCP ..... *Phencyclidine*
PET ..... *Positron emission tomography*
PIR ..... *Passive infrared*
PPI ..... *Paired-pulse inhibition*
PV ..... *Parvalbumin-positive*
REM ..... *Rapid-eye movement*
SCN ..... *Suprachiasmatic nucleus*
SCZ ..... *Schizophrenia*
SD ..... *Standard deviation*
SNP ..... *Single nucleotide polymorphism*
SPW-R ..... *Sharp-wave ripple*
SWS ..... *Slow-wave sleep*
TBP ..... *Theta-burst pairing*
VTA ..... *Ventral tegmental area*
WT ..... *Wildtype*
α1 ..... *Alpha-1*

1

Chapter 1

Introduction

1.1. Introduction

Our understanding of the aetiology of psychiatric conditions remains very limited, hampering the treatment of psychiatric disease. In the past 40 years, there have been few major improvements in the effectiveness of drug treatments for psychiatric illness and the discovery of novel compounds with therapeutic potential has been sparse in comparison to other areas of health care (Krystal and State, 2014). This has resulted in pharmaceutical companies, the main drivers of therapeutics, shifting funding away from psychiatric treatment development (Abbott, 2011, Hyman, 2013), a move which has adverse implications for the ~20-35% (Kessler et al., 2009, Whiteford et al., 2013) of the population affected by these disorders. One area that has defied this trend has been psychiatric genetics which has seen significant advances over the past two decades, amounting to what could be described as a genetic revolution that is uncovering key insights into the aetiology of these disorders (Malhotra and Sebat, 2012, Kendler, 2013, McCarroll and Hyman, 2013, Owen, 2014, Tansey et al., 2015). The hope is that these new understandings of psychiatric disease may turn the tide, enabling the field to emerge from relative dormancy and instigate a revival of neurobiological understanding and treatment discovery.

1.1.1. Heritability of Psychiatric Illness

Genetic contributions to psychiatric illness have been acknowledged for over a century (Rudin, 1916). Family, twin and adoption studies over this time period (Rudin, 1916, Luxenberger, 1928, Heston, 1966) all point to the same conclusion: genetics play a key role in the predisposition to mental illness, in conjunction with a large swathe of environmental risk factors (McDonald and Murray, 2000, Kendler et al., 2003, Dean and Murray, 2005). Heritability estimates are as high as 75-80% for disorders such as Autism (ASD) and Schizophrenia (SCZ)

(Gejman et al., 2010, Lichtenstein et al., 2010, Polderman et al., 2015, Tick et al., 2016, Smoller et al., 2019). For disorders with generally lower genetic contributions, such as Major Depressive Disorder (MDD) and anxiety disorders, the genetic component is still significant, with heritability estimates ranging from 27-37% (Sullivan et al., 2000, Hettema et al., 2001, Sartor et al., 2012).

The results of this research provided the impetus to begin a search to find DNA variants that alter an individual's risk of developing a psychiatric condition. The initial focus in the search was on candidate genes – genes selected as potential risk genes on the basis of their function and what was known about the underlying mechanisms of these disorders. By and large, this proved to be an unsuccessful endeavour (Burmeister et al., 2008, Sanders et al., 2008, Farrell et al., 2015, Smoller et al., 2019). One reason for this failure, was that these studies used low sample sizes and thus had inadequate statistical power to detect risk genes (Farrell et al., 2015, Smoller et al., 2019).

From 2008, researchers began to publish the results of large-scale Genome-Wide Association Studies (GWAS) undertaken to identify risk gene variants. These studies, through the collaborative efforts of large groups of researchers such as the Psychiatric Genomics Consortium (https://www.med.unc.edu/pgc/), benefit from larger case and controls samples (>10,000) and have since discovered a wealth of robust significant psychiatric disease-associated risk genes (International Schizophrenia Consortium, 2008, Stefansson et al., 2008, Purcell et al., 2009, Stefansson et al., 2009, Schizophrenia Working Group of the Psychiatric Genomics Consortium, 2014, Ripke et al., 2020). Broadly speaking, the genes uncovered in these GWAS fall into two camps. First are common genetic risk variants comprising associations with Single Nucleotide Polymorphisms (SNPs, DNA variations at single base-pairs), for which the most recent GWAS for schizophrenia from the Psychiatric Genomics Consortium identified 270 distinct risk loci (Ripke et al., 2020). These variants are relatively common in the population, but individually confer a low risk for psychiatric disorder with odds ratios typically around 1.1-1.3 (1.1-1.3x the risk of the general population) (Purcell et al., 2009, Stefansson et al., 2009, Gaugler et al., 2014, Harrison, 2015, Smoller et al., 2019). These variants may accumulate in an individual however, giving rise to an on enhanced 'polygenic risk' for psychiatric illness (Purcell et al., 2009, Bergen et al., 2019). A second major grouping are the rare genetic variants such as copy number variants (CNVs) and frank single nucleotide point mutations (e.g. *SETD1A* (Takata et al., 2014). Despite a low incidence in the population (~1 in 300-2000 for CNVs; (Kirov et al., 2014), these variants, in particular those variants arising spontaneously (*de-novo*) in offspring, confer a much higher risk for psychiatric disease, with odds ratios of up to 60 (Stefansson et al., 2008, Malhotra and Sebat, 2012, Purcell et al., 2014, Rees et al., 2014, Genovese et al., 2016, Marshall et al., 2017, Kendall et al., 2019).

In summary, these findings point towards a complex genomic architecture for psychiatric disease in which liability is the result of the collective action of many common SNPs, in combination with contributions from a much lower number of highly penetrant variants, most of which are CNVs. Combined with environmental risk factors, our genetic liability conspires in ways we are yet to fully understand, to give rise to one's overall risk for psychiatric disorders.

A wealth of important insights have come out of these large GWAS and other genetic approaches, though two in particular warrant further discussion:

1. Psychiatric disorders possess significant levels of genetic overlap
2. Risk gene associations converge on specific biological pathways

1) Psychiatric disorders possess significant levels of genetic overlap

Most early GWAS looked for gene variants conferring risk for specific psychiatric disorders. Gene samples were stratified into control samples and case samples (samples from individuals with a diagnosis for a particular psychiatric condition) and gene variants that occurred in the case population at a sufficiently high incidence compared to the control population were assessed to determine whether they met the stringent statistical threshold for genome-wide significance (International Schizophrenia Consortium, 2008, Stefansson et al., 2008, Ma et al., 2009). However as more GWAS were carried out for a range of psychiatric conditions, many genetic risk variants for one condition appeared to be implicated in other conditions (Purcell et al., 2009, Cross-Disorder Group of the Psychiatric Genomics Consortium, 2013, Lee et al., 2013, Zhang, 2016). Analysis of the crossover between the risk variants for different psychiatric conditions reveals in some instances high correlations between diagnostically distinct disorders (Carroll and Owen, 2009, Cross-Disorder Group of the Psychiatric Genomics Consortium, 2013, Lee et al., 2013, Cardno and Owen, 2014, Doherty and Owen, 2014). Bipolar disorder (BPD) and SCZ for example, display a genetic correlation of ~0.6 (Cardno and Owen, 2014), demonstrating a striking degree of overlap in their genetic background. In some ways this finding is not surprising; as psychiatrists appreciate, there is a substantial degree of heterogeneity of symptoms within any psychiatric disease (Buchsbaum and Haier, 1978, Tsuang et al., 1990, Goldberg, 2011, Wardenaar and de Jonge, 2013) in addition to considerable comorbidity among individuals with a psychiatric condition (Stahlberg et al., 2004, Buckley et al., 2009, Plana-Ripoll et al., 2019). There is also significant overlap in symptoms between individuals with otherwise distinct psychiatric conditions (Craddock and Owen, 2005). This points to a likely inadequacy in our current diagnostic criteria to accurately characterize symptoms of psychiatric disease.

Outside of the psychiatric genetics domain, attempts have been made to understand the underlying biological dimensions of psychiatric dysfunction more accurately, by performing statistical analyses on symptom co-occurrence. These have demonstrated that current diagnostic categories do indeed inaccurately cluster psychiatric symptoms. Instead, most psychiatric disease symptoms appear to reflect a much smaller number of common underlying factors (Lahey et al., 2012, Caspi et al., 2014). Psychiatric genetics supports this finding with high degrees of pleiotropy observed among psychiatric risk genes (Solovieff et al., 2013). Principal component analysis on correlations between psychiatric risk genes provides support for the hypothesis that diverse psychiatric diseases reflect a common underlying dimension of dysfunction (Selzam et al., 2018). These findings have important implications for our understanding and treatment of psychiatric disorders. These disorders are largely understood as individual diseases and treated as such (Owen, 2014). Viewing these disorders as possessing shared underlying biological mechanisms will require a move towards less diagnosis-specific treatments.

2) Risk gene associations converge on specific biological pathways

The wealth of gene associations uncovered by GWAS has enabled researchers to characterise the role of specific risk genes to assess whether particular biological pathways may be commonly implicated in psychiatric risk. This line of analysis has indeed pointed towards a convergence of these genes on specific pathways for some disorders (Maier, 2008, Jia et al., 2011, Nurnberger et al., 2014, Schizophrenia Working Group of the Psychiatric Genomics Consortium, 2014, Network and Pathway Analysis Subgroup of Psychiatric Genomics Consortium, 2015, Pardiñas et al., 2018). One particular area of enrichment is for genes involved in synaptic signalling (Maier, 2008, Jia et al., 2011, Nurnberger et al., 2014, Schizophrenia Working Group of the Psychiatric Genomics Consortium, 2014, Network and Pathway Analysis Subgroup of Psychiatric Genomics Consortium, 2015, Pardiñas et al., 2018). This includes genes involved in glutamatergic transmission such as *GRIN2A* (Schizophrenia Working Group of the Psychiatric Genomics Consortium, 2014, Burnashev and Szepetowski, 2015), a gene for a protein that forms a subunit of the N-methyl D-aspartate (NMDA) receptor (Burnashev and Szepetowski, 2015, Addis et al., 2017), *CYFIP1* (Doornbos et al., 2009, Tam et al., 2010), a gene for a protein involved in regulation of the cytoskeleton in the post-synaptic density (Napoli et al., 2008) and *GRM3* (Schizophrenia Working Group of the Psychiatric Genomics Consortium, 2014, Saini et al., 2017), a gene for a metabotropic glutamate receptor (García-Bea et al., 2017). Additionally, calcium channel signalling genes such as *CACNA1C* and *CACNA1I* are also implicated (Nyegaard et al., 2010, Cross-Disorder Group of the Psychiatric Genomics Consortium, 2013, Nurnberger et al., 2014, Schizophrenia

Working Group of the Psychiatric Genomics Consortium, 2014, Pardiñas et al., 2018, Ripke et al., 2020). Overall there is strong emerging evidence for a major role for synaptic (dys)function in risk for psychiatric illness.

Other areas of potential disease-related enrichment include genes for proteins involved in dopaminergic signalling such as DRD2, the gene encoding the dopamine D2 receptor (Schizophrenia Working Group of the Psychiatric Genomics Consortium, 2014, Lencz and Malhotra, 2015) – confirming a role for dopaminergic dysfunction in Schizophrenia (Schizophrenia Working Group of the Psychiatric Genomics Consortium, 2014); genes involved in histone methylation (Schizophrenia Working Group of the Psychiatric Genomics Consortium, 2014, Network and Pathway Analysis Subgroup of Psychiatric Genomics Consortium, 2015); and genes related to immune function (Jia et al., 2011, Schizophrenia Working Group of the Psychiatric Genomics Consortium, 2014, Network and Pathway Analysis Subgroup of Psychiatric Genomics Consortium, 2015). These gene studies have importantly both confirmed previously held theories regarding the aetiology of psychiatric illness such as dopamine dysfunction in SCZ (Howes et al., 2017) but also opened up new lines of enquiry. Glutamatergic dysfunction, though previously suspected to play a role in disorder like SCZ due to the ability of NMDA receptor antagonists to recapitulate SCZ-like symptoms in healthy patients (Stodieck, 1983, Krystal et al., 2005b), has now been corroborated as a clear contender underlying psychiatric disease symptoms. Calcium channel signalling genes represent another potential line of enquiry that may both complement the role of genes in glutamatergic transmission or signify a new area of dysfunction in psychiatric illness.

1.1.2. Shifting Sands of Psychiatric Research

These new genetic-driven insights represent a turning point in psychiatric disease research. Researchers and clinicians are now equipped with genetically rationalised pathways to begin searching for mechanisms underlying psychiatric risk in addition to a new understanding of psychiatric disease; one in which there are not distinct disease categories, but instead in a radical rethink, a continuum of dysfunction. Though a change is yet to be seen within the medical community, diagnoses here still mainly relying on classifying individuals into specific disease categories (American Psychiatric Association, 2013, World Health Organization 2020), the research community have instigated a shift in their approach to one focused not on understanding specific psychiatric diseases, but instead on trying to understand underlying dimensions of dysfunction across psychiatric disease categories (Cuthbert, 2014, Owen, 2014). This approach is highlighted by the National Institute of Mental Health's (NIMH)

Research Domain Criteria (RDoC) which sets out a framework for research built upon a brain circuit-based understanding of psychiatric disease (Cuthbert and Insel, 2013, Cuthbert, 2014).

An important concept underpinning this new understanding of psychiatric disease research is that of the endophenotype (Anderzhanova et al., 2017). This refers to phenotypes of disease that bear a closer relationship to underlying pathophysiology than classical psychiatric disease symptoms. Under this conception complex psychiatric disorders can be broken down into more fundamental components and research should aim to interrogate these rather than any disease category as a single unit (Gottesman and Shields, 1973, Gould and Gottesman, 2006, Flint and Munafò, 2007). The original conception of the endophenotype had a very specific definition (Gottesman and Shields, 1973) some consider to be too narrow and thus some prefer the term intermediate phenotype, to simply refer to any phenotype more closely aligned with underlying pathophysiology (Lenzenweger, 2013, Donaldson and Hen, 2015). Here I will use both interchangeably but refer to the latter more broadly defined concept.

1.1.3. Animal Models of Psychiatric Disease

To effectively interrogate brain circuits in order to identify new psychiatric-relevant endophenotypes there are many possible routes of entry. One employed extensively in the present work is the use of animal models to enable invasive brain recordings of specific neuronal circuits. Newly identified psychiatric risk genes may present a new method by which one can model psychiatric relevant brain dysfunction in addition to more rigorously characterising the physiological roles of these genes. Previous animal models of psychiatric risk were based on the effects of currently available treatments (Nestler and Hyman, 2010). For example, a commonly used behavioural assay for MDD is the tail suspension test, which assesses the time taken for a rodent to become immobile as a metric for ‘helplessness’. This measure is altered by administration of antidepressants lending this assay a degree of predictive validity (Cryan et al., 2005). Additionally for SCZ, hypersensitivity to psychostimulant administration is a commonly used assay for positive symptoms, this time on the basis that anti-psychotic medications reduce this effect (Seeman, 2011). However many of these commonly used medications were discovered serendipitously on the basis that they treat symptoms but do not necessarily treat underlying dysfunction (Berton and Nestler, 2006, Ramachandraiah et al., 2009). As such these models lack any real evidence of construct validity (Nestler and Hyman, 2010).

Transgenic techniques of researching psychiatric risk target the underlying dysfunction in psychiatric disease and therefore arguably possess some degree of construct validity (Donaldson and Hen, 2015). The original conception of the endophenotype saw each core component of psychiatric risk as a heritable module and as such gene manipulations may

accurately model specific endophenotypes (Gottesman and Shields, 1973, Gould and Gottesman, 2006). Importantly these are not models of a psychiatric disorder itself. Psychiatric risk genes may be of low penetrance in which case they will not fully recapitulate psychiatric dysfunction. Or they may be of high penetrance yet confer risk across disease boundaries and so cannot be said to model any one disorder (Nestler and Hyman, 2010). Given the arbitrary nature of these disease boundaries it is unlikely any model could accurately model a psychiatric disease as a whole. However, genetically altered animals offer useful neurobiological tools to interrogate the brain dysfunction that may underlie important disease symptoms.

1.2. CACNA1C

1.2.1. CACNA1C Genetic Variation

One of the most commonly implicated psychiatric risk genes, and the main focus of this thesis, is the calcium voltage-gated channel subunit alpha1c (*CACNA1C*) gene. This gene was first implicated in a GWAS for BPD (Ferreira et al., 2008) and has since been consistently associated with risk for a range of psychiatric disease categories including SCZ (Green et al., 2010, Nyegaard et al., 2010, Hori et al., 2012, Cross-Disorder Group of the Psychiatric Genomics Consortium, 2013, Guan et al., 2014, He et al., 2014, Ivorra et al., 2014, Zheng et al., 2014), MDD (Casamassima et al., 2010, Green et al., 2010, Liu et al., 2011, Wray et al., 2012, Cross-Disorder Group of the Psychiatric Genomics Consortium, 2013) and ASD (Cross-Disorder Group of the Psychiatric Genomics Consortium, 2013, Li et al., 2015) as well as gaining further support for its role in BPD (Lett et al., 2011, Liu et al., 2011, Gonzalez et al., 2013, Green et al., 2013, Ruderfer et al., 2014).

There are at least 62 currently identified SNPs contained within this gene (Bremer et al., 2006) and at least 8 of these are associated with psychiatric risk (Moon et al., 2018). The most commonly identified of these is rs1006737 and the risk variant (A) is common within the population at a frequency of 0.33 (Heyes et al., 2015). These SNPs are typically found within intronic regions of the DNA and appear to be expression quantitative trait loci (eQTL) for *CACNA1C* (Bigos et al., 2010, Gershon et al., 2014, Roussos et al., 2014, Yoshimizu et al., 2015, Eckart et al., 2016, Jaffe et al., 2020) (that is they explain variance in gene expression levels). The direction of their effect on *CACNA1C* expression has been reported both as an increase (Bigos et al., 2010, Yoshimizu et al., 2015) and a decrease (Gershon et al., 2014, Roussos et al., 2014, Eckart et al., 2016, Jaffe et al., 2020) depending on the brain region sampled. These eQTL effects appear to relate to the enrichment of these SNPs within

enhancer regions where they interact with transcription start-sites to affect gene transcription (Roussos et al., 2014).

SNPs are not the only form of genetic variation that alter *CACNA1C* with regard to psychiatric disease. There is also evidence of de novo mutations in *CACNA1C* in psychiatric disease patients including a splice-acceptor mutation (Purcell et al., 2014) – a mutation that alters the splicing characteristics of this gene and a protein truncating mutation (Jiang et al., 2013, Purcell et al., 2014), a mutation that shortens the gene coding sequence in patients with SCZ and ASD. *CACNA1C* is also implicated in the genetic disorder Timothy Syndrome. This disorder results from a missense mutation and is thought to result in a gain of function whereby the calcium channel product of *CACNA1C* loses inactivation (Splawski et al., 2004) and is characterised by generalised organ dysfunction including cardiac impairments, immune deficiency and ASD (Splawski et al., 2004). Additionally, though most patients don't survive beyond childhood (Han et al., 2019), a case study of a patient who did survive into adulthood reveals the development of BPD symptoms (Gershon et al., 2014).

1.2.2. CACNA1C Genetic Animal Models

A variety of methods have been used to model genetic variation in *CACNA1C* in both mice and rats. A germline homozygous knockout of *Cacna1c* is embryonically lethal (Seisenberger et al., 2000) however some researchers have made use of conditional knockout of *Cacna1c* to successfully generate homozygous models. These include forebrain (Moosmang et al., 2005, White et al., 2008), prefrontal cortex (Lee et al., 2012, Kabir et al., 2017b) and CNS (Langwieser et al., 2010) conditional knockout models. A model of Timothy Syndrome has also been generated. The human disorder is the result of a mutation in exon 8A however a similar homozygous or heterozygous mutation in mice is lethal. Retention of the neomycin cassette, a section of DNA introduced during gene exchange, allows these animals to survive to adulthood when harbouring a heterozygous mutation, where they go on to exhibit Timothy Syndrome-like phenotypes. It is thought the neomycin cassette sequence may limit the expression of dysfunctional L-Type Calcium Channels (LTCCs) to non-lethal levels. This mouse model is termed the TS2_Neo$^{+/-}$ model (Bader et al., 2011). Finally a heterozygous *Cacna1c (Cacna1c*$^{+/-}$*)* model is also commonly used, whereby one copy of the *Cacna1c* gene is deleted (Dao et al., 2010, Bavley et al., 2017, Moon et al., 2018, Tigaret et al., 2020). This model arguably exhibits closer resemblance to the human condition by modelling the reduction in gene dosage (Gershon et al., 2014, Roussos et al., 2014, Eckart et al., 2016, Jaffe et al., 2020) that results from variation in Cav1.2 enhancer regions. In this thesis I make use of a *Cacna1c*$^{+/-}$ rat model generated with a 4-breakpoint deletion in exon 6 giving rise to a truncating mutation.

1.2.3. L-Type Calcium Channel Properties

CACNA1C encodes the alpha-1 (α1) subunit of the LTCC. There are 10 different α1 subtypes and the L-Type channels are encoded by *CACNA1S,C,D* and *F.* Collectively, these channel-types are referred to as Cav1 channels and *CACNA1C* encodes the Cav1.2 subtype (Catterall et al., 2003). Cav1.1 is found predominantly in skeletal muscle with little expression in the brain (Striessnig et al., 2014), Cav1.2 is expressed in cardiac and smooth muscle, secretory cells and throughout the brain (Striessnig et al., 2014) while Cav1.3 has some expression in the brain but is more prominently expressed in heart and cochlear hair cells (Platzer et al., 2000, Mangoni et al., 2003). Within the brain, Cav1.2 expression, as demonstrated through the prevalence of *CACNA1C* mRNA, appears to be expressed within most major brain regions including the cerebellum, throughout the cortex and in subcortical structures such as the hippocampus and the amygdala (see https://www.proteinatlas.org/ENSG00000151067-CACNA1C/brain) (Uhlén et al., 2015). In rodents, a sub-regional specific assessment of *Cacna1c* expression in the prefrontal cortex, the hippocampus and the cerebellum reveals dense expression within all subregions and cell layers (Sykes et al., 2018) highlighting a likely important role for this channel in normal brain function. At a cellular level, immunolabelling combined with electron microscopy in the hippocampus reveals expression of Cav1.2 in the cell soma, dendritic spines, and axon terminals (Tippens et al., 2008, Leitch et al., 2009). The expression appears to be most prominent within the soma and post-synaptic density, particularly around microdomains (Leitch et al., 2009), again pointing towards an important role for post-synaptic density genes in psychiatric risk (Schizophrenia Working Group of the Psychiatric Genomics Consortium, 2014).

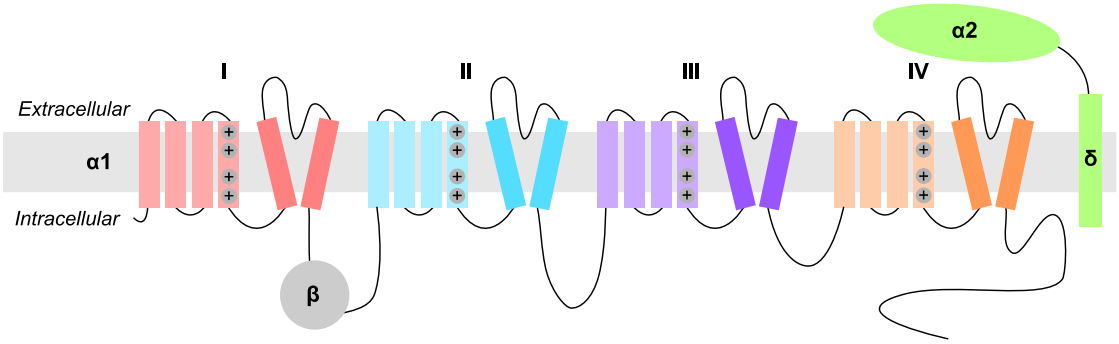

***Figure 1.1* | Voltage-gated calcium channel structure and subunits**
Calcium channel subunit structure depicting α1, α2δ and β subunits. The α1 subunit is comprised of 4 transmembrane regions (I-IV) each with 6 transmembrane helices. The fourth helix in each transmembrane region contains a voltage sensor and the fifth and sixth helices (indicated by darker colours) comprise the pore-forming segments.

The α1 subunit encoded by *CACNA1C* is depicted in **Figure 1.1**. This subunit has 4 transmembrane regions, each made up of 6 transmembrane helices. Each of these regions has a voltage sensor and 2 pore-forming helices. The role of this subunit both in forming the pore of the channel and the voltage sensor means that most key properties of the LTCC including voltage-dependence, conductance and pharmacology are largely determined by this subunit (Heyes et al., 2015). The other subunits are the β subunit and the α2δ complex which are involved in trafficking of the protein (Dolphin, 2012).

LTCCs require a high degree of membrane depolarization to open compared to other calcium channel sub-types and support a long-lasting calcium current. Additionally like all other classes of calcium channel, after a sustained membrane depolarization they will undergo an inactivation to prevent accumulation of calcium that could lead to cytotoxicity (Stotz et al., 2004). In LTCCs this effect appears to be mediated through calmodulin tethered to the C-tail of the α1 subunit (Peterson et al., 1999).

The effect of LTCC calcium influx is to activate a variety of downstream signalling pathways involved in gene expression for proteins that regulate synaptic function (Flavell and Greenberg, 2008). This includes the activation of calcium/calmodulin-dependent protein kinase II (CamKII) which in turn activates the transcription factor CREB (Nanou and Catterall, 2018). This pathway appears to be mediated both through calcium influx through the LTCC and via a conformational change to the channel itself (Li et al., 2016). LTCCs also promote activation of the transcription factor Nuclear Factor of Activated T-Cells (NFAT) via coupling at the C-terminal to the phosphatase calcineurin (CaN) protein (Murphy et al., 2014). These pathways in addition to others regulated via LTCCs are summarized in **Figure 1.2**.

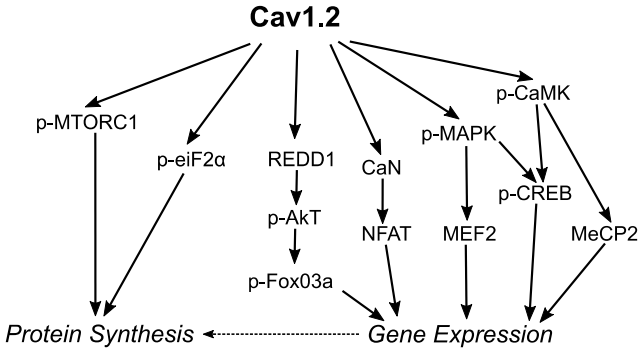

***Figure 1.2* | Cav1.2 cellular signalling pathways**
Diagram indicating signalling pathways linked to Cav1.2. Solid arrows indicate currently identified pathways. Dotted arrows indicate potential pathways. (mTORC1) mammalian target of rapamycin complex 1 (Workman et al., 2013); (P-eIF2α) phosphorylated eukaryotic initiation factor 2 alpha (Kabir et al., 2017a); (REDD1) regulated in development and DNA damage response 1 (Kabir et al., 2017b); (CaN) calcineurin (Murphy et al., 2014); (P-MAPK) phosphorylated mitogen-activated protein kinase (Moosmang et al., 2005); (P-CaMK) phosphorylated CAM-dependent protein kinase (Wheeler et al., 2008); (P-Akt) phosphorylated protein kinase B; (P-Foxo3a) Phosphorylated forkhead box class O 3a;

(NFAT) nuclear factor of activated T cells; (MEF2) myocyte enhancer factor 2; (P-CREB) phosphorylated cAMP response element-binding protein; (MeCP2) Methyl CpG binding protein 2. Adapted from Kabir et al. (2017) (Kabir et al., 2017c).

1.2.4. L-Type Calcium Channels & Synaptic Plasticity

Neurons exhibit activity-dependent alterations in their synaptic strengths, a process termed plasticity or long-term potentiation/depression (LTP/LTD). This plasticity is widely accepted as the synaptic basis of learning and memory (Bliss and Lomo, 1973, Morris et al., 1986, Bliss and Collingridge, 1993, Malenka and Nicoll, 1999, Nicoll, 2017). The capacity of LTCCs to activate downstream intracellular signalling cascades may instigate changes in synaptic function that can contribute to synaptic plasticity (Herring and Nicoll, 2016); several lines of evidence support this.

Though calcium entry to the cell has long been known to be important to plasticity (Lynch et al., 1983), this was initially shown to rely on calcium entry through the NMDA receptor (Collingridge et al., 1983, MacDermott et al., 1986, Ascher and Nowak, 1988). However under certain stimulation protocols, calcium channels also display an important contribution to synaptic plasticity. In the Schaffer-collateral pathway of the hippocampus (neurons projecting from CA3-CA1 region), a tetanus stimulation protocol (multiple trains of 100Hz stimulation) can induce a form of LTP independent of NMDA receptors but dependent on LTCCs, as evidenced by inhibition of this LTP through LTCC antagonists (Grover and Teyler, 1990). Additionally in the mossy fibre pathway of the hippocampus (the DG→CA3 pathway), brief high frequency stimulation LTP is blocked through the use of nimodipine, an LTCC antagonist (Kapur et al., 1998).

Outside of the hippocampus calcium channels also play an important role in LTP. In a pathway from the thalamus to the amygdala, associative plasticity – a form of plasticity reliant on concurrent pre and post synaptic stimulation – was blocked by nifedipine, another LTCC antagonist (Weisskopf et al., 1999). Additionally LTP in the ventral tegmental Area (VTA) is blocked with an LTCC blocker (Degoulet et al., 2016). Plasticity in vivo also relies on LTCCs. In anaesthetized rats high frequency stimulation dependent LTP of Schaffer-collateral synapses is impaired with LTCC antagonism (Freir and Herron, 2003), again highlighting the important role of these channels in LTP here. While these studies highlight the importance of LTCCs for LTP, they are not subtype specific and so it unknown whether this effect is mediated through Cav1.2. Some studies have observed the effects of Cav1.2 on plasticity more directly however.

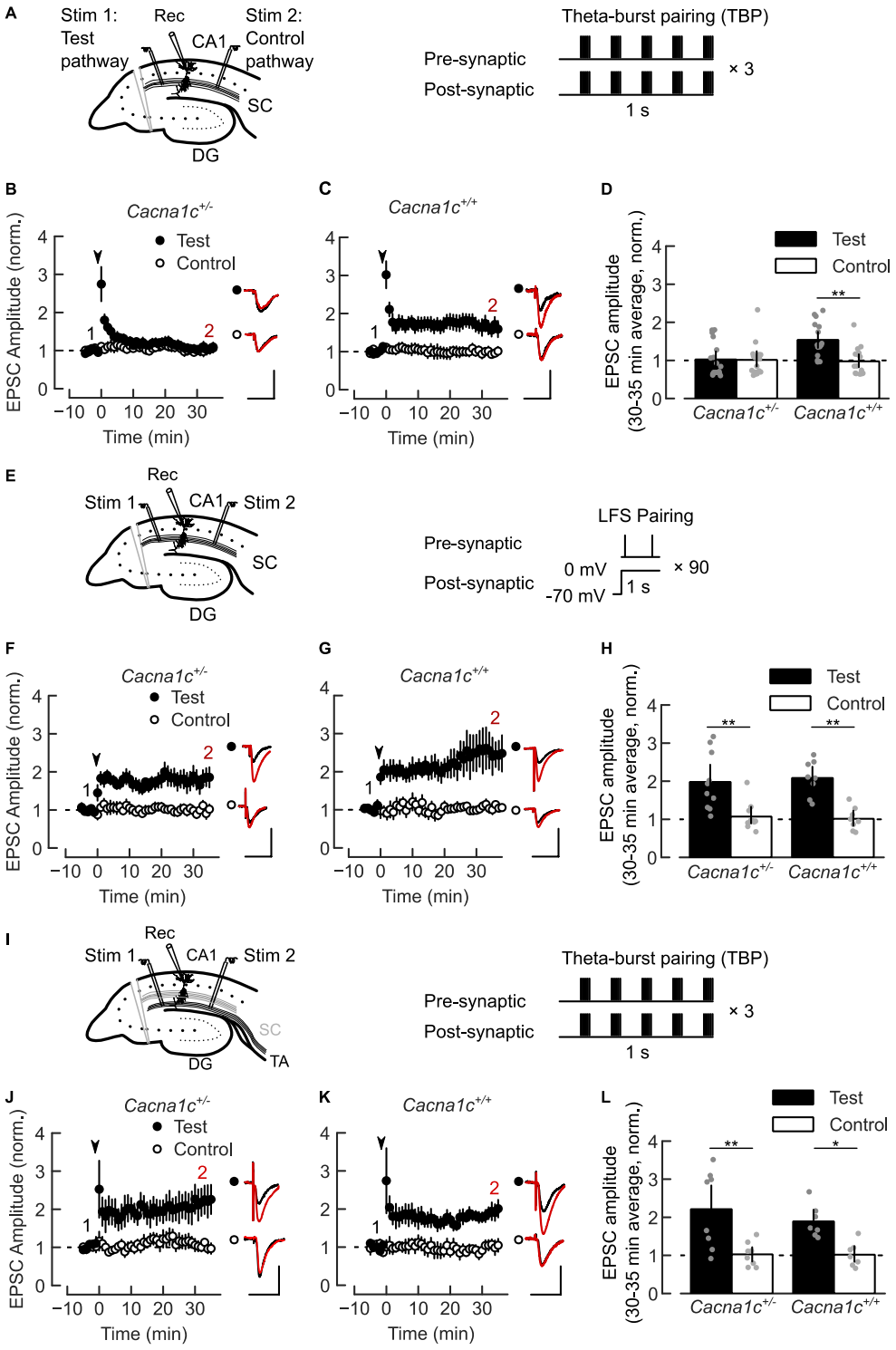

***Figure 1.3* | Impaired Schaffer-collateral long-term potentiation in *Cacna1c* heterozygous rats**
(A) Electrodes placements (left) and theta-burst pairing (TBP) protocol (right) for LTP at SC-CA1 synapses. **(B)** No TBP-induced LTP at SC-CA1 synapses in Cacna1c$^{+/-}$ slices. **(C)** Robust TBP-induced homosynaptic LTP at SC-CA1 in Cacna1c$^{+/+}$ slices. **(D)** Summary of normalized change in EPSC amplitude at 30-35 min shown in **B** and **C**. (Genotype effect: $p<0.05$; genotype × pathway interaction:

**p<0.01; Pairwise comparisons of Test vs Control pathway for Cacna1c$^{+/-}$: p>0.05, n=17/12; Cacna1c$^{+/+}$: **p<0.01, n=16/9).
(E) Electrodes placements (left) and low-frequency stimulation (LFS-pairing) protocol (right) for SC-CA1 LTP. **(F,G)** LFS-pairing induces SC-CA1 LTP in Cacna1c$^{+/-}$ **(F)** and Cacna1c$^{+/+}$ slices **(G)**. **(H)** Summary of EPSC amplitude change at 30-35 min shown in **F** and **G**. (No genotype or genotype × pathway interaction: p>0.05; Pairwise Test vs Control for Cacna1c$^{+/-}$: **p<0.01, n=10/7; Cacna1c$^{+/+}$: **p<0.01, n=8/6).
(I) Electrode placements (left) and TBP protocol (right) for LTP at TA-CA1 synapses. **(J,K)** TBP induces homosynaptic TA-CA1 LTP in slices from Cacna1c$^{+/-}$ **(J)** and Cacna1c$^{+/+}$ animals **(K)**. **(L)** Summary of changes in normalized EPSC amplitude at 30-35 min shown in **J** and **K.** (No genotype or genotype × pathway interaction: p>0.05; Contrast Test versus Control pathways, in Cacna1c$^{+/-}$: **p<0.01, n=8/7; Cacna1c$^{+/+}$: *p<0.05, n=7/5).
*(Plots show EPSC amplitude time-course in Test and Control pathways, normalized to 5 min average before LTP induction (arrowheads). Insets: 5 min average EPSC waveforms before (1, black) and 30-35 min after (2, red) LTP induction; scale bars: 50 pA, 50 ms. Sample sizes given as cells/animals. Data presented as means ± SEM. *p <0.05, **p<0.01 determined by two-way ordinal regression (cumulative link model) followed by analysis of deviance.)* Taken with permission from Tigaret et al. (2020).

In one study mice were bred with a mutation in Ser^{1928} – a PKA phosphorylation site found in the C-terminal of the Cav1.2 α1 subunit. Prolonged theta-burst LTP at Schaffer-collateral synapses was impaired in these mice though only when administered alongside β2-adrenergic receptor activation (Qian et al., 2017), highlighting a limited role for Cav1.2 in this context. More immediately relevant to the LTCC antagonist studies above, one study made use of a Cav1.2^{HCKO} mouse model (neocortex and hippocampus conditional knockout) to assess plasticity. Schaffer-collateral plasticity under a theta-burst stimulation protocol was normal, yet 200Hz tetanic stimulation was impaired. Additionally CREB phosphorylation was impaired in these mice following the LTP stimulation protocol (Moosmang et al., 2005), highlighting not only an important role for Cav1.2 in hippocampal plasticity but also the importance of cellular signalling pathways to this form of LTP.

More recently, a study has observed hippocampal plasticity in the *Cacna1c*$^{+/-}$ model, the same model used throughout this thesis, and the results of this study are shown in **Figure 1.3**. In this study plasticity was induced using a theta-burst pairing (TBP) protocol, a protocol thought to engage the activity both of LTCCs and NMDA receptors (Magee and Johnston, 1997, Tigaret et al., 2016). This protocol failed to induce LTP in *Cacna1c*$^{+/-}$ rats but was intact in Wild-Types (WTs) (**Figure 1.3A-D**). To demonstrate that this was not simply the result of a global LTP deficit they also induced LTP at this synapse using low-frequency stimulation, an NMDA receptor dependent stimulation protocol (Perkel et al., 1993), and revealed intact plasticity in *Cacna1c*$^{+/-}$ rats here (**Figure 1.3E-H**). Additionally, plasticity at the temporo-ammonic pathway (EC→CA1) was intact indicating a specific CA3-CA1 signalling deficit (**Figure 1.3I-L**) (Tigaret et al., 2020). This study highlights not only the importance of Cav1.2 channels for LTP but additionally a hippocampal signalling deficit that results from reduced

gene dosage of *Cacna1c* which may have important implications for hippocampal function in individuals with variations of this gene.

1.2.5. Behavioural Effects of CACNA1C Gene Variation

The effects of *Cacna1c* genetic variation on synaptic plasticity may have significant behavioural implications. Several studies, including those previously mentioned with regards to synaptic plasticity, have characterised behavioural abnormalities in animals harbouring *Cacna1c* gene mutations. In conditional knockout models spatial learning deficits have been observed. A loss of long-term spatial memory was observed in a forebrain conditional knockout model (White et al., 2008), the Cav1.2^{HCKO} model displayed spatial discrimination deficits (Moosmang et al., 2005) and a neuron-specific conditional knockout model displayed impairments in context discrimination and spatial memory (Temme et al., 2016). These findings are in line with a hippocampal deficit (Olton et al., 1978, Morris et al., 1982, Blum et al., 1999) which is concordant with the impairments to hippocampal plasticity. In *Cacna1c*$^{+/-}$ models a range of emotional impairments have been observed (Dao et al., 2010, Dedic et al., 2018). This includes a range of sex-specific deficits such as enhanced anxiety in female *Cacna1c*$^{+/-}$ mice combined with reduced locomotion and exploratory behaviour (Dao et al., 2010). Deficits in reversal learning have also observed and these impairments were analogous to those observed in human participants harbouring *CACNA1C* risk variants. This was found to correspond to a reduction in BDNF in the prefrontal cortex highlighting a role for this brain region in behavioural abnormalities here (Sykes et al., 2019).

Cacna1c$^{+/-}$ rats also display a deficit in latent inhibition. In this behavioural protocol animals undergo a contextual fear conditioning protocol; however, prior to conditioning they are pre-exposed to the context for 4-hours (Weiner, 2001). In WTs this pre-exposure period led to a reduction in the normal fear response however no reduction was observed in *Cacna1c*$^{+/-}$ rats (Tigaret et al., 2020). This behaviour is thought to rely on the hippocampus (Holt and Maren, 1999), again suggesting a role for hippocampal deficits in *Cacna1c* gene variant-mediated deficits.

Human work also reveals behavioural deficits in individuals carrying risk associated *CACNA1C* SNPs. In SCZ patients with the risk allele for rs1006737, deficits in logical memory performance were observed, though these deficits were not observed in healthy carriers of the risk allele (Hori et al., 2012). Similarly in individuals carrying the risk allele for rs2007044, working memory was impaired but this effect was predominantly driven by those with a SCZ diagnosis (Cosgrove et al., 2017). Though these studies point to a potential role for *CACNA1C* SNPs in cognitive impairment, the lack of impairment in healthy carriers would indicate other factors interact here to give rise to these deficits. In support of this notion, a range of

CACNA1C SNPs were shown to interact with adverse life events to give rise to depressive symptoms in humans (Dedic et al., 2018).

In infants harbouring *CACNA1C* SNPs, several SNPs were significantly associated with changes to sleep, specifically sleep onset latency (Kantojärvi et al., 2017). Several GWAS have also pointed to a role for *CACNA1C* in sleep disturbance (Shimada et al., 2010, Byrne et al., 2013, Parsons et al., 2013). This relationship may result from *CACNA1C* expression within the suprachiasmatic nucleus (SCN) (Nahm et al., 2005) - the brain's circadian pacemaker - and given the prevalence of sleep disturbance in psychiatric disease (Kupfer and Foster, 1972, Waller et al., 1989, Emslie et al., 1990, Nofzinger et al., 1991, Zanini et al., 2015), such a relationship may have important significance for the development of psychiatric symptoms in *CACNA1C* risk SNP carriers (see Chapter 4).

1.2.6. Effects of CACNA1C Gene Variants on Brain Activity

Behavioural deficits in animals and humans harbouring *CACNA1C* gene variants point towards underlying brain abnormalities that may result from the effects of these variants on synaptic plasticity. Indeed functional and structural imaging work in risk allele carriers reveals brain deficits across multiple structures. Functional MRI (fMRI) studies of *CACNA1C* risk allele carriers reveal a range of associated deficits. In an n-back task - a working memory-dependent task (Gevins and Cutillo, 1993) – prefrontal cortex-hippocampus connectivity was elevated in homozygous carriers of the risk allele (Paulus et al., 2014). Similarly during emotional processing, enhanced hippocampal activation in risk allele carriers was observed (Bigos et al., 2010). In contrast during episodic memory recall a reduction in hippocampal activation in carriers of risk variants has also been observed (Erk et al., 2014). Importantly these deficits were observed in healthy carriers implying that these were not simply brain alterations resulting from a psychiatric disorder. Brain structural changes have also been observed. The rs1006737 risk allele was associated with increased medial orbitofrontal cortex thickness (Soeiro-de-Souza et al., 2017) and diffusion tensor imaging (DTI) revealed structural abnormalities in the occipital and parahippocampal gyri in addition to the cerebellum, optic radiation and certain temporal gyri (Mallas et al., 2017). These abnormalities were only observed in SCZ patients however, so may result from interaction with other genetic or environmental factors.

Despite clear evidence of a) synaptic plasticity deficits, b) behavioural deficits and c) human functional and structural brain deficits with regard to *CACNA1C* genetic variation, there is a lack of research in-vivo into the effects of reduced gene dosage on brain activity. In particular the field would benefit from some understanding of how this gene affects brain function at a temporal and spatial scale that imaging studies are unable to resolve. In this thesis I aim to bridge this gap in the research into *CACNA1C* by characterising single unit and

local field potential activity in *Cacna1c*$^{+/-}$ rats. Across all levels of enquiry reviewed in this introductory section, deficits in hippocampal function have been observed. At the synaptic level, impairments in Schaffer-collateral plasticity are present (Moosmang et al., 2005, Tigaret et al., 2020). At the behavioural level, spatial memory deficits (White et al., 2008, Temme et al., 2016) in addition to latent inhibition impairments (Tigaret et al., 2020) have been observed and at the brain-wide level, alterations in hippocampal activation during various tasks (Bigos et al., 2010, Erk et al., 2014, Paulus et al., 2014) are evident in addition to structural abnormalities in the parahippocampal region (Mallas et al., 2017). The focus of the research here will therefore primarily be on this brain structure and circuitry in order to understand how brain alterations related to *Cacna1c* heterozygosity manifest at the cellular and network level in-vivo.

1.3. The Hippocampus

1.3.1. The Roles of the Hippocampus

Early work in patients with hippocampal damage revealed profound memory deficits (Penfield and Milner, 1958). One of the most famous of these patients was 'Patient HM', a man who received a bilateral medial temporal lobe resection to treat his severe epilepsy. Though the seizures subsided, he was left with severe anterograde amnesia – an inability to form new episodic memories (Scoville and Milner, 2000). This patient also had structures proximal to the hippocampus removed, yet later work in 'Patient RB' revealed anterograde amnesia following a lesion localised entirely to the CA1 field of the hippocampus (Zola-Morgan et al., 1986) and work since then has revealed that damage to the Hippocampus alone is sufficient to produce severe episodic memory deficits (Rempel-Clower et al., 1996). There is now little dispute that the human hippocampus plays a key role in episodic memory (Cohen and Eichenbaum, 1993, Burgess et al., 2002, Moscovitch et al., 2016).

Early animal work in the hippocampus also revealed an important memory function here. John O'Keefe's Nobel Prize winning discovery of place cells revealed hippocampal cells that fired only in response to select regions of an environment (O'Keefe and Dostrovsky, 1971) and navigation to an escape platform on a water-maze is impaired in animals with hippocampal lesions (Morris et al., 1986). These studies would imply a role for the hippocampus in spatial navigation and indeed a wide body of literature supports a role for both the rodent and human hippocampus in spatial navigation (Aguirre et al., 1996, Maguire et al., 1998, Burgess et al., 2002, Ekstrom et al., 2003, Martin and Clark, 2007, Eichenbaum, 2017).

How do we marry these two proposed hippocampal functions? Edward Tolman in 1948 proposed a cognitive map theory of the brain (Tolman 1948). This holds that rather than

understand behaviour purely in terms of stimulus-response connections, the brain is capable of developing internalised representations or maps of an environment that establish the relationships between items within that map. John O'Keefe and Lynn Nadel in 1978 published *The Hippocampus as a Cognitive Map* where they argued that the hippocampus supports this very function (O'Keefe and Nadel, 1978), enabling the establishment of a relational framework that is capable of mapping items in space to support a spatial map and by extension spatial navigation, or events within their spatial and temporal context, enabling the support of episodic memory (Buzsáki and Moser, 2013, Eichenbaum and Cohen, 2014).

1.3.2. The Hippocampus in Psychiatric Disease

A wealth of studies report structural abnormalities, usually manifesting as a reduction in volume, in the hippocampi of patients with SCZ (Lawrie and Abukmeil, 1998, Nelson et al., 1998, Wright et al., 2000), BPD (Driessen et al., 2000, Brambilla et al., 2002, Schmahl et al., 2003) and MDD (Sheline et al., 1996, Sheline et al., 1999, Bremner et al., 2000). Hippocampal volume alterations have also been observed in prodromal and first-episode SCZ patients (Bogerts et al., 1990, Lawrie et al., 1999, Pantelis et al., 2003a) indicating that these alterations are fundamental, or at least closely aligned, to the dysfunction underlying psychiatric disease symptoms.

Post-mortem studies also reveal cellular alterations in the hippocampal formation of patients. For example in MDD patients, pyramidal cell and granule cell density is reduced in addition to a reduction in soma size (Stockmeier et al., 2004) and in SCZ patients molecular changes indicative of reductions in glutamatergic transmission have been demonstrated (Tamminga, 1998, Gao et al., 2000). Functional imaging studies have revealed alterations in hippocampal activation in psychiatric disease. PET scans show reduced hippocampal activation during recall in SCZ patients (Heckers et al., 1998), though in contrast, elevated activity levels measured via blood flow to the CA1 (Schobel et al., 2009) and hippocampal metabolic activity (Molina et al., 2003) have also been reported, with the direction of change in activity potentially reflecting the task demands.

Alterations in hippocampal activation are in keeping with those seen in healthy *CACNA1C* risk allele carriers (Bigos et al., 2010, Erk et al., 2014) suggesting these activity changes may precede the emergence of psychiatric symptoms. In support of this notion, a study observing hippocampal activation via changes in hippocampal metabolism in high risk SCZ individuals found that elevated metabolic activity was highly predictive of conversion to psychosis in these individuals (Lieberman et al., 2018), implying a role here for hippocampal abnormalities in the development of psychosis symptoms. Given the potential role of the hippocampus in supporting cognitive maps, abnormalities observed in this structure may reflect the widespread cognitive impairments observed in most psychiatric disorders

(Heinrichs and Zakzanis, 1998, Austin et al., 2001, Daban et al., 2006, Trivedi, 2006, Millan et al., 2012). Current drug treatments for psychiatric disorders have poor efficacy in treating these cognitive deficits (Mishara and Goldberg, 2004, Keefe et al., 2007, Shilyansky et al., 2016, Solé et al., 2017), thus there is a need to better understand the brain dysfunction giving rise to these symptoms.

The hippocampus is highly conserved across mammalian species with regards to its internal circuitry, its anatomical connectivity (Clark and Squire, 2013), its spatial coding scheme (Thome et al., 2017), and its connectivity to the prefrontal cortex during spatial cognition (Bähner et al., 2015). As such, study of the hippocampus in rodents may be a translational metric by which to probe cognitive function and dysfunction in relation to psychiatric disease.

1.3.3. Hippocampal Electrophysiology

The research in this thesis aims to understand how hippocampal function and dysfunction in relation to *CACNA1C* genetic variation may underlie symptoms of psychiatric disease including cognitive symptoms. I assess this through tetrode recordings in the dorsal CA1 (dCA1) region of *Cacna1c*$^{+/-}$ rats, enabling the extracellular recording of single unit and local field potential activity during active behaviour and natural rest/sleep. In order to provide a basis for this research, I will first summarise the current literature on hippocampal electrophysiology here; more specifically relevant information will be provided in each subsequent experimental chapter.

1.3.3.1. Place Cells

Hippocampal pyramidal cells (in CA1 and CA3) and granule cells (in DG) exhibit spatial firing characteristics such that their firing rate increases within particular regions of an environment termed the ‘place-field’. Any cell that exhibits spatial firing characteristics is referred to as a ‘place-cell’ (O'Keefe and Dostrovsky, 1971, O'Keefe, 1976). In any environment, loosely spatially tuned activity is present in around half of recorded cells from the outset of the recording and this activity stabilizes within minutes (Wilson and McNaughton, 1993, Frank et al., 2004) and can persist over durations of several months (Thompson and Best, 1990). This persistent place-field stability appears to be contingent upon CA1 plasticity, with interventions designed to block plasticity here giving rise to a loss of place-field stability (McHugh et al., 1996, Rotenberg et al., 1996, Kentros et al., 1998). The activity of place-cells in one environment appears to bear little resemblance to their activity in a separate environment, implying separate maps exist for distinct contexts (O'Keefe, 1976, Alme et al., 2014) and lending weight to the possibility that the hippocampus supports cognitive maps. Within the

same environment a place cell may alter its coding scheme if features of that environment are sufficiently altered, by changing its firing rate within the place-field – a phenomenon termed rate remapping (Muller and Kubie, 1987, Bostock et al., 1991, Muller et al., 1991).

How does the hippocampus generate spatially tuned firing? One of its main inputs, the entorhinal cortex (EC), may offer some clues. The cells in this region appear to vary their firing in an environment in a regular grid-like pattern that forms a hexagonal structure. These cells, termed grid-cells, display variable sized grids with different grid locations and orientations for each cell (Fyhn et al., 2004, Hafting et al., 2005). Computational work reveals that by summing the input from multiple variably oriented grid-cells, one can form single place-fields (Solstad et al., 2006) pointing to a possible spatial coding mechanism for hippocampal place-cells.

1.3.3.2. Hippocampal Rhythmic Activity

The summation of neuronal transmembrane currents can produce variations in the extracellular medium (Mitzdorf, 1985, Viswanathan and Freeman, 2007) detectable through broadband extracellular recordings (Marshall et al., 1937, Galambos, 1941), referred to as local field potentials (LFP). Recordings of this kind within the hippocampus reveal a range of characteristic rhythmic oscillations:

i) Theta

During mobility, a ~6-10Hz oscillation is present across all hippocampal subregions (Grastyan et al., 1959, Vanderwolf, 1969, Buzsáki, 2002). This rhythm, termed theta, is most prominent during exploratory and preparatory behaviour (Vanderwolf, 1969) and can also be present during immobility such as during rapid-eye movement (REM) sleep (Jouvet, 1969) and while an animal engages in working memory tasks (Tesche and Karhu, 2000) indicating an association with behaviours engaging cognition such as decision-making and recall.

Theta is ubiquitous across mammalian species (Grastyan et al., 1959, Raghavachari et al., 2001, Buzsáki, 2002, Lee et al., 2005) and is also present across many other brain structures (Mitchell and Ranck, 1980, Leung and Borst, 1987, Paré and Collins, 2000), though not necessarily in coherence with hippocampal theta (Raghavachari et al., 2001). Lesion to the medial septum appears to abolish theta in the hippocampus (Stumpf et al., 1962) suggesting the rhythm originates in this structure; though damage to other structures also leads to theta impairments (Bland, 1986, Vertes and Kocsis, 1997) suggesting the medial septum is not solely responsible. Under one of the earliest models of theta generation, the medial septum is hypothesized to provide rhythmic drive to basket interneurons in CA1 which in turn provide rhythmic inhibitory input to CA1 pyramidal cells. Concurrent perforant path input from the EC provides coherent excitatory input and the interaction between these two

interacting input sources generates a theta rhythm in the CA1 (Holsheimer et al., 1982, Buzsáki et al., 1983).

This model appears to be somewhat of an oversimplification. In anaesthetized rats, absent of any background theta oscillation, dendritic depolarization of CA1 pyramidal cells can generate a locally self-sustained theta rhythm (Kamondi et al., 1998). Furthermore in an isolated hippocampus, theta rhythms can emerge in the CA1 even after dissection of the CA3 (Goutagny et al., 2009) implying that there is an intrinsic component to CA1 theta and there is now some suggestion that multiple independent theta oscillators exist and coherent hippocampal theta emerges from the interaction of these various oscillators (Lubenov and Siapas, 2009).

Hippocampal theta appears to support memory consolidation and recall. In human participants, intracranial EEG recordings from epileptic patients with implanted hippocampal electrodes reveals an elevation of theta prior to successful memory recall (Fell et al., 2011) and in rats, loss of the hippocampal theta rhythm following medial septum lesion leads to spatial memory deficits (Winson, 1978). The importance of hippocampal theta to spatial navigation has also been observed in human participants through the use of MEG recordings, where successful navigation of a virtual water maze was preceded by elevated theta in the septal hippocampus (Cornwell et al., 2012).

ii) Gamma

Another prominent hippocampal rhythm is gamma (Stumpf 1965, Leung et al., 1982). The term gamma encompasses two rhythms a ~25-55Hz slow gamma rhythm and a ~65-140Hz fast gamma rhythm (Colgin et al., 2009). Gamma also occurs during mobility (Buzsáki et al., 1983) and cognitive tasks (van Vugt et al., 2010) and is therefore often found to co-occur with theta (Stumpf 1965, Leung et al., 1982). This co-occurrence is not coincidental. Both oscillations display temporal coupling such that the amplitude of gamma rhythms is highest during the trough of a theta oscillation (Bragin et al., 1995, Canolty et al., 2006); a phenomenon described as phase-amplitude coupling (PAC).

The finding that gamma encompasses two sub-bands of slow and fast gamma is a relatively recent one and as such many older papers refer to all oscillations from ~25-140Hz as gamma. However current source density (CSD) analysis combined with lesioning reveals the presence of two distinct oscillations within this range. During hippocampal gamma oscillations the highest excitatory currents are found in the DG molecular layer – the termination zone of the EC (Bragin et al., 1995, Charpak et al., 1995). However in animals with a lesioned EC, excitatory currents are found within the stratum radiatum layers indicative of CA3 input. Additionally the gamma rhythm in these lesioned animals is of a lower frequency compared to non-lesioned animals (Bragin et al., 1995). A comparison of the coupling of CA1

gamma rhythms to CA3 and EC gamma rhythms demonstrates slower frequency CA1 gamma oscillations coupled to CA3 gamma and higher frequency CA1 gamma coupled to EC gamma (Colgin et al., 2009). Together these findings support the idea that there are two gamma generators, the CA3 and EC respectively, and these give rise to two distinct gamma oscillations in the CA1.

At a cellular level, gamma oscillations appear to emerge as a result of the activity of inhibitory interneurons. Early support for this theory came from intracellular CA1 and CA3 recordings which found that chloride ion injection (analogous to an IPSP) into a pyramidal cell induces a gamma frequency oscillating membrane potential (Soltesz and Deschênes, 1993). Additionally basket cells display gamma frequency burst firing during gamma oscillations (Penttonen et al., 1998) and direct manipulation of fast-spiking interneurons through optogenetics, though in the cortex in this instance, induces a gamma oscillation in vivo (Cardin et al., 2009).

Hippocampal gamma in humans predicts successful memory encoding (Sederberg et al., 2007) and the extent of theta-gamma PAC is also predictive of working memory performance in human participants (Axmacher et al., 2010) and spatial memory in rats (Shirvalkar et al., 2010). In T-maze tasks in rats, the point at which a rat must choose a correct maze arm, termed the choice-point, is also incidentally the point at which theta-gamma PAC is highest (Tort et al., 2008) demonstrating the importance to hippocampal function of these rhythms not only in isolation but also in combination.

iii) Sharp-Wave Ripples

Though theta and gamma oscillations are predominantly active during alert behaviour, additional characteristic oscillatory activity is observed in the hippocampus during resting wake behaviour in addition to slow-wave sleep (SWS). Sharp-wave ripples are brief (~150ms) oscillations characterised by a large amplitude fluctuation termed a ‘sharp-wave’ followed by a ~100-200Hz oscillation termed a ‘ripple’ collectively referred to as a sharp-wave ripple (SPW-R). The two components of the SPW-R are thought to emerge separately: the sharp-wave, from recurrent collaterals within the CA3 (Buzsáki et al., 1983), and ripples from an interplay between excitatory and inhibitory cells in both CA3 and CA1 (Schlingloff et al., 2014, Buzsáki, 2015). Like theta and gamma oscillations, SPW-Rs support memory consolidation with the density of SPW-Rs during sleep predictive of behavioural performance in an associative memory task in rats (Ramadan et al., 2009). Additionally suppression of ripple activity following spatial learning in rats impairs subsequent performance (Girardeau et al., 2009, Ego-Stengel and Wilson, 2010).

1.3.3.3. How do Hippocampal Rhythms Relate to Coordinated Cell Firing?

i) Theta

Rhythmic oscillations are found throughout the brain and have been hypothesized to provide a clocking mechanism for the activity of single neurons (Singer, 1999, Varela et al., 2001). Research into the role of hippocampal oscillations does indeed reveal important associations with the activity of individual neurons. Several studies have highlighted the importance of theta-timing in synaptic plasticity, demonstrating that LTP is most effective when stimulation is delivered at the peak of a theta-wave (Huerta and Lisman, 1996, Hölscher et al., 1997, Orr et al., 2001). The significance of this relationship to place-cells in vivo appears to be more complicated. Here, concurrent single unit and LFP recordings reveal that as an animal enters a place-field, the place-cells' firing is phase-locked to the late-phase of a theta-wave and firing progresses to earlier phases as the animal traverses the field (O'Keefe and Recce, 1993, Skaggs et al., 1996) (see **Figure 1.4A**). Importantly this theta 'phase precession' means that theta-phase varies with location and therefore provides an additional metric for encoding spatial information. This is evidenced by the fact that estimates of an animal's position on the basis of place-cell firing are improved in accuracy when incorporating theta-phase information (Jensen and Lisman, 2000).

In addition to providing another spatial information metric, phase-precession may support the encoding of sequences. In a scenario where multiple place-fields overlap, the place-field the animal runs through first will fire at the earliest theta phase and the last at the latest. The result is such that the sequence of place-cell firing in a theta cycle corresponds to the ordering of place-cells on the track (Skaggs et al., 1996, Gupta et al., 2012). Indeed, impairments to phase-precession in animals lead to a loss of coordinated timing among place-cells and memory impairments as a result (Lenck-Santini and Holmes, 2008, Robbe and Buzsáki, 2009).

The mechanism by which theta phase precession emerges may relate to the effects of theta on membrane potential. Intracellular CA1 recordings reveal a rhythmic somatic hyperpolarising effect of theta. Applying a ramping depolarising current results in cells firing at progressively earlier theta phases, mirroring phase-precession (Kamondi et al., 1998, Magee, 2001). This occurs due to the conflict between the hyperpolarizing effects of theta and the depolarising effects of the current injection and thus at higher currents neurons can overcome the hyperpolarising effects of theta at earlier phases. In the instance of place-cells, this takes the form of a ramping of membrane potential as an animal traverses a place field (Harvey et al., 2009b).

ii) Gamma

In gamma, place-cell phase-locking is also observed, though this appears to remain fixed through runs (Dragoi and Buzsáki, 2006, Senior et al., 2008). Interestingly place cells appear to show independent phase-locking to slow and fast-gamma (Kitanishi et al., 2015) suggesting these oscillations may function as a mechanism to segregate CA3 and EC input to CA1. In addition, phase-locking to each serves a different role. In the instance of slow-gamma, phase-locking occurs when place-cells are firing in response to upcoming locations, while phase-locking to fast-gamma occurs when firing in response to the animals' present location (Bieri et al., 2014). This, alongside phase-precession, may enable sequences to be encoded more robustly.

Given the hyperpolarising effect of theta, one might consider whether gamma exerts a similar effect. Certainly rhythmic fluctuations in membrane potential are present (Penttonen et al., 1998), though in the instance of gamma it may be the case this oscillation is the result of cell firing patterns rather than the cause. Model excitatory-inhibitory (EI) networks based around those found in the hippocampus display emergent gamma rhythms as a result of the co-ordinated activity of interneurons (Buzsáki and Wang, 2012) and this may serve to synchronize pyramidal cell firing, giving rise to the synchronous firing patterns during gamma cycles observed in the cortex and hippocampus (Singer and Gray, 1995, Csicsvari et al., 2003).

The importance of EI network interactions during gamma cycles is highlighted by the E%-Max model of gamma oscillations. Here, the most excitable cell fires first during the depolarising phase of a gamma-cycle and initiates feedback inhibition. Only cells which are then sufficiently excitable within the delay between the first cell firing and feedback inhibition are capable of firing a cell within that gamma-cycle (de Almeida et al., 2009). This enables the coordination of a small subset of the most excitable cells within any gamma cycle. In addition, the feedback inhibition initiated by the first cell in the cycle creates a brief time-window for firing in that cycle, which is potentially what gives rise to phase-locking. This may serve an important integration function. Cells that fire within 6ms sum supralinearly, enabling more effective integration of inputs (Losonczy and Magee, 2006). The length of a gamma cycle is longer than this, thus phase-locking increases the likelihood of synchronous firing leading to downstream activation of neurons. Phase-locking also provides longer time-windows between subsequent firing of different cell subsets. This enables downstream neurons to discriminate between inputs more efficiently (Lisman and Jensen, 2013).

In summary this would suggest that gamma has an important role in bringing together cells to form ensembles as well as segregating separate ensembles. This may explain the importance of theta-gamma coupling. By operating in synchrony, theta phase-precession enables the correct sequencing of place-cells while gamma segregates the firing of each place-cell. This is essential for the correct interpretation of sequences by structures

downstream of the hippocampus and thus disruption to this process would undoubtedly give rise to cognitive deficits.

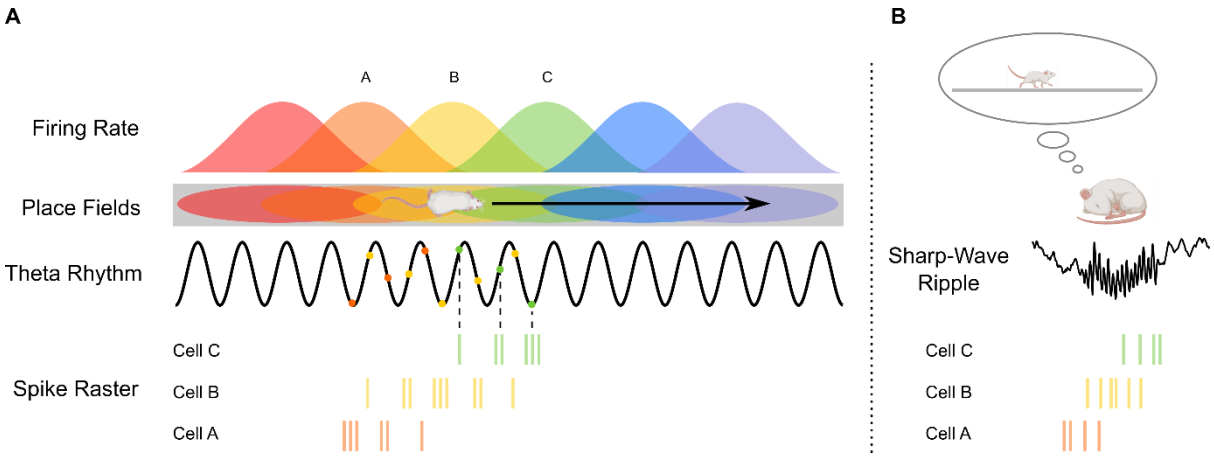

***Figure 1.4* | Schematic depicting place-cell single unit and oscillatory activity during wake and sleep**
(A) Place-cell activity during exploration of a linear track. The firing rate of a place-cell varies as the animal traverses its place-field. Spike rasters are shown for 3 cells: A,B and C. As the animal traverses the place-field of each, they fire at progressively earlier phases relative to the hippocampal theta rhythm. **(B)** Place-cell activity during rest. The cell's shown in **(A)** fire again during sharp-wave ripples in the same sequential order as during wake yet on a compressed timescale.

iii) Sharp-Wave Ripples

Recording the activity of single units during SPW-R's reveals the highly synchronous nature of these oscillations with around 10-20% of recorded CA1 neurons active in any SPW-R event (Ylinen et al., 1995). Initial work comparing the activity of neurons during wake to those active during SPW-Rs revealed high temporal correlations between cell pairs that were temporally correlated during wake (Wilson and McNaughton, 1994). Subsequent analysis revealed that the sequential activation of place-cells observed during wake, matched that of place-cells during sleep and rest, in particular during SPW-R events. This sleep reactivation of an animal's trajectory during wake occurred on a much finer timescale (approximately 10-fold difference) (Lee and Wilson, 2002), a phenomenon termed replay (see **Figure 1.4B**). Given the important role of SPW-Rs in memory consolidation, replay may serve a memory function by enhancing the plasticity between learned sequences. Reactivation in vitro, of place-cell sequences recorded in vivo does indeed lead to LTP but only when supported by a sharp-wave ripple-like stimulation (Sadowski et al., 2016).

1.3.3.4. Behavioural Dependence of Hippocampal Rhythms

Given the phase relationship between individual neurons and oscillatory activity, assuming consistent rhythmic activity during a task, the phase at which spikes fired would vary

depending on the rate of progression through a firing field. In the case of place-cells on a track, theta and gamma spike-phase would vary with running speed. This raises problems if the phase relationship provides an important information metric. Experimental evidence however shows that the frequency of theta and gamma rhythms is running speed dependent (Pickenhain and Klingberg, 1967, Vanderwolf, 1969, Ahmed and Mehta, 2012) enabling consistent phase as running speed varies (Geisler et al., 2007). In animals displaying an impairment in this theta run-speed dependence, spatial memory is also impaired (Richard et al., 2013). Additionally the strength of the association is predictive of spatial memory performance (Young et al., 2020).

The power of hippocampal oscillations is also running speed dependent (Chen et al., 2011, Li et al., 2012b, Penley et al., 2013) though the function here is less clear. Given the hyperpolarising effect of theta, one might expect this to correspond to a reduction in the firing rate of place-cells, though this does not appear to be the case and instead firing rate displays a positive-running speed correlation (Lu and Bilkey, 2010). Alternatively, the firing rate of place-cells may rise with running speed independently of theta (Fuhrmann et al., 2015), and the increased frequency and greater degree of hyperpolarisation of theta shortens the firing window of these cells. This is evidenced by the increased instantaneous firing rate with running speed exhibited by place cells and yet a relatively consistent spike count with variations in running speed (Geisler et al., 2007). The result is that firing curves and therefore place-fields remain fairly constant with running speed variations.

1.3.3.5. Hippocampal Electrophysiology in Psychiatric Disease

Though there is a great deal of literature demonstrating structural deficits in the hippocampus and alterations in hippocampal activation in relation to psychiatric disease, the literature characterising hippocampal electrophysiology is relatively sparse. A MEG study of patients carrying the risk allele for *ZNF804A*, a psychiatric risk gene, revealed a reduction in hippocampal theta compared to non-risk allele carriers (Cousijn et al., 2015) and outside of the hippocampus, alterations to cortical theta (Haenschel et al., 2009), gamma (Grent-'t-Jong et al., 2016) and theta-gamma coupling are reported in SCZ patients (Barr et al., 2017), possibly indicative of a wider oscillatory deficit (Uhlhaas and Singer, 2010, Phillips and Uhlhaas, 2015). Studying oscillatory impairments in relation to psychiatric disease may be of particular utility due to the relative ease with which oscillatory properties can be characterised both in humans and animal models thus providing a translational metric by which to characterise network activity in psychiatric disease.

There is also a small animal literature characterising hippocampal electrophysiological activity in animal models of psychiatric risk. Alterations in place-cell activity (Mesbah-Oskui et al., 2015, Kaefer et al., 2019) and oscillatory activity (Suh et al., 2013) have been reported

here (discussed in full in Chapters 3 and 4). To date a similar assessment in *Cacna1c*$^{+/-}$ animals is lacking.

1.4. Thesis Aims

CACNA1C gene variants confer risk across a range of psychiatric disease categories, implying an important role for this gene in the development of psychiatric symptoms. The broad aim of this thesis is to understand how this gene affects brain and behaviour to identify intermediate phenotypes that may underlie the symptoms of psychiatric disease. In particular I will focus on single unit and local field potential activity within the CA1 region of the dorsal hippocampus (dCA1) with the aim of linking findings related to *Cacna1c* at the synaptic level to those at the behavioural and brain imaging level.

- In Chapter 3 I quantify recordings of dCA1 hippocampal activity in *Cacna1c*$^{+/-}$ rats during wake as they freely explore a familiar linear track and a novel open-field. Here I will quantify place-cell activity to understand the effects of reduced gene dosage on spatial coding. In addition I will characterise oscillatory activity within the theta and gamma bands as a measure of network activity.
- In Chapter 4 I explore sleep behaviour in *Cacna1c*$^{+/-}$ rats. Here I use infrared camera-based actigraphy to monitor home-cage activity levels in order to quantify circadian rhythms in *Cacna1c*$^{+/-}$ and gain an understanding of the effects of this gene on sleep architecture.
- In Chapter 5 I quantify hippocampal electrophysiology during sleep and quiescent wake. Here I investigate sharp-wave ripple oscillations and associated spiking activity in the rest period prior to and following runs on the linear track in order to better understand 'offline' network activity and reactivation of spatial learning in relation to *Cacna1c* heterozygosity.
- Finally in Chapter 6 I will assess how *Cacna1c* genetic variation interacts with another form of dysfunction pertinent to psychiatric disease, NMDA receptor hypofunction. Here I administer the NMDA receptor antagonist ketamine to *Cacna1c*$^{+/-}$ rats during exploration of an open-field while simultaneously recording hippocampal oscillatory activity and behaviour.

2

Chapter 2

General Methods

2.1. Animals

All procedures were carried out in accordance with the UK Animals (Scientific Procedures) Act 1986 with approval from the University of Bristol Ethical Review Board. *Cacna1c* heterozygous rats on a Sprague Dawley background were bred by Cardiff University from a colony maintained at Charles River, UK. These were generated from cryo-preserved embryos (Sage Research Labs, Pennsylvania, USA) using zinc-finger nuclease technology to target exon 6, resulting in a 4-breakpoint deletion. At a minimum age of 9 weeks rats were shipped to Bristol University with an equivalent number of WT littermate controls.

All animals were group-housed upon arrival to Bristol, and single-housed prior to surgery. Animals were maintained on a 12:12 hour light-dark cycle and given ad libitum access to food and water. All animals were handled regularly from arrival.

2.2. In Vivo Electrophysiology

2.2.1. Tetrode Design & Construction

Figure 2.1 shows a schematic of the tetrode microdrive construction. From the base upwards, the microdrive consisted of a 10-gauge guide cannula containing at least twenty 30-gauge cannulae (Coopers Needleworks). Each 30-gauge cannula was inserted at the top into a 19-gauge cannula which was glued at the top to a hole within a 'bottom-piece' – a piece of Delrin with three holes for shuttling cannulae and screws up and down; a 23-gauge hole, a 19-gauge hole and a threaded screw-hole. Bottom-pieces were arranged in a ring at the top and attached to one another with dental cement. The base of 30-gauge cannulae were also surrounded by dental cement to fix in place. 'Top-pieces' – two 23-gauge cannulae and a screw (Tenable Screw Company), held together at the top by dental cement – were inserted into each bottom-piece and in the centre of the microdrive (**Figure 2.1B**), raised above the height of the top-

pieces, an electrode-interface board (EIB-36 16TT, Neuralynx) was held by a column of dental cement.

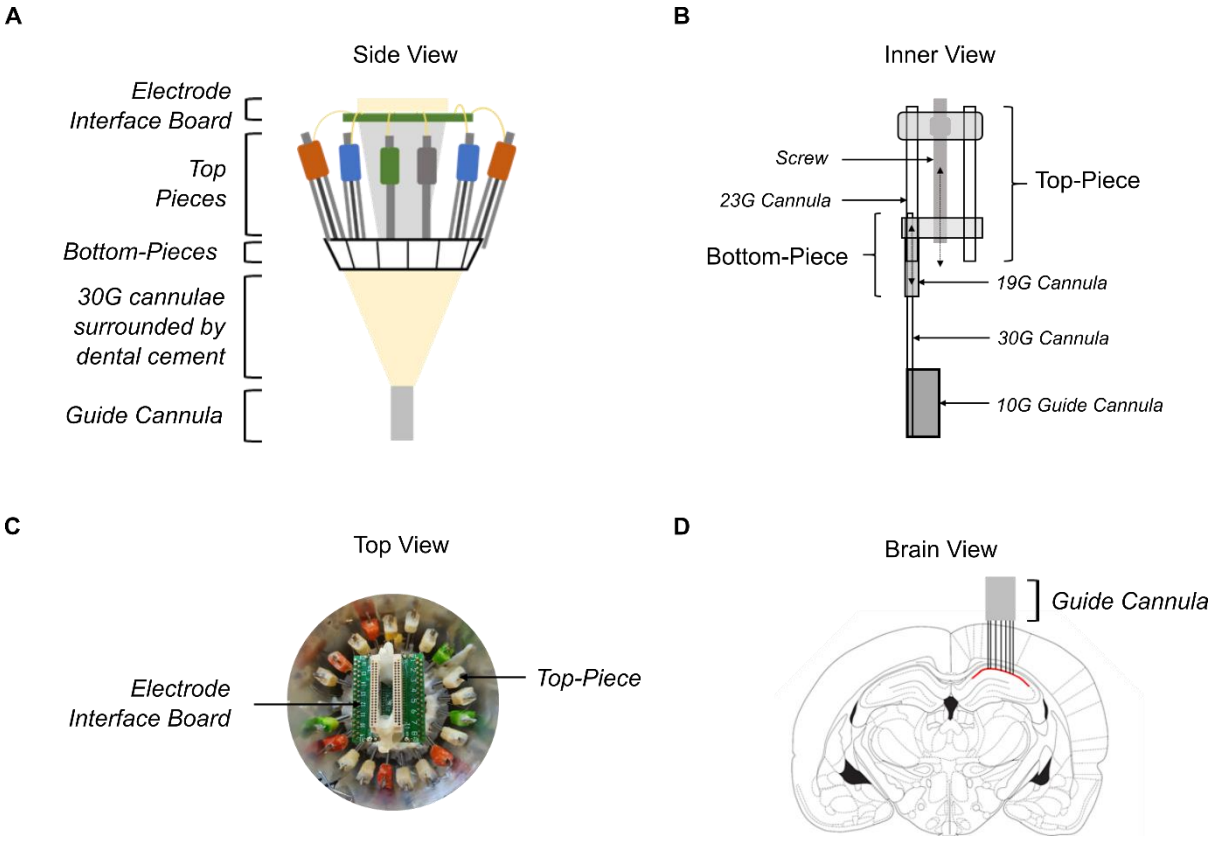

***Figure 2.1* | Tetrode microdrive construction.**
(A) Microdrive schematic viewed from the side.
(B) Inner view of tetrode microdrive depicting arrangement of cannulae within drive and movement of top-pieces; double-arrows indicate direction of top-piece movement.
(C) Photo of microdrive viewed from the top showing electrode interface board and array of top pieces.
(D) Position of guide cannula during surgery and targeting of tetrodes to dCA1 of hippocampus. Red line indicates dCA1 cell layer.

Tetrode wires were made from 12µm polyimide-coated nichrome. This was folded and twisted together by hand twice before attaching the wire bundle to a stand by a loop of wire at the top and to a crocodile clip attached to a rotating motor at the base. The wire was then automatically twisted 80 times in a clockwise direction and a further 40 times in an anti-clockwise direction. A heat-gun set to 350°C was used to melt the polyimide coating. Tetrode wires were inserted into the 23-gauge cannulae contained within top-pieces and lowered with tweezers into the 30-gauge cannulae. The loop of wire at the top of each tetrode was cut and each individual wire was threaded into an individual channel on the electrode-interface board. These were fixed in place with gold-pins (Neuralynx) and the wire was attached by glue to polyimide tubing contained within the 23-gauge cannulae in the top-pieces. This enabled each tetrode wire to be independently shuttled up and down through the microdrive by turning the

screw in the top-piece (1 turn = 320µM). Tetrode wires were cut using fine scissors (World Precision Instruments) to at least 4mm of length from the base of the microdrive (when the top-piece was at its lowest possible position) to allow enough distance to reach the dCA1 region of the hippocampus after surgery. Each microdrive contained 16 tetrodes and 4 references.

The ends of each tetrode wire were plated with gold to reduce the impedance to at least 200kΩ by placing the end in a non-cyanide gold solution (SIFCO) and applying a -0.3µA current (NanoZ, Neuralynx). Four 0.25mm Teflon-coated silver wires (World Precision Instruments) were attached by solder to the ground-holes in the electrode interface board to act as grounding wires. Two of these were attached by silver-paint to an aluminium cone placed around the exterior of the microdrive. This cone acted to both protect the microdrive from damage following surgery and to shield from electromagnetic interference. The other two grounding wires were attached to ground screws during surgery (more details ***2.2.2***).

2.2.2. Surgical Procedure

Prior to surgery rats were moved into single high-top cages and handled daily for at least one week. All surgeries were carried out using aseptic technique to minimize the risk of infection through the use of autoclaved surgical equipment, sterile gowns and gloves, and sterile drapes covering all surfaces. Anaesthesia was induced with 4% isoflurane in oxygen and maintained throughout surgery at 1.5-3%. Rats were weighed at the beginning of surgery and had their heads shaved prior to transfer to a sterile heat-mat and head-fixed in place to a stereotaxic frame (Kopf model 1900). The rat's vital signs including body temperature (via a rectal probe) and heart rate and blood-oxygen saturation level (via a paw sensor) were monitored throughout surgery (Kent Scientific). The rat's eyes were protected from corneal drying with LacriLube and shielded from surgical lights with tape. Hydration levels were maintained throughout surgery with 5ml sub-cutaneous injections of 0.9% saline. Prior to incision, the rat's scalp was sterilized with chlorhexidine and 70% ethanol and the surgical plane of anaesthesia was gauged from the toe-pinch withdrawal reflex. Once the rat was sufficiently anaesthetized a sub-cutaneous injection of 0.1ml of lidocaine with adrenaline was administered down the midline.

A scalpel incision (~3cm) was made down the midline and held open with skin clips. Connective tissue was removed with a scalpel, scissors and cotton buds to expose the skull region from bregma to lambda. The skull surface was roughened with a curette to encourage adherence of dental cement to the skull surface later in the surgery. The skull was levelled with a stereotaxic alignment indicator and the co-ordinates for the craniotomy were marked according to the rat brain atlas (Watson & Paxinos, 2007; 3.6mm posterior to bregma; 2.5mm lateral to midline) along with the positions for 7 skull screws. Screw holes were drilled using a

tungsten carbide burr with 2 positioned anterior to bregma and 3 left of the midline, posterior to bregma and anterior to lambda, for support screws. A further 2 holes were drilled posterior to lambda, above the cerebellum, for the ground screws – screws with a length of silver wire attached with solder. These holes went through the skull to ensure low impedance. After ground screws were screwed in place the impedance was checked to ensure a good connection. Following insertion of structural and ground screws, metabond dental cement (C&B Metabond) was applied to the base of the screws to secure them to the skull surface.

A 2.5mm sized craniotomy was made at the previously marked position using the tungsten carbide burr. Once the skull was removed and the brain exposed, the layer of dura above the brain was removed with a 30-gauge needle bent to form a hook and fine tweezers. The microdrive was lowered such that the edge of the guide cannula sat just within the craniotomy, above the brain (**Figure 2.21D**). Petroleum jelly (Vaseline) was placed around the edge of the craniotomy and Gentamycin dental cement (DePuY) was placed around the base of the skull screws up to the guide cannula to secure the microdrive to the skull surface. The ground wires attached to the microdrive were soldered to the ends of the ground wire attached to the skull screws. Following implantation of the microdrive, all tetrodes and references were lowered 4 turns (1280μM). The skin anterior and posterior to the implant was sutured with Teflon sutures (Ethicon) and antibiotics (Surolan) were applied to the edges of the incision.

The rat was taken off anaesthesia and returned to a clean cage. Once reflexes had returned the animal was given an intraperitoneal injection of 0.025mg/kg buprenorphine (Vetergesic). For one-week post-surgery the rat was given a mixture of recovery gel (DietGel) and mashed rat chow. Weight was recorded daily and food and water intake were monitored.

2.2.3. Data Acquisition System

For recording electrophysiological signals, microdrives were plugged into a head stage pre-amplifier (HS-36, Neuralynx) which was connected to a fine-wire tether and in turn connected to a Digital Lynx SX (Neuralynx) system to amplify signals and convert from analogue to digital. The Digital Lynx system was connected to a PC installed with Cheetah software (Neuralynx) which was used to record local field potentials (LFP) (sampled at 1000Hz; filtered between 0.1-600Hz) and single units (sampled at 32kHz; filtered between 600-6000Hz). The polarity of all signals was inverted, and signals were referenced to 1 of the 4 reference tetrodes. For single unit recordings a noise threshold was set manually for each individual tetrode.

To track the position of the rat during behavioural sessions, a light-emitting diode was attached to the head stage and recorded with overhead cameras (sampled at 25 frames/second; 720x560 pixel resolution) with Cheetah software.

2.2.4. Tetrode Targeting

Following surgery rats were placed daily in a sound-attenuating chamber (**Figure 2.2A**) on a raised platform. Over a duration of 2-4 weeks each tetrode was lowered, to begin with, at larger increments (80-160µM), and as tetrodes neared the hippocampus (~2mm depth), at smaller increments (20-40µM). Each tetrode was lowered until in line with the pyramidal cell layer of the dCA1 region of the hippocampus (~2.2mm depth). The depth of each tetrode was determined by SPW-R activity in the LFP signal and bursting spike activity. Reference tetrodes were targeted towards the white matter situated below the cortex and above the dCA1.

2.3. Habituation & Behaviour

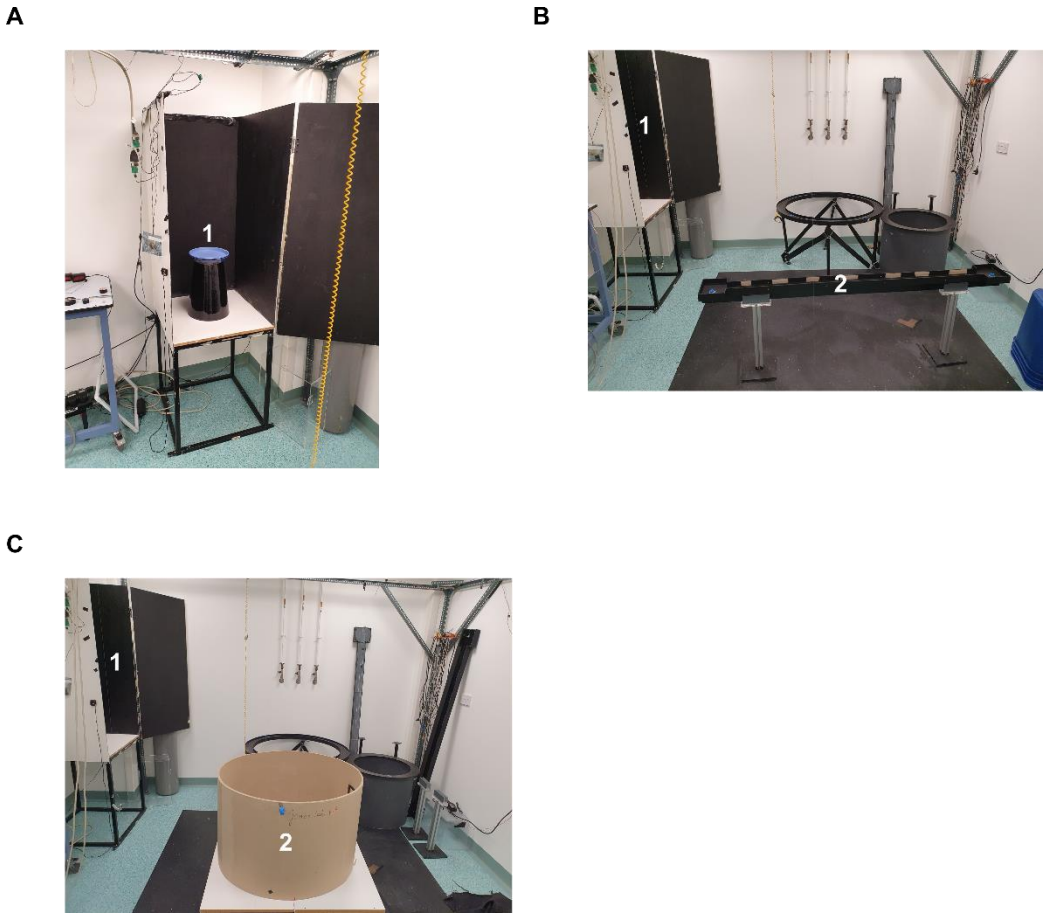

***Figure 2.2* | Recording room setup.**
(A) The Sleep-Box: a sound attenuating chamber used for sleep/rest recordings, with a raised platform (1) for the animal.
(B,C) Full recording room with sleep box (1) in corner and open space for in centre of room for linear track (**B**,2) or open-field **(C**,2).

2.3.1. Recording Room Setup

Figure 2.2 displays the recording room setup. Sleep/rest data were acquired in the sound-attenuating box (sleep-box) and all behavioural recordings (linear track and open field) were taken from the open space situated adjacent to the sleep-box. A pulley system of weights was used to counter-balance the weight of the animal with the weight of the head-stage and tether such that the animal could move freely both in the sleep-box and in the behavioural environment.

2.3.2. Habituation

Prior to surgery rats were habituated to the sleep-box. At least one week after surgery rats were placed on food restriction to ≥85% of their initial weight and habituated to the linear track over a duration of 1-4 weeks (alongside lowering of tetrodes). Each day rats were allowed to freely explore the linear track for sucrose solution rewards that alternated between each end of the track, only after the rat had run the full length of the track in one direction. Experimental recordings began once rats had reached a minimum criterion of 10 complete circuits on the linear track (10 runs in both directions).

2.4. Verification of Electrode Position

2.4.1. Lesioning & Perfusion

After completion of all recording sessions rats were terminally anaesthetized with sodium pentobarbital (60mg/kg). Following confirmation of loss of toe-pinch withdrawal reflex, a 30µA current was passed through each tetrode for 10 seconds to create an electrolytic lesion at the tetrode tip. Rats were then transcardially perfused with 0.9% saline followed by 4% paraformaldehyde, administered through a peristaltic pump connected to a blunt needle inserted into an incision in the heart. Brains were then dissected out and transferred to 4% paraformaldehyde solution for at least 3 days. Prior to sectioning, the brain was transferred to sucrose solution for at least 2 days.

2.4.2. Histology

Using a freezing microtome, 50µM coronal sections of the brain were cut and transferred to adhesive SuperFrost Plus Slides (ThermoScientific). After being left to dry for 24 hours, slides were nissl-stained with thionin. The sections were viewed under an optical microscope with a digital camera attached and the lesion sites were cross-checked against the rat brain atlas (Watson & Paxinos, 2007).

2.5. Data Analysis

All data analysis was carried out using Matlab (Mathworks) with custom-made scripts and open-source toolboxes (see experimental chapter methods for further details).

2.5.1. Spike Sorting

Spike-sorting of single unit data was carried out automatically first, using KlustaKwik (http://klustakwik.sourceforge.net/) based on the peak amplitude, the first principle component of the waveform and the spike energy. Automatically defined clusters were then manually curated using MClust (Redish, 2014). Clusters were required to meet a minimum criterion for inclusion in data analysis (Isolation Distance ≥ 12; less than 1% interspike intervals below 2ms; mean firing rate ≥ 0.2 spikes per second). Interneuron clusters were separated from pyramidal cell clusters using a hierarchical clustering algorithm on the basis of spike-width, peak-valley ratio and firing rate.

2.5.2. Statistics

All statistical analyses were carried out using Matlab and SPSS (IBM). All data were tested for normality with the Shapiro-Wilk test and appropriate parametric and non-parametric statistical tests were selected accordingly (see experimental chapter methods for further details).

3

Chapter 3

Place-Cell & Network Physiology During Free Exploration in *Cacna1c* Heterozygous Rats

3.1. Introduction

Psychiatric risk is associated with hippocampal dysfunction (Heckers et al., 1998, Lawrie and Abukmeil, 1998, Bremner et al., 2000, Driessen et al., 2000, Stockmeier et al., 2004) and similar impairment have been described in individuals harbouring variants of *CACNA1C* (Bigos et al., 2010, Erk et al., 2014, Paulus et al., 2014, Mallas et al., 2017). Moreover, animal models of *CACNA1C* genetic variation display deficits in Schaffer-collateral plasticity indicating dysfunction to hippocampal synaptic signalling (Moosmang et al., 2005, Tigaret et al., 2020). Yet despite these findings it is unknown how reduced *CACNA1C* expression impacts on individual neuron and network signalling in vivo. Given the important role of the hippocampus in cognition (O'Keefe and Nadel, 1978, Eichenbaum, 2004), dysfunction to hippocampal neurophysiology as a result of *CACNA1C* genetic variation could engender cognitive impairment. In this chapter I explore hippocampal neurophysiology in *Cacna1c* heterozygous rats during wakeful exploration of familiar and novel environments in order to deepen our understanding of how reduced *CACNA1C* expression might underlie hippocampal dysfunction in psychiatric risk.

3.1.1. Hippocampal Electrophysiology in Psychiatric Disease

The literature on hippocampal electrophysiology in relation to psychiatric risk is sparse, though several studies have described neurophysiological alterations that may underlie dysfunction in psychiatric disease. In order to consider how *Cacna1c* heterozygosity might impact on hippocampal neurophysiology, I will summarise what is known about place-cell and oscillatory activity in relation to psychiatric risk in genetic animal models (summarised in **Table 1**), in addition to several other psychiatric relevant human and animal studies.

Table 1. Summary of research into hippocampal place-cell and network physiology in relation to genetic models of psychiatric risk

Animal Model	Subfield	Behavioural Task	Place-Cell Phenotype	Oscillatory Phenotype	Reference
DISC1 - L100P Mouse	CA1	Free exploration (novel open-field)	Enlarged place-fields Fewer place-fields per place cell	Reduced theta power	Mesbah Oskui et al. (2015)
tgDISC1 Rat	CA1	Free exploration (novel & familiar open-field)	Smaller place-fields Increased spatial information Reduced decoding error of position	Reduced theta & gamma phase-locking	Kaefer et al. (2019)
Forebrain specific calcineurin-KO mouse	CA1	Free exploration (linear track)	Normal place-cell activity	Increased sharp-wave ripple power and abundance Increased spiking activity during sharp-wave ripples	Suh et al. (2013)
Df(16)A$^{+/-}$ mouse	CA1	Goal-oriented learning task (head-fixed, treadmill running)	Smaller place-fields Fewer place-fields per place cell Reduced spatial information Reduced place-field stability	N/A	Zaremba et al. (2017)
NLG3-KO mouse	CA2 & CA3	Anaesthetized	N/A	Reduced theta, slow-gamma and fast-gamma	Modi et al. (2019)

3.1.1.1. Place Cell Physiology

Though a well-studied phenomenon in relation to hippocampal function, few studies have attempted to link place-cell dynamics to psychiatric risk. A small body of research is beginning to emerge, though the results here are conflicting.

Two such studies have exploited models of DISC1 variants in order to quantify place-cell neurophysiology (Mesbah-Oskui et al., 2015, Kaefer et al., 2019). DISC1 is a gene heavily implicated in SCZ among other psychiatric disorders (St Clair et al., 1990, Hovatta et al., 1999, Blackwood et al., 2001, Ekelund et al., 2001, Hodgkinson et al., 2004). A study of a large Scottish family revealed a translocation in this gene that conferred risk for SCZ at an odds ratio of ~7 (St Clair et al., 1990, Blackwood et al., 2001); strikingly high compared to most other psychiatric risk associated genes (Harrison, 2015). The gene product of DISC1 is a scaffolding protein which appears to play an important role in synaptic spine morphology through its interaction with other synaptic proteins (Jaaro-Peled et al., 2009, Hayashi-Takagi et al., 2010). Spine density reductions have been observed in animals with DISC1 deletions (Hayashi-Takagi et al., 2010), highlighting the important role of the post-synaptic density in psychiatric risk.

In the first of these studies, the authors made use of the L100P mouse model, a model whereby a mutation in one exon of DISC1 gives rise to a replacement amino acid in the protein

product. This model has previously been shown to recapitulate certain SCZ-like phenotypes (Clapcote et al., 2007). CA1 recordings from mice as they explored an open-field revealed larger place-fields in DISC1-L100P mice. Further interrogation of this finding revealed it to be the result of fewer place-fields per place-cell in DISC1-L100P. Place-field stability was also assessed through a cue rotation experiment and this was not altered between genotypes, nor were place-field properties as the cue was returned to the original position, indicating intact spatial stability. Importantly the altered place-field properties were observed upon first exposure to the novel open-field, potentially indicating a deficit here in place-field formation (Mesbah-Oskui et al., 2015).

The second of these studies made use of the tgDISC1 rat model. This model is not strictly a genetic model per se, rather it makes use of a transgene introduced into the rat to cause overexpression of intact DISC1, leading to protein misassembly (Trossbach et al., 2016). CA1 recordings from rats as they explored novel and familiar open-fields revealed smaller place-fields, enhanced spatial information and a reduction in Bayesian decoding error of spatial position in the tgDISC1 animals (Kaefer et al., 2019). The pattern of changes observed in this study might imply an improvement in spatial coding rather than a deficit. The authors also quantified firing rate variability of place-cells and found a reduction in the tgDISC1 rats which they posited might reflect an impairment in encoding non-spatial features. Conversely this could also have reflected enhanced place-cell stability in the tgDISC1 rats. Future behavioural research in this animal model could elucidate further the effects on cognitive function of this particular pattern of changes to hippocampal neurophysiology.

In another study, researchers made use of a forebrain-specific calcineurin knockout mouse model (Suh et al., 2013) to quantify place-cell physiology. Calcineurin is a protein phosphatase, implicated in SCZ through genetic association with the gene for the gamma subunit of this protein, PPP3CC (Gerber et al., 2003). In addition to its association with psychiatric risk, calcineurin has more direct relevance to *CACNA1C* due its role in calcium mediated synaptic signalling cascades (Saitoh and Schwartz, 1985, Day et al., 2002), in particular NFAT signalling (Li et al., 2012a), which may have some importance in the regulation of synaptic plasticity (Furman et al., 2016). In this study CA1 place-cells were recorded as animals explored a linear track. All measures of place-cell activity here were reported to be normal, including place-field size and spatial information.

Finally, place-cell activity was quantified in the Df(16)A $^{+/-}$ mouse model. This is a model of 22q11.2 deletion, one of the strongest genetic risk factors for SCZ (Karayiorgou et al., 1995, Xu et al., 2008, Levinson et al., 2012), with an odds ratio of 67 having been previously reported (Marshall et al., 2017). This model involves a chromosomal deletion in region Df1 in the mouse; thought to be analogous to the 22q region in humans (Lindsay et al., 1999). This study made use of CA1 calcium imaging in head fixed mice as they performed a goal-oriented

learning task on a treadmill, which involved licking in particular locations of the context to elicit a water reward. Df(16)A$^{+/-}$ mice here were reported to display smaller place-fields, fewer place-fields per place-cell and a reduction in the number of place-cells exhibiting significant spatial information. Additionally day-to-day place-cell stability was impaired and these changes corresponded to a modest impairment in task performance (Zaremba et al., 2017).

3.1.1.2. Oscillatory Activity

Several of the previously mentioned studies, in addition to others have also sought to characterise hippocampal oscillatory activity in relation to psychiatric risk. In the DISC1-L100P mouse model, a reduction in theta power was observed. This also corresponded to alterations in Parvalbumin-positive (PV) interneurons, with the direction of alteration varying across the dorsoventral axis (Mesbah-Oskui et al., 2015). In the tgDISC1 animal model, though the properties of theta and gamma oscillations were not reported, tgDISC1 animals displayed a reduction in phase-locking both to theta and gamma. The change in gamma phase-locking here manifested only during exploration in the novel environment (Kaefer et al., 2019). Prior research in rats lacking a GluR1 AMPA receptor subunit also revealed a reduction in gamma phase-locking that manifested only in a novel environment and this appeared to be the result of impaired Schaffer-collateral plasticity (Kitanishi et al., 2015) indicating a similar mechanism may have been at play in the tgDISC1 rats. Another study made use of NLG3 knockout mice. NLG3 is one of the neuroligin genes, mutations and deletions to which have been implicated in ASD (Jamain et al., 2003, Gilman et al., 2011, Sanders et al., 2011). In this study, LFP from CA2 and CA3 were recorded in anaesthetized rats revealing a reduction in theta, slow-gamma and fast-gamma. These effects, as in the DISC1-L100P study, were purported to result from inhibitory deficits as evidenced by the loss of CCK-mediated IPSPs in CA2 pyramidal cells in the NLG3 mice (Modi et al., 2019).

Hippocampal oscillatory impairments have also been studied in relation to non-genetic models of psychiatric risk. Administration of polyriboinosinic–polyribocytidilic acid to mice during pregnancy to mimic prenatal infection, a risk factor for SCZ (Brown and Derkits, 2010), resulted in a lower density of PV interneurons in CA1 which corresponded to a reduction in theta power (Ducharme et al., 2012). Use of psychotomimetics – pharmacological compounds thought to recapitulate symptoms of SCZ - also produces alterations in hippocampal gamma power (Ma and Leung, 2000, Kittelberger et al., 2012) in addition to impairments to theta-gamma coupling (see Chapter 6 for full details) (Caixeta et al., 2013, Michaels et al., 2018).

Deficits in hippocampal oscillatory activity in relation to psychiatric disease have additionally been reported in a study of human participants. Here healthy participants harbouring psychiatric risk associated SNPs for ZNF804A underwent MEG and fMRI hippocampus and prefrontal cortex scans at rest. This analysis revealed a loss of hippocampal

theta power (Cousijn et al., 2015), lending some translatability to animal studies reporting similar deficits.

3.1.1.3. Applicability of Findings to Cacna1c Heterozygotes

Though several of these studies describe hippocampal neurophysiological dysfunction, the results are relatively inconsistent, indicating that there is not one common form of hippocampal dysfunction underlying psychiatric risk. Do any of these animal models have specific relevance to *Cacna1c* heterozygosity? The calcineurin knockout model, as discussed, disrupts a protein involved in calcium signalling, and calcineurin appears to interact with Cav1.2 (Day et al., 2002, Li et al., 2012a) indicating a convergence on similar biological pathways. Under this assumption one might expect minimal place-cell alterations in *Cacna1c*$^{+/-}$ rats. Yet plasticity deficits observed in this animal model do not mirror those observed in *Cacna1c*$^{+/-}$ rats, with normal Schaffer-collateral LTP reported yet an impairment in LTD observed in calcineurin mice (Zeng et al., 2001). Additionally calcineurin mediated NFAT signalling represents just one of many signalling pathways for which Cav1.2 channels are involved (see Chapter 1).

DISC1, like *CACNA1C*, also appears to have a role in the erk/MAPK pathway (Hashimoto et al., 2006), and impairments to Schaffer-collateral plasticity have been reported in relation this gene (Cui et al., 2016), indicating some shared biology with this animal model also. The plasticity deficits observed here were in relation to the L100P model. If such deficits underlie either place-field changes or theta oscillation impairments, one might expect similar effects with regard to *Cacna1c* heterozygosity.

None of the models described here however show any direct relevance to LTCC signalling. Though their common role in psychiatric risk provides some remit to anticipate place-cell alterations and oscillatory deficits in relation to *Cacna1c* heterozygosity, to better understand how *Cacna1c* heterozygosity might impact in vivo hippocampal neurophysiology I will first review the role of calcium channel signalling in relation to hippocampal neurophysiology.

3.1.2. Calcium Channels & Place-Cells

Direct study of the role of calcium channels, in particular Cav1.2, in hippocampal place-cell physiology is limited. One study has sought to characterise the role of Cav2.1 channels through the use of conditional knockout animals. Key place-cell properties were revealed to be normal yet the ability to re-orient place-cell locations back to their original position following a cue rotation experiment revealed a deficit in the knockout animals (Jung et al., 2016). Though this reveals a potential role for calcium channels in place-cell remapping, it is unclear how relevant such a finding is to Cav1.2.

Despite a lack of direct research into the role of Cav1.2 channels in place-cell dynamics, research into the physiology underlying place-field formation indirectly points towards a potentially prominent role for LTCCs. Calcium imaging of CA1 cells in mice during exploration of a virtual environment reveals an important role for dendritic spiking in place-field formation (Sheffield and Dombeck, 2015, Sheffield et al., 2017). In the first of these studies, regenerative dendritic spiking was recorded in CA1 place-cells and this appeared to be predictive of the spatial precision of that cell (Sheffield and Dombeck, 2015). The follow-up to this study characterised this spiking on a finer temporal resolution and found that regenerative dendritic spiking preceded the onset of somatic spiking in pyramidal cells upon formation of location-specific firing (Sheffield et al., 2017), indicating an important role for dendritic spiking in place-cell formation. Such dendritic spiking appears to be contingent upon voltage-gated calcium channels. In particular, compound spiking at the dendrite – whereby a fast-spike is followed by secondary spikes – appears to depend on sodium influx for the fast-component and LTCC mediated calcium influx for the secondary components, as evidenced by the loss of this spiking with nifedipine administration (Andreasen and Lambert, 1995).

Dendritic spiking has also been characterised in relation to *Cacna1c* heterozygosity. Here back-propagation of action potentials was quantified through the use of calcium imaging in CA1 pyramidal cells. This revealed a significant attenuation of these action potentials as they travelled down the dendrite in *Cacna1c*$^{+/-}$ rats compared to WTs (Tigaret et al., 2020). It is unclear whether the dendritic spiking events underlying place-field formation are the result of back-propagation or more localized spike generation, though the order of spiking from dendritic event first, followed by somatic spiking would imply the latter. Yet localised spike generation also shows an important dependence on LTCCs. In vitro recordings from CA1 cells reveal that LTP at the dendrite does not require backpropagating action potentials but is instead reliant on spatially localised, locally generated dendritic spikes, and importantly this spiking activity is blocked with nimodipine, also highlighting a role for LTCCs here (Golding et al., 2002).

The importance of dendritic spiking in LTP (Magee and Johnston, 1997, Schiller et al., 1998, Golding et al., 2002) could underlie the Schaffer-collateral LTP deficits reported in *Cacna1c*$^{+/-}$ rats (Tigaret et al., 2020), and several studies have considered the role of such LTP in relation to place-cell activity. In one study the NMDAR1 gene was knocked out in CA1 pyramidal cells in mice, generating dysfunctional NMDA receptors and a loss of Schaffer-collateral plasticity as a result. Place-cell recordings during free exploration of a track revealed larger place-fields and impaired decoding of spatial trajectories (McHugh et al., 1996). Such an alteration in place-field size is broadly similar to what has been reported in the DISC1-L100P mouse model (Mesbah-Oskui et al., 2015) which incidentally also displays impairments in Schaffer-collateral plasticity (Cui et al., 2016). On this basis one might expect to observe a

similar enlargement of place-fields in *Cacna1c*$^{+/-}$ rats. In another study CA1 plasticity was blocked through the use CPP, an NMDA receptor antagonist. This resulted in a loss of long-term stability of place-fields though place-field formation here was not impaired (Kentros et al., 1998). In the aforementioned research relating dendritic spiking to place-field formation, some cells exhibited somatic spiking from the outset of exposure to a novel environment (Sheffield et al., 2017), indicating that plasticity is not necessary for the formation of place-fields. The authors posited that dendritic spike-mediated plasticity may serve to refine place-cell activity, both in terms of spatial precision and stability over time. This was highlighted in mice exhibiting a mutation in αCaMKII, a downstream signalling molecule important in NMDA receptor dependent CA1 plasticity (Giese et al., 1998a, Yasuda et al., 2003). Here, though spatial tuning of place-fields over time was observed in wild-type animals, this was absent in the mutant animals (Cacucci et al., 2007). As such, in *Cacna1c*$^{+/-}$ rats, place-field formation may not be impaired per se, yet one may expect to observe dysfunction in the refinement of place-fields over time.

In summary, this research reveals that place-cell formation and refinement is regulated via spiking activity at the dendrite and corresponding plasticity. On this basis I hypothesize that place-cell properties such as place-field size will be impaired in *Cacna1c* heterozygous rats.

3.1.3. Calcium Channels in Hippocampal Network Activity

To date, no direct assessment of *CACNA1C* in relation to network activity in vivo has been reported. However in human induced pluripotent stem cell cultures, a loss of synchronous firing activity was observed in response to LTCC blockade (Plumbly et al., 2019), indicating an important role for LTCCs in regulating EI networks. In the hippocampus, PV interneurons appear to rely on LTCCs for their maturation in slice cultures, as evidenced by the respective effects of LTCC agonist and antagonist administration (Jiang and Swann, 2005). Such an effect on interneuronal development may in part underlie the loss of emergent network activity observed in culture. Theta, gamma, and the coupling of these two rhythms have all been shown previously to depend on PV interneuron activity (Cardin et al., 2009, Sohal et al., 2009, Wulff et al., 2009) and thus it seems reasonable to hypothesize that *Cacna1c* heterozygosity might lead to deficits in hippocampal theta and gamma oscillatory activity.

At a synaptic level LTCCs may also play an important role in oscillatory activity. At apical dendrites in CA1 pyramidal cells, slow spiking – a rhythmic dendritic depolarization at approximately the frequency of theta – can be induced with dendritic depolarization. These membrane oscillations were blocked with nimodipine indicating a reliance on LTCCs. Additionally a theta-like current injection (6Hz sine wave) generated a dendritic oscillation. The amplitude of this oscillation increased as a function of initial membrane potential yet

nimodipine and a range of other LTCC blockers attenuated this amplification (Hansen et al., 2014). This research demonstrates an intrinsic theta-oscillatory component at the level of the dendrite that may serve to amplify field theta. In vivo, a loss of LTCCs could impair the magnitude of theta oscillations or alternatively this could manifest as an inability to amplify theta oscillations in response to behavioural changes.

The role of LTCCs in dendritic responses to theta could also disrupt the spiking of individual cells in relation to oscillatory activity. An in vitro model of phase-precession made use of concurrent somatic and dendritic theta frequency stimulation. Such stimulation generated dendritic spiking activity which in turn caused a phase advance of somatic action potential activity (Magee, 2001). Though the role of LTCCs was not tested here, their importance towards dendritic spike generation might lead to impairments in theta phase-precession in *Cacna1c*$^{+/-}$ rats.

Phase locking of CA1 pyramidal cells to gamma oscillations as mentioned earlier, appears to rely on Schaffer-collateral plasticity as evidenced by the impaired phase-locking observed in rats lacking GluR1 AMPA receptor subunits (Kitanishi et al., 2015) – an effect also seen in tgDISC1 animals (Kaefer et al., 2019). Assuming Schaffer-collateral plasticity deficits do underlie these effects, then a similar disruption might be observed in *Cacna1c*$^{+/-}$ rats.

These studies collectively, point towards a possible role for LTCCs in hippocampal oscillatory activity and spiking activity relative to hippocampal rhythms, yet direct study is necessary to fully elucidate their role here. The results presented in this chapter will aim to uncover more precisely, the role of LTCCs in hippocampal oscillatory activity.

3.1.4. Chapter Aims

A small body of research points towards an association between psychiatric risk genes and dysfunction at the cellular and network level in the hippocampus in vivo. Moreover LTCCs play an important role in the dendritic activity underlying the formation and refinement of place-cells in addition to a possible role in the regulation of network activity. Yet there is a lack of research quantifying either the effects of *Cacna1c* reduced gene dosage on hippocampal neurophysiology, or more broadly, the role of LTCCs in this domain.

In this chapter I aim to characterise hippocampal place-cell neurophysiology by taking electrophysiological recordings from rats during runs on a linear track, runs on the same track in a novel orientation and free exploration of a novel open field. In addition I will also assess hippocampal oscillatory properties during linear track runs to quantify network hippocampal properties in *Cacna1c*$^{+/-}$ rats during engagement in a task. Finally I will quantify single unit coupling to network oscillations. Here I will characterise the phase relationships of cells to individual frequency bands and assess the degree of phase precession relative to theta in each genotype.

CACNA1C is associated with hippocampal cellular deficits and hippocampal-dependent behavioural deficits. The research in this chapter will further our understanding of how these are related at a network level which may ultimately broaden our understanding of deficits underlying psychiatric disease.

3.2. Methods

Table 2. Summary table of number of animals used.
Summary table of number of animals and across number of sessions. Total number of cells across all animals given with range of cells recorded from individual animals in brackets.

Section	Number of Recording Days	Number of Sessions	Genotype	Number of animals	Number of cells	Number of place-cells
Spike properties	1	3 (Pre-sleep, Run and Post-Sleep)	WT	5	Pyr: 126 (2-51), IN: 34 (2-18)	N/A
			Cacna1c$^{+/-}$	7	Pyr: 144 (4-54), IN: 25 (1-7)	N/A
Familiar linear track	1	1	WT	5	126 (2-51)	77 (2-24)
			Cacna1c$^{+/-}$	7	144 (4-54)	95 (2-38)
Linear track in novel orientation	1	1	WT	5	100 (2-51)	69 (2-31)
			Cacna1c$^{+/-}$	7	112 (2-42)	81 (2-32)
Open-field	1	1	WT	5	128 (2-52)	84 (2-36)
			Cacna1c$^{+/-}$	7	94 (2-36)	73 (2-24)

3.2.1. Behavioural Protocol

3.2.1.1. Apparatus

The linear track used was 175cm in length with 3.5cm high walls. The central portion of the track was 149cm in length with a width of 7cm while the ends of the track (reward zones) were

expanded to have a width of 16cm and were 13cm in length. These enabled the animal sufficient space to turn. The track was raised 50cm off the ground.

The track was built from acrylic and painted matt black to reduce the smoothness of the surface, enabling the animal to run and to avoid reflection of LED's on the animal's headstage on the surface of the track. Reward ports were placed in each reward zone. These were built from plastic caps with an indentation in the top to hold a sucrose solution and a metal cannulae held by glue in a hole in the cap. The reward port was placed in a hole drilled in the reward zone, enabling sucrose solution to be pumped into the port from below, through rubber tubing. Sucrose solution release was controlled by pinch valves enabling individual drops of sucrose solution to be released upon successful completion of a run.

For the novel open field, a cardboard cylinder 50cm in radius with 50cm high walls (see **Figure 2.2**) was used as an open field. The cylinder was placed upon two raised wooden platforms and covered in sawdust. A box and a cross were attached to the sides of the open field walls to act as visual cues.

3.2.1.2. Familiar Track Protocol

Figure 3.1 describes the behavioural protocol used. Animals were placed in a rest-box (described in ***2.3.1***) and left to rest for approximately 30 minutes. Following pre-rest animals were placed on the linear track and allowed to run freely for sucrose rewards. Rewards were delivered at the end of every run in one direction (half circuit) and only if the run had been completed without turning around. After the run, animals were placed back in the rest-box for a 'Post-Rest' session and were left to rest for a further 30 minutes. The animal was tethered to the Neuralynx system throughout the protocol, enabling concurrent recording of electrophysiological signals as well as position and behaviour. All recordings took place in the animal's light phase. Lights were left on for the pre and post rest recordings but were turned off during the run to enable better tracking of the LEDs. Recordings took place in both the morning and the afternoon, but these were counterbalanced between genotypes to avoid time-of-day effects.

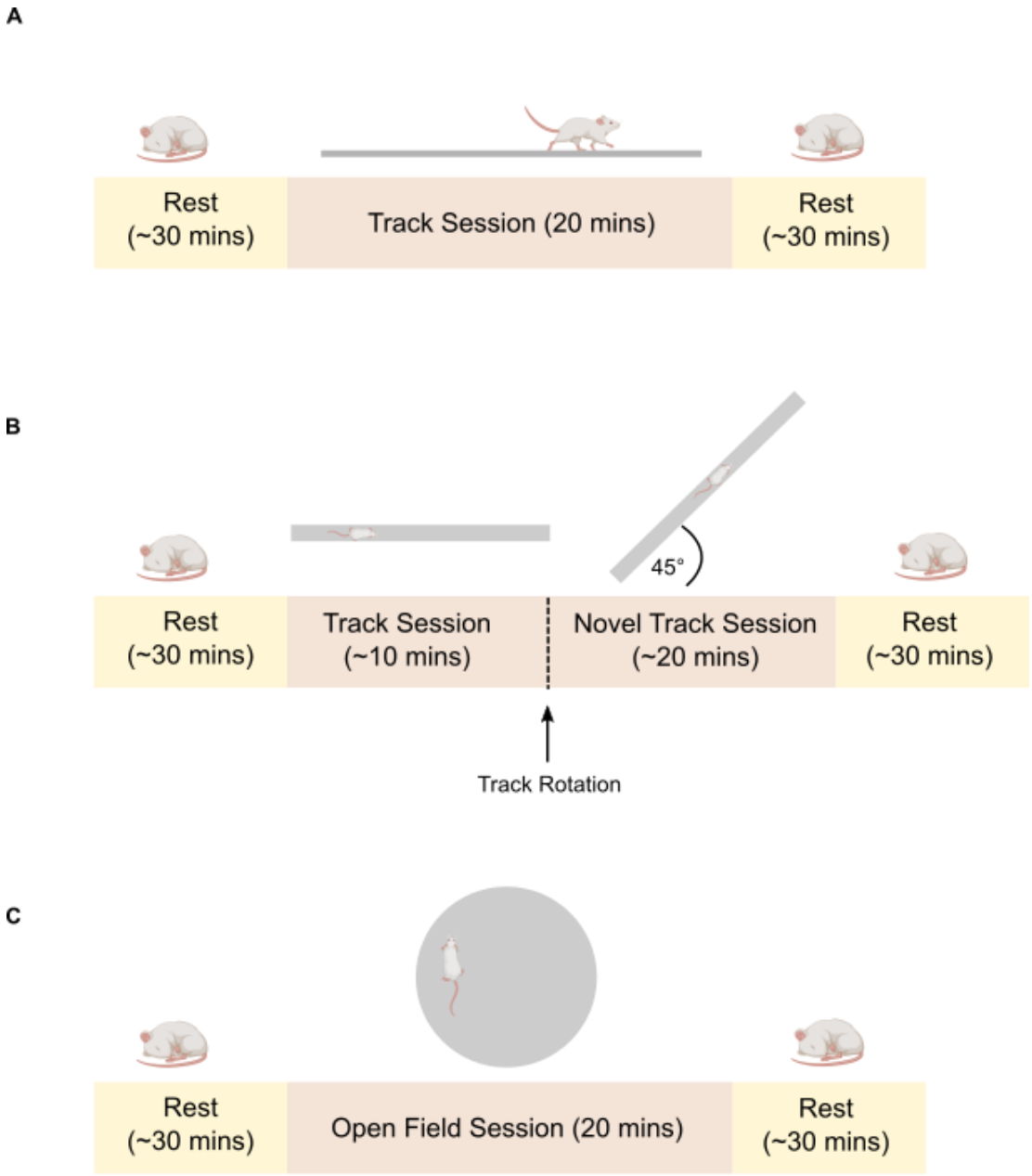

***Figure 3.1* | Behavioural protocol** Schematic depicting behavioural protocol for **(A)** familiar linear track session, **(B)** novel linear track session and **(C)** open field session

3.2.1.3. Novel Track Orientation Protocol

Animals were subject to this protocol following at least one session on the familiar linear track. First animals were first placed in the rest-box for ~30 minutes of pre-rest before being placed on the linear track in the 'familiar' position to run for sucrose rewards. After at least 5 complete circuits on the track, animals were taken off the track, the track was rotated 45°, and they were placed back on to continue running for sucrose rewards, now through a different portion of the recording room. Following at least 10 complete circuits in the novel track orientation, animals were placed back in the rest-box for a further ~30 minutes.

3.2.1.4. Novel Environment

At least one day following the track sessions, animals were subject to the novel environment protocol. Animals had received no prior experience of the novel environment before this session. The pre-rest and post-rest protocol did not differ to that used for either of the linear track protocols. After pre-rest, animals were put into the novel open field for 20 minutes and allowed to freely explore, followed by the post-rest session.

Both the novel track orientation and novel environment sessions occurred during the light phase with lights on for rest sessions, but off for the run sessions. Recordings occurred during both morning and afternoon and these times of day were counterbalanced between genotypes.

3.2.2. Data Analysis

All data analysis was carried out in Matlab (Mathworks).

3.2.2.1. Spike Properties

Analysis of firing rate and bursting was carried out as described by Mizuseki & Buzsaki (2013). A burst was defined as 3 or more spikes occurring less than 8ms apart and the burst index was defined as the ratio of spikes in bursts vs. all spikes.

3.2.2.2. Place Cell Analysis: Linear Tracks

For all linear track place cell analysis, position data was collapsed onto the x-axis and analysis was carried out on one dimensional place fields. Track runs were only included when the animal was running above a speed threshold of 5cm/s. This ensured runs incorporating periods of immobility, which may have contained ripples, were not included in the analysis.

To compute place fields, an occupancy map was initially generated by dividing the track into 29 (~6cm) bins and calculating average dwell time in each bin across all trials. Place fields were calculated by dividing the spike count in each bin by the occupancy map and averaging across trials. Occupancy and spike counts were computed for runs in each direction separately, to assess whether cells showed bidirectionality in their firing properties. Place fields were smoothed using a gaussian smoothing kernel (SD = 1.5). A cell was regarded as a ‘place cell’ if it had a minimum firing rate of 0.2Hz and a peak firing rate of at least 5Hz (McHugh et al., 1996, Pastalkova et al., 2008). Only cells which met this criterion were included in all subsequent analysis. The place field was defined as a contiguous region surrounding a firing rate peak with a minimum firing rate at least one third of the peak firing

rate. Firing rate peaks greater than 25% of the main peak were regarded as additional place fields and place fields in each direction were counted separately.

Spatial information was calculated according to the following formula:

$$Spatial\ Information = \sum_{i=1}^{N} p_i \lambda_i log_2 \frac{\lambda_i}{\lambda}$$

where I = 1,…,N represents each bin, p_i denotes the probability of the animal being in that bin, λ_i denotes the mean firing rate in that bin and λ is the overall mean firing rate(Skaggs et al., 1993).

Bidirectionality index was calculated according to the formula:

$$BD_{index} = \frac{|F1 - F2|}{F1 + F2}$$

Where F1 denotes the firing rate in the left → right direction and F2 denotes the firing rate in right → left direction. A value of 0 indicates no difference in firing rate between each direction while 1 indicates unidirectional firing.

3.2.2.3. Place Cell Analysis: Open Field

All analysis of place cells in the open-field was performed on periods when the animal's running speed was above 5cm/s. An occupancy map was produced by dividing the open field into 50x50 bins and measuring the occupancy in each. A rate map for each cell was produced by taking the spike count in each bin and dividing by the occupancy map.

Analysis of place-fields in the open-field was carried out in the same way as place-field analysis in the linear track sessions.

3.2.2.4. Position Decoding

Position decoding was carried out using the Bayesocampus Matlab toolbox (https://github.com/lukearend/bayesocampus) which implements a Bayesian decoder to estimate an animal's position from raw spike trains. Full details of this method have been described previously (Zhang et al., 1998) but in brief, Bayesian decoding computes a posterior probability of the animal being in each position at individual time-points on the basis of spike counts from all cells. This method assumes spike trains follow a Poisson distribution, with each cell's firing assumed to be independent of one another.

For the purposes of decoding position data across the linear track session, the decoder was trained on data from one half of the recording and implemented on the other half. The

analysis was then re-run with the halves of data used for training and implementation reversed. The results from both were then collated.

Posterior probability distributions of animal position were computed across 271 positional bins using a time-window of 40ms and occupancy maps were smoothed with a 10-pixel gaussian smoothing window. Spikes from all individual cells (including non-place cells) from every animal during periods of running were used to decode position (see **Table 2** for numbers used).

Confusion matrices were calculated by generating a histogram of decoded position probabilities for each real position on the track. Decoding error was estimated by taking the decoded position value with the highest probability and comparing it to the animal's real position. A trajectory was built out of all peak probabilities across a run and the correlation coefficient was computed between the real and peak decoded probability.

3.2.2.5. Place Cell Remapping

Place cell remapping analysis was performed on a cell by cell basis by comparing properties prior to and following track rotation. Rate remapping was defined as:

$$Rate\ Remapping = \frac{|Rate_2 - Rate_1|}{Rate_2 - Rate_1}$$

Where $Rate_1$ denotes mean firing rate in position 1 (familiar position) and $Rate_2$ denotes mean firing rate in position 2 (novel orienation). A score of 0 indicates no change in rate between positions and a score of 1, an infinite firing rate change.

General remapping was defined by two measures: the spatial correlation between a cell's place field in position 1 and position 2 and the shift in place field centre, measured as the absolute difference between the place-field centre of mass in position 1 and position 2 (Leutgeb et al., 2005).

3.2.2.6. Power Spectral Analysis

All power analysis of local field potentials was carried out using Chronux toolbox (http://chronux.org/) (Mitra and Bokil, 2008). Spectral analysis of local field potential signals can lead to high variance and bias in power estimates due to the stochastic nature of these signals. Chronux mitigates these issues by making use of multitaper spectral analysis. This involves multiplying the signal by multiple orthogonal tapers and computing a power spectrum for each. By averaging across each spectra this method reduces the bias that would result from using a single taper or taking the Fourier transform of the signal. This method also makes use of a moving window to smooth the signal which results in lower variance in the power

spectra (Babadi and Brown, 2014). All power analysis used a time-bandwidth product of 3, 5 tapers, and a window length of 2.5 seconds.

To compute power spectra, LFPs were taken from track run periods and combined, and power spectra were computed on the combined signal. Bandpower for each frequency band was calculated as the mean power at 6-10Hz for theta, 25-55Hz for slow-gamma, and 60-140Hz for fast-gamma. These frequency bands were used for all subsequent LFP analysis.

When comparing between the familiar and novel track orientation, data from the previous day's familiar track session were used. To account for variation in the number of runs and therefore the length of the local field potential signal used in analysis, a matched number of runs were pseudo-randomly selected from the session with more track runs (typically the familiar track session).

3.2.2.7. Phase-Amplitude Coupling Analysis

PAC was computed with a PAC toolbox described by Onslow et al., (2011). This method detects whether the amplitude of a signal filtered at a higher frequency is modulated by the phase of a signal filtered at a lower frequency and as a result is capable of observing cross-frequency coupling between oscillations in the brain.

To compute PAC, the modulation index method was used. This takes the signal and filters it at a lower frequency, denoted Y_{fph}, and at a higher frequency, denoted Y_{famp}. The instantaneous phase of Y_{fph} is calculated using the phase angle of the Hilbert transform of this signal and denoted Φ_{fph}. Next the amplitude envelope of Y_{famp} is calculated by taking the absolute value of the Hilbert transform of this signal and is denoted A_{famp}. These transformed signals are depicted in **Figure 3.13A**. A composite signal is generated of these two signals by the formula:

$$Z_{fph,famp}(t) = A_{famp}(t).e^{i\Phi_{fph}(t)}$$

Where t indicates the amplitude and phase values at each timepoint in the signal. The modulation index value is calculated as the absolute value of the average of the composite signal. A non-zero value indicates co-occurrence of the phase and amplitude signals in time, indicative of cross-frequency coupling. As a non-zero modulation index value can result from non-uniformity of the signal, the modulation index value was compared against a set of surrogate values generated by introducing a lag between Φ_{fph} and A_{famp} (Canolty et al., 2006).

The above calculation was computed for 20 phase frequency values ranging from 1-20Hz and 20 amplitude frequency ranging from 1-200Hz to generate a cross-frequency coupling matrix. To generate the cross-frequency coupling matrix, local field potential signals

were taken from periods when the animal was running on the linear track and combined. The analysis was then performed on the combined local field potential signal.

3.2.2.8. Phase-Locking Analysis

To assess phase-locking of place cells to hippocampal oscillations, local field potentials were filtered at the frequency range of interest (theta, slow-gamma and fast-gamma) and only periods where the signal was 1 SD above the mean absolute amplitude of the signal were used. The instantaneous phase of the signal was calculated as described in ***3.2.2.7***.

Phase-locking was calculated as described by Kitanishi et al., (2015). Spikes which occurred during periods of high amplitude oscillatory activity were denoted a phase value. Phase-locking strength was determined by the resultant vector length r, denoted by the formula:

$$r = \sum_{j=1}^{N} \frac{e^{i\Phi_j}}{N}$$

Where j = 1,…,N represents each spike, Φ_j denotes the phase value of that spike and N is the total number of spikes. Resultant vector length varied between 0, indicating uniform distribution among all phase values, and 1, indicating identical phase values for all spikes. To account for large variations in the number of spikes per cell, a bootstrapping procedure was performed whereby the resultant length was computed for 30 spikes randomly selected without replacement from the total number of spikes and repeated until all spikes had been sampled. The final resultant vector value given for each cell was the mean of each subsampled resultant vector value.

To estimate chance levels of phase-locking, 200 sets of surrogate data were produced through random assignment of a phase value to every spike. The resultant vector was computed for all sets of data and chance-levels represent the mean of all surrogate resultant vectors.

3.2.2.9. Phase Precession Analysis

Theta phase precession was computed first by filtering the LFP at theta frequency and assigning a phase value to every spike as described in ***3.2.2.8***. Next, spikes occurring within the boundaries of a place field were isolated, as well as the animal's position, to obtain a position-phase vector for every traversal through a place field. Position was normalised to the peak of the place field to allow comparisons between place fields of different widths. Place

field traversals with fewer than 30 spikes or in which the cell fired for less than half of the traversal were discarded.

3.2.2.10. Oscillatory Activity vs. Running Speed Analysis

To assess the relationship between running speed and LFP oscillations, instantaneous velocity was calculated for every run on the linear track and smoothed with a gaussian kernel (SD=2) to minimize the effects of movement artifacts. Velocity for every run was calculated as mean instantaneous velocity. For each run, mean power at all frequency ranges (theta, slow-gamma, fast-gamma) and peak frequency values within that range were computed to obtain a velocity-power and velocity-peak frequency tuple to be used in linear regression analysis (see ***3.2.3.3***).

3.2.3. Statistical Analysis

To compare group means between genotypes a student's t-test was used unless stated otherwise. For non-parametric data, if the dataset was large enough, a non-parametric equivalent was used. When comparing individual animal means a student's t-test was used as the n was too small for a non-parametric test to have sufficient power to detect differences. When comparing group means between environments a two-way ANOVA was used.

3.2.3.1. Phase-Locking Significance

To calculate significance of phase-locking, each cell was tested for deviation from circular uniformity with the Rayleigh test. A cell was regarded as displaying significant phase-locking if it had a p-value < 0.05. The proportion of cells displaying significant phase-locking within each genotype were compared for significance with the chi-squared test.

3.2.3.2. Phase Precession

To quantify the relationship between animal position relative to the place field peak and theta phase, circular linear regression analysis was performed on each cell's position–phase scatter plot. This analysis generated slope estimates as well as r-squared values which were compared between genotypes. Circular regression analysis also produced a p-value quantifying the significance of the relationship between position and theta-phase, and the proportion of cells exhibiting significant phase-precession were defined as cells with a p-value < 0.05. The proportion of cells displaying significant phase precession were compared with the chi-squared test.

3.2.3.3. Linear Regression Analysis

To assess the relationship between running speed and band-power or frequency, the velocity–power or velocity–frequency value pairs for every run from each animal were subject to a linear regression analysis. Running speed and genotype were entered as predictor variables with two dummy indicator variables used for each genotype. The results of this regression were subject to an ANOVA to test the significance of the relationship between running speed, genotype, and running speed x genotype, with the dependent variable (bandpower or frequency). To assess the running speed-power/frequency relationship within each genotype a separate linear regression analysis was run for each to generate slope, intercept, and r-squared values. When assessing the impact of novelty, track orientation was also entered as a predictor variable with a dummy indicator variable used for each track orientation. Error bars for the beta coefficients reflect the coefficient standard errors (SE) computed as the root-mean squared error of the coefficient variances.

3.3. Results

3.3.1. Single-Cell Firing Properties

Before relating the activity of individual neurons to behaviour, I first characterised the properties of cells across all behavioural sessions. *Cacna1c* heterozygosity is associated with an increased attenuation of backpropagating action potentials (Tigaret et al., 2020) and this attenuation has been shown to relate to the shape of subsequent cell spikes (Tsubokawa et al., 2000, Golding et al., 2001). The amplitude of both pyramidal cell and interneuron extracellular action potentials (measured as the peak to trough height) was comparable between WTs and *Cacna1c*$^{+/-}$ rats (**Figure 3.2A**; Pyramidal cells, p=0.804; Interneurons, p=0.286; Wilcoxon rank-sum test). However, *Cacna1c*$^{+/-}$ rats showed an increased spike-width (measured as peak-trough distance) for both cell-types (Pyramidal cells, p=5.67x10-4; Wilcoxon rank-sum test). This may relate to the role of LTCCs in afterhyperpolarization following an action potential (Cloues and Sather, 2003).

An increased spike-width may reduce the rate at which action potentials can fire by lengthening the repolarization time. To assess this, I first characterised the mean firing rates of all pyramidal cells. Both genotypes showed a comparable lognormal distribution of firing rates among cells (**Figure 3.2B**; p =0.991; Two-sample Kolmorgorov-Smirnov test). I next looked at whether increased spike-width might result in a longer duration between spikes by assessing the interspike-interval (ISI) (**Figure 3.2C**). Both genotypes displayed a narrow peak between ~2 and 10ms and a wider peak between ~50 and 300ms, indicating ISIs between

spikes within bursts and outside of bursts respectively. *Cacna1c*$^{+/-}$ rats however appeared to display a slight reduction in ISIs with a short peak yet a comparatively larger proportion of spikes with ISIs falling between a short and wide peak. Analysis of the distributions revealed these were significantly different between genotypes (p=1.23x10-4; Two-sample Kolmorgorov-Smirnov test).

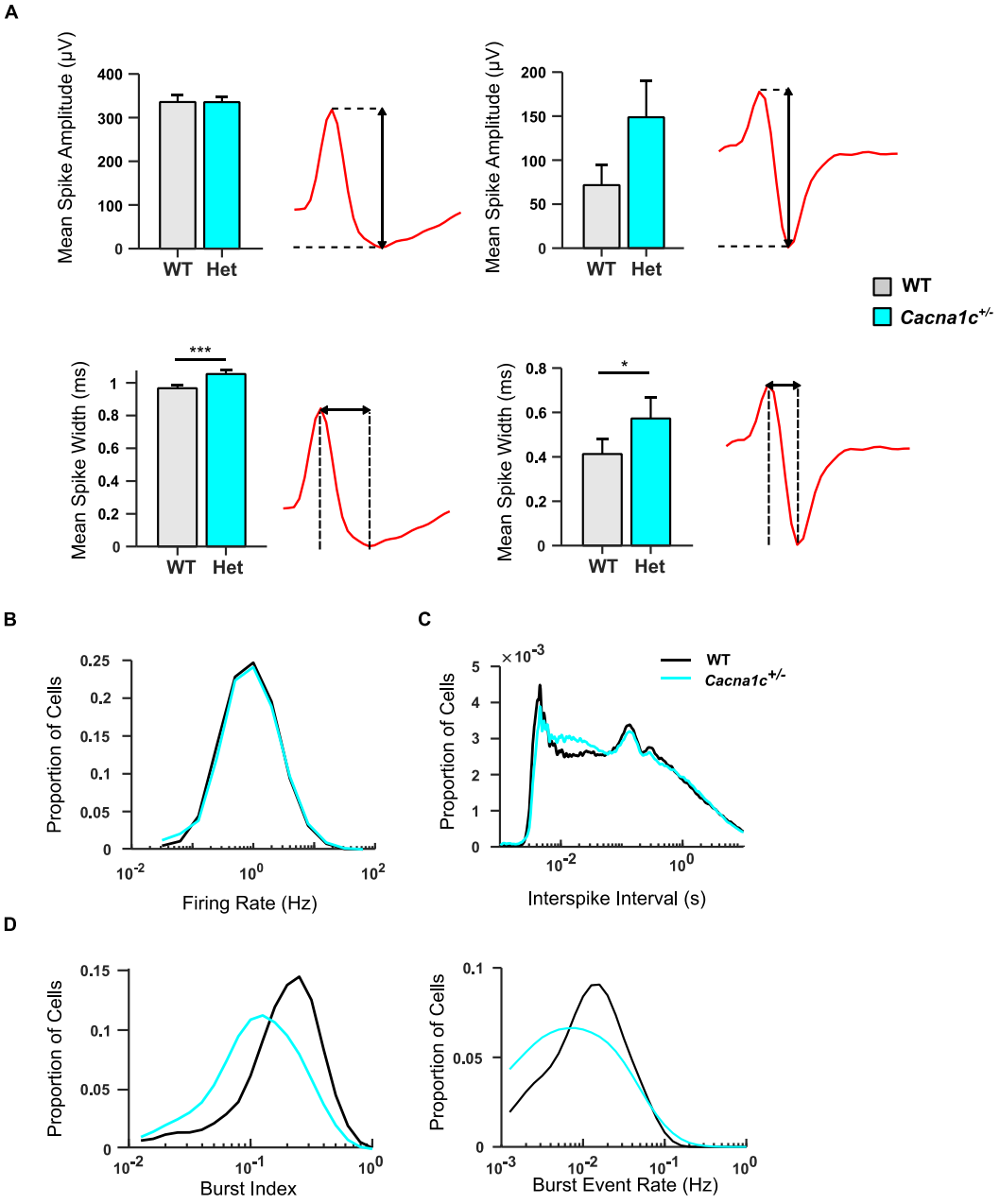

***Figure 3.2* | Spike and firing rate properties of CA1 pyramidal cells and interneurons**
(A) Mean spike waveform properties of pyramidal cells (left) and interneurons (right) taken from all cells recorded over full familiar track recording session. (Top) Spike amplitude did not significantly differ between genotypes for pyramidal cells (p>0.05; Wilcoxon rank-sum test) or Interneurons (p>0.05; Wilcoxon rank-sum test). (Bottom) *Cacna1c*$^{+/-}$ rats showed a signicant increase in pyramidal cell spike width (*p<0.05; Wilcoxon rank-sum test) and Interneuron spike width (*p<0.05; Wilcoxon rank-sum test) compared to WTs. Representative spike waveforms taken from one WT animal shown in red to the right

of each bar plot (Dashed lines indicate peak and trough of waveform and double-headed arrow indicates measurements used in bar plots). *(Data presented as mean±SEM)*
(B) Distribution of pyramidal cell firing rates across full recording session for both genotypes shown on a lognormal scale.
(C) Distribution of pyramidal cell inter-spike intervals across full recording session for both genotypes shown on a lognormal scale.
(D) Bursting characteristics of individual pyramidal cells across full recording session. (Left) Lognormal burst index distributions for individual pyramidal cells across full recording session (Burst index defined as the proportion of spikes occurring <8ms apart). (Right) Lognormal distribution of burst event rates for individual pyramidal cells across full recording session (Burst event defined as ≥3 consecutive spikes occurring <8ms apart).
(Wildtypes (WT): n=126 Pyramidal cells, n=34 Interneurons; Cacna1c$^{+/-}$ rats (Het): n=144 Pyramidal cells, n=25 Interneurons. WT in black, Cacna1c$^{+/-}$ in cyan)

To better understand the implications of this result I assessed the bursting properties of cells in each genotype. First, I looked at the burst index of all cells, defined as the proportion of spikes in bursts (3 or more spikes less than 8ms apart) vs. all spikes (**Figure 3.2D**, *left*). Burst indices were comparable between genotypes (p=0.771; Two-Sample Kolmorgorov Smirnov Test). Next, I assessed the burst event rate (**Figure 3.2D**, *right*), defined as the rate at which bursts (as defined for burst index) occurred for each cell. Again, this was comparable between genotypes (p=0.537; Kolmorgorov-Smirnov test).

These results indicate that reduced calcium channel expression may alter spike shape, generating an increase in spike-width. This however does not impair the frequency at which spikes fire and bursting remains largely normal.

3.3.2. Behaviour on the Linear Track

Before comparing hippocampal properties on the linear track I first assessed behavioural differences to test whether neurophysiological changes may be downstream of behavioural differences between genotypes. First, I scored the time taken both in number of sessions and minutes on the track to reach the minimum criterion of runs (10 in each direction); neither measure was different between genotypes (**Figure 3.3A**; Minutes to criterion, p=0.718; Sessions to criterion, p=0.716; Student's t-test). The learning curves, as assessed by the mean number of runs per recording day are also shown (**Figure 3.3B**).

To compare the animal's behaviour on the track during the recording day (familiar track session) I assessed the proportion of time spent in motion vs. stationary and for both genotypes this was approximately one third of the recording session (**Figure 3.3C**, *right*; p=0.511; Student's t-test). Additionally, the time spent on the central linear portion of the track (defined as 75% of the track length measured from the centre) vs time spent on the track edges (the remaining 25% of the track) was not significantly different between genotypes (**Figure 3.3C**, *left*; p=0.425, Student's t-test). Based on these results, behaviour in *Cacna1c*$^{+/-}$ rats was not overtly impaired on the linear track.

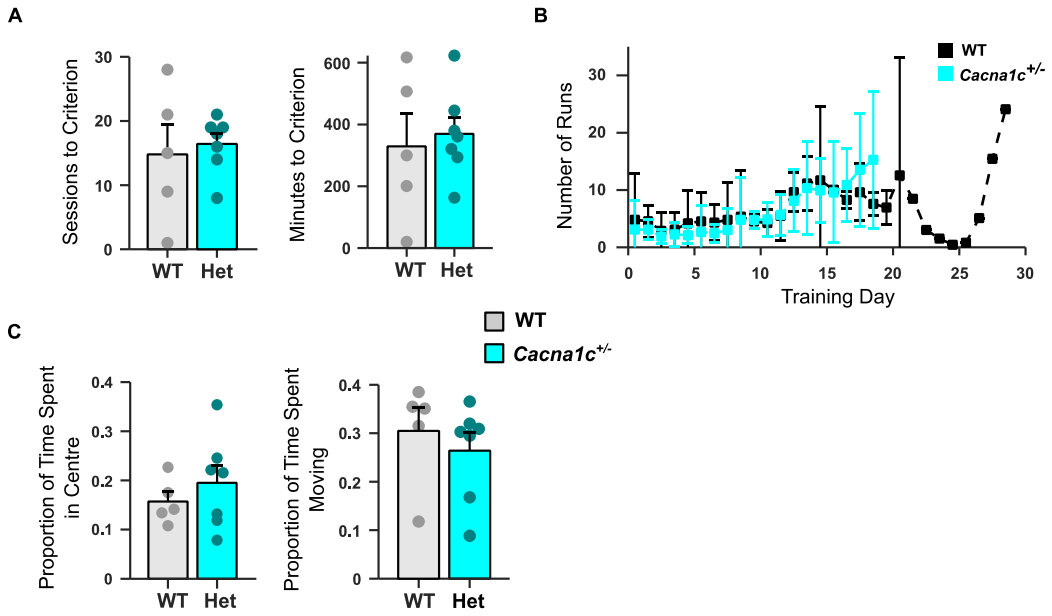

***Figure 3.3* | Behaviour on the linear track**
(A) Time on the track taken to reach a minimum criterion of 10 runs in both directions in (left) minutes ($p = 0.7551$; student's t-test) and (right) sessions ($p>0.05$; student's t-test).
(B) Learning curves for each genotype depicting mean number of runs per day until reaching criterion.
(C) (Left) Proportion of time during familiar track recording spent on the central portion of linear track (75% of total track area from the centre of the track) vs. time spent on the track edges (25% of track area from outer edges) ($p>0.05$; student's t-test). (Right) Proportion of time on track during familiar track recording spent moving vs. proportion of time spent stationary ($p>0.05$; student's t-test).
(*Data presented as mean ± SEM; WT: n=5; Cacna1c$^{+/-}$: n=7. WT in black, Cacna1c$^{+/-}$ in cyan)*

3.3.3. Place Cell Properties on the Familiar Linear Track

To assess place-cell properties I characterised the firing rates of cells recorded as animals ran down the central portion of the linear track and from this data was able to plot mean positional firing rate curves for each cell (**Figure 3.4A**).

Firing field analysis revealed slightly larger place-fields in *Cacna1c*$^{+/-}$ rats compared to WTs, as was hypothesized on the basis of place-field alterations observed in animals with deficient Schaffer-collateral plasticity (McHugh et al., 1996, Mesbah-Oskui et al., 2015). **(Figure 3.4B**; $p=0.038$, Student's t-test). As the spatial information metric described by Skaggs et al., (1993) is dependent upon the firing rate curves of place-cells I sought to assess whether larger place-fields results in a reduction in spatial information (**Figure 3.4D**) and this did appear to be the case ($p=0.043$; Student's t-test).

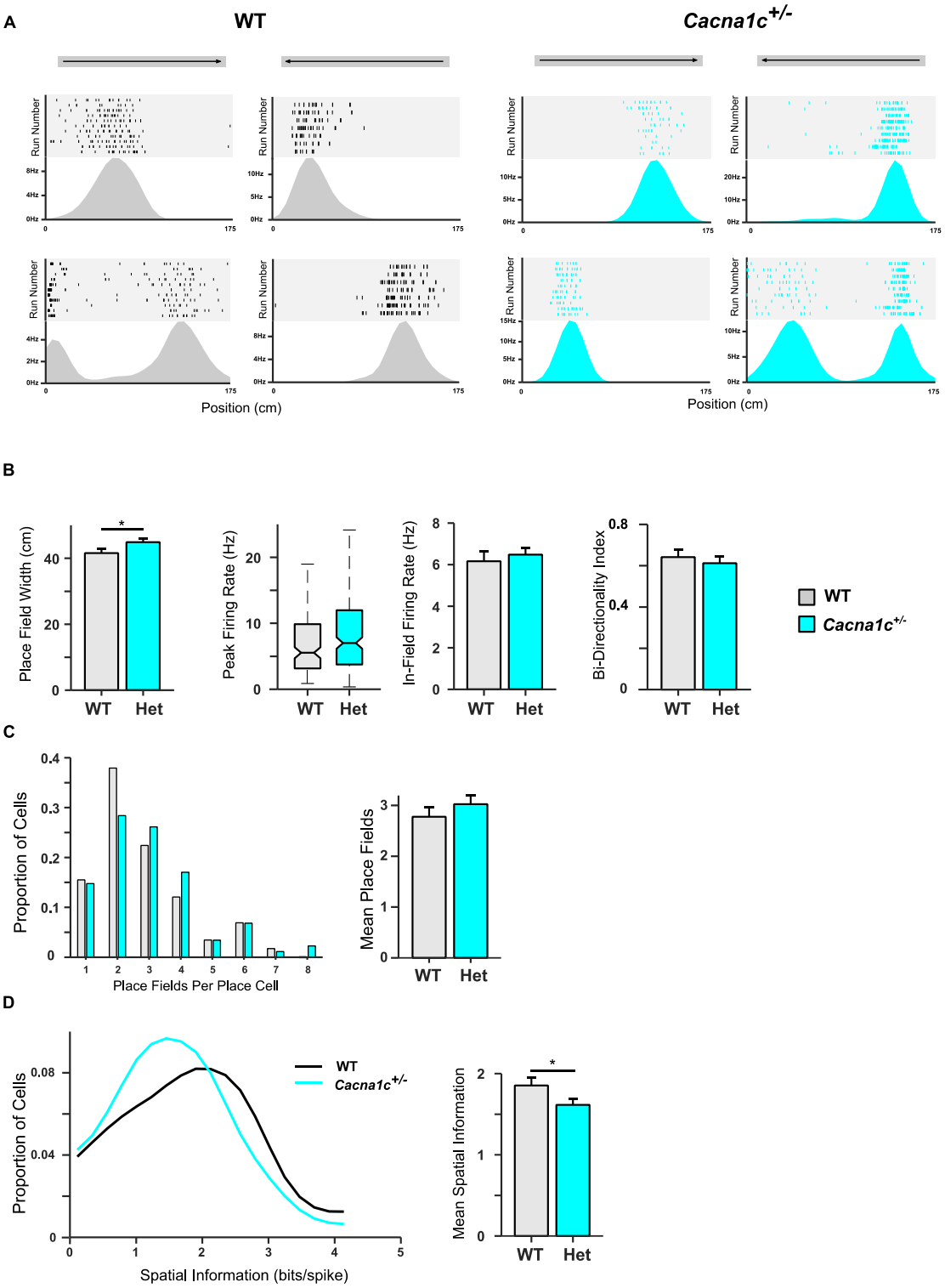

***Figure 3.4* | Place-field properties on the familiar track in WTs and *Cacna1c*$^{+/-}$ rats**
(A) Example place fields of individual cells taken from one WT and one *Cacna1c*$^{+/-}$ rat, from runs in the left→right direction (left) and right→left direction (right). Each plot shows a spike raster for each run in that direction (top) and the mean firing rate curve (bottom). (Note the presence of cells with multiple place fields in each animal).
(B) Comparisons of place field key properties (from left to right): Place field width, peak firing rate, mean in-field firing rate and bi-directionality index. Place field width was higher in *Cacna1c*$^{+/-}$ rats than WTs (*p<0.05; Student's t-test) while all other properties were similar between genotypes (p>0.05; Data

presented as mean±SEM except for peak firing rate which is presented as the median and the upper and lower quartiles due to the high deviation from normal distribution).
(C) Number of place fields per place cell. (Left) Place field number distribution (Right) The mean number of place fields per place cell (p>0.05; Data presented as mean±SEM).
(D) Spatial information contained within spiking activity of individual cells. (Left) Spatial information distribution. (Right) Mean spatial information was significantly lower in *Cacna1c*$^{+/-}$ rats than WTs (*p<0.05; Student's t-test. Data presented as mean±SEM)
(WT: n=77 cells; Cacna1c$^{+/-}$*: n=95 cells. WT in black; Cacna1c*$^{+/-}$ *in cyan)*

Despite the increase in place-field size in *Cacna1c*$^{+/-}$ rats, place field firing rate remained normal. This included two firing rate measures: 1) Mean firing rate within the boundaries of a place-field (**Figure 3.4B**; p=0.116; Student's t-test) and 2) Peak firing rate (p=0.096; Student's t-test).

Previous work in the DISC1 model of SCZ has revealed, in addition to an increased place-field width, a reduced number of place-fields per place cell (Mesbah-Oskui et al., 2015). This analysis however showed that in *Cacna1c*$^{+/-}$ rats, the number of place-fields are normal (**Figure 3.4C**; p=0.258; Student's t-test). Finally, to assess whether place-cells displayed any bias in their directionality I compared the bidirectionality index (**Figure 3.4B**) between genotypes. Both genotypes displayed a tendency towards bidirectionality (>0.5 index) but did not significantly differ (p=0.478; Student's t-test).

Given the loss of spatial information and the increase in place-field size of individual place cells in *Cacna1c*$^{+/-}$ rats, how might population encoding of spatial information be affected? To quantify this, I applied a Bayesian decoding algorithm to population spike data from individual runs on the linear track to see how well run trajectories could be reconstructed. For both genotypes, the distribution of predicted position probabilities tended to align closely with the animal's real position (**Figure 3.5A,B**). To quantify genotype differences, I took the root-mean-square error between the peak decoded position value and the animal's real position at each timepoint (**Figure 3.5C,** *middle*). Here *Cacna1c*$^{+/-}$ rats showed a small but significant increase in decoding error ($p=3.39x10^{-4}$; Wilcoxon rank-sum test) in line with the reduction in spatial information content of individual place cell spike trains. As an additional metric of decoding error, I assessed the correlation between peak decoded trajectories and real trajectories (**Figure 3.5C,** *right)* though correlation coefficients were not significantly different between genotypes (p=0.087; Student's t-test).

In summary, assessment of place-cell properties on the familiar linear track revealed as predicted, an increase in place-field size in *Cacna1c*$^{+/-}$ rats with all other properties remaining intact. This corresponded to a reduction in spatial information which as a result led to increased error in decoding run trajectories.

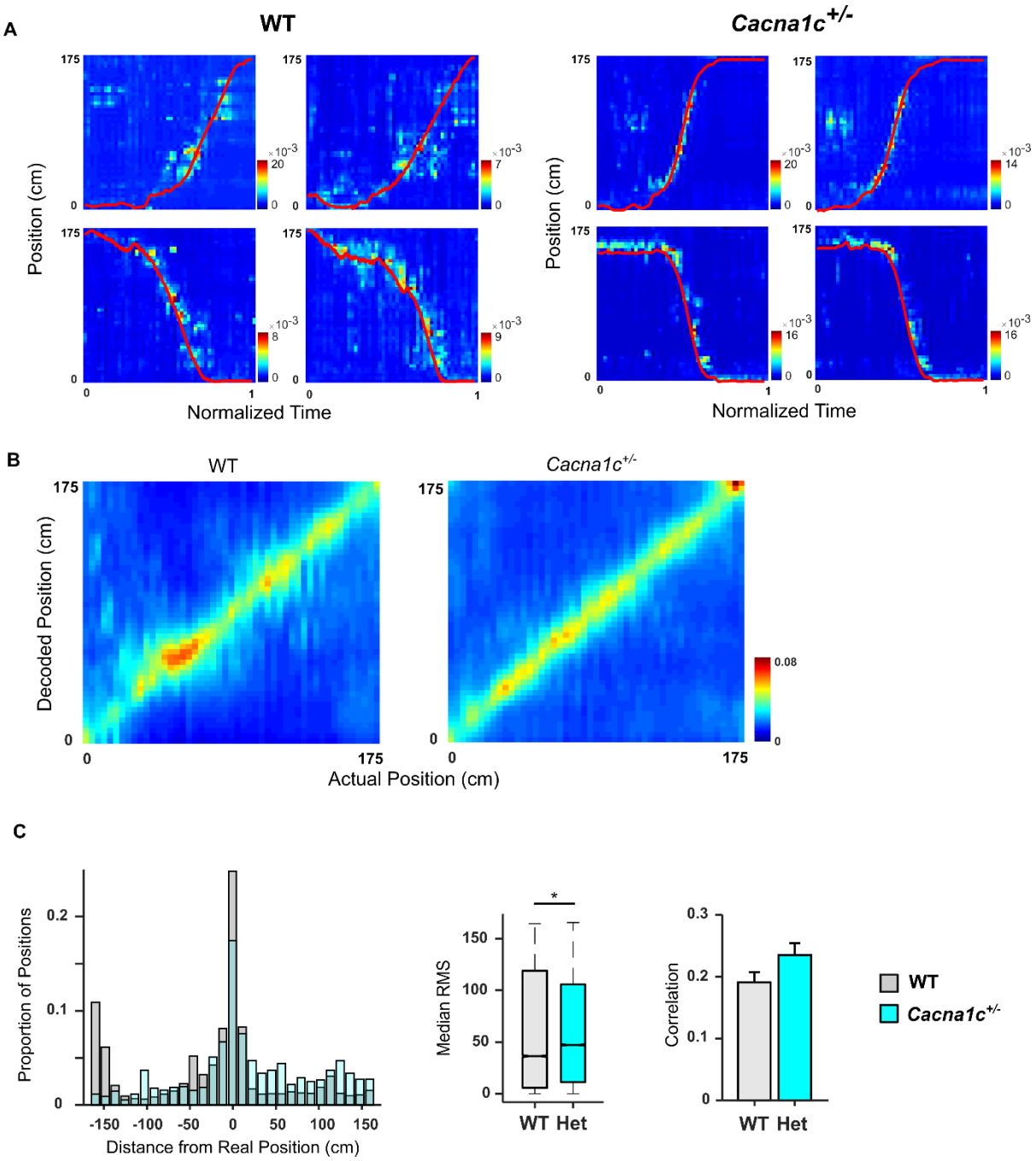

***Figure 3.5* | Decoding spatial trajectories with a Bayesian decoding algorithm**

(A) Example run trajectories from individual animals. Each panel depicts a single run trajectory with time on the x-axis and x-position on the y-axis. The decoded posterior probability distribution at each timepoint is depicted by colour (Normalized, arbitrary units) and the red line depicts the real position. (WTs shown on the left; *Cacna1c*$^{+/-}$ rats shown on the right. Left→Right runs shown top; Right→Left runs shown bottom).

(B) Confusion matrices for all animals across all runs. Each matrix shows the distribution of decoded posterior probabilities at each real x-position. Colour indicates probability values. (WTs shown on the left; *Cacna1c*$^{+/-}$ rats shown on the right).

(C) Decoding error between decoded position values and real position values. (Left) Distribution of distances between real x-position values and peak decoded position values at each timepoint. (Centre) Root-mean-square error between peak decoded position values and real position values at each timepoint (Data presented as median with upper and lower quartiles shown. *p<0.05 Wilcoxon Rank-Sum Test). (Right) Correlation between real run trajectories and trajectories of peak decoded position values (Data presented as mean±SEM. p>0.05; Student's t-test).

(WT: n=137 runs; Cacna1c$^{+/-}$: n=140 runs. WT in black; Cacan1c$^{+/-}$ in cyan).

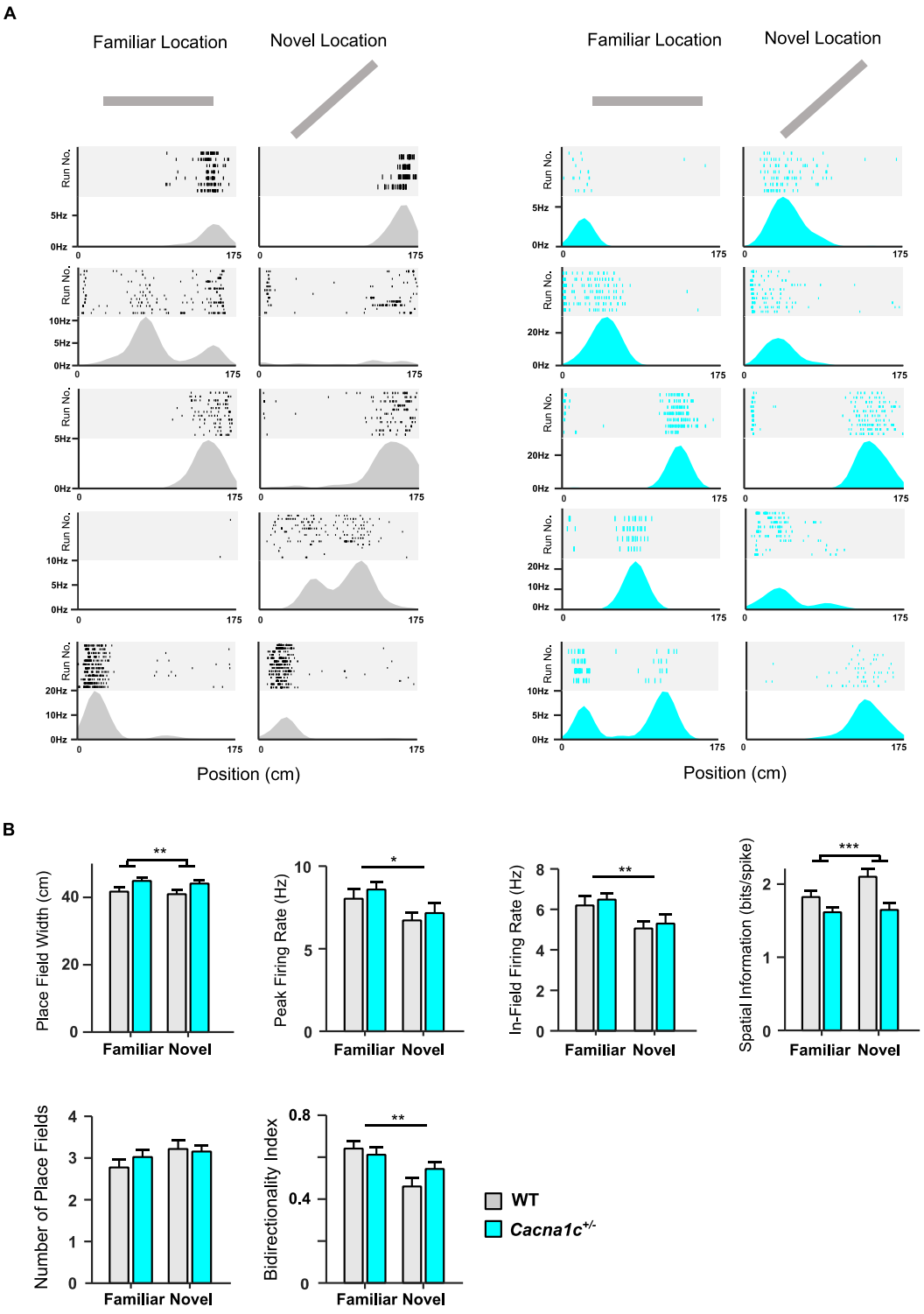

***Figure 3.6* | Comparison of place field properties between a familiar and novel track orientation**
(A) Firing maps of individual cells in a familiar and novel environment. Each row depicts an individual cell with a spike raster for every run shown (top) and a mean firing rate curve shown (bottom). Each column depicts runs in the familiar and novel track orientation respectively. (WTs shown on the left, *Cacna1c*$^{+/-}$ rats shown on the right).

(B) Comparison of Place-field properties in the familiar and novel environment. From left to right: Place-field width, peak firing rate, mean in-field firing rate, spatial information, number of place fields and bidirectionality index. A significant main effect of genotype was seen for place-field width and spatial information (**p<0.01,***p<0.001 respectively, ANOVA) and a significant main effect of environment was seen for peak firing rate, mean firing rate and bidirectionality index (*p<0.05,**p<0.01 ANOVA). (Data presented as mean±SEM).
(WT: n=77 cells familiar track, n=57 cells novel track; Cacna1c$^{+/-}$: n=95 cells familiar track, n=82 cells novel track. WT in black, Cacna1c$^{+/-}$ in cyan)

3.3.4. Place-Cell Properties in a Novel Track Location

The alterations in place-field properties described in ***3.3.3*** are indicative of an impairment in the refinement of fields place-cells undergo with increasing familiarity of an environment, as a result of plasticity. I therefore set out next to determine what place-fields looked like in a previously unexplored, novel space in *Cacna1c*$^{+/-}$ rats. Here, I recorded from animals as they ran on the same linear track however part-way through the recording period the track was rotated 45°.

I first assessed place-cell activity by characterising the properties of place-fields shown in **Figure 3.6A** and made comparisons with place-fields from the familiar track session to assess the effect of novelty. Analysis here, in line with the results from ***3.3.3*** revealed a significant effect of genotype on place-field width (**Figure 3.6B**, $F_{1,741}$=7.06, p=0.0081, Two-Way ANOVA) though unexpectedly, no effect of environment ($F_{1,741}$=0.3, p=0.584) or a genotype x environment interaction ($F_{1,741}$=0.01, p=0.9433). The increased place-field width corresponded, as in ***3.3.3,*** to a reduction in spatial information (**Figure 3.6B**, Genotype effect: $F_{1,460}$=13.74, p=0.0002, Two-Way ANOVA) though again, there was no effect of environment ($F_{1,460}$=2.44, p=0.119) or a genotype x environment interaction ($F_{1,460}$=1.48, p=0.225).

As in the familiar location, a reduction in spatial information resulted in a modest increase in decoding error when reconstructing trajectories in the novel location from spike data. (**Figure 3.7C**, *centre*; p=7.24x10^{-231}, Wilcoxon rank-sum test). Again however, the correlation between peak decoded trajectories and real trajectory did not differ between genotypes (**Figure 3.7C**, *right*; p=0.693, Student's t-test)

Interestingly, firing rate measures did display an environment effect. (**Figure 3.6B**, Peak firing rate: $F_{1,741}$=6.77, p=0.0095; Mean in-field firing rate: $F_{1,741}$=8.48, p=0.0037) though no effect of genotype (Peak firing rate: $F_{1,741}$=0.96, p=0.329; Mean in-field firing rate: $F_{1,741}$=0.53, p=0.468). Additionally, both genotypes showed a reduction in bidirectionality with novelty (**Figure 3.6B,** $F_{1,284}$=11, p=0.001) with no effect of genotype ($F_{1,284}$= 0.38, p=0.538).

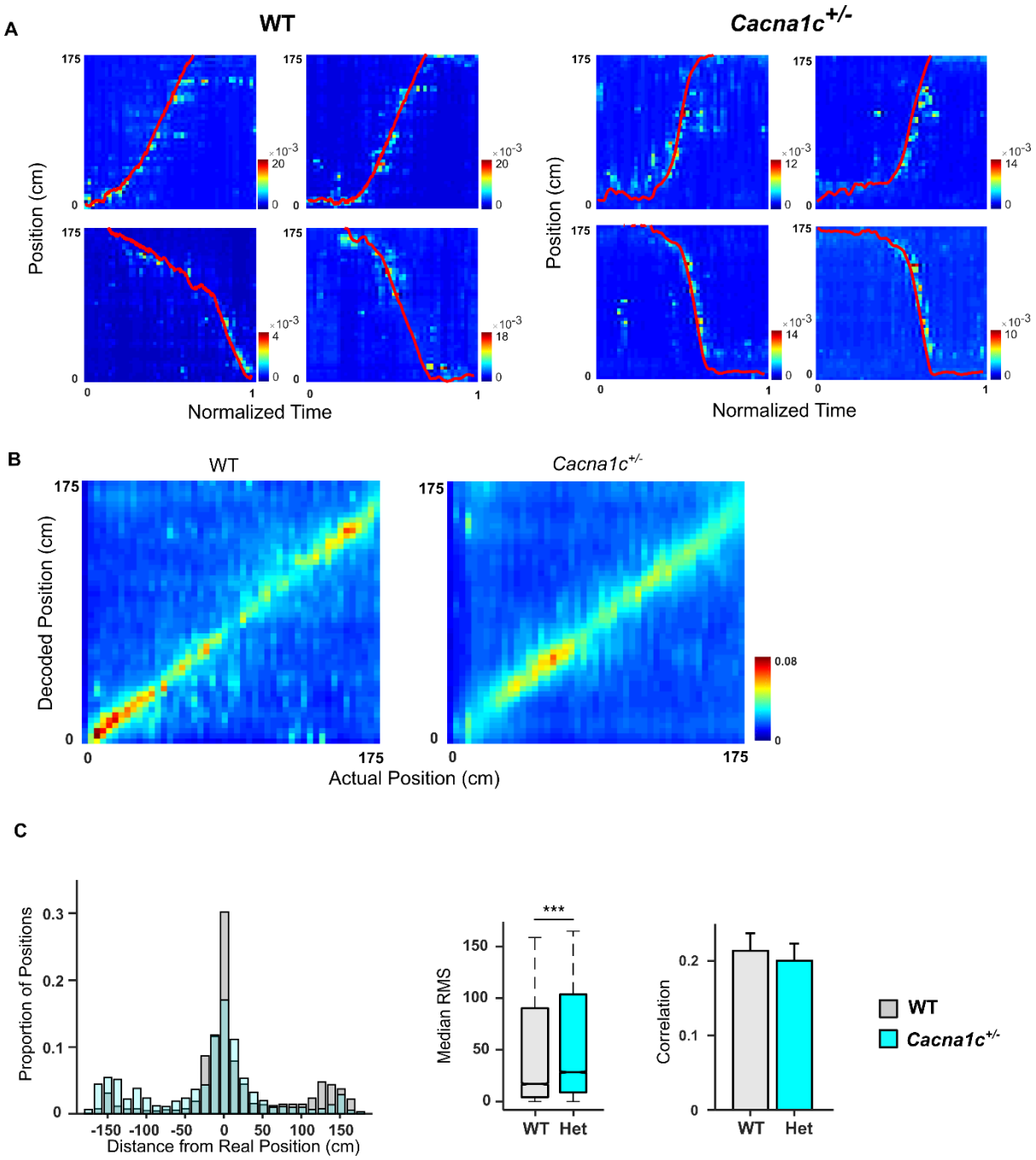

***Figure 3.7* | Decoding spatial trajectories in a novel track orientation**

(A) Example run trajectories from individual animals in the novel track orientation. Each panel depicts a single run trajectory with time on the x-axis and x-position on the y-axis. The decoded posterior probability distribution at each timepoint is depicted by colour and the red line depicts the real position. (WTs shown on the left; *Cacna1c*$^{+/-}$ rats shown on the right. Left→Right runs shown top; Right→Left runs shown bottom).

(B) Confusion matrices for all animals across all runs. Each matrix shows the distribution of decoded posterior probabilities at each real x-position. Colour indicates probability values. (WTs shown on the left; *Cacna1c*$^{+/-}$ rats shown on the right).

(C) Decoding error between decoded position values and real position values. (Left) Distribution of distances between real x-position values and peak decoded position values at each timepoint. (Centre) Root-mean square error between peak decoded position values and real position values at each timepoint (Data presented as median with upper and lower quartiles shown. ***p<0.001 Wilcoxon Rank-Sum Test). (Right) Correlation between real run trajectories and trajectories of peak decoded position values (Data presented as mean±SEM. p>0.05; Student's t-test).

(WT: n=72 runs; Cacna1c$^{+/-}$: n=89 runs. WT in black; Cacna1c$^{+/-}$ in cyan).

The changes to firing rate in the novel position are reminiscent of rate-remapping, a phenomenon whereby alterations to an environment lead to changes in the firing rates of place-cells while the location-dependent firing remains intact (Bostock et al., 1991). This might imply that the rotated track was being represented as an altered environment as opposed to a novel one. To assess the degree of novelty imparted by track rotation I next looked at how individual cells changed their firing properties before and after position-change and whether this differed between genotypes.

First, to quantify rate remapping I assigned a rate remapping index to every cell – an index of how much the firing rate changes between track locations. Both genotypes showed rate remapping indices ranging from 0 to 1 (**Figure 3.8A**) implying a high degree of variability among cells in encoding environment change. The mean degree of rate remapping was close to 0.5 in both genotype and did not significantly differ (p=0.239, Student's t-test).

Next, I assessed how spatial properties varied between positions as a metric of global remapping – a phenomenon observed among place-cells when in a completely novel environment, whereby place-field positions and sizes shift entirely (Leutgeb et al., 2005). First, I looked at the spatial correlation between place-fields in each location (**Figure 3.8B**). Again, both genotypes displayed a high degree of variability in place-field correlations indicating a mixed response among place-cells to the change in track position. These responses however were comparable between genotypes (p=0.395, Student's t-test). I also looked at the shift in the centre of mass of the place-field as an additional metric of global remapping (**Figure 3.8C**). This was also comparable between genotypes (p=0.207, Student's t-test).

These results show that the responses of individual place cells to position-change varied dramatically. However, combining the responses of all cells implies that neither genotype regarded the change in track position as entirely novel or familiar and instead it was encoded as an altered rather than new environment.

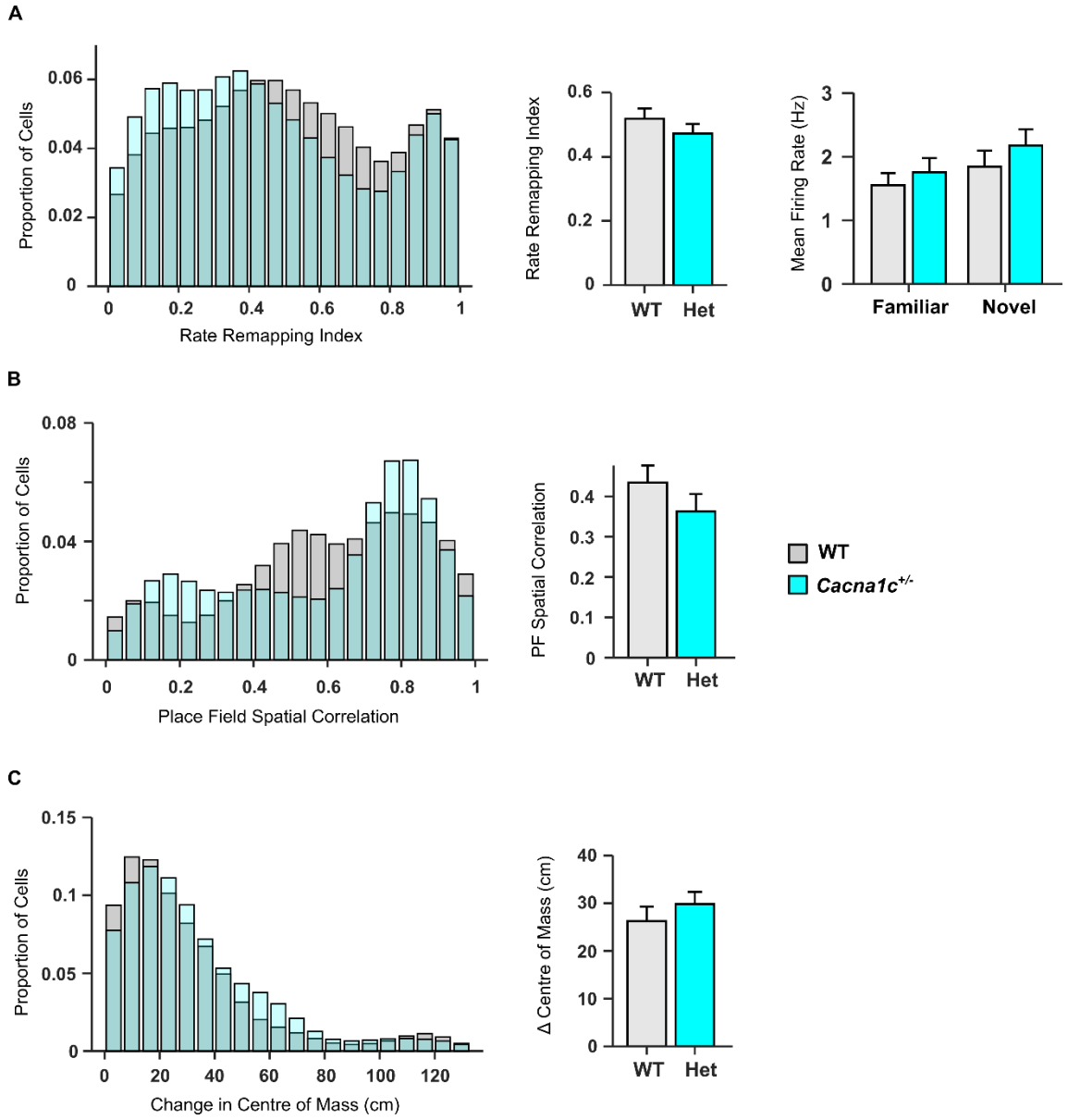

***Figure 3.8* | Place cell remapping between familiar and novel track orientation**

(A) Changes in the mean firing rate between environment. (Left) Rate remapping index distribution. (Centre) Mean rate remapping index was not significantly different between genotypes ($p>0.05$, student's t-test). (Right) Mean firing rate did not significantly differ between genotypes in either environment ($p>0.05$, ANOVA).

(B) Spatial correlation between place fields of individual cells in each environment. (Left) Spatial correlation distribution. (Right) Mean spatial correlation was not significantly different between genotypes ($p>0.05$, student's t-test).

(C) Shifts in the place-field centre (centre of mass) between environments. (Left) Distribution of shifts in the place-field centre of mass. (Right) Mean change in place-field centre of mass did not significantly differ between genotypes ($p>0.05$ student's t-test).

(Data presented as mean±SEM; WT: n=57 cells; Cacna1c$^{+/-}$: n=82 cells. WT in black, Cacna1c$^{+/-}$ in cyan).

3.3.5. Place-Cell Properties in a Novel Open-Field

In light of the remapping analysis, it seemed fit to also assess place-fields in a completely novel environment. For this, recordings were taken from animals as they explored a novel open field. Importantly no animals had received any prior exposure to such an environment.

Before assessing place-cells, as per the track session, I also characterised behaviour. Previous work in animal models of SCZ has revealed hyperlocomotion in an open-field (van den Buuse, 2010) thus I first assessed novel environment locomotory activity. Both genotypes showed a reduction in locomotion as the recording progressed (**Figure 3.9A**) however mean locomotion did not differ between genotypes (p=0.771, Student's t-test). In addition I characterised time spent in the central portion of the open-field compared to time in the periphery – a measure of anxiety behaviour in rodents (Seibenhener and Wooten, 2015). This was also similar between genotypes (**Figure 3.9B**, p=0.432, Student's t-test).

In summary this analysis revealed that open-field behaviour was normal in *Cacna1c*$^{+/-}$ rats.

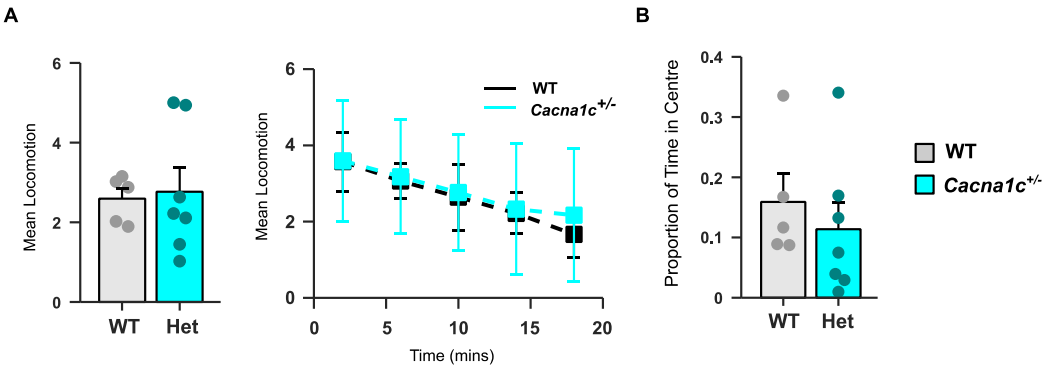

***Figure 3.9* | Behaviour in the novel open field**
(A) Mean Locomotion in the novel open field for the whole session (left) and in 5-minute bins (right). Locomotion did not differ between genotypes (p>0.05, Student's t-test).
(B) Proportion of time spent in the centre of the open field vs. periphery was comparable between genotypes (p>0.05, Student's t-test). Centre defined as the inner 50% of the field.
(Data presented as mean±SEM; WT: n=5; Cacna1c$^{+/-}$: n=7. WT in black, Cacna1c$^{+/-}$ in cyan)

To assess place-cells in the novel environment, spiking activity from periods in which the animal ran over 5cm/s was analysed. In contrast to the linear track, novel place-field sizes were not significantly different between genotypes (**Figure 3.10B**, p=0.722, Student's t-test). As a result, spatial information was also comparable (**Figure 3.10B**, p=0.206, Student's t-test). Likewise, mean and peak firing rates within place-fields also did not vary between genotypes (**Figure 3.10B**, p=0.161, p=0.371 respectively; Student's t-test).

These results demonstrate that in previously unexplored space, *Cacna1c*$^{+/-}$ rats exhibit similar place-cell properties to WTs. This would support the hypothesis that deficits in plasticity impair the refinement of place-fields that occur as an environment becomes familiar, hence

place field differences in *Cacna1c*$^{+/-}$ rats only manifest after repeated exposure to an environment.

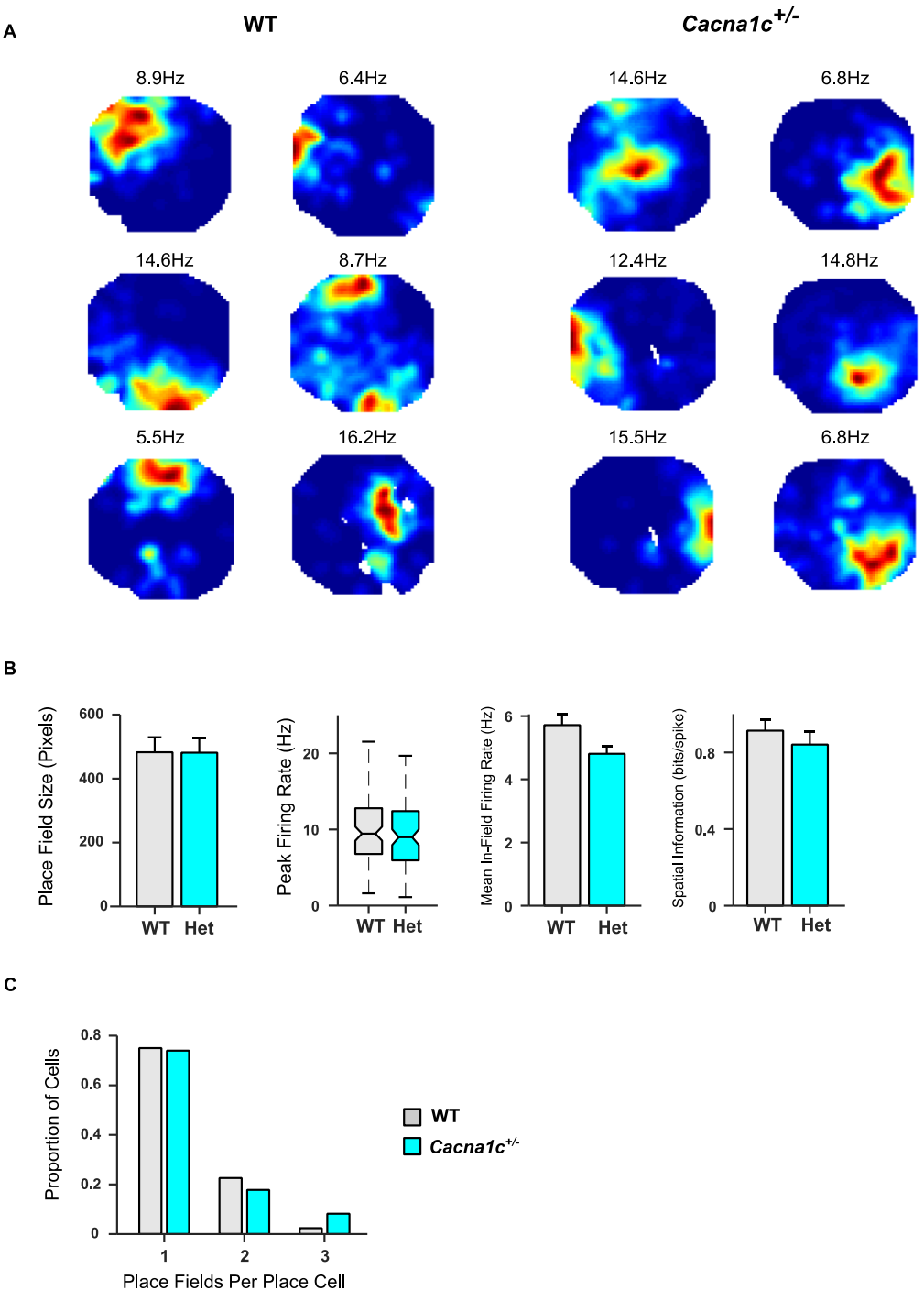

***Figure 3.10* | Place field properties in a novel open field are similar between genotypes**
(A) Example rate maps of individual cells in WTs (left) and *Cacna1c*$^{+/-}$ rats (right) taken during exploration of a novel open field. Colour depicts firing rate. Peak firing rate is shown above each plot. **(B)** Comparisons of place field key properties (from left to right): Place field width, peak firing rate, mean in-field firing rate and spatial information. Place field properties were comparable between genotypes ($p>0.05$, Student's t-test; Data presented as mean±SEM except for peak firing rate which is presented as the median and the upper and lower quartiles due to the high deviation from normal distribution).

(C) Number of place fields per place cell. Most cells exhibited only one place field in the novel open field in both genotypes.
(WT: n=84 cells; Cacna1c$^{+/-}$: n=66 cells. WT in black, Cacna1c$^{+/-}$ in cyan).

3.3.6. Hippocampal Rhythms on The Linear Track

I next catalogued hippocampal rhythmic activity while animals ran on the linear track.

First, I characterised power spectral densities on the familiar linear track. Both genotypes displayed clear theta activity in their LFP (**Figure 3.11A**) as revealed by prominent peaks in their power spectra around the theta band (6-10Hz) (**Figure 3.11B**). This rhythmic activity did not differ in either genotype (**Figure 3.11C**, *left,* p=0.692, Student's test). Likewise, both bands of gamma were comparable between genotypes (**Figure 3.11C**, Slow-Gamma (25-55Hz), p=0.522, Fast-Gamma (60-140Hz), p=0.594; Student's t-test).

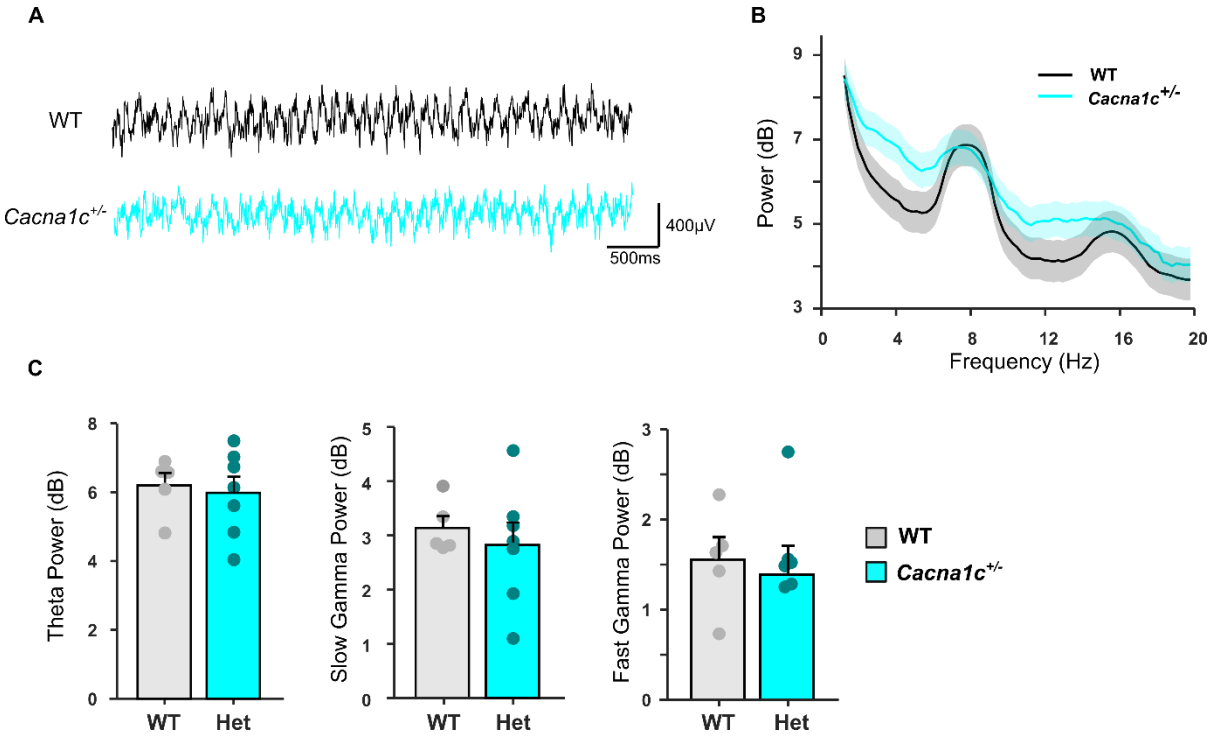

***Figure 3.11* | Power spectral density during track runs**
(A) Representative broadband local field potential traces (0.1-475 Hz) taken from individual animals in a 5 second window while running on the track.
(B) Mean power spectra in the theta range taken from track runs.
(C) Mean bandpower shown (left) for theta (6-10Hz), (centre) for slow gamma power (25-55Hz) and (right) for fast gamma power (60-140Hz). Bandpower did not differ between genotypes at any frequency band (p>0.05, Student's t-test. Solid circles indicate individual animals).
(Data presented as mean±SEM. WT: n=5 animals; Cacna1c$^{+/-}$: n=7 animals. WT in black, Cacna1c$^{+/-}$ in cyan)

Additionally, I compared power spectral densities as animals ran on the linear track in the novel orientation (**Figure 3.12**). Again, theta and both gamma bands were comparable

between genotypes (**Figure 3.12B**, Theta, p=0.467; Slow-Gamma, p=0.122; Fast-Gamma, p=0.248; Student's t-test).

These results indicate that the cellular and network mechanisms involved in the generation of hippocampal oscillations are intact in *Cacna1c*$^{+/-}$ rats.

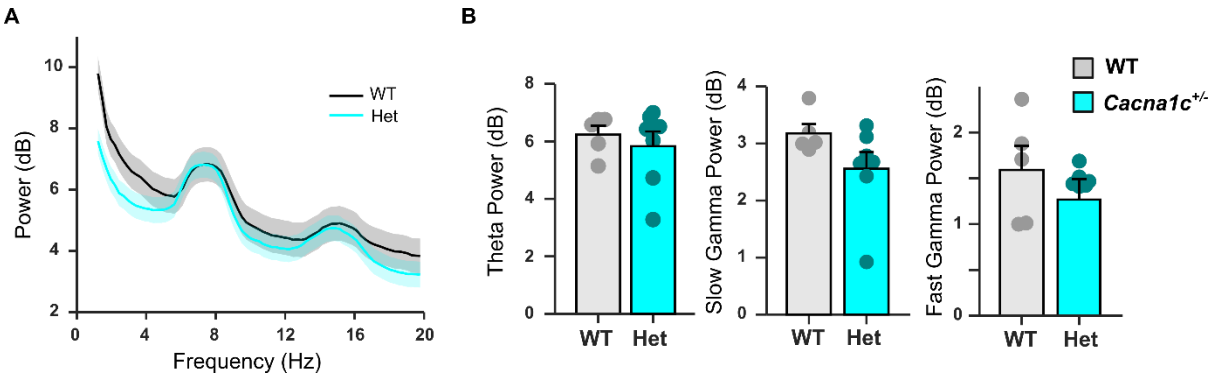

***Figure 3.12* | Power spectral density during track runs in the novel track orientation**
(A) Mean power spectra in the theta range taken from track runs.
(B) Mean bandpower shown (left) for theta (6-10Hz), (centre) for slow gamma power (25-55Hz) and (right) for fast gamma power (60-140Hz). Bandpower did not differ between genotypes at any frequency band (p>0.05, Student's t-test. Solid circles indicate individual animals).
(Data presented as mean±SEM; WT: n=5 animals; Cacna1c$^{+/-}$*: n=7 animals. WT in black, Cacna1c*$^{+/-}$ *in Cyan)*

While individual oscillations were intact, the temporal coupling of oscillations may have been affected. To assess this, I calculated PAC with LFP data from track runs. PAC comodulograms (**Figure 3.13B**, *left column*) appeared similar between genotypes on the familiar track. Closer inspection of MI values within theta-gamma regions revealed comparable PAC between both theta and slow gamma (p=0.918) and theta and fast-gamma (p=0.709, Student's t-test), indicative of intact phase-amplitude coupling while running on the track.

PAC comodulograms on the novel track, while broadly similar to familiar conditions in the WTs, appeared to show a distinct attenuation across a range of frequencies in the *Cacna1c*$^{+/-}$ rats (**Figure 3.13B**, *right column*). Band MI values revealed a reduction in slow-gamma coupling in the *Cacna1c*$^{+/-}$ rats compared to the WTs (p=0.026) while theta-fast gamma coupling, though reduced, was not significantly different (p=0.058, Student's t-test).

These results imply a context-dependent deficit in oscillatory coupling within *Cacna1c*$^{+/-}$ rats.

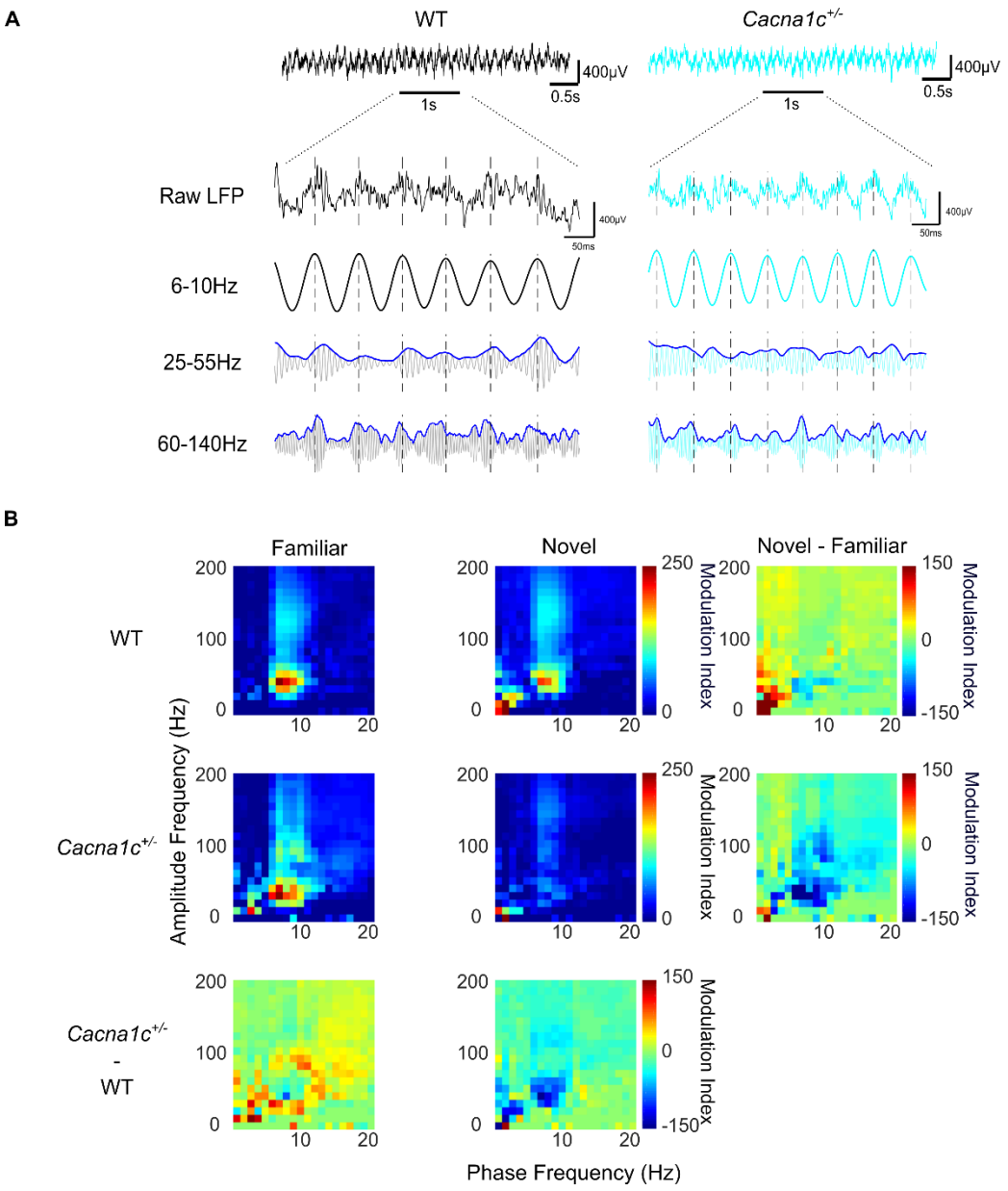

***Figure 3.13* | Phase-amplitude coupling during track runs**
(A) Local field potentials taken from tracks runs on the familiar track. (Top) Representative broadband LFP traces (0.1-475Hz) in a 5 second window while running. (Bottom) 1 second expanded segment showing raw unfiltered LFP (top) and bandpass filtered theta (6-10Hz), slow gamma (25-55Hz) and fast gamma (60-140Hz) (bottom). Phase-amplitude coupling measures the degree to which the amplitude envelope (blue traces shown for slow and fast gamma) is modulated by the phase signal (theta filtered LFP). (Dashed vertical lines indicate timings of theta cycle peaks).
(B) Mean Phase Amplitude Coupling comodulograms taken from track runs on the linear track. Phase frequencies (1-20Hz) shown on the x-axis and amplitude frequencies (1-200Hz) shown on the y-axis. Differences between environments and genotypes are shown next to the mean plots as labelled. Colour depicts the modulation index.
(WT: n=5 animals; Cacna1c$^{+/-}$: n=7 animals. WT in black, Cacna1c$^{+/-}$ in Cyan)

Given the important relationship between oscillatory activity and behaviour (Pickenhain and Klingberg, 1967, Vanderwolf, 1969) I next set out to assess how hippocampal oscillations varied with running speed. First, I characterised the running speeds of all animals to ensure

that any differences observed were not the result of inherent differences between running speed. Both genotypes displayed a normal distribution of running speeds (**Figure 3.14A**, *left*) and mean running speed was comparable (p=0.435, Student's t-test) indicating similar running behaviour on the linear track.

Next, I assessed the relationship between running speed and theta frequency on the familiar track by entering each speed-theta frequency pair across every run on the track into a linear regression analysis. This analysis, as expected, revealed a significant effect of running speed on theta frequency (**Figure 3.14B**, $F_{1,373}$=31.2, p=4.51x10^{-8}) however did not reveal a running speed x genotype interaction ($F_{1,371}$=2.95, p=0.087), therefore indicating intact running speed – theta frequency dependence.

I then performed the same analysis, this time to assess the relationship between theta power and running speed (**Figure 3.14D**). This analysis revealed a very significant genotype x running speed interaction ($F_{1,373}$=47.7, p=2.11x10^{-11}). Further examination revealed a strong association between theta-power and running speed in the WTs (t=16.6, p=5.29x10^{-40}) but no significant relationship in the *Cacna1c*$^{+/-}$ rats (t=-1.09, p=0.277).

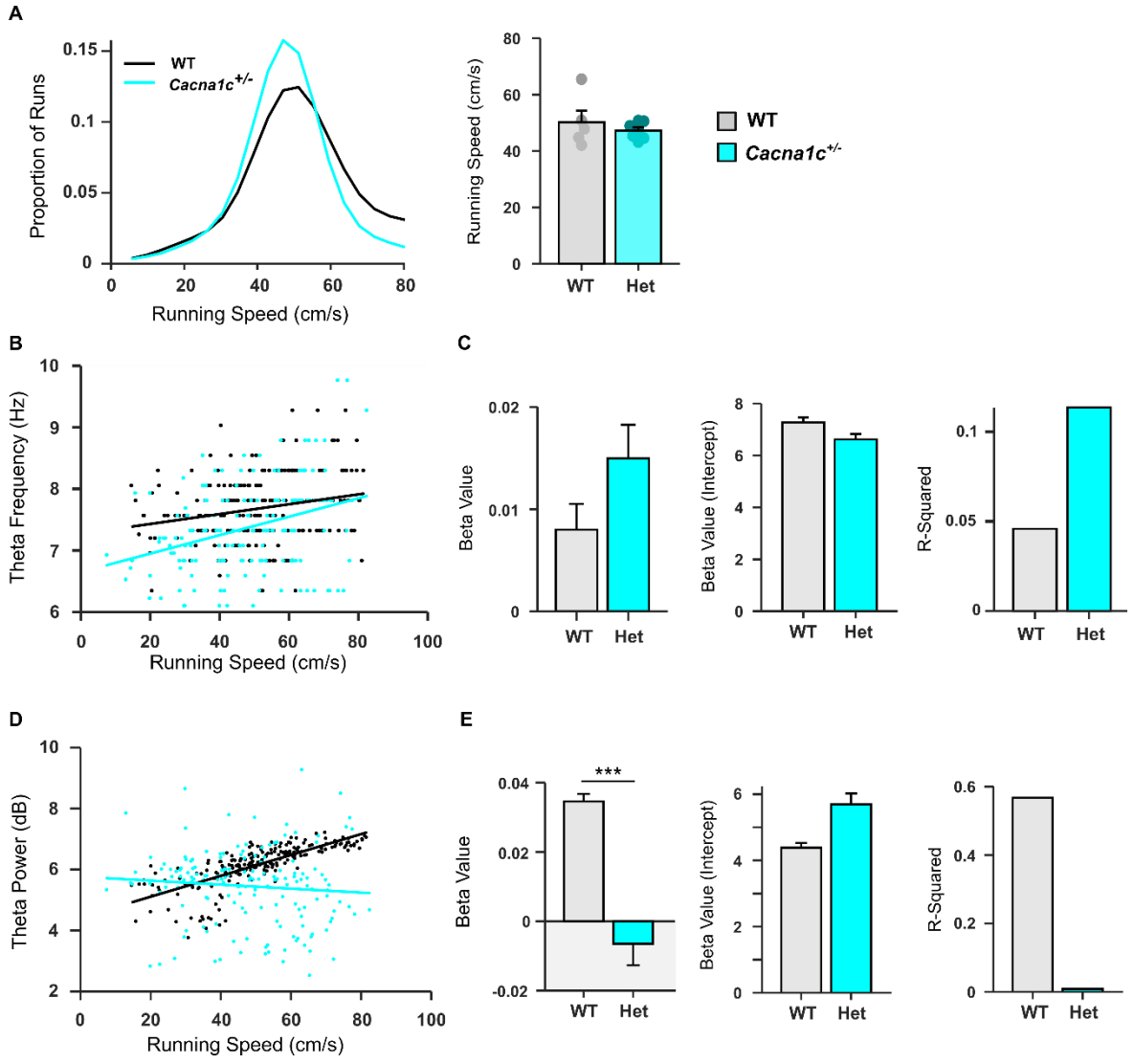

***Figure 3.14* | Speed modulation of theta power & frequency**
(A) Velocity on the linear track. (Left) Distribution of mean running speeds for individual runs. (Right) Mean running speed did not differ between genotypes (p>0.05; Student's t-test).
(B) Speed modulation of theta frequency. Mean trial running speed vs. theta (6-10Hz) frequency. (Solid line depicts linear regression fit)
(C) Slope statistics for scatter plot shown in **(B)**. (Left) Correlation coefficients between running speed and theta-frequency did not reveal a significant difference between genotypes (p>0.05). (Centre) Intercept (β-value). (Right) R-squared values. (Data presented as mean±SEM)
(D) Speed modulation of theta power. Mean trial running speed vs. log theta power. (Solid line depicts linear regression fit).
(E) Slope statistics for scatter plot shown in **(D)**. (Left) Correlation coefficients between running speed and theta power. Analysis revealed a significant effect of genotype (***p<0.001). (Centre) Intercept (β-value). (Right) R-squared values.
(Data presented as mean±SE; WT: n=186 runs; Cacna1c$^{+/-}$: n=124 runs. WT in black, Cacna1c$^{+/-}$ in Cyan).

Previous work has revealed an effect of novelty on the theta-run speed association (Penley et al., 2013). I therefore performed the same analysis incorporating runs in the novel track orientation. First, I applied this analysis to theta frequency (**Figure 3.15A**). As previously described, this analysis revealed a significant context x run-speed interaction on theta frequency ($F_{1,414}$=4.69, p=0.03), with both genotypes displaying a reduction in slope in the novel orientation (**Figure 3.15B**). Analysis however showed no effect of genotype on this interaction ($F_{1,413}$=0.618, p=0.432) indicating robust theta frequency dependency on run speed in *Cacna1c*$^{+/-}$ rats.

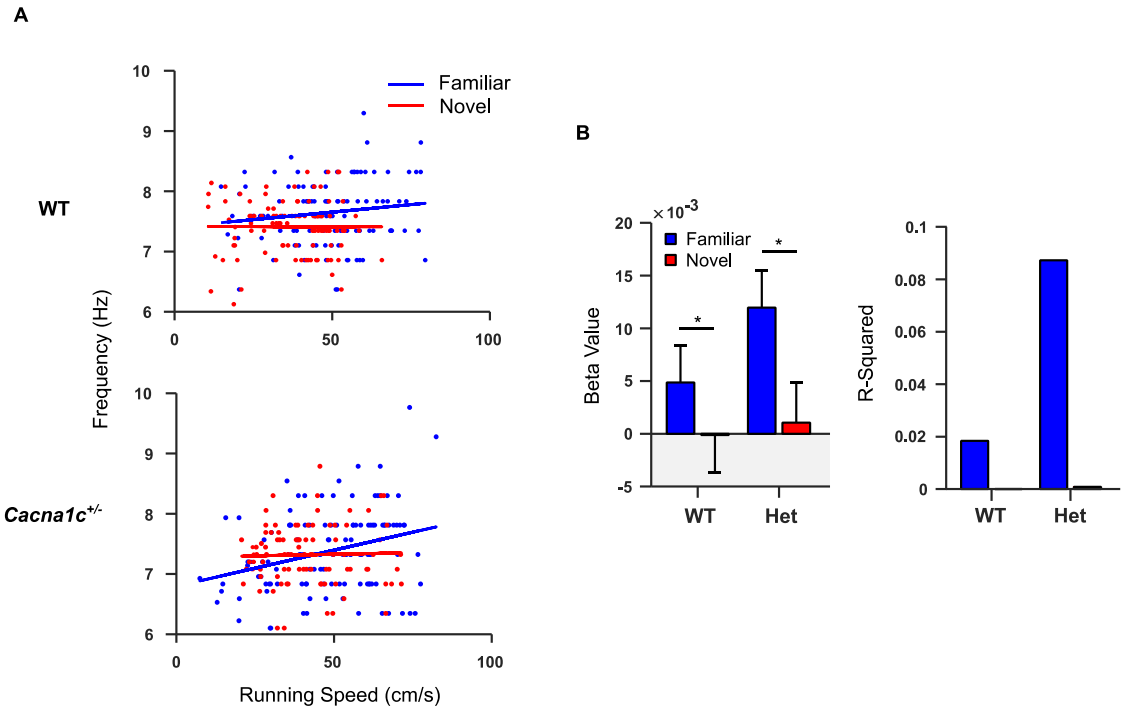

***Figure 3.15* | Running speed vs. theta frequency on the familiar and novel linear track**
(A) Speed modulation of theta frequency on both familiar and novel linear track. Mean trial running speed vs. theta (6-10Hz) frequency shown for WTs (top) and *Cacna1c*$^{+/-}$ rats (bottom). (Solid line depicts linear regression fit)

(B) Slope statistics for scatter plots shown in **(A)**. Analysis revealed a significant effect of context (*p<0.05) but not genotype (p>0.05).
(Data presented as mean±SE; Familiar track: WT, n=104 runs, Cacna1c$^{+/-}$, n=123 runs; Novel track: WT, n=100 runs, Cacna1c$^{+/-}$, n=94 runs. Familiar track in blue, novel track in red)

Next, I assessed the novel track running speed relationship with regards to theta power (**Figure 3.16A**). This analysis did not reveal an effect of novelty on the relationship here ($F_{1,413}$=2.08, p=0.15) but again showed a very significant effect of genotype ($F_{1,413}$=21.2, p=5.51x10^{-4}). Individual genotype analysis showed a lack of relationship between running speed and theta power in the *Cacna1c*$^{+/-}$ rats (t=-0.69, p=0.49) while a significant relationship remained in the WTs (t=4.75, p=6.84x10^{-6}).

These results demonstrate an intact relationship between theta frequency and running speed, yet a marked loss of relationship between theta power and running speed in *Cacna1c*$^{+/-}$ rats.

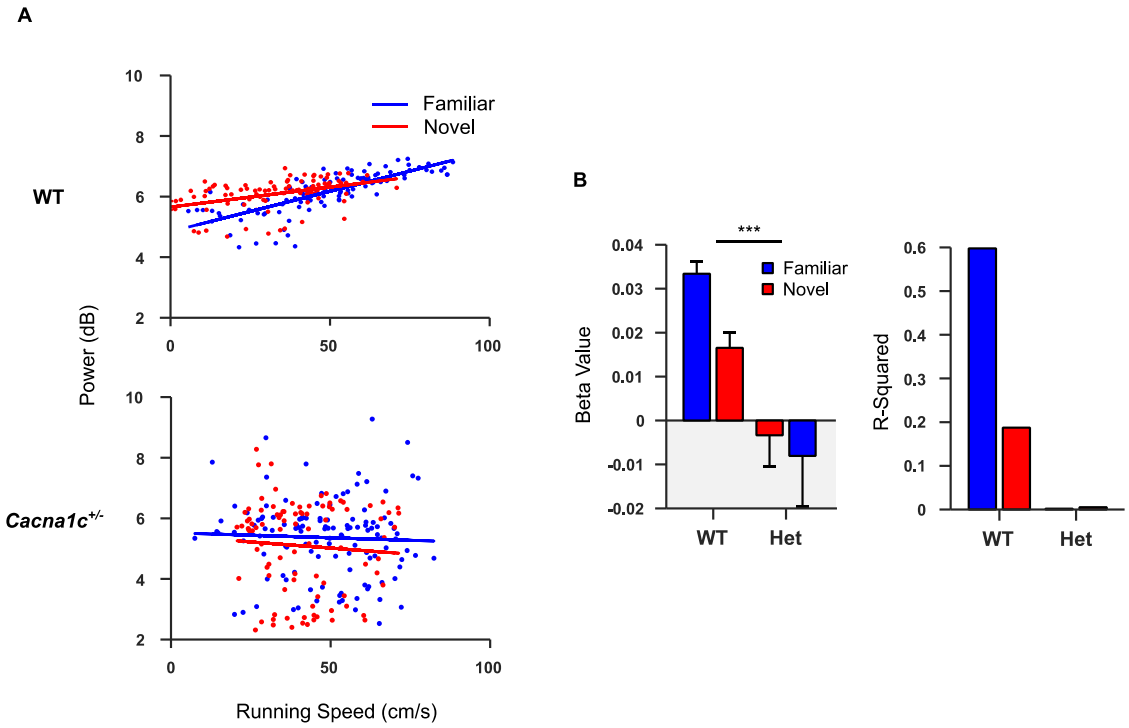

***Figure 3.16* | Running speed vs. theta power on the familiar and novel linear track**
(A) Speed modulation of theta power on both familiar and novel linear track. Mean trial running speed vs. theta (6-10Hz) power shown for WTs (top) and *Cacna1c*$^{+/-}$ rats (bottom). (Solid line depicts linear regression fit)
(B) Slope statistics for scatter plots shown in **(A)**. Analysis revealed a significant effect of genotype (*p<0.05) but not context (p>0.05).
(Data presented as mean±SE; Familiar track: WT, n=104 runs, Cacna1c$^{+/-}$, n=123 runs; Novel track: WT, n=100 runs, Cacna1c$^{+/-}$, n=94 runs. Familiar track in red, novel track in blue)

I next assessed the same dependencies on running speed at the gamma frequency band. As slow gamma has been previously shown to display a very weak relationship to running speed

(Zheng et al., 2015) analysis here was restricted to fast gamma. A comparison between fast-gamma frequency and running speed in each genotype and across contexts (**Figure 3.17**) revealed a significant interaction between genotype and running speed ($F_{1,413}$=7.62, p=0.006). Unexpectedly this relationship was the result of a significant association in the *Cacna1c*$^{+/-}$ rats (t=4.19, p=4.08x10^{-5}) and not in the WTs (t=1.01, p=0.314).

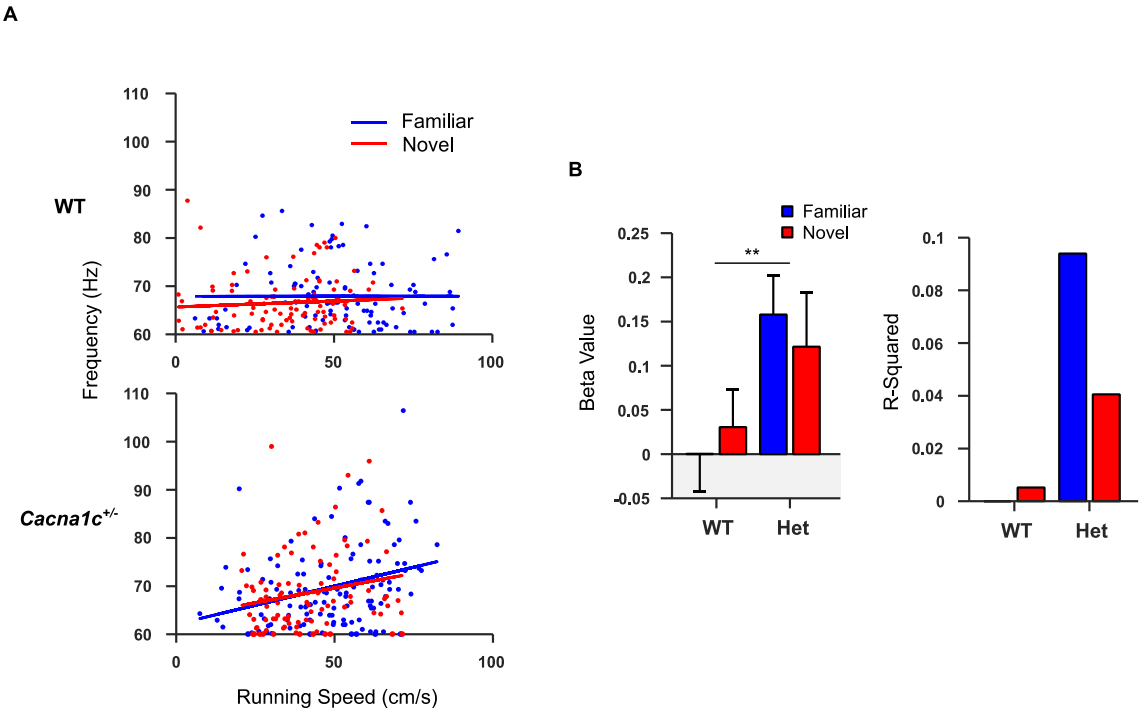

***Figure 3.17* | Running speed vs. fast gamma frequency on the familiar and novel linear track**
(A) Speed modulation of fast-gamma (65-140Hz) frequency on both familiar and novel linear track. Mean trial running speed vs. theta (6-10Hz) power shown for WTs (top) and *Cacna1c*$^{+/-}$ rats (bottom). (Solid line depicts linear regression fit)
(B) Slope statistics for scatter plots shown in **(A)**. Analysis revealed a significant effect of genotype (**p<0.01) but not context (p>0.05).
(Data presented as mean±SE; Familiar track: WT, n=104 runs, Cacna1c$^{+/-}$*, n=123 runs; Novel track: WT, n=100 runs, Cacna1c*$^{+/-}$*, n=94 runs. Familiar track in red, novel track in blue)*

Fast-gamma power vs. running speed analysis (**Figure 3.18**) revealed a significant effect of genotype ($F_{1,413}$=14.2, p=1.9x10^{-4}) which in this instance was the result of a significant association in the WTs (t=4.83, p=2.67x10^{-6}) but not in the *Cacna1c*$^{+/-}$ rats (t=-0.6, p=0.55). In neither instance was an effect of context observed on the running speed relationship to fast gamma. (Fast-Gamma Frequency: $F_{1,413}$=0.01, p=0.917; Fast-Gamma Power: $F_{1,413}$=1.8 p =0.18).

Together, this implies an elevation of fast gamma frequency dependence on running speed in *Cacna1c*$^{+/-}$ rats yet, as was the case with theta, a loss of dependency of power on running speed.

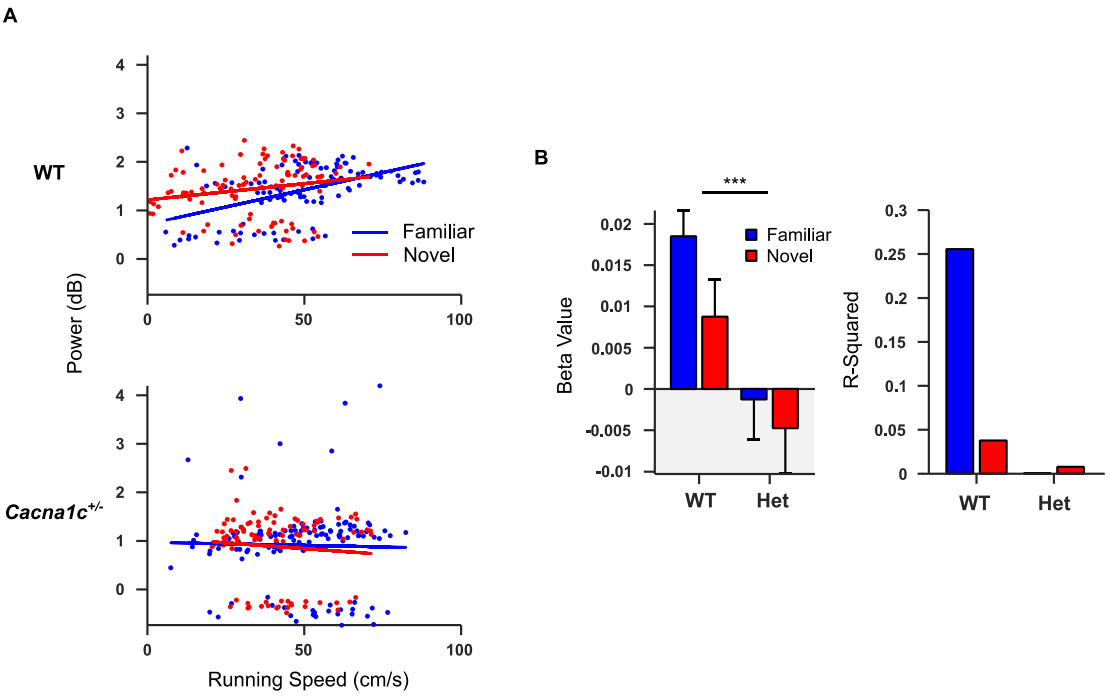

***Figure 3.18* | Running speed vs. fast gamma power on the familiar and novel linear track**
(A) Speed modulation of fast-gamma power on both familiar and novel linear track. Mean trial running speed vs. fast-gamma power shown for WTs (top) and *Cacna1c*$^{+/-}$ rats (bottom). (Solid line depicts linear regression fit)
(B) Slope statistics for scatter plots shown in **(A)**. Analysis revealed a significant effect of context (***p<0.001) but not genotype (p>0.05).
(Data presented as mean±SE; Familiar track: WT, n=104 runs, Cacna1c$^{+/-}$*, n=123 runs; Novel track: WT, n=100 runs, Cacna1c*$^{+/-}$*, n=94 runs. Familiar track in red, novel track in blue)*

The results of the analysis into hippocampal rhythmic activity revealed that on the surface, hippocampal oscillations appear intact in *Cacna1c*$^{+/-}$ rats. However closer inspection reveals a coupling deficit in the theta-slow gamma band, contingent upon environmental context. Additionally, the modification of rhythmic activity by running speed, while intact in relation to frequency is lost in relation to oscillatory power in *Cacna1c*$^{+/-}$ rats. To better understand the functional importance of these deficits, the next stage in the analysis was to assess the effects on single unit activity.

3.3.7. Phase Relationships Between Single Unit Activity & Hippocampal Rhythms

To quantity how rhythmic activity modulated the activity of individual pyramidal cells, I took spiking activity from the run session on the familiar linear track and assessed the phase relationships to different frequency bands.

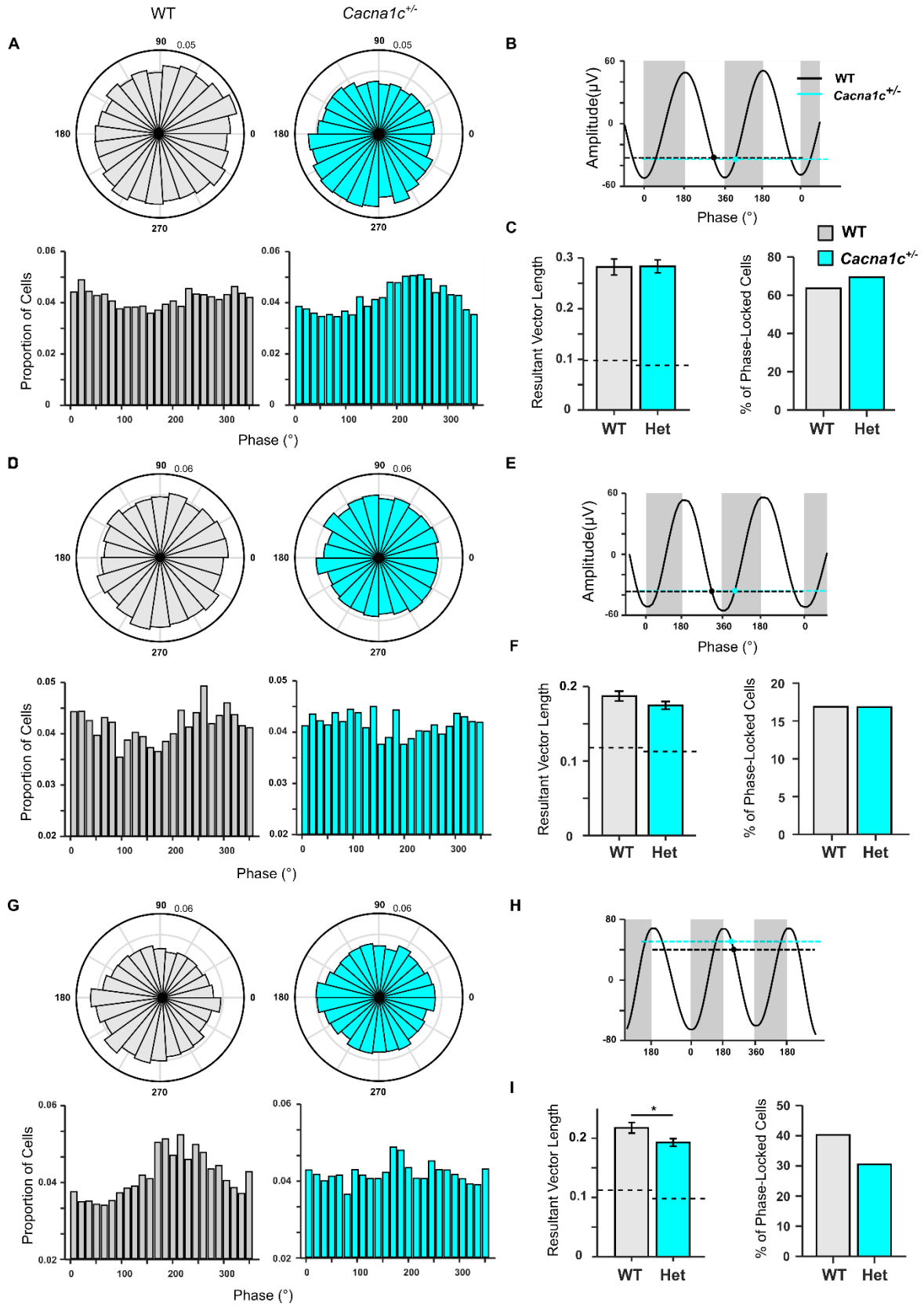

***Figure 3.19* | Phase-locking of pyramidal cell firing to hippocampal oscillations**
Phase distributions of pyramidal cell firing shown for periods of high theta (6-10Hz) **(A)**, slow-gamma (25-55Hz) **(D)** and fast gamma (60-140Hz) **(G)** during the track session. Circular phase histogram shown (top) and standard phase histogram shown (bottom).

(B,E & H) Raw local field potential traces taken from an individual animal filtered at theta, slow-gamma and fast-gamma respectively. Filled circles indicate mean preferred phase and dotted line indicates circular standard deviation of all cells.
(C,F & I) Quantifying phase-locking. Resultant vector lengths shown for theta, slow-gamma and fast-gamma respectively (left). Both genotypes showed above-chance levels (black dotted line) of phase-locking to all frequency bands. Phase-locking to fast-gamma was lower in *Cacna1c*$^{+/-}$ rats than WTs (*p<0.05, Student's t-test) and similar for theta and slow-gamma (p>0.05 student's t-test; Data presented as mean±SEM). Proportion of cells showing significant phase-locking (*p<0.05, Rayleigh test) to theta, slow-gamma and fast-gamma (right) shown. Both genotypes showed a similar proportion of significantly phase-locked cells (p>0.05; Chi-squared test).
(Data presented as mean±SEM; WT: n=77 Cells; Cacna1c$^{+/-}$*: n=95 cells. WT in black; Cacna1c*$^{+/-}$ *in cyan).*

First, I assessed the phase relationship of single units to theta (**Figure 3.19A**). To quantify the degree of phase-locking I took the resultant vector length of all phase values from individual cells (**Figure 3.19C**, *left*). Both genotypes displayed above-chance levels of phase-locking (*p<0.05, one-sample t-test), though the degree of phase-locking did not significantly differ between either genotype (p=0.947, Student's t-test). In addition, the number of cells defined as showing significant phase-locking (**Figure 3.19C**, *right*; p<0.05, Rayleigh test) was comparable (p=0.518, χ^2 test). Phase-locking to slow-gamma (**Figure 3.19D**) was also above-chance in both genotypes (**Figure 3.19E**, *left*) and not significantly different (p=0.145, Student's t-test), nor were the proportion of cells with significant phase-locking (**Figure 3.19F**, *right*; p=0.843, χ^2 test). Finally, I assessed phase-locking to fast-gamma (**Fig. 3.19G**). Both genotypes displayed above-chance levels of phase-locking however this was significantly reduced in *Cacna1c*$^{+/-}$ rats (**Figure 3.19I**, *left*; p=0.042). Meanwhile, the proportion of significantly phase-locked cells (**Figure 3.19I**, *right*) was not significantly different (p=0.242, χ^2 test).

These results reveal intact phase-locking to theta and slow-gamma yet a loss of phase-locking to fast-gamma in *Cacna1c*$^{+/-}$ rats. This was surprising, given the increased running speed relationship to fast-gamma frequency observed in *Cacna1c*$^{+/-}$ rats.

Phase-locking to hippocampal rhythms is altered upon exposure to a novel environment (Kitanishi et al., 2015). To assess this, I next performed the same analysis on the run session from the novel track orientation. Phase-locking to theta (**Figure 3.20A**), as in the familiar orientation, was above-chance for both genotypes and not significantly different (**Figure 3.20C**, *left*; p=0.64, Student's t-test), yet peculiarly the proportion of cells with significant phase-locking was reduced in the WTs compared to the *Cacna1c*$^{+/-}$ rats (**Figure 3.20C**, *right*; p=0.0036, χ^2 test).

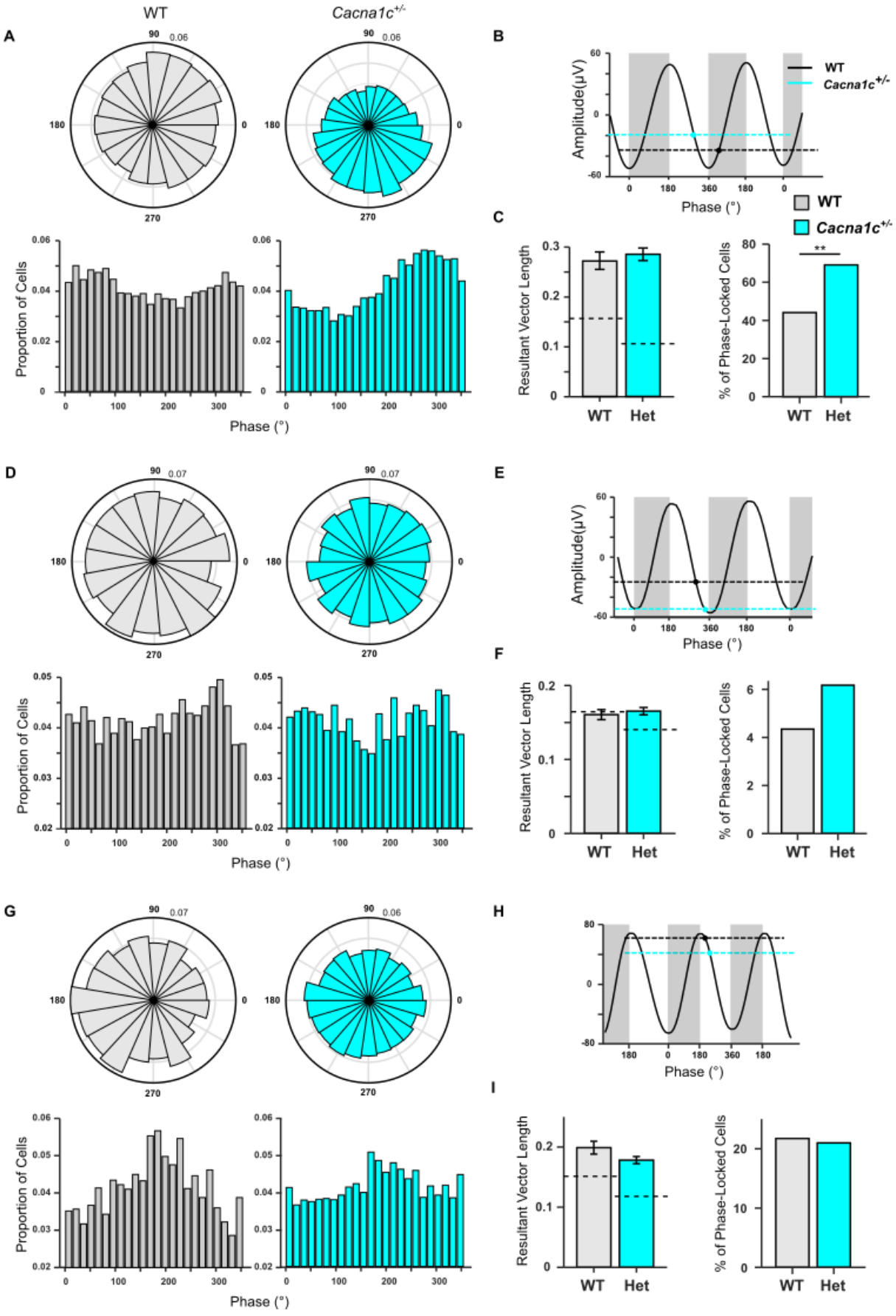

Figure 3.20 **| Phase-locking of pyramidal cell firing to hippocampal oscillations during runs in a novel track orientation**

Phase distributions of pyramidal cell firing shown for periods of high theta (6-10Hz) **(A)**, slow-gamma (25-55Hz) **(D)** and fast gamma (60-140Hz) **(G)** during the novel track session. Circular phase histogram shown (top) and standard phase histogram shown (bottom).
(B,E & H) Raw local field potential traces taken from an individual animal, filtered at theta, slow-gamma and fast-gamma respectively. Filled circles indicate mean preferred phase and dotted line indicates circular standard deviation of all cells.
(C,F & I) Quantifying phase-locking. Resultant vector lengths shown for theta, slow-gamma and fast-gamma respectively (left). Both genotypes showed above-chance levels (black dotted line) of phase-locking to theta and fast-gamma, however WTs did not show above-chance phase-locking to slow gamma ($p>0.05$, one-sample t-test). Phase-locking to all frequency bands was comparable between genotypes ($p>0.05$ student's t-test; Data presented as mean±SEM). Proportion of cells showing significant phase-locking ($p>0.05$, Rayleigh test) to theta, slow gamma and fast-gamma (right) shown. The proportion of significantly phase-locked cells was similar between genotypes for slow and fast-gamma ($p>0.05$) while WTs showed a significantly lower proportion of theta phase-locked cells compared to *Cacna1c*$^{+/-}$ rats (**$p<0.01$; Chi-squared Test).
(Data presented as mean±SEM; WT: n=57 Cells; Cacna1c$^{+/-}$*: n=82 cells. WT in black; Cacna1c*$^{+/-}$ *in cyan).*

Slow-gamma phase-locking in the novel track orientation was markedly reduced with the proportions of significantly phase-locked cells low in both genotypes, though this was not significantly different (**Figure 3.20E**, *right*; p=0.9, χ^2 test). Additionally, resultant vector lengths revealed no differences in phase-locking between genotypes (**Figure 3.20E**, p=0.531, Student's t-test) though in the WTs phase-locking was not above-chance levels. This result may reflect the reduction in slow-gamma input observed in novel environments (Penley et al., 2013) as a result of increased reliance on EC inputs. Finally, phase-locking to fast-gamma was comparable between genotypes (**Figure 3.20I**, *left*; p=0.145) as was the proportion of significantly phase-locked cells (**Figure 3.20I**, *right*; p=0.93, χ^2 test).

These results indicate intact oscillatory phase-locking in *Cacna1c*$^{+/-}$ rats in a novel environment. The similarity of fast gamma phase-locking in a novel but not familiar environment in *Cacna1c*$^{+/-}$ rats, may indicate a role for synaptic plasticity in phase-locking changes that occur with the increasing familiarity of an environment.

Theta phase-locking was both present and comparable between genotypes in both track orientations, however as discussed in ***1.3.3.3***, theta phase-relationships are not fixed across runs on a track but instead show a precession of phase as the animal progresses through a place-field. To assess this, I next looked at the phase relationship to theta for every place-cell (**Figure 3.21A**), during runs on the familiar linear track. To assess the degree of phase-precession, I performed circular linear regression analysis on the position relative to the centre of the place-field vs. the phase of all spikes fired by an individual cell. The proportion of cells displaying a significant position-phase relationship ($p<0.05$, deviation from circular normal distribution) was comparable between genotypes (**Figure 3.21B**, *right*; p=0.692, χ^2 test). Similarly, the strength of the relationship in cells that showed this significant relationship was

comparable (**Figure 3.21B**, *left*; p=0.42, Student's t-test). The direction of the position-phase relationship (Regression slope value) however, was significantly different between genotypes (p=0.002; Student's t-test) Surprisingly though, this was the result of a mean positive position-phase slope in the WTs (**Figure 3.21B**, *centre*) and a negative slope in the *Cacna1c*$^{+/-}$ rats. This result runs counter to previous research into phase-precession which describes a negative position-phase relationship with theta (O'Keefe and Recce, 1993, Skaggs et al., 1996) implying that phase-precession was "more normal" in the *Cacna1c*$^{+/-}$ rats that the WTs. The genotype difference observed here could not therefore be described as evidence of an impairment in the *Cacna1c*$^{+/-}$ rats given that their phase-precession relationship was more characteristic of normal phase-precession than the WTs.

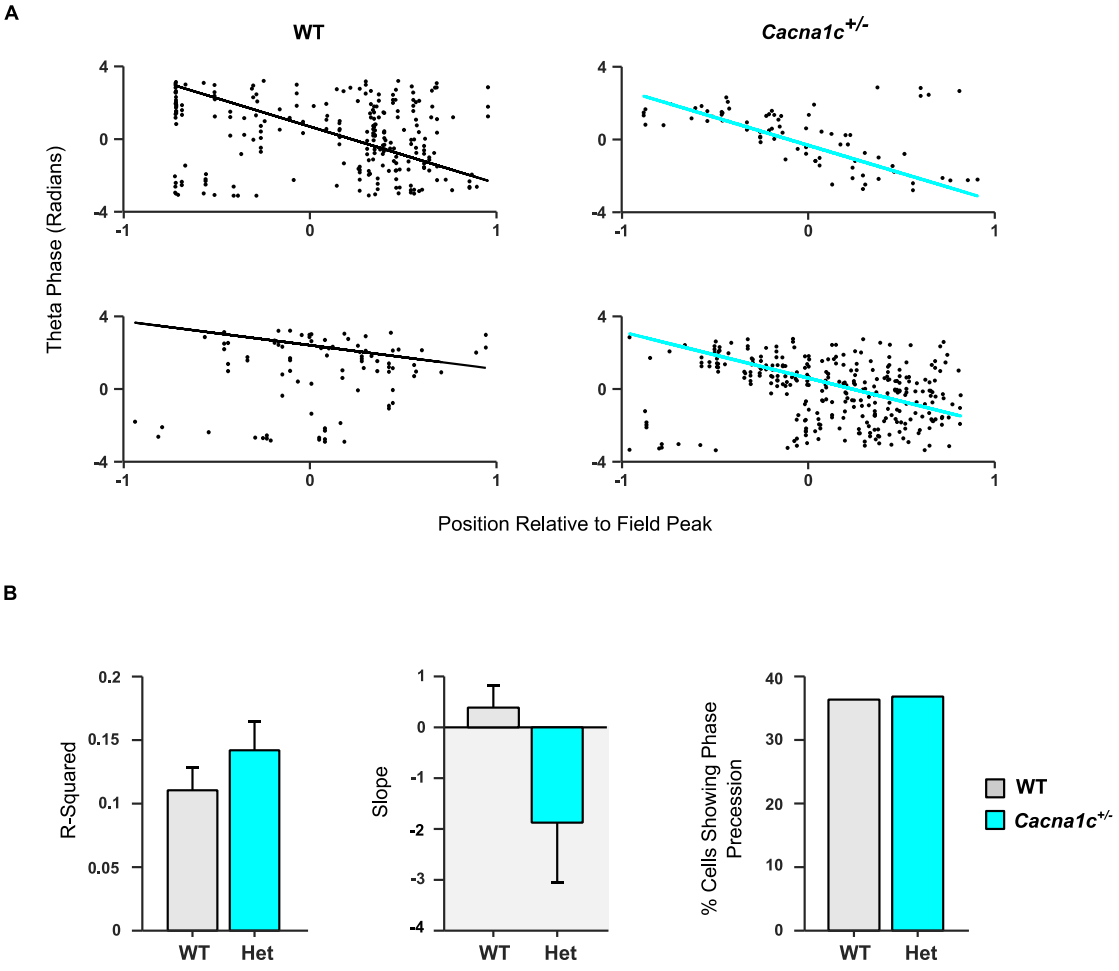

***Figure 3.21* | Phase precession of pyramidal cell firing relative to theta oscillations**
(A) Representative phase-precession plots shown for individual cells from WTs (left) and *Cacna1c*$^{+/-}$ rats (right). Plots depict theta-phase of spikes (black dots) vs. position relative to the centre of the place-field. Solid line through dots indicates circular regression fit.
(B) Circular regression slope statistics. Mean R-squared (left) and slope (centre) values of circular regression fits did not significantly differ between genotypes (p>0.05; Student's t-test; Data presented as mean±SEM). Percentage of cells showing significant phase precession (p-value of regression slope < 0.05) (right) were similar between genotypes.
(WT: n=77 cells; Cacna1c$^{+/-}$*: n=95 cells. WT in black; Cacna1c*$^{+/-}$ *in cyan).*

As phase-precession analysis on the familiar linear track was unable to detect normal phase-precession in WT animals, I next characterised phase-precession on the novel linear track to assess whether the prior finding was robust to changes in novelty. Here both genotypes displayed characteristic negative position-phase slopes (**Figure 3.22B**, *centre*) though these were not significantly different between genotypes (p=0.695, Student's t-test). Similarly, the proportion of cells displaying a significant position-phase relationship, in addition to the strength of the relationship, was also comparable between genotypes (**Figure 3.22B**, p=0.87, χ^2 test; p=0.739; Student's t-test, respectively).

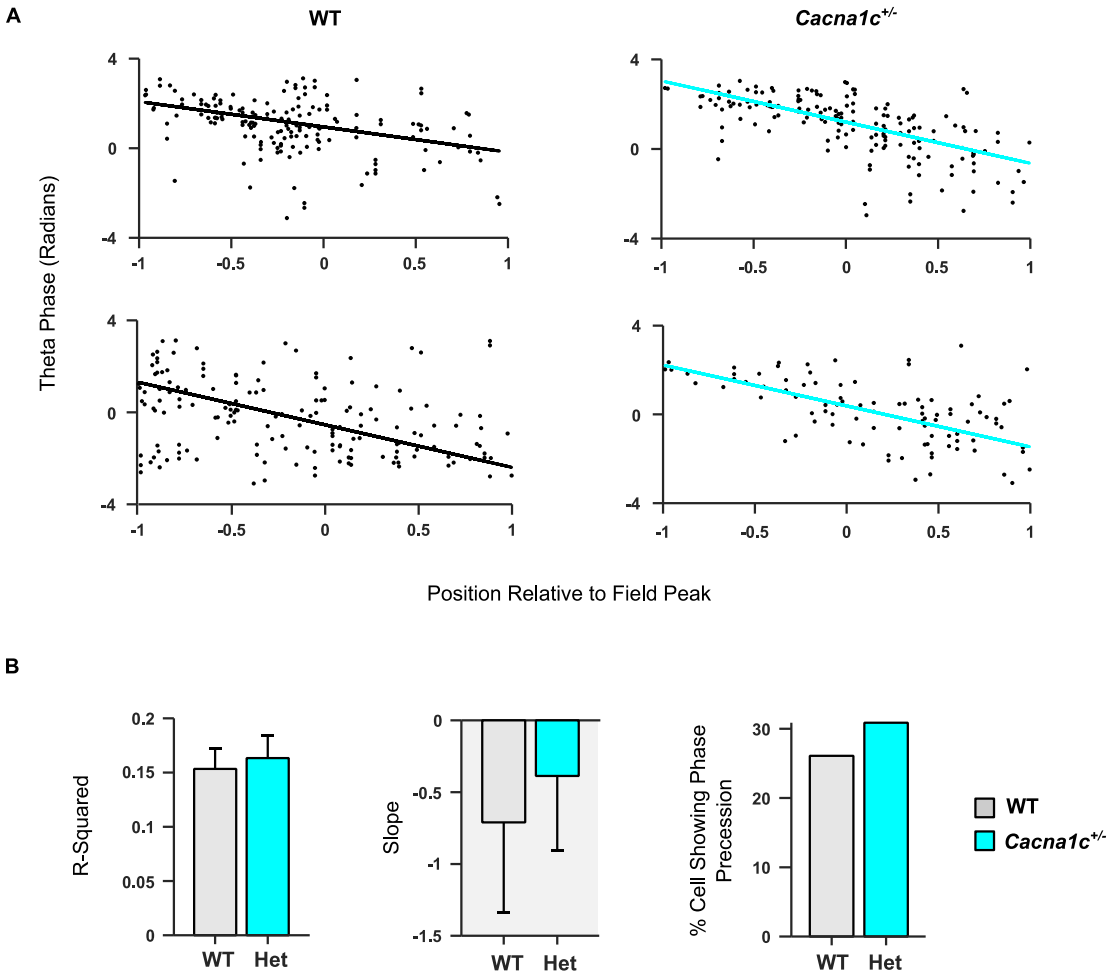

***Figure 3.22* | Phase precession of pyramidal cell firing relative to theta oscillations during novel track runs**

(A) Representative phase-precession plots shown for individual cells from WTs (left) and *Cacna1c*$^{+/-}$ rats (right). Plots depict theta-phase of spikes (black dots) vs. position relative to the centre of the place-field. Solid line through dots indicates circular regression fit.

(B) Circular regression slope statistics. Mean R-squared (left) and slope (centre) values of circular regression fits did not significantly differ between genotypes (p>0.05; Student's t-test; Data presented as mean±SEM). Percentage of cells showing significant phase precession (p-value of regression slope < 0.05) (right) were similar between genotypes.

(WT: n=77 cells; Cacna1c$^{+/-}$*: n=95 cells. WT in black; Cacna1c*$^{+/-}$ *in cyan).*

These results indicate that mechanisms of phase-precession are intact in *Cacna1c*$^{+/-}$ rats.

Table 3. Summary of findings reported in Chapter 3.

Test	Session	Effect	Statistical significance
Spike properties	Familiar linear track (incl. pre and post sleep)	Similar Pyr Cell and IN spike amplitude	p>0.05
		Increased Pyr cell and IN spike width in Cacna1c$^{+/-}$	p<0.001, p<0.01
		Comparable firing rate, burst index and burst event rate	p>0.05
		Altered ISI distribution	p<0.001
Behaviour	Familiar linear track	Comparable time to criterion (in minutes and session)	p>0.05
		Comparable behaviour on track (time spent moving and time spent in centre)	p>0.05
	Open-field	Comparable levels of locomotion and time spent in centre of field	p>0.05
Place-cells	Familiar linear track	Increased place-field width and reduced spatial information in *Cacna1c*$^{+/-}$	p<0.05, p<0.05
		Comparable place-field firing rates, number of place-fields per place cell and bidirectionality of place-cells	p>0.05
	Linear track in novel orientation	Increased place-field width and reduced spatial information in *Cacna1c*$^{+/-}$	p<0.01, p<0.001
		Comparable place-field firing rates, number of place-fields per place cell and bidirectionality of place-cells	p>0.05
	Open-field	Comparable place-field size, place-cell spatial information, place-field firing rates and number of place-fields	p>0.05
Bayesian decoding	Familiar linear track	Increased decoding error in *Cacna1c*$^{+/-}$	p<0.05
	Linear track in novel orientation	Increased decoding error in *Cacna1c*$^{+/-}$	p<0.001
Place-cell remapping	Familiar and novel orientation linear track	Comparable reduction in place-cell firing rate from familiar -> novel	p>0.05
		Comparable rate-remapping index, place-field spatial correlation and change in place-field centre of mass	p>0.05
Oscillatory activity	Familiar linear track	Comparable theta and gamma power	p>0.05
		Comparable theta slow-gamma and theta fast-gamma coupling	p>0.05

	Linear track in novel orientation	Comparable theta and gamma power	p>0.05
		Reduced theta slow-gamma coupling in *Cacna1c*$^{+/-}$	p<0.05
Oscillatory coupling to behaviour	Familiar linear track	Comparable correlation between running speed and theta-frequency	p>0.05
		Increased correlation between running speed and fast-gamma frequency in *Cacna1c*$^{+/-}$	p<0.001
		Reduced correlation between running speed and theta power in *Cacna1c*$^{+/-}$	p<0.001
		Reduced correlation between running speed and fast-gamma power in Cacna1c$^{+/-}$	p<0.001
	Linear track in novel orientation	Comparable reduction in correlation between running speed and theta frequency from familiar -> novel	p>0.05
		Increased correlation between running speed and fast-gamma frequency in *Cacna1c*$^{+/-}$	p<0.01
		Reduced correlation between running speed and theta power in *Cacna1c*$^{+/-}$	p<0.001
		Reduced correlation between running speed and fast-gamma power in Cacna1c$^{+/-}$	p<0.001
Phase-locking to oscillatory activity	Familiar linear track	Comparable phase-locking of Pyr-cell firing to theta and slow-gamma	p>0.05
		Reduced phase-locking of Pyr-cell firing to fast-gamma	p<0.05
	Linear track in novel orientation	Increased phase locking of Pyr-cell firing to theta in *Cacna1c*$^{+/-}$	p<0.01
		Comparable phase-locking of Pry-cell firing to slow and fast-gamma	p>0.05
Phase Precession Analysis	Familiar linear track	Increased phase-precession of Pyr cell firing relative to theta in *Cacna1c*$^{+/-}$	p<0.05
	Linear track in novel orientation	Comparable phase-precession of Pry cell firing relative to theta	p>0.05

3.4. Discussion

3.4.1. Key Findings

In this chapter I recorded behaviour and extracellular dCA1 electrophysiology as rats explored three environments: A familiar linear track, a linear track in a novel orientation and a novel

open-field. This analysis revealed normal behaviour across all environments yet electrophysiological deficits during linear track runs. This included alterations in spike properties and place-field properties indicative of impairments at a single unit level. LFP analysis also revealed a loss of coupling on the rotated linear track at the theta and slow-gamma band. Finally, in *Cacna1c*$^{+/-}$ rats I observed a complete loss of bandpower dependency on running speed. Here, I shall explore these deficits further to understand how they relate to one another in addition to known *CACNA1C* related deficits.

3.4.2. Spike properties

Analysis of spike properties revealed normal spike amplitudes yet an increased spike-width in both pyramidal cells and interneurons in *Cacna1c*$^{+/-}$ rats. Spike-width broadening without change to amplitude is observed when the afterhyperpolarization (AHP) period of an action potential is extended (Shao et al., 1999). This change is mediated through calcium influx (Giese et al., 1998b, Shao et al., 1999, Jaffe et al., 2011) which would imply that reduced calcium channel expression would give rise to a shortening of the AHP – the opposite of what was observed here. The mechanism governing the AHP itself though is dependent on potassium channels (Jaffe et al., 2011) and the exact role of LTCCs here is yet to be elucidated. The similar effect at interneurons makes this an interesting result that would nonetheless be worth investigating further, though this would require detailed intracellular measures typically made in vitro.

AHP properties alter the speed at which a cell can depolarise and repolarise (Storm, 1987) which appears to affect neuronal firing rates (Gu et al., 2007). I did not however see any changes to the firing rates or bursting properties of neurons in *Cacna1c*$^{+/-}$ rats. An altered ISI distribution was observed in *Cacna1c*$^{+/-}$ rats, importantly though this distribution essentially characterises two ISI event populations: Spikes observed in and outside of bursts. Establishing whether one or both populations gave rise to this change remains undetermined, but the lack of effect on bursting neurons would imply this was an effect at higher ISI events, and as such any link between this alteration and spike-width is made more tenuous.

One important caveat to this line of research is that it was blind to the state of each animal. Many of these properties show dependence on behavioural state (Mizuseki and Buzsáki, 2013) and without knowing what proportion of each animal's recording session consisted of sleep, active periods and waking rest it would be difficult to determine whether these changes are intrinsic cellular properties or simply a reflection of altered behaviour.

3.4.3. Place Cell Properties in Cacna1c$^{+/-}$ Rats

Analysis of place-cells across multiple environments showed that place-fields are larger in *Cacna1c$^{+/-}$ rats* in a familiar and novel orientation but not in a novel context. This result implies that place-field formation is intact, but that regulation of place-field size is impaired. Spatial information was also lower in *Cacna1c$^{+/-}$* rats than WTs in both linear track sessions but not the novel context. This measure is contingent upon the firing rate specificity and thus larger place-fields, higher firing rates and trial to trial variability can give rise to lower spatial information scores. Firing rate measures across all sessions were similar for both genotypes, while in the two sessions in which *Cacna1c$^{+/-}$* rats exhibited larger place-fields, they also displayed a reduction in place-field size, indicating that their spatial information deficits were the result of place-field size changes. This change in spatial information may have given rise to the modest reduction in position decoding observed in *Cacna1c$^{+/-}$* rats compared to WTs.

Research into the importance of place-field size in spatial encoding is conflicting. CA1-specific NMDAR1 knockout mice display larger place fields in addition to impaired Schaffer-collateral plasticity and spatial memory deficits (McHugh et al., 1996) and exposure to a novel environment has been shown to lead to an increase in place-field size that reduces with experience (Barry et al., 2012). Additionally, a progressive increase in place-field size is seen along the dorsal-ventral axis of the hippocampus and this coincides with a progressive decrease in spatial encoding ability (Fanselow and Dong, 2010, Royer et al., 2010, Yartsev, 2010). In contrast, place-fields have also been observed to expand with experience (Mehta et al., 2000). In these instances, this relates to an increased skewing of the place-field as a result of spike-timing dependent plasticity. As such, the size of the place field may matter less here than the resultant asymmetry. Additionally mice lacking the HCN1 gene display larger place-fields, yet an improvement in spatial memory (Hussaini et al., 2011). Here, the effects on place-field properties appear to relate to EC input as HCN1 is not highly expressed in CA3; thus the changes in place-field size here may arise from a different mechanism to the place-field changes observed in NMDAR1 knockout mice.

As discussed in ***3.1***, in psychiatric disease animal models, place-fields may also be disrupted, yet the results are conflicting. In DISC1-L100P mice, an increase in place-field size is observed that results from having fewer place-fields typically active over larger regions of space (Mesbah-Oskui et al., 2015) yet tgDISC1 rats exhibit smaller place-fields (Kaefer et al., 2019). These conflicting results may reflect a U-shaped relationship. Place fields that are too large may lack specificity, but too small and the hippocampus may fail to fully encode spatial experience. In the instance of *Cacna1c*, the impairments in spatial information and position decoding imply that this increase in place field size is in fact a deficit and results from reduced specificity. Notably the increase in place-field size was small, and thus position decoding, though mildly reduced compared to WTs, was still broadly accurate.

The increase in place-field size is broadly in line with the change observed in CA1-NMDAR1 knockout mice. In *Cacna1c*$^{+/-}$ rats, plasticity deficits are observed specifically at Schaffer-collateral synapses (Moosmang et al., 2005, Tigaret et al., 2020), implicating this pathway in the observed changes. The lack of impairment in place-field properties in the novel open-field may reflect this pathway specific deficit. Place-field formation, as would occur upon first exposure to an environment, is coincident with dendritic spiking and place field formation can be induced with artificial dendritic spikes. Importantly, these are mediated through EC input while CA3 input simply alters their duration (Bittner et al., 2015). As a result, place-field formation only depends on EC, but concurrent CA3 input may serve to provide backpropagating action potentials to enable associative plasticity (Magee and Johnston, 1997) giving rise to a refinement of place-field properties over time. In *Cacna1c*$^{+/-}$ rats, perforant path plasticity is intact, and as such one would expect place-field formation to appear largely normal as I observed here. The potential role for CA3 in providing backpropagating action potentials fits with the increased attenuation of these action potentials seen in *Cacna1c*$^{+/-}$ rats which may also underlie the plasticity deficits (Tigaret et al., 2020). I hypothesize that this reduction in plasticity prevents a CA3-mediated increase in specificity of place-fields over time and as such, in more familiar environments *Cacna1c*$^{+/-}$ rats exhibit place-field deficits not observed upon first exposure.

It is unknown whether these place-field alterations have any functional importance to spatial memory, as is the case in NMDAR1 knockout mice. In forebrain specific knockout of *Cacna1c*, spatial learning deficits are observed (Moosmang et al., 2005) however this model results in complete knockout rather than heterozygosity in the hippocampus, unlike the model used here. In heterozygous models, while memory deficits have been described (Tigaret et al., 2020), spatial memory appears intact (Braun et al., 2018). This may be due to the relatively small place-field changes observed and thus any influence on behaviour may be more subtle. Importantly, the hippocampus does more than simply encode spatial information and so while spatial memory might be intact, functional deficits to single unit firing properties may underlie other important hippocampal contingent behaviours such as latent inhibition which is impaired in *Cacna1c*$^{+/-}$ rats (Tigaret et al., 2020). This behavioural measure tests the ability of animals to inhibit subsequent fear conditioning following an extended pre-exposure period (Weiner, 2001). This relies on the ability of the hippocampus to balance two competing representations and as such a reduced encoding specificity may impair ability here. Additionally, the hippocampus functions by binding together experiences into episodes. Consequently we must consider the role of population activity in combination with individual neurons to fully understand hippocampal activity with regard to *Cacna1c*.

3.4.4. Hippocampal Rhythmic Activity

The power and frequency of hippocampal rhythms was comparable between genotypes across linear track sessions yet coupling showed impairment on the rotated linear track, specifically at the theta-slow gamma band. Theta-slow gamma PAC relates to coupling between CA3 and CA1 (Colgin et al., 2009) thus deficits here may reflect a deficit in connectivity between these two regions, underlying the effects on plasticity observed in relation to *Cacna1c*. Importantly though, the lack of deficit in slow-gamma power implies no change in input itself to CA1, rather an alteration in the coupling of CA1 theta modulation to the gamma rhythm of CA3 – this might result from a loss of plasticity and indeed plasticity has been observed to occur alongside elevated theta-gamma coupling though here it appears that theta-gamma coupling gives rise to, rather than results from plasticity (Bikbaev and Manahan-Vaughan, 2008). The effect observed in *Cacna1c*$^{+/-}$ rats may therefore be an additional deficit that enhances the loss of plasticity in *Cacna1c*$^{+/-}$ rats rather than resulting from it. Moreover, this loss of coupling was observed only in relation to the novel orientation. Previous work has revealed an elevation in the phase-locking of individual neurons to slow-gamma upon first exposure to a novel environment that reduces with experience. This effect is impaired in animals displaying a virus-mediated loss of Schaffer-collateral plasticity (Kitanishi et al., 2015). This might relate to the place-field refinement role of CA3 mediated plasticity discussed in ***3.4.3***. Phase-locking to slow-gamma was also attenuated on the rotated track in *Cacna1c*$^{+/-}$ rats, however a similar deficit was observed in WTs and so this doesn't explain the coupling deficit.

One important thing to bear in mind however was that remapping analysis revealed that in neither genotype was full global remapping observed, indicating that this novel orientation was not encoded as fully novel. Interestingly in a study making use of a modified path – a 45° rotation of just one half of the track, no alteration to either theta or gamma power was observed (Penley et al., 2013). This intervention, though not identical, is certainly comparable to the one used here and as such the coupling deficit may not be reflective of the oscillatory changes observed with novelty. There is scant literature characterising theta-gamma coupling changes following small environmental changes capable of inducing rate remapping. Hippocampal subregions vary in their sensitivity to such changes however, with CA3 cells showing a shift in place field centre immediately following cue changes while CA1 cells show a comparable change a day later (Lee et al., 2004). This implies that the cue change exerts an effect primarily on CA3 while CA1 may serve to integrate this new information with current sensory input from EC, giving rise to the delayed changes in place-fields. Importantly this would rely on concurrent input from CA3 and EC, presumably to enable associative plasticity. Impaired theta-slow gamma coupling in *Cacna1c*$^{+/-}$ rats may reflect a failure to integrate new information from CA3. Unfortunately, the lack of subsequent recordings on the

rotated track prevents analysis of CA1 place-field changes that might emerge later as a result of such a process.

Despite what appeared to be intact generation of theta and gamma oscillations in *Cacna1c*$^{+/-}$ rats, behavioural dependence of these rhythms revealed important deficits possibly indicative of an impairment in rhythmic modulation. Theta rhythms, though showing normal frequency dependence on running speed displayed a complete loss of a power-running speed relationship in *Cacna1c*$^{+/-}$ rats. This effect did not appear contingent upon novelty, but again this might reflect the lack of complete novelty imparted by track rotation. Indeed, in the aforementioned 'modified path' study, the power and frequency running speed relationship did not vary compared to the familiar environment for theta or fast gamma (Penley et al., 2013).

The origin of this relationship appears to reside in the septal hippocampal pathway. Firing of neurons in the medial septum precede the onset of locomotion and locomotion speed appears intrinsically linked to the firing patterns of these neurons. Additionally hippocampal theta is entrained to the firing frequency of these neurons (Fuhrmann et al., 2015). These projections also regulate the inhibition of CA1 cells and thus impairments here may also accentuate plasticity deficits observed in *Cacna1c*$^{+/-}$ rats. On the other hand, theta oscillations appear to also affect this relationship in the opposite direction. Stimulation of hippocampal projections to the lateral septum at theta frequency alters running speed in a frequency dependent manner implying a two-way hippocampal-septal interaction (Bender et al., 2015). It is unknown exactly how these pathways relate to *CACNA1C*. To date, the expression of *CACNA1C* in this region is unknown, though the effect could result from expression within the hippocampus as well.

This deficit may at least partially underlie some of the place-field changes. A study which observed the importance of self-motion signals to hippocampal encoding by putting rats in cars on a track and comparing place-cell properties to runs on that track, found that the animals in cars exhibited a loss of theta dependence on velocity, concurrent with larger place-fields (Terrazas et al., 2005). As such the deficit observed in place fields may in fact reflect a more widespread failure to incorporate sensorimotor information in the hippocampus. In humans, theta and sensorimotor integration are intrinsically linked. During motor planning, when incorporating sensory information with motor signals is most prominent, theta signals are also highest (Caplan et al., 2003). Interestingly there is also a vast literature implicating corollary discharge deficits in SCZ (Ford et al., 2001, Mathalon and Ford, 2008). Corollary discharges are copies of motor signals sent to sensory regions to enable anticipation of the sensory feedback from a motor action (Wurtz and Sommer, 2004). This form of sensorimotor integration relies on theta, as evidenced by the loss of motor-auditory cortical theta coherence observed in SCZ patients (Ford and Mathalon, 2004). Sensorimotor deficits may also disrupt

the integration of motor signals by the hippocampus giving rise to the loss of the theta power – running speed relationship observed in the hippocampus of *Cacna1c*$^{+/-}$ rats. Though an equivalent deficit has not been previously related to SCZ, the DISC1 animal model exhibits a loss of firing rate dependence on running speed (Kaefer et al., 2019) which may reflect similar underlying sensorimotor dysfunction.

Similar running-speed power dysfunction was also seen for fast-gamma in *Cacna1c*$^{+/-}$ rats. Given that coupling between theta and fast gamma was intact, it is possible this deficit simply reflects the theta deficit. If the power of gamma is modulated by theta then one would expect gamma in turn to be modulated by running speed in healthy animals and an impairment in *Cacna1c*$^{+/-}$ rats. That being said, there is some evidence of medial septum influence on gamma. Deep brain medial septum stimulation reverses the increase in gamma power observed after administration of an NMDA receptor antagonist (Leung and Ma, 2018). Interestingly NMDA receptor antagonism is used as a model for SCZ (Coyle, 2012) lending more weight to the possibility that medial septum dysfunction underlies symptoms of psychiatric disease. It is unknown whether this medial septal influence has any bearing on the running-speed gamma relationship, though this study did observe elevated locomotion with NMDA receptor antagonism that was reduced with medial septum stimulation in concurrence with the effects on gamma.

These findings highlight the importance of sensorimotor integration in hippocampal function and possibly shed light on a deficit underlying aspects of psychiatric disease. While there is a possibility this deficit may have some bearing on place-field properties for example, it is important to consider the effect of rhythmic activity on single unit activity to better understand the implications of dysfunction at a population level.

3.4.5. Spike-Phase Relationships

Spike-phase analysis revealed intact phase-locking of place-cells to theta and slow-gamma but an impairment to fast-gamma in *Cacna1c*$^{+/-}$ rats on the familiar linear track. This is perhaps counter-intuitive given that fast gamma reflects EC input and plasticity deficits have been observed in relation to CA3 input. Alternatively, this result may be reflective of the deficit in running speed-power interactions, though one might also expect to observe a theta phase-locking deficit. The relationship between gamma and running speed has been suggested to play a role in enabling faster transitions between different gamma cycles in line with the increased traversal speed of an environment (Ahmed and Mehta, 2012). Predominantly this relies on the frequency of gamma rather than the power, which was not observed to be impaired in *Cacna1c*$^{+/-}$ rats, though it is possible a power relationship aids in this phenomenon also. As previously mentioned, fast and slow gamma phase locking appears to serve different roles. Slow gamma phase locking relates to upcoming positions on a track and as such would

be expected to be most prominent early in the place-field while fast-gamma relates to retrospective coding, thus peaking in prominence later (Bieri et al., 2014). As you may recall, familiarity-mediated expansion of place-fields gives rise to an enhanced asymmetry of the place-field, leaning more heavily towards the approach-end (Mehta et al., 2000). As such, larger place-fields may result in less emphasis on fast-gamma phase-locking. There are still a few problems with this explanation though. Firstly, on the rotated track no deficit in fast-gamma phase-locking was observed despite an increased place-field size in *Cacna1c*$^{+/-}$ rats. Moreover it is unknown whether the increased place-field size in *Cacna1c*$^{+/-}$ rats was an asymmetric increase, and this change to place-field shape is thought to aid in healthy hippocampal function whereas in the *Cacna1c*$^{+/-}$ rats it appeared to have a dysfunctional role, at least in spatial encoding. As such the significance of this phase-locking impairment remains elusive.

Additionally a curious reduction in the proportion of significantly theta-phase locked cells was observed in WTs during runs in the novel track orientation yet not observed in *Cacna1c*$^{+/-}$ rats. There is some evidence that theta-phase locking alters in response to novelty, though this relates to the specific phase cells fire at, rather than the strength of phase-locking (Lever et al., 2010). That being said, in the tgDISC1 animal model, an elevation in the theta phase-locking strength of individual neurons was observed in the tgDISC1 animals and this manifested only in a novel environment (Kaefer et al., 2019) indicating dysfunction to the hippocampus could enhance phase-locking as well as leading to impairments. However in this model a concurrent loss of population level phase-locking was observed in the tgDISC1 animals whereas in *Cacna1c*$^{+/-}$ rats this was normal. Furthermore the change observed here appeared to be the result of a specific impairment in the WTs rather than a change to phase-locking in the *Cacna1c*$^{+/-}$ rats. Accordingly, though it is unclear why the proportion of theta-phase locked cells dropped in the WTs during runs in the novel orientation, in *Cacna1c*$^{+/-}$ rats theta-phase locking appears normal.

Theta phase-precession analysis revealed intact phase precession in *Cacna1c*$^{+/-}$ rats though peculiarly, a deficit in WTs on the familiar track. This impairment may have reflected a lack of sufficient power to detect phase precession rather than an impairment per se. Place field properties were otherwise normal in WTs and as phase-precession is an essential component of hippocampal function, it is unlikely such a striking deficit would be present without also observing deficits in other faculties of hippocampal processing.

The robust phase-precession observed in *Cacna1c*$^{+/-}$ rats however, alongside mostly normal phase-locking, implies an imperviousness of place-cell activity in the phase domain to changes in the firing rate domain. This may enable a certain degree of redundancy in hippocampal encoding, where loss of specificity in place-cell firing rates can be accounted for by intact encoding by phase relationships. This may explain why measures of simple

hippocampal functioning such as contextual fear conditioning still appear intact in *Cacna1c*$^{+/-}$ rats (Tigaret et al., 2020).

3.4.6. Conclusion

The results in this chapter highlight a potential role for Schaffer-collateral plasticity in refining place-fields during spatial encoding. As such *Cacna1c* heterozygosity leads to reduced place-field specificity in a familiar environment that corresponds to a reduction in spatial encoding. Additionally, the modulation of certain hippocampal rhythms shows impairments that may reflect deficits in connectivity within the hippocampus, but also connectivity with other regions such as the medial septum.

Importantly these deficits may underlie certain hippocampal contingent behavioural deficits observed in animal models of *CACNA1C* genetic variation and these deficits may reflect the broader cognitive impairments associated with SCZ. In addition, impairment in integrating sensory signals in the hippocampus may give rise to some of the sensorimotor deficits observed in SCZ or at least reflect more widespread sensorimotor dysfunction.

The contingency of many of these deficits on experience, implies an encoding impairment. In this chapter I have discussed the importance of plasticity here. Yet encoding also reflects a form of consolidation of memory, which may at least in part be at fault. This analysis has reported these changes in the context of active periods on a track, yet memory consolidation is intimately linked to sleep. To fully understand how the encoding of memories is impaired one must also consider offline brain activity. In the next two chapters we will explore the role of sleep in memory consolidation to provide more context to the research explored in this chapter.

4

Chapter 4

Circadian Rhythms in *Cacna1c* Heterozygous Rats

4.1. Introduction

4.1.1. The Importance of Sleep

Sleep comprises 15-85% of the average mammal's lifetime (Elgar et al., 1988) and is ubiquitous across the animal kingdom (Keene and Duboue, 2018). This is not a behaviour that serves any single role but instead a plethora of different roles, such as an immune function, playing an essential role in the production of antibodies (Besedovsky et al., 2012), an important metabolic function such as regulating hormonal levels (Leproult and Van Cauter, 2010), and most relevant to this thesis, a multitude of important roles within the brain, from a memory function, to regulation of emotion.

Though there are a wealth of important reasons to study sleep, to do so here is particularly relevant for 2 reasons:

1. Sleep abnormalities are ubiquitous to psychiatric disease
2. Normal hippocampal function is highly contingent upon its 'offline' activity as well as its activity during engagement in a task

In this chapter I address the first point by exploring sleep architecture through the use of infrared actigraphy monitoring to better understand how *Cacna1c* heterozygosity impacts on circadian rhythmic activity. In the subsequent chapter I address the second point by quantifying sleep-associated hippocampal neurophysiology.

4.1.2. Sleep in Psychiatric Disorders

Abnormalities in sleep are widespread across most psychiatric disorders. An estimated 90% of patients suffering from MDD exhibit sleep difficulties (Thase, 1999) and display altered sleep properties. Typically patients display a reduction in REM sleep onset in addition to a greater proportion of total REM sleep (Kupfer and Foster, 1972, Waller et al., 1989, Emslie et al., 1990). In BPD, during manic phases patients will exhibit insomnia and during the depressed phase, hypersomnia (Nofzinger et al., 1991, Harvey et al., 2009a). Like MDD, patients with BPD also display an increase in total REM and a reduction in REM onset (Hudson et al., 1988). In SCZ around 80% of patients report sleep difficulties (Sharma et al., 2016). Additionally patients may exhibit insomnia prior to a psychotic relapse (Herz and Melville, 1980). This touches on an important point: Is the altered sleep a symptom of these disorders or can it actually precipitate or exacerbate the illness? Adolescents identified as at-risk for both SCZ and BPD display disrupted sleep even before showing symptoms of these disorders (Lunsford-Avery et al., 2013, Zanini et al., 2015). This would suggest that sleep disruption may play a role in the development of more classical symptoms of these disorders. In the case of MDD this relationship has been tested more rigorously. A genetic study of insomnia found a correlation between risk genes for insomnia and both depressive symptoms and MDD. The authors here used mendelian randomization, a method that makes use of the non-reverse causality associated with genetic risk to ask whether the genes associated with insomnia increased the risk of depression through an insomnia effect, or vice versa. They found that in fact insomnia was the cause of depression (Jansen et al., 2019). A similar approach has been applied to SCZ though here it uncovered a bidirectional effect – sleep impairments may worsen SCZ, though SCZ also gives rise to sleep impairment (Dashti et al., 2019).

The importance of this research is to show that sleep may have a mechanistic role in the aetiology of psychiatric conditions. As such, when investigating genetic factors in these disorders, it is essential we assess their role in sleep. If risk genes do impair sleep it could be in one of two ways: Genetic factors may directly disrupt the mechanisms governing sleep; this could be regarded as an endophenotype in and of itself. Alternatively, the effect may be indirect; a non-sleep related endophenotype may indirectly give rise to impairments in sleep. Here the role of sleep in non-sleep related symptoms would be less clear. In this chapter I will present research which aims to assess the role of *Cacna1c* in governing sleep in rodents but first we will consider what is already known in this domain.

4.1.3. CACNA1C & Sleep

Sleep cycles are governed by the SCN - a bundle of cells behind the optic chiasm that drive circadian rhythms through their 24-hour rhythmic activity (Hastings, 1997). Interestingly this rhythmic activity appears intrinsic to each cell, i.e. – they fire with a circadian rhythmic activity

even when isolated from all other cells (Welsh et al., 1995). The mechanism governing such rhythmic activity appears to be encoded into the DNA itself. Two proteins, CLOCK and BMAL1 activate transcription of the clock genes *Per* and *Cry*. As time progresses, these proteins accumulate and bind to each other. The new heterodimer compound is capable of entering the nucleus where it supresses further encoding of these protein's mRNA. This forms a negative feedback loop that progresses over a roughly 24-hour period, giving rise to the 24-hour circadian rhythm (Hastings, 1998).

Importantly, *Cacna1c* is expressed in the SCN and appears to play some role in this function (Nahm et al., 2005). Blocking calcium channels abolishes rhythmic clock gene expression, though this study used a non-selective antagonist and as such the role of LTCCs here is unclear (Nahm et al., 2005). Conversely, calcium channel activity may be governed by the activity of clock genes. *CACNA1C* expression appears to display rhythmic activity in time with clock gene expression (Schmutz et al., 2014, McCarthy et al., 2016) and a reduction in rhythmic intracellular calcium is observed following the inhibition of *Per* (Noguchi et al., 2017). Interestingly this rhythmic *CACNA1C* expression is reduced in BPD patients (McCarthy et al., 2016), hinting at a potential sleep-mediated role of this gene in psychiatric risk.

The presence of LTCCs within the brain's circadian machinery unsurprisingly gives rise to circadian behavioural effects when *Cacna1c* expression is altered. In heterozygous mice this manifests as an increase in sleep onset latency which also leads to reduced activity during wake periods (Kumar et al., 2013). Additionally intervening in an animal's normal circadian rhythm appears to reveal *Cacna1c* associated deficits: a light pulse during an animal's dark period gives rise to a circadian phase-shift in WT mice, while in brain-specific *Cacna1c* knockout mice this effect is lost (Schmutz et al., 2014). Additionally following sleep deprivation, a loss of REM rebound is observed in heterozygous *Cacna1c* mice (Kumar et al., 2015) - a phenomenon whereby REM sleep increases in response to sleep loss.

Human work also reveals a role for *CACNA1C* in sleep regulation. Genetic studies of sleep deficits consistently implicate *CACNA1C* and so far this gene has been associated with narcolepsy (Shimada et al., 2010), sleep onset latency (Byrne et al., 2013, Kantojärvi et al., 2017) and sleep quality (Parsons et al., 2013). Direct study of sleep in patients harbouring risk associated *CACNA1C* SNPs is yet to be undertaken however at the time of writing a clinical trial into the effects of the LTCC antagonist nicardipine on psychiatric symptoms and sleep is underway, and all participants will be genotyped for *CACNA1C* to understand its effects here (Atkinson et al., 2019).

4.1.4. Chapter Aims

Collectively, this evidence supports a role for *CACNA1C* in modulating circadian rhythms. As such, sleep deficits may represent a *CACNA1C* mediated psychiatric-disease relevant

endophenotype. To investigate this further, here I monitor circadian rhythms in *Cacna1c* heterozygous rats using camera-based actigraphy (see section ***4.2*** for more details). This is a method that provides an indirect measure of sleep cycles by continually monitoring activity levels. Despite being an indirect measure, actigraphy shows very high agreement with polysomnography - a direct method to measure sleep (McCall and McCall, 2012) and there is a wide body of literature using actigraphy as an effective measure of sleep in psychiatric conditions (Tahmasian et al., 2013).

I will first characterise these animal's circadian rhythms by taking activity recordings under their standard 12:12 hour light-dark cycle. I will then interfere with this rhythm by switching animals to a reversed light-dark cycle to observe how their circadian rhythms adapt. Given the importance of *CACNA1C* to circadian activity, alterations to both normal circadian activity and adaptations of circadian activity to changing light-dark cycles may be observed in *Cacna1c*$^{+/-}$ rats.

4.2. Methods

4.2.1. Animals

6 Heterozygous *Cacna1c* rats and 3 WTs (obtained as described in Chapter 2) were used. These recordings were undertaken in 2 batches, the first with 5 *Cacna1c*$^{+/-}$ rats and 2 WTs and the second with one *Cacna1c*$^{+/-}$ rat and one WT.

Table 4. Summary table of number of animals used.

Section	Number of Recording Days	Batch	Genotype	Number of animals
Normal lighting	14	1	WT	2
			Cacna1c$^{+/-}$	5
		2	WT	1
			Cacna1c$^{+/-}$	1
Reverse lighting	28	1	WT	2
			Cacna1c$^{+/-}$	5
		2	WT	1
			Cacna1c$^{+/-}$	1

4.2.2. Actigraphy Setup

Actigraphy recordings were obtained using hardware developed in-lab by Aleks Domanksi. Movement was detected through the use of Passive Infrared (PIR) sensors as described by

Brown et al. (Brown et al., 2016) and data was collected via an embedded ATmega328 microcontroller (Arduino) in 10s bins at a sampling rate of 0.01Hz. Each 10s bin was defined as a percentage activity count.

For the first batch of recordings animals were single-housed in Techniplast 2154F cages. These have wire-tops enabling infrared signals to pass through the top relatively unobstructed. PIR sensors were positioned above the cages, mounted to the top of the cage-rack. To enable full coverage of the cage, cameras were mounted 28cm from the cage floor and 17cm from the front of the cage. Additionally each cage was separated by thick black card to avoid interference from other cages.

For the second batch of recordings, both animals were implanted with tetrode microdrives and as such were required to remain in high-top cages. As these have plastic lids, sensors had to be placed within the cage to avoid obstruction of infrared signals. Here sensors were placed 38cm from the cage floor and 30cm from the front of the cage. The sensors had a 46° angle of detection thus this positioning still allowed full coverage of the cage. Each cage was positioned 18cm away from the rack edge to avoid detection of IR signals from elsewhere in the room and each cage was separated by thick black card.

4.2.3. Actigraphy Recording Protocol

Recordings were taken after at least 12 days of habituation to the recording room. All recordings were initially taken in a reverse light-dark room maintained on a 12:12 hour light-dark cycle (Lights-on: 8:15pm; Lights-off: 8:15am). These first recordings lasted 2 weeks in total. Following this 2-week initial recording period, all animals were moved into a normal light-dark room also maintained on a 12:12 hour light dark-cycle but 12 hours out of phase with the reverse lighting room (Lights-on: 8:15am; Lights-off: 8:15pm). These secondary recordings lasted 4 weeks in total.

4.2.4. Data Analysis

Circadian rhythms were first characterised by a set of non-parametric measures laid out by Witting et al. (1990). Actigraphy data from the reverse-lighting period was subdivided into 60 minute bins and sleep fragmentation was defined by intradaily variability (IV):

$$IV = \sum_{n=2}^{N} \frac{(X_n - X_{n-1})^2/(N-1)}{\sum_{n=1}^{N}(X_n - \bar{X})^2/N}$$

whereby X_n denotes the activity in successive one-hour bins, N is the total number of bins and $\overline{X}$ denotes mean activity. High IV values indicate a tendency towards daytime sleep bouts and night-time activity bouts (Gonçalves et al., 2014).

Interdaily stability (IS) measures the adherence to a 24-hour rhythm and is defined by:

$$IS = \frac{\sum_{h=1}^{P}(X_h - X_m)^2 \, N}{p \sum_{i=1}^{N}(X_i - X_m)^2}$$

This measure involves defining a mean 24-hour profile denoted by the mean activity X_h at each hour of the mean day. Mean total activity is denoted X_m, the number of samples per mean day (24 here) is denoted p and X_i denotes activity at each hour across the whole recording. High IS values indicate a high degree of adherence to a 24-hour rhythm.

Additional circadian analysis was carried out using Clocklab (https://www.actimetrics.com/), a software package designed for the use of circadian rhythm analysis. Sleep bouts were identified by periods absent of activity bouts, defined as a minimum of 5 bouts per minute, for at least 10 minutes. Activity onsets and offsets were identified using a template matching algorithm which defined the 20th percentile of activity and characterised all activity as falling above or below the 20th percentile. This binary characterisation was convolved with an off-on template to determine activity onset and an on-off template to determine activity offset. This template-matching approach was combined with additional manual curation to identify any cases where the algorithm appeared to mis-characterise onsets and offsets.

4.2.5. Statistical Analysis

To compare two groups a t-test or non-parametric equivalent was used. To compare sleep onset latencies across time a two-way ANOVA with repeated measures was used. All data is presented as mean±SEM or median±inter-quartile range for non-parametric data, unless stated otherwise.

4.3. Results

4.3.1. Circadian Analysis

To assess gross sleep architecture I first compared circadian rhythms between genotypes over a 2-week period in the reverse light-dark condition (**Figure 4.1)**. Non-parametric analysis of activity rhythms (**Figure 4.1C**) revealed an IS close to 0.5 for both genotypes. This did not differ between genotypes (p=0.777; Student's t-test) indicating that both genotypes showed a comparable degree of adherence to a consistent 24-hour rhythm. IV was also comparable between genotypes (p=0.611; Student's t-test) indicating a similar tendency towards daytime naps and night-time awakenings in both genotypes.

To better understand daytime napping and night-time awakening behaviour I next characterised the mean sleep bout length in addition to the number of sleep bouts for each animal at every circadian time (**Figure 4.1B**). Both genotypes showed clear evidence of circadian activity with sleep bouts shortening in length during the active period meanwhile the number of sleep bouts increased, indicating a tendency to be more active. Analysis here as expected revealed a significant effect of time (Sleep Bout Length: $F_{23,161}$ = 12.5, p=2.64x10^{-25}; Sleep Bout Number: $F_{23,161}$=8.02, p=5.6x10^{-17}; Repeated measures ANOVA) however no effect of genotype was observed (Sleep Bout Length: $F_{23,161}$ =0.192, p=1; Sleep Bout Number: $F_{23,161}$=0.629, p=0.9; Repeated measures ANOVA).

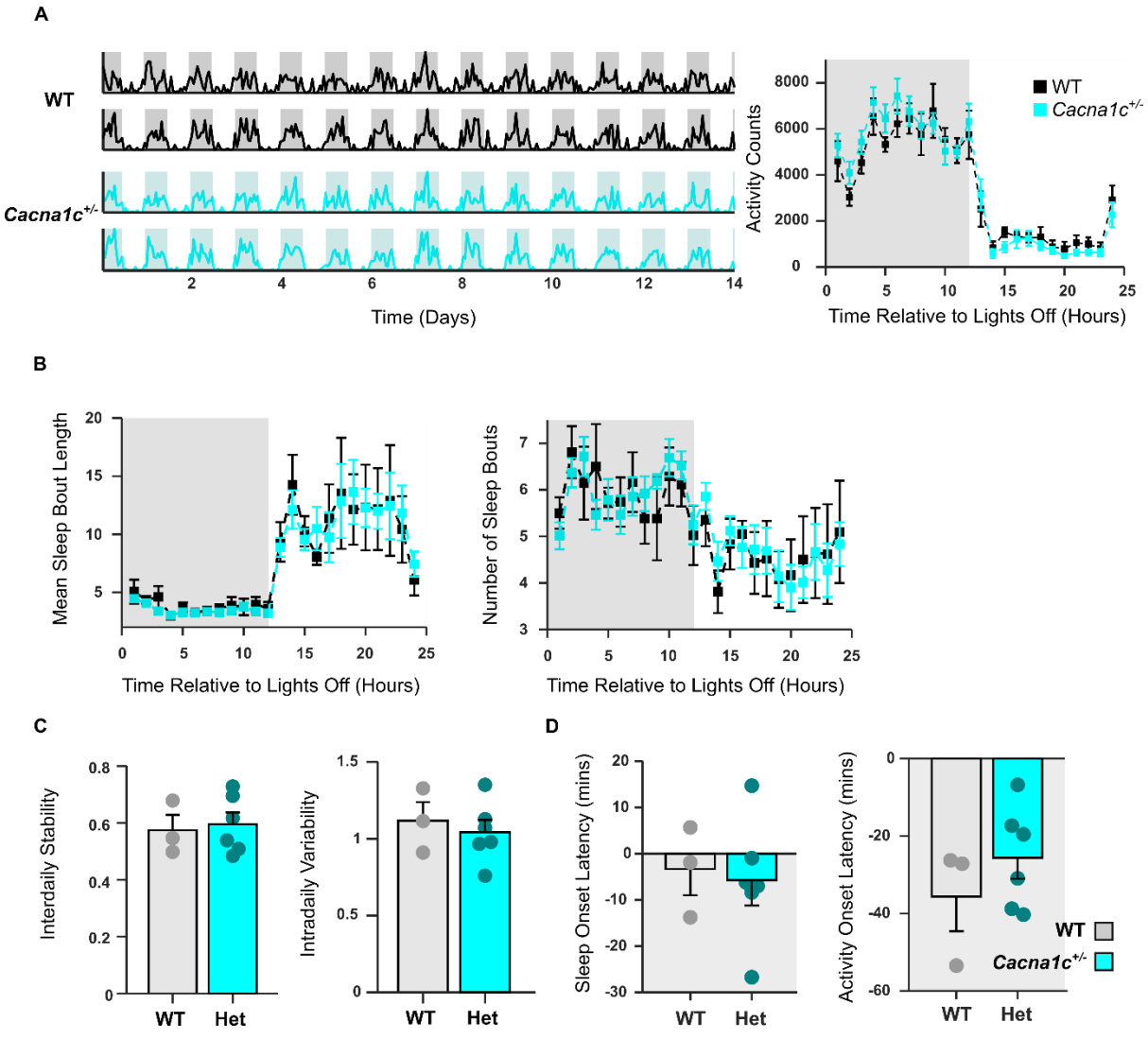

***Figure 4.1* | Robust circadian rhythms in WTs and *Cacna1c*$^{+/-}$ rats**
(A) (Left) Example actograms taken from two WTs (top rows, black) and two *Cacna1c*$^{+/-}$ rats (bottom rows, cyan) recorded over a duration of 14 days. Actograms indicate activity patterns over time (shaded area denotes lights-off period). (Right) Mean Activity profile for both genotypes. Activity profile depicts the hourly mean activity counts over the duration of the recording relative to lights-off.

(B) Mean immobility-defined sleep properties. (Left) Hourly mean sleep bout length. (Right) Hourly mean number of sleep bouts.
(C) Non-parametric measures of Circadian Rhythmicity. (Left) Interdaily stability. A measure of the stability of the circadian rhythm between days. (Right) Intradaily variability. A measure of the fragmentation of the circadian rhythm within days. Neither measure differed between genotypes (p>0.05, Student's t-test).
(D) Sleep latency measures. (Left) Latency between lights-off and sleep onset. (Right) Latency between lights-on and activity onset. Sleep latency was comparable between genotypes. (p>0.05, Student's t-test).
(Data presented as mean±SEM; WT: n=3; Cacna1c$^{+/-}$: n=6. WT in black, Cacna1c$^{+/-}$ in cyan. Shaded areas denote lights-off period)

CACNA1C has previously been associated with alterations in sleep onset latency both in rodents (Kumar et al., 2013) and humans (Byrne et al., 2013, Kantojärvi et al., 2017). To assess this here I compared sleep onset times relative to lights-on in both genotypes (**Figure 4.1D**). This analysis revealed sleep onset times slightly in advance, though close to lights-on in both genotypes. These times did not differ between genotypes (p=3.42; Student's t-test). I also characterised activity onsets relative to lights-off and similarly this was comparable between genotypes (p=0.791; Student's t-test).

In summary this analysis revealed robust circadian rhythms in *Cacna1c*$^{+/-}$ rats that did not differ between genotypes.

4.3.2. Circadian Re-Entrainment

While circadian rhythms were robust in *Cacna1c*$^{+/-}$ rats, previous work in *Cacna1c* knockout mice has revealed a loss of phase-shifting of circadian activity to light-pulses despite otherwise normal circadian activity (Schmutz et al., 2014). This might indicate a failure in these animals to entrain their circadian rhythms to changing light levels.

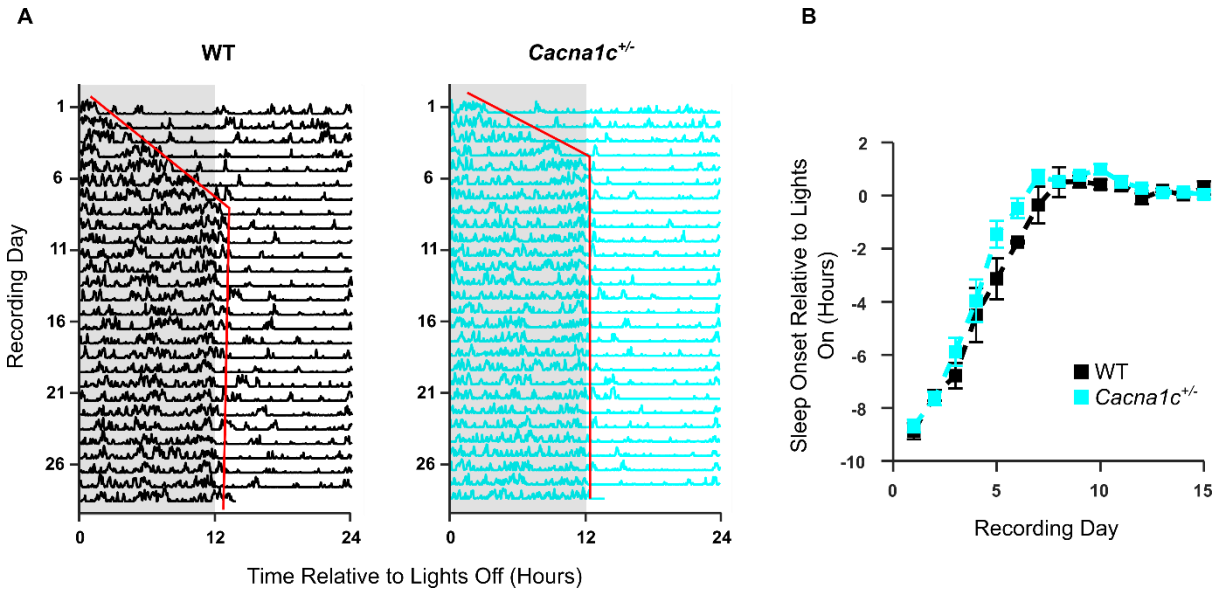

***Figure 4.2* | Re-entrainment of circadian rhythm to a 12-hour phase-shift**
(A) Example actograms taken from a WT (left) and *Cacna1c*$^{+/-}$ rat (right). Each row denotes one day of recording. The red line depicts sleep-onset (activity offset) which shifts over time in line with the new light-dark cycle. Shaded area denotes lights-off.
(B) Sleep onset time relative to lights-off. Time taken to adjust circadian rhythms to the new light-dark cycle did not differ between genotypes. (p>0.05, Repeated measures ANOVA). (Data presented as mean±SEM).
(WT: n=3; Cacna1c$^{+/-}$*: n=6. WT in black, Cacna1c*$^{+/-}$ *in cyan)*

To assess circadian re-entrainment here, I moved all animals from a reverse-lighting room to a normal lighting room thus phase-shifting their day by 12 hours. In response to the shifted light-dark cycle all animals showed an advanced sleep onset relative to their new lights-on time that became progressively less advanced over the following days (**Figure 4.2A**). To compare this between genotypes I assessed sleep onset latency every day following the phase-shift (**Figure 4.2B**). In both genotypes, their sleep onsets approached 0 around the 8th day of recording and then flattened off indicating a re-entrainment of their circadian activity to the new light-dark cycle. This analysis revealed a significant effect of time ($F_{14,98}$=138.4, p=5.93x10^{-58}) but no effect of genotype ($F_{14,98}$=1.02, p=0.441; Repeated measures ANOVA) indicating normal circadian re-entrainment in *Cacna1c*$^{+/-}$ rats.

Together with the circadian analysis in reverse-lighting conditions, this analysis reveals normal circadian activity in *Cacna1c*$^{+/-}$ rats that displays an adaptability to changing light-levels in line with that of WT counterparts.

4.4. Discussion

4.4.1. Key Findings

In this chapter I assessed circadian rhythms in *Cacna1c*$^{+/-}$ rats and found these to be normal. Additionally *Cacna1c*$^{+/-}$ rats showed robust re-entrainment of circadian rhythms to a circadian phase-shift.

4.4.2. Circadian Activity

To assess circadian rhythms I recorded activity across 2 weeks under reverse-lighting conditions and observed changing activity levels with changing light-levels as a metric for sleep. This analysis revealed that across all measures of circadian rhythms, *Cacna1c*$^{+/-}$ rats were normal. In some respects, this finding was surprising; *CACNA1C* shows a clear genetic relationship to sleep disorders (Shimada et al., 2010, Byrne et al., 2013, Parsons et al., 2013, Kantojärvi et al., 2017) and this gene shows widespread expression within the SCN (Nahm et al., 2005). On the other hand, previous animal work using these very same measures to

investigate sleep rhythms in relation to *Cacna1c* has revealed broadly normal circadian rhythms (Schmutz et al., 2014). This isn't a reflection on the method per se; actigraphy shows wide agreement with polysomnographic measures of sleep (McCall and McCall, 2012), but it may reveal a species-specific effect on sleep as all of the aforementioned genetic associations with sleep were in regard to human participants.

Alternatively the sleep deficits associated with *CACNA1C* may reflect a genotype x environment interaction effect. Sleep deficits in *Cacna1c* heterozygous mice have been observed, but only following a sleep deprivation or restraint stress protocol (Kumar et al., 2013). This might indicate an enhanced susceptibility to sleep deficits rather than a simple impairment. Though analysis here did not look at sleep rhythms following any kind of environmental insult, I did assess the adaptability of circadian rhythms following a 12-hour phase-shift. This kind of phase-shift is analogous to the jetlag that would arise after travelling half-way around the world. In both humans and rodents, typically ~1 day per hour of phase-shift is required to re-entrain circadian rhythms (Eastman and Burgess, 2009, Sellix et al., 2012). In both genotypes it appeared that a lower ~8 days was the required time, though the re-entrainment rate is highly variable and contingent on whether the shift is an advance or a delay (Eastman and Burgess, 2009); with a 12-hour shift it could be regarded as either. Importantly however this did not differ between genotypes. One might have expected to observe deficits given that SCZ is associated with an impairment in the entrainment of sleep rhythms to light-levels (Wulff et al., 2012), though this deficit is not related to the entraining of rhythms to shifting phases and it is not clear that there is any link between jetlag effects and SCZ (Katz et al., 2001). The previously mentioned *Cacna1c* actigraphy study did observe an effect of phase-shifting of rhythms to light-pulses (Schmutz et al., 2014), though this is not directly comparable to a complete phase-shift of the light-dark cycle and additionally this study used a *Cacna1c* knockout rather than heterozygous model.

4.4.3. Conclusion

In conclusion all the analysis presented here would suggest that in *Cacna1c*$^{+/-}$ rats, circadian rhythms are normal. It is important to acknowledge here that the n was low, particularly in relation to WTs. However very clear circadian patterns were still observable in *Cacna1c*$^{+/-}$ rats and so if there is any genuine circadian deficit in *Cacna1c*$^{+/-}$ rats that was missed by this analysis, it is most likely very subtle. This analysis did also concern only sleep-wake activity; many psychiatric disease related deficits are sleep stage specific (Kupfer and Foster, 1972, Waller et al., 1989, Emslie et al., 1990) and as such, a full EEG based study may shed more light on global sleep structure in relation to *CACNA1C* in the future.

5

Chapter 5

Offline Hippocampal Neurophysiology in *Cacna1c* Heterozygous Rats

5.1. Introduction

5.1.1. Sleep, Memory & The Hippocampus

The hippocampus has an essential role in 'offline' brain function, particularly in relation to sleep-dependent memory consolidation (Peigneux et al., 2004, Ramadan et al., 2009), and impairments to its function during sleep have been implicated in psychiatric disease (Phillips et al., 2012a, Suh et al., 2013, Altimus et al., 2015). Furthermore the characteristic electrophysiological signatures observed in this brain structure during sleep may rely on the activity of LTCCs (Chiovini et al., 2014, Kouvaros et al., 2015).

In this chapter I explore hippocampal neurophysiology during sleep and rest prior to and following exploration of the linear track in *Cacna1c*$^{+/-}$ rats, to understand how LTCCs support hippocampal function here, in addition to understanding how any deficits associated with *Cacna1c* heterozygosity may more broadly underlie sleep-associated deficits identified in psychiatric disorders.

5.1.2. The Memory Function of Sleep

Sleep has an essential role in fostering the consolidation of memory. Declarative memories show improvement not only after sleep (Plihal and Born, 1997) but also after naps, even as short as 60 minutes (Tucker et al., 2006, Lahl et al., 2008). This improvement appears to primarily be contingent upon the density of slow-wave sleep. Additionally, procedural memories, studied through motor tasks also show drastic improvements with sleep (Plihal and Born, 1997, Walker et al., 2003, Fischer et al., 2005, Korman et al., 2007), though this appears more reliant on REM sleep (Plihal and Born, 1997). Interestingly this improvement does not

correlate with the degree of performance participants achieved prior to sleep, indicating that this memory mechanism is distinct from that operating during wake (Walker et al., 2003). Memory of emotional events, over and above neutral events, is also improved with sleep (Payne et al., 2008), a phenomenon purported to be a REM sleep dependent effect (Nishida et al., 2009).

5.1.3. The Hippocampus in Memory Consolidation

The memory function of sleep appears to be heavily supported by the hippocampus. SWS shows an increase in hippocampal activation and this elevation in activity correlates with the degree of overnight memory improvement (Peigneux et al., 2004). Additionally SPW-Rs increase their occurrence during this time (Eschenko et al., 2008) and the frequency of their occurrence is predictive of memory improvement (Ramadan et al., 2009). In rats, disrupting or blocking SPW-Rs in the rest period following training on a radial-arm maze impairs memory consolidation (Girardeau et al., 2009, Ego-Stengel and Wilson, 2010).

How do SPW-Rs support memory consolidation? The answer to this appears to be dependent both on activity within this structure but also its relation to activity within the cortex. As discussed in Chapter 1, during SPW-Rs, place-cells recorded during exploration are reactivated in the same order on a compressed timescale, a phenomenon termed replay (Wilson and McNaughton, 1994, Lee and Wilson, 2002). Such replay is not merely a sleep phenomenon, with replay found during SPW-Rs occurring during immobility or in brief pauses in exploration (Foster and Wilson, 2006, Jackson et al., 2006, Karlsson and Frank, 2009). Replay also does not always occur in the same direction either, with 'reverse-replay' following the reverse direction to that of place-cell activation during wake (Foster and Wilson, 2006, Csicsvari et al., 2007, Diba and Buzsáki, 2007, Davidson et al., 2009). The type of replay occurring appears to be largely influenced by the animal's behavioural state (Wikenheiser and Redish, 2013). Replay may have an important role in plasticity. In one study CA3 and CA1 spike sequences recorded in vivo were reactivated in vitro. This reactivation was capable of inducing Schaffer-collateral plasticity but only when accompanied by dendritic depolarization set to match the envelope of depolarization observed during SPW-R activity in vivo (Sadowski et al., 2016). The authors hypothesized that such replay on a compressed timescale supported by SPW-R depolarization, may serve to enable spike-timing dependent plasticity so as to boost connectivity between learned place-cell sequences (Sadowski et al., 2011).

Outside of the hippocampus, cortical oscillatory activity may also have an important role in memory consolidation. NREM sleep is characterised by cortical slow-waves. These are high amplitude, low frequency (0.5-4Hz) synchronous oscillations that traverse the entire cortex as a travelling wave (Massimini et al., 2004). Importantly, the strength of these oscillations correlates with overnight memory improvement (Huber et al., 2004) and artificial

enhancement of slow-waves boosts memory consolidation further still (Marshall et al., 2006). In addition, NREM sleep (stage N2 in humans) is interspersed with faster 11-16Hz oscillations termed spindles (Morrison and Dempsey, 1941). These occur synchronously between the cortex and thalamus (Contreras et al., 1996) and are also predictive of overnight memory consolidation both in terms of their strength and their frequency of occurrence (Nishida and Walker, 2007).

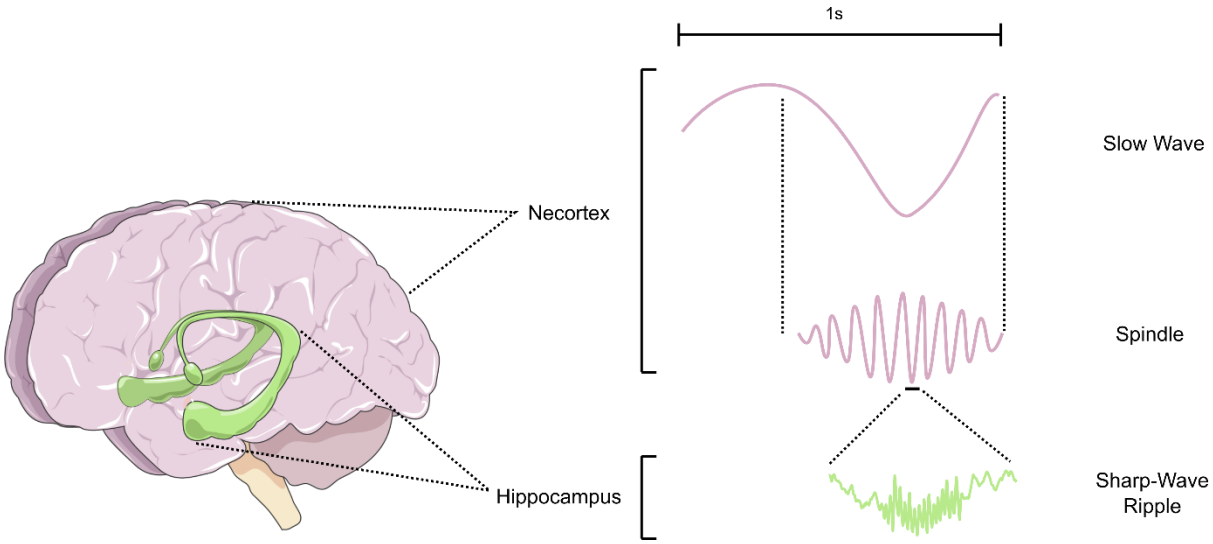

***Figure 5.1* | Two-stage model of memory consolidation schematic**
Schematic of temporal coupling between oscillatory activity in the hippocampus and cortex during sleep-dependent memory consolidation.

Concurrent cortical and hippocampal recordings reveal a high degree of temporal coupling between slow-waves, spindles and SPW-Rs (**Figure 5.1**) (Siapas and Wilson, 1998, Clemens et al., 2007, Staresina et al., 2015). The coupling here is revealed to be a 'top-down' phenomenon: The slow-waves modulate the timing of spindles, which in turn exact a modulating effect on SPW-Rs (Staresina et al., 2015). The role of such coupling has been hypothesized to relate to the 'Two-Stage Model' of sleep consolidation. This model supposes that memories are stored temporarily in the hippocampus but are integrated into more permanent storage in the cortex (Buzsáki, 1989) hence the integrity of remote memories even following hippocampal damage (Squire et al., 2010). Indeed activation of the hippocampus appears to reduce over repeated retrievals of a memory while cortical sites show the opposite pattern (Ross and Eichenbaum, 2006), implying an increased reliance on the cortex over time. Under the two-stage model, sleep-dependent coupling of these oscillations times the hippocampus to enable transfer of information to the cortex (Sirota and Buzsáki, 2005). Closer inspection of individual neuronal activity displays a loop-like activation pattern. Cortical cellular activation during slow-waves and spindles, entrains activation patterns in the hippocampus

during SPW-Rs. These in turn entrain the subsequent activity of cell populations in the cortex (Rothschild et al., 2017).

A loss of temporal rhythmic coordination unsurprisingly gives rise to memory deficits. With age, precise rhythmic timing is lost and as a result impaired sleep-dependent memory consolidation results (Muehlroth et al., 2019). Additionally in rodent studies, disruption to the timing of these rhythms impairs memory (Latchoumane et al., 2017). Artificially enhancing the precise timing of this rhythmic activity has the opposite effect, boosting overnight memory consolidation, both in rodents (Maingret et al., 2016, Latchoumane et al., 2017) and humans (Niknazar et al., 2015).

5.1.4. Memory Consolidation in Psychiatric Disease

Sleep-dependent memory consolidation is impaired in individuals with psychiatric disorders. This is most pronounced in SCZ patients with impairments observed both in declarative (Baran et al., 2018) and procedural (Wamsley et al., 2012, Genzel et al., 2015) sleep-dependent consolidation, but in patients with MDD a loss of overnight improvement in procedural learning is also observed (Dresler et al., 2011, Genzel et al., 2015). Importantly these effects are observed even after controlling for time spent asleep and consequently cannot arise purely as a result of the sleep-loss associated with these disorders.

These deficits may emerge from oscillatory impairment. Sleep spindle deficits for example are highly pronounced in patients with SCZ (Wamsley et al., 2012, Manoach et al., 2016, D'Agostino et al., 2018, Manoach and Stickgold, 2019) to the extent that this has been proposed as an endophenotype (Manoach et al., 2016, D'Agostino et al., 2018). It seems highly probable that this deficit, at least to some extent, underlies the loss of sleep-dependent memory consolidation in SCZ. Spindle deficits may reflect a broader impairment in oscillatory coupling observed in psychiatric disorders. In patients, PAC between spindles and slow-waves reveals a reduced co-ordination which in turn corresponds to a loss of overnight memory consolidation (Bartsch et al., 2019). Additionally in the MAM SCZ animal model, a neurodevelopmental model of SCZ generated through prenatal administration of methylazoxymethanol acetate (MAM) (Lodge, 2013), disrupted timing between SPW-Rs, spindles and slow-waves was observed. At a cellular level, this disrupted timing corresponded to a loss of cross-correlated activity between CA1 and prelimbic cortical pyramidal cells (Phillips et al., 2012a).

SPW-R oscillatory properties also appear to be altered in relation to psychiatric disease. In a mouse expressing a dominant negative mutation in DISC1, a SCZ-associated risk gene (Hennah et al., 2006), elevated SPW-R amplitude and abundance was reported (Altimus et al., 2015). A similar pattern of changes was observed in mice exhibiting a forebrain specific knockout of a calcineurin regulatory subunit. Additionally at a cellular level, this mouse

model displayed an enhancement of CA1 spiking activity during SPW-R events. Paradoxically however, this corresponded to an impairment in SPW-R associated replay (Suh et al., 2013).

To date, no assessment of SPW-R activity has been undertaken in animals expressing genetic variation in *CACNA1C*. Though not directly related to calcium signalling, DISC1 converges on many of the same downstream synaptic signalling pathways as Cav1.2 (Hashimoto et al., 2006, Kim et al., 2009), while calcineurin is directly involved in calcium mediated cellular signalling in synapses (Baumgärtel and Mansuy, 2012). Combined with the important role of *CACNA1C* in sleep, it seems feasible that disordered SPW-R oscillatory and cellular activity may be observed in *Cacna1c*$^{+/-}$ rats. To better understand how *Cacna1c* heterozygosity might be expected to impact on SPW-R activity we must first consider the role of LTCCs here.

5.1.5. L-Type Calcium Channels in Sharp-Wave Ripples

The literature on the role of LTCCs in SPW-Rs is sparse, though some evidence points to their important role in the regulation of these oscillatory events. In one study, LTCCs were shown to be critical in the activity of PV interneurons during SPW-R events. This study combined the use of glutamate uncaging with 3D two-photon imaging and found that at the level of the dendrite, PV interneurons exhibited supralinear summation of inputs generating a dendritic spike that propagated to other regions of the dendrite. The strength of this signal was shown to tightly correlate with the action potential output of the interneuron which incidentally occurred at ripple frequency. Use of nimodipine drastically reduced the magnitude of these dendritic spikes highlighting a key role for LTCCs here (Chiovini et al., 2014). Importantly PV interneurons have been demonstrated to be largely responsible for the driving of SPW-Rs within CA1 (Stark et al., 2014, Ognjanovski et al., 2017). The above study indicates that this may be reliant on the activity of LTCCs in the dendrite.

In vivo, use of the LTCC antagonist nifedipine, enhances the amplitude of the sharp-wave component of the SPW-R, though this was an age-dependent effect with the effect observed in adult but not aged rats (Kouvaros et al., 2015). Alterations in hippocampal LTCC density are observed with age which might explain the results here, yet this was observed as an increased LTCC density with age, which one would expect to give rise to the opposite effect to that observed in the prior study (Thibault and Landfield, 1996).

5.1.6. Chapter Aims

Though in vivo the effects are less clear, evidence for the importance of LTCCs in SPW-Rs would imply that *Cacna1c* heterozygosity might disrupt the mechanisms generating these oscillations. Additionally the clear pattern of disruption to these oscillations observed in other

genetic animal models of psychiatric risk indicate that disrupted SPW-Rs may underlie some symptoms of psychiatric disease.

In this chapter I will assess SPW-R properties in *Cacna1c*$^{+/-}$ rats to understand how reduced gene dosage of *Cacna1c* impacts SPW-R properties. In addition, SPW-Rs underlie the reactivation of individual neurons, possibly as part of the two-stage model of sleep dependent memory consolidation. To assess whether cellular activity patterns are altered during sleep and SPW-Rs as a result of *Cacna1c* heterozygosity I will also quantify cellular activation patterns in combination with oscillatory activity.

5.2. Methods

5.2.1. Animals

The same animals used in Chapter 3 were used here and these recordings were taken from the same sessions in which familiar and rotated linear track recordings were taken (see **Figure 3.1**).

Table 5. Summary table of number of animals used.
Number of animals used across number of session. Total number of recorded cells across all animals shown with range of cell numbers recorded in individual animals denoted in brackets.

Section	Number of Recording Days	Number of Sessions	Genotype	Number of animals	Number of cells	Number of place-cells
Sharp-wave ripple properties	1	2 (pre-sleep and post-sleep)	WT	5	N/A	N/A
			Cacna1c+/-	7	N/A	N/A
Sharp-wave ripple single unit activity	1	2 (pre-sleep and post-sleep)	WT	5	126 (2-51)	N/A
			Cacna1c+/-	7	144 (4-54)	N/A
Sharp-wave ripple pairwise activity	1	3 (pre-sleep, run and post-sleep)	WT	5	N/A	77 (2-24)
			Cacna1c+/-	7	N/A	95 (2-38)

Bayesian decoding (familiar linear track)	1	2 (run and post-sleep)	WT	5	126 (2-51)	N/A
			Cacna1c+/-	7	144 (4-54)	N/A
Bayesian decoding (linear track in novel orientation)	1	2 (run and post-sleep)	WT	5	100 (2-51)	N/A
			Cacna1c+/-	7	112 (2-42)	N/A

5.2.2. Recording Protocol

All sleep electrophysiology recordings were taken prior to and following the linear track session (as described in ***3.2***).

5.2.3. Data Analysis

5.2.3.1. Ripple Detection

Ripples were detected using an automated algorithm developed in-lab by Ullrich Bartsch. LFP signals were first bandpass filtered between 120 and 250Hz (**Figure 5.2A**) and z-scored to normalise. Signals were then rectified and the amplitude envelope of the rectified signal was obtained using cubic spline interpolation. Ripples were defined as events 3.5SDs greater than the mean amplitude envelope, with a duration of 25-500ms and at least 50μV in amplitude. The start and end times were defined as the point at which the signal fell below 1SD of the mean envelope. Individual ripple characteristics were obtained by taking the fourier transform of LFP segments falling between the start and end times of individual ripples.

5.2.3.2. Spike-Ripple Analysis

Spike participation in SPW-Rs was characterised as described by Suh et al. (2013). Spikes were defined as ripple-associated if occurring any time between 300ms before the start time of the SPW-R and up to 300ms after the end-time. Spikes per ripple was defined as the mean number of ripple-associated spikes for any cells with at least one spike in at least one SPW-R event. Spike participation was defined as the fraction of SPW-R events in which a cell fired at least one spike.

5.2.3.3. Cross-Correlation

Cross correlations were computed using in-lab toolboxes. Frist spike trains were taken from all cells identified as place-cells in Chapter 3. For each pair of spike trains, $f_1, \dots, f_m$ and $g_1, \dots, g_n$, the time lags between all $m \times n$ pairs of spike times were computed as $lag_{ij} = |g_j - f_i|$. These lags values were used to generate a cross-correlation histogram with a bin-size of 10ms within a 1s window. As cross-correlations are highly sensitive to the firing rates of individual cells (de la Rocha et al., 2007) the cross-correlations were normalized by the number of spikes fired by each cell.

To compute the significance of the cross-correlation, 1000 surrogate correlations were computed for each cell pair by shuffling the ISI. This disrupts the firing patterns between cell pairs but maintains the interval structure and firing rates of individual cells (Gerstein, 2004). Cell-pairs were regarded as significantly correlated if their correlation coefficient was >95% of the correlation values generated from surrogate data.

To compute cross-correlations during sleep sessions, spike trains were limited to periods between the start and stop time of SPW-Rs and cross correlations were computed on these. For cross-correlations during active periods, spike trains were limited to periods from the familiar track session when the animal ran above 5cm/s.

For place-field distance correlograms, place-field distance was estimated as the absolute distance between place-field peaks. For cell-pairs that were active in both run directions the average distance in each direction was used. All cross-correlations were normalized by z-scoring for the purposes of visualisation and the cross-correlations of cell-pairs with equivalent distances between place-fields were averaged. To perform linear regression, the time-lag at which the peak cross-correlation was found was used to generate a time-lag - place-field distance tuple for every cell-pair.

5.2.3.4. Replay Detection

To detect replay, a Bayesian decoding algorithm was trained on data from the linear track session using the method described in ***3.2.2.4***. This algorithm was then applied to spike trains occurring within SPW-R windows to obtain a posterior probability matrix for each SPW-R, however using a shorter time window of 10ms than that used to decode position during wake. The decoding algorithm was applied to each run direction separately and thus a posterior probability matrix corresponding to each run direction was obtained for each SPW-R event.

For this analysis, spikes from all individual cells across every animal during periods of running were used to decode position (see **Table 5** for numbers used).

To characterise the strength of replay, a weighted correlation was calculated for each posterior probability matrix as described by Wu & Foster (2014). This first involved calculating the weighted mean as denoted by:

$$m(x;w) = \frac{\sum_{i=1}^{N} w_i x_i}{\sum_{i=1}^{N} w_i}$$

Whereby w_i denotes each successive probability matrix pixel value, x_i denotes the time value of that pixel and N, the total number of pixels. This same calculation is also applied to the position domain to obtain a value for both the weighted mean with respect to time, m(x;w), and the weighted mean with respect to position m(y;w).

Next, weighed covariance is given by the formula:

$$cov(x,y;w) = \frac{\sum_{i=1}^{N} w_i (x_i - m(x;w))(x_i - m(y;w))}{\sum_{i=1}^{N} w_i}$$

Time-time covariances, cov(x,x;w) and position-position covariances, cov(y,y;w) are also obtained by using the weighed mean, m(x;w) in place of m(y;w) or vice versa.

Finally, the weighted correlation is denoted by:

$$corr(x,y;w) = \frac{cov(x,y;w)}{\sqrt{cov(x,x;w)cov(y,y;w)}}$$

Probability matrices were defined as exhibiting replay if they had a minimum weighted correlation of 0.4 and displayed a coverage of at least 50% of the total track length. Coverage of any position bin was defined by a peak probability > 1 / number of position bins.

The replay directionality ratio was defined as:

$$Directionality\ Ratio = \frac{|Corr_1 - Corr_2|}{Corr_1 + Corr_2}$$

Whereby $Corr_1$ denotes the weighted correlation for replay in left→right run direction and $Corr_2$ denotes the weighted correlation for replay in the right→left run direction.

5.2.4. Statistical Analysis

To compare two groups a t-test or non-parametric equivalent was used. When comparing distributions the Kolmogorov-Smirnov test was used. A chi-squared test was used to compare proportions. For the comparison of more than two groups, appropriate ANOVA's were used. To compare variances, Bartlett's test was used. When performing multiple comparisons Tukey post hoc tests were used if statistically significant results had been identified by the prior statistical test.

For the linear regression analysis presented in ***5.3.3.3*** place-field distance, genotype and sleep session were entered as predictor variables with dummy indicator variables used for genotype and sleep session.

All data is presented as mean±SEM or median±inter-quartile range for non-parametric data, unless stated otherwise.

5.3. Results

5.3.1. Sharp-Wave Ripple Characterisation

To characterise sleep electrophysiology in both genotypes I first quantified SPW-R characteristics before and after track runs in the familiar and novel orientation. SPW-Rs were clearly visible in the LFP of both genotypes (**Figure 5.2A**) and their filtered waveforms looked comparable between genotypes (**Figure 5.2B**, *left*). To further investigate this I characterised key properties of all ripple events including the frequency, amplitude, and event length (**Figure 5.2B**). Distributions of all key properties across every ripple event during each sleep session were comparable between genotypes (p>0.05; Kolmorgrov-Smirnov test).

Ripple properties have previously been observed to change following learning (Eschenko et al., 2008). To assess whether running on a track resulted in any changes to the ripple properties I next assessed whether these properties differed between the pre and post sleep periods by comparing mean values (**Figure 5.2C**). Analysis here revealed comparable ripple properties both pre and post the run session in both genotypes (ripple frequency: $F_{1,20}$=0.16, p=0.692; ripple amplitude: $F_{1,20}$=0.7, p=0.414; ripple length: $F_{1,20}$=0.09, p=0.767; Two-way ANOVA). Additionally no effects of genotype or genotype interaction effects were observed (p>0.05, Two-way ANOVA). Ripple density (**Figure 5.2D**), a measure of the frequency of occurrence of ripples was also comparable between genotypes ($F_{1,20}$=0.14, p=0.71; Two-Way ANOVA) with no change observed between sleep sessions ($F_{1,20}$=, p=0.226; Two-way ANOVA).

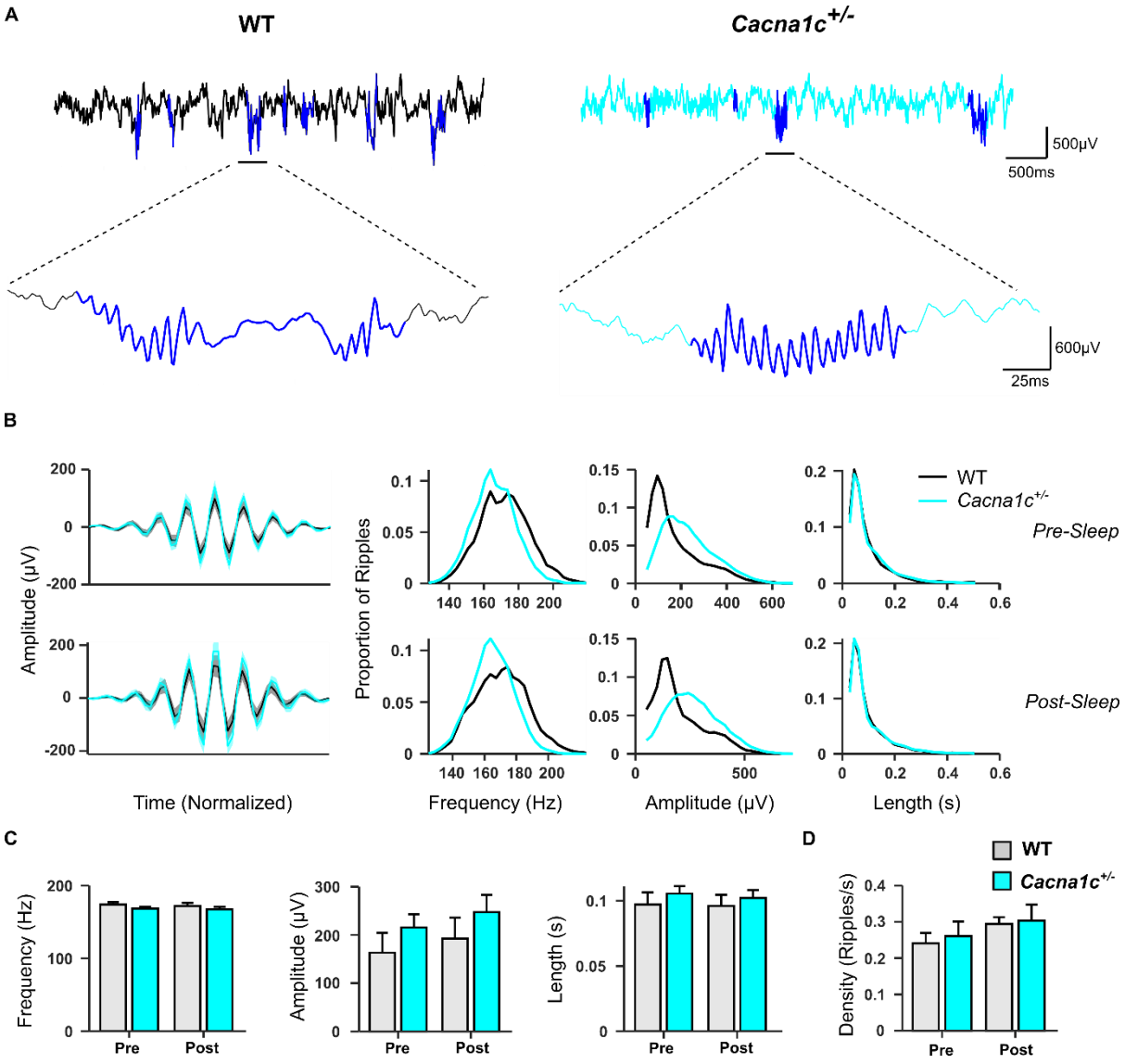

***Figure 5.2* | Sharp-wave ripple properties during sleep pre & post runs on a familiar track**
(A) Raw LFP taken from post-sleep periods from a WT (*left*) and *Cacna1c*$^{+/-}$ rat (*right*). Top trace shows 5s of LFP with detected ripples shown in blue. Bottom trace shows zoomed in 300ms depicting individual sharp-wave ripples.
(B) Key ripple properties shown for pre and post-sleep periods. Distributions of ripple properties did not differ between genotypes in either condition. ($p>0.05$, Kolmogorov-Smirnov test).
(C) Comparison of mean ripple properties between pre and post-sleep periods. No genotype or sleep period effect were observed for any ripple properties (Mean±SEM; $p>0.05$, Two-way ANOVA).
(D) Ripple density (number of ripples per second) was comparable between genotypes (Mean±SEM; $p>0.05$, Two-Way ANOVA).
(Pre-sleep: WT, n=2683; Cacna1c$^{+/-}$*, n=4260 ripple events; Post-sleep: WT, n=2868; Cacna1c*$^{+/-}$*, n=5046 ripple events. WT: n=5 rats; Cacna1c*$^{+/-}$*: n=7 rats. WT in black, Cacna1c*$^{+/-}$ *in cyan)*

While SPW-Rs were observed to be normal in *Cacna1c*$^{+/-}$ rats, I next set out to assess whether the modulation of spiking activity by these oscillations was intact. Ripple-modulated spikes were visible in both genotypes (**Figure 5.3A**). To quantify the degree of this modulation I first assessed the number of spikes fired per place-cell per SPW-R event (**Figure 5.3B**) both in

the pre and post sleep sessions. This revealed a significant effect of genotype with *Cacna1c*$^{+/-}$ rats displaying increased spiking per ripple ($F_{1,337}$=6.44, p=0.012) though no effect of session ($F_{1,337}$=0.04, p=0.842; Two-way ANOVA).

I next assessed whether the proportion of all ripple events that cells were active in (**Figure 5.3C**) was also altered. This measure was not contingent upon session in either genotype (session effect: $F_{1,337}$=0.41, p=0.522), however again *Cacna1c*$^{+/-}$ rats showed a significant increase in spike-ripple participation across both sessions ($F_{1,337}$=22.5, p=3.07x10^{-6}). Together, this analysis reveals an enhanced propensity for spiking – presumably due to increased excitability of cells – in *Cacna1c*$^{+/-}$ rats during SPW-R events.

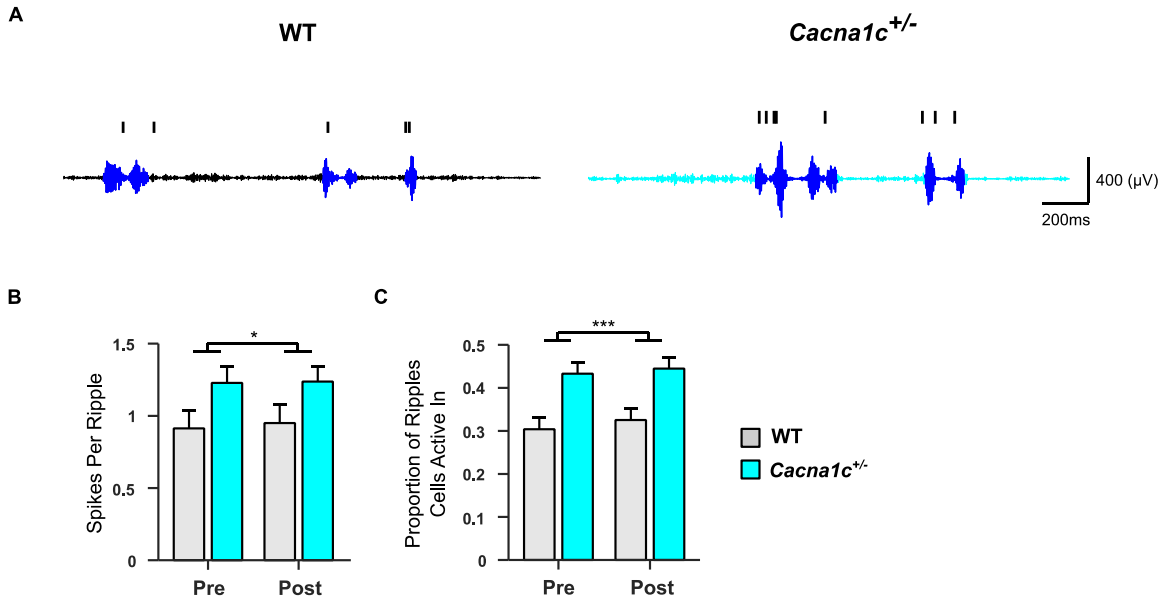

***Figure 5.3* | Spike participation in sharp-wave ripples**
(A) Representative ripple-modulated spiking. Ripple-frequency-filtered (120-250Hz) LFP shown (*bottom*) with spike trains from single cell shown (*top*) from a post-sleep period following a familiar track run session. (Sharp-wave ripple events in blue).
(B) Mean spikes fired per ripple per cell shown for pre and post-sleep period. *Cacna1c*$^{+/-}$ rats showed significantly more spikes per ripple in both sleep sessions (*p<0.05, Two-way ANOVA).
(C) Mean proportion of sharp-wave ripple events cells fired at least one spike in shown for pre and post sleep period. *Cacna1c*$^{+/-}$ rats fired spikes in significantly more sharp-wave ripple events than WTs in both sleep sessions. (***p<0.001, Two-way ANOVA).
(Data presented as mean±SEM; WT: n=77 cells; Cacna1c$^{+/-}$*: n=95 cells. WT in black, Cacna1c*$^{+/-}$ *in cyan)*

5.3.2. CA1 Network Activity

SPW-R activity corresponds to robust increases in synchronous firing in the hippocampus (Ylinen et al., 1995). As such the alterations in SPW-R activity in *Cacna1c*$^{+/-}$ rats may give rise to more highly synchronous firing. To assess this I next assessed ripple-associated cross correlated firing between place-cell pairs during pre and post sleep (**Figure 5.4**) in addition to cross-correlated firing during track runs.

This analysis revealed a significant genotype x session effect (**Figure 5.4A**; $F_{2,3720}$=20.6, p=1.27x10^{-9}; Factorial ANOVA). However, a session by session comparison between genotypes revealed a significant reduction in peak cross correlation values during ripples in *Cacna1c*$^{+/-}$ rats compared to WTs (p<0.001; Tukey Test) during sleep sessions. Additionally WTs showed a reduction in peak correlations in the post-sleep session compared to pre-sleep (p<0.001; Tukey Test) while in *Cacna1c*$^{+/-}$ rats the magnitude of correlated firing was comparable between sleep sessions (p>0.05; Tukey Test).

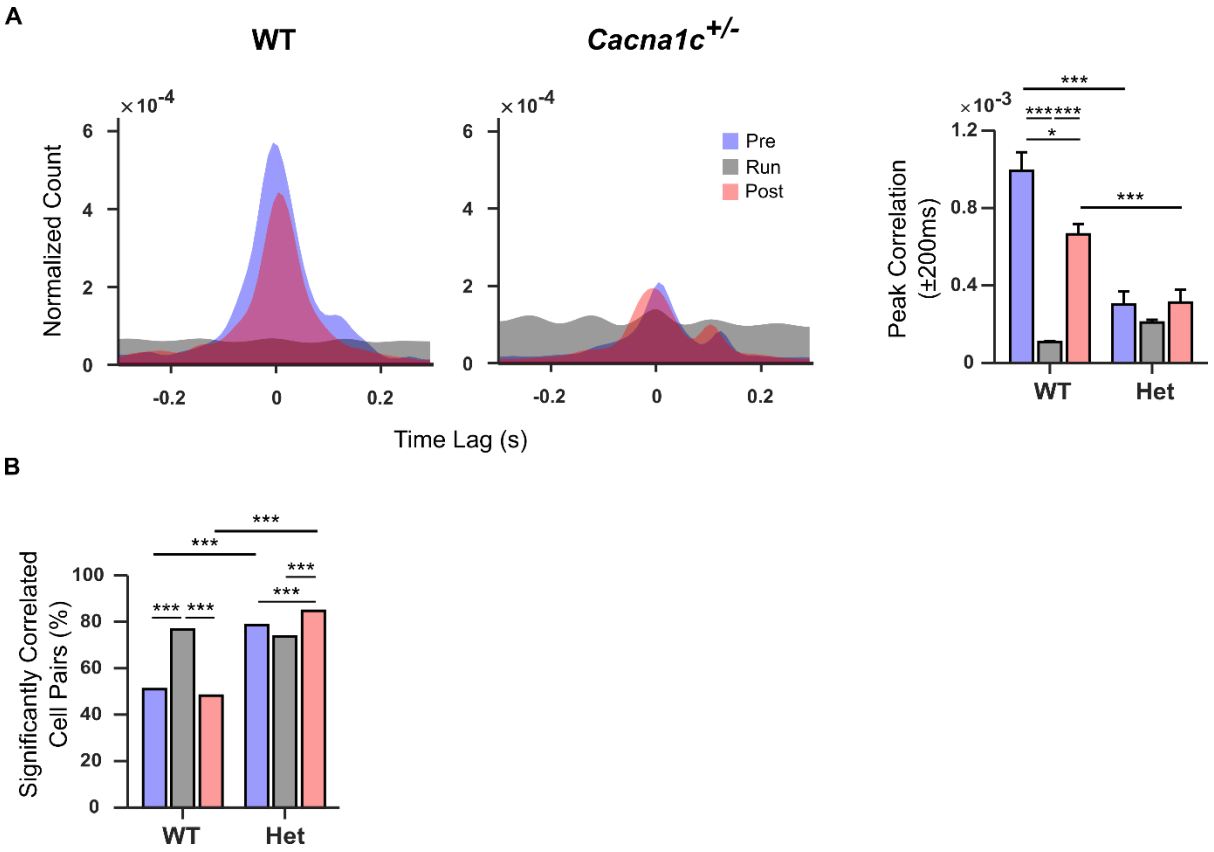

***Figure 5.4* | Cross correlations during sharp-wave ripple events in sleep vs. activity during wake on the familiar linear track**

(A) Cross correlations between all significantly correlated place-cell pairs. (Left) Mean cross-correlograms shown for WTs (*left*) and *Cacna1c*$^{+/-}$ rats (*right*) during ripple periods during sleep and while running above 5m/s during wake. (Right) Peak cross correlation values during 200ms window either side of zero lag. *Cacna1c*$^{+/-}$ rats showed a significant reduction in ripple-associated cross-correlated firing compared to WTs (mean±SEM; ***p<0.001; Factorial ANOVA with Tukey post-hoc tests).

(B) Proportion of cell pairs exhibiting significant (p<0.05, shuffle-corrected correlation co-efficient) cross correlations across each session of the familiar track session. *Cacna1c*$^{+/-}$ rats showed a significant increase in the proportions of cell-pairs with significantly correlated ripple-associated firing during sleep compared to WTs (***p<0.001, χ^2 test with Tukey post-hoc tests).

(WT: Pre-sleep n=371 cell pairs, run n=558 cell pairs, post-sleep n=351 cell pairs, Cacna1c$^{+/-}$*: Pre-sleep n=809 cell pairs, run n=759 cell pairs, post-sleep n=873 cell pairs; Pre-sleep in blue, run in black, post-sleep in Red)*

Next, I assessed the proportions of cell pairs with significantly correlated firing (**Figure 5.4B**). Again this analysis revealed very significant differences in the proportions of cell pairs with correlated firing ($p<0.001$; χ^2 test). A session by session comparison between genotypes revealed very significant increases in the proportions of correlated cell pairs in *Cacna1c*$^{+/-}$ rats during ripples compared to WTs ($p<0.001$; Tukey test). In WTs the proportion of correlated cell pairs during pre and post sleep was reduced compared to the run ($p<0.001$; Tukey test) while in *Cacna1c*$^{+/-}$ rats it increased in the post-sleep session ($p<0.001$; Tukey test).

This result indicates that in WTs the proportion of correlated cells reduces during ripple windows while the magnitude of correlated firing increases, while in *Cacna1c*$^{+/-}$ rats, the reverse is true.

5.3.3. Relationship of Ripple-Associated Firing to Behaviour

The distinct alterations to spike firing during ripple windows in the *Cacna1c*$^{+/-}$ rats could conceivably reflect or contribute to disrupted mechanisms of sleep-dependent memory consolidation**.** To investigate this I next sought to relate the changes in cross-correlated firing observed during sleep to firing patterns observed during wake.

The sequential reactivation of place-cells observed during SPW-Rs (Wilson and McNaughton, 1994, Lee and Wilson, 2002) implies that place-cells with fields in close proximity will be reactivated more closely in time than those with fields further apart (Karlsson and Frank, 2009). To assess this I sorted cell-pairs by distance between place-field peaks and arranged their cross-correlations accordingly (**Figure 5.5A**). This method of analysis has been previously shown to produce a 'v-shape' whereby cell-pairs in close proximity display a cross-correlation peak closer to zero lag than those with fields further apart (Karlsson and Frank, 2009). Though it was unclear that such a 'v-shape' was present in either genotype, *Cacna1c*$^{+/-}$ rats appeared to display more cross-correlated firing centred on zero and an analysis of the variance of time-lags revealed a significant increase in variance in the WTs compared to the *Cacna1c*$^{+/-}$ rats ($p<0.001$; Bartlett's test).

To further quantify the association of time-lag with place-field distance, I next performed a linear regression in which the absolute cross-correlation peak time-lag for each cell pair was plotted as a function of place-field distance. This analysis revealed a significant genotype x session x place-field distance effect (**Figure 5.5B**; $F_{1,2396}=5.72$, $p=0.017$). This effect was the result of a significant association between place-field distance and time-lag in the WTs but not the *Cacna1c*$^{+/-}$ rats during the post-sleep session (WTs: $\beta=4.6\text{x}10^{-4}\pm1.3\text{x}10^{-4}$, $t=3.4$, $p=6.4\text{x}10^{-4}$; Hets: $t=0.6$, $p=0.54$) while no association was observed between place-field distance and cross-correlation time-lag in either genotype in the pre-sleep session ($p>0.05$).

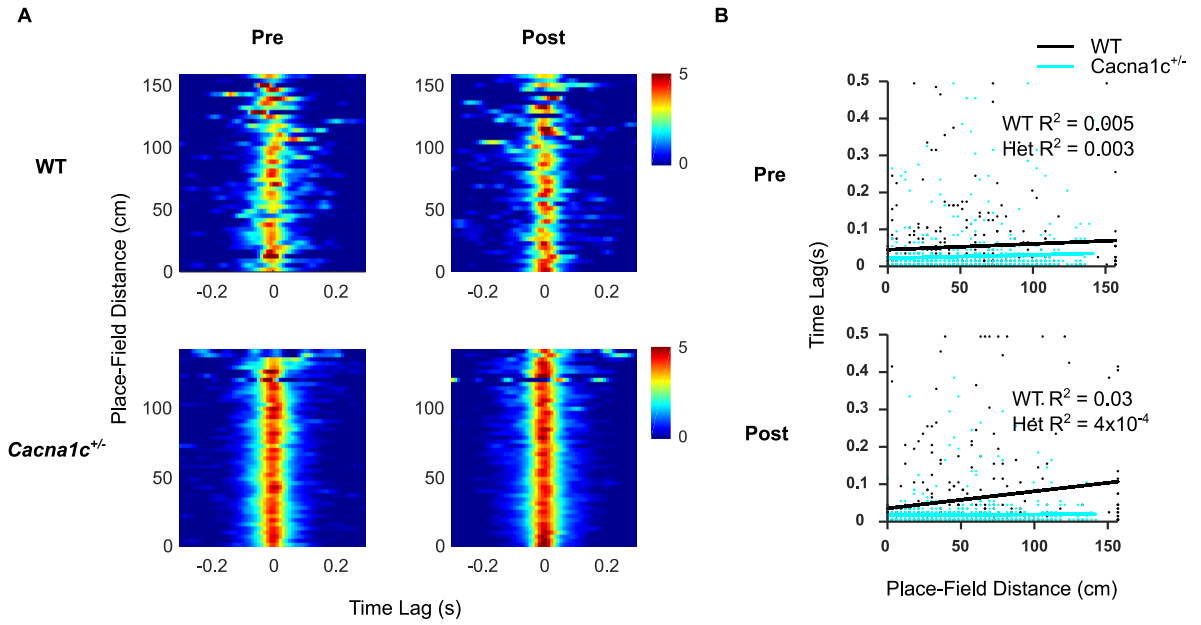

***Figure 5.5* | Relationship between spike-timing and place-field distance between place-cell pairs**
(A) Cross-correlation vs. place-field separation for all cell pairs. Each correlogram shows rows depicting normalized cross-correlations between cell pairs sorted in the y-axis by distance between place-field peaks. Each row is averaged over all cell-pairs with an equivalent place-field separation. Colour indicates strength of cross-correlation at each time-lag. Cross-correlograms shown for pre-sleep (*left*) and post-sleep (*right*) and for WTs (*top*) and *Cacna1c*$^{+/-}$ rats (*bottom*).
(B) Time-lag between cell-pairs plotted as a function of place-field separation for pre-sleep (*top*) and post-sleep (*bottom*). Neither genotype showed a significant association between place-field separation in the pre-sleep period ($p>0.05$, linear regression) while WTs but not *Cacna1c*$^{+/-}$ rats showed a significant association between place-field separation in the post-sleep period (WTs: ***$p<0.001$, *Cacna1c*$^{+/-}$ rats: $p> 0.05$, linear regression) (Solid line depicts linear regression fit)
(WT: Pre-sleep n=371 cell pairs, post-sleep n=351, Cacna1c$^{+/-}$*: Pre-sleep n=809 cell pairs, post-sleep n=873 cell pairs. WT in black, Cacna1c*$^{+/-}$ *in cyan)*

5.3.4. Replay of Run Trajectories During Sleep

The association between place-field distance and spike separation in the post-sleep session in WTs but not *Cacna1c*$^{+/-}$ rats might be indicative of an impairment in the reactivation of spatial trajectories. To investigate this further I next performed Bayesian decoding on spike trains from within ripple windows in the post-sleep period following the familiar linear track session (**Figure 5.6**). The decoder was trained separately on runs in the left→right direction and right→left direction and applied to the post-sleep period to detect replay of each trajectory direction.

To assess the strength of replay I computed the weighted correlation for every posterior probability matrix – a measure of the correlation between position and time. The distribution of weighted correlation values (**Figure 5.6B**, *left*) revealed a left-skewed distribution in both genotypes indicating a low propensity towards replay. In *Cacna1c*$^{+/-}$ rats however, a small but significantly increased weighted correlation was observed (**Figure 5.6B**,

right; p=2.12 x 10^{-16}; Wilcoxon rank-sum test) indicating an increase rather than an impairment in replay.

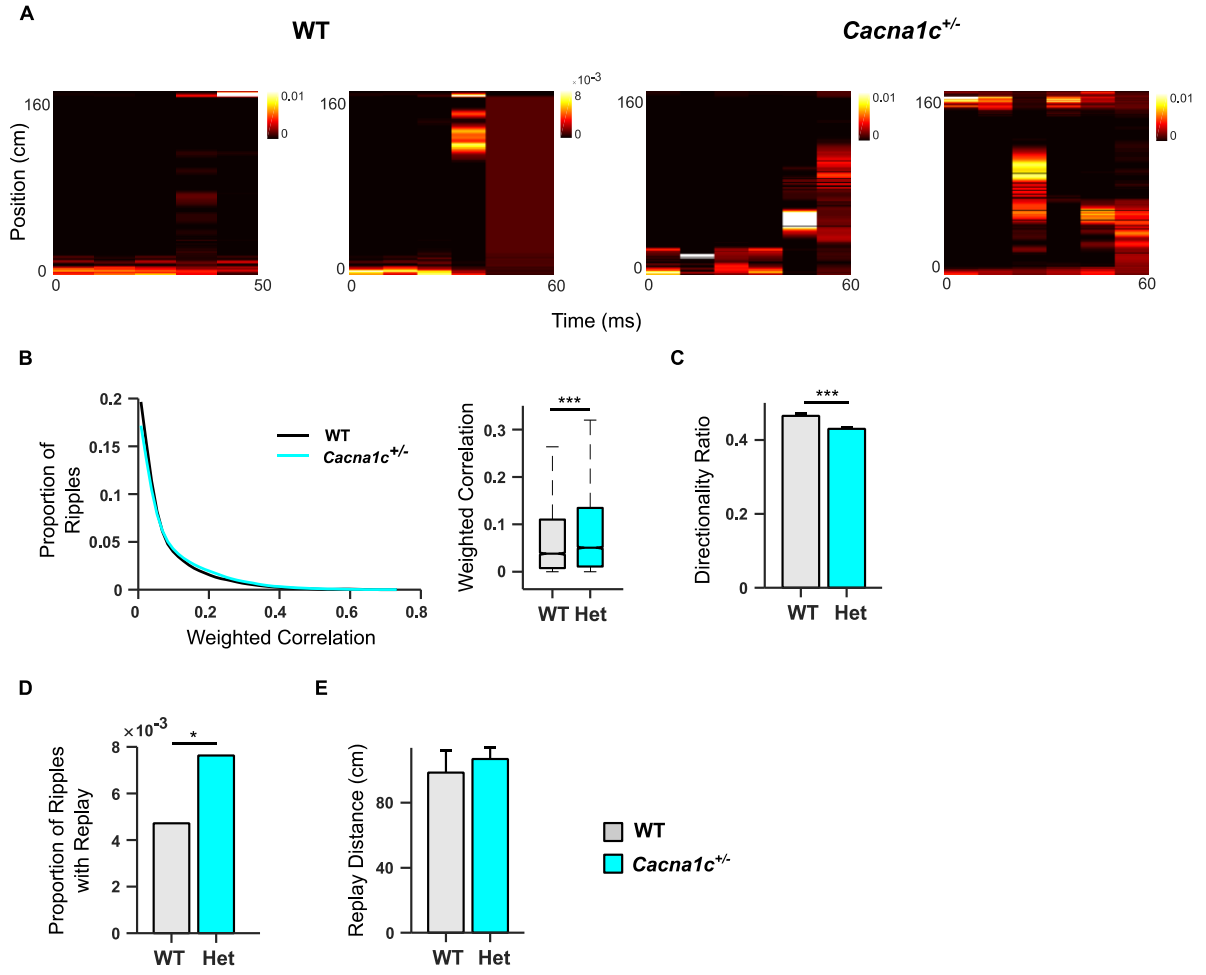

***Figure 5.6* | Replay of run trajectories during sleep following the familiar track run session**
(A) Example posterior probability matrices depicting decoded position during each 10ms bin of a ripple window, shown for WTs (*left*) and *Cacna1c*$^{+/-}$ rats (*right*).
(B) Weighted correlation scores of posterior probability matrices. (Left) Distribution of weighted correlation scores across all decoded ripple events. (Right) Median weighted correlation across all ripple events. *Cacna1c*$^{+/-}$ rats showed a significant increase in weighted correlation compared to WTs (Median±Upper/Lower quartiles, ***p<0.001; Wilcoxon rank-sum test).
(C) Directionality of replay defined as ratio between weighted correlation in the left→right and right→left direction. *Cacna1c*$^{+/-}$ rats displayed a reduction in replay directionality (Mean±SEM, p<0.001; Student's t-test).
(D) Proportion of ripple events exhibiting significant replay was higher in *Cacna1c*$^{+/-}$ rats than WTs (*p<0.05; χ^2 test).
(E) Mean distance covered by replay trajectories of significant replay events. (Mean±SEM; p>0.05; Student's t-test)
(WT: n=2426 ripple events, Cacna1c$^{+/-}$*: n=5046 ripple events. WT in black, Cacna1c*$^{+/-}$ *in cyan)*

To further assess this, I next quantified the number of candidate events that jointly satisfied a minimum weighted correlation threshold in addition to sufficient coverage of the track area and defined these events as replay events. The proportion of replay events was

very low in both genotypes (WTs: 0.47%, *Cacna1c*$^{+/-}$ rats: 0.76%), yet in *Cacna1c*$^{+/-}$ rats this proportion was higher (**Figure 5.6D**; p=0.035; χ^2 test).

While the degree of replay appeared higher in *Cacna1c*$^{+/-}$ rats, I next quantified the properties of these events to observe whether these were different between genotypes. First I assessed bias in the directionality of replay by characterising the ratio between weighted correlation values in each run direction (**Figure 5.6C**). Both genotypes had mean values below 0.5 indicating a tendency towards bidirectional replay however this was lower in *Cacna1c*$^{+/-}$ rats than WTs (p=9.78x10^{-7}; Student's t-test) indicating more bidirectional replay in *Cacna1c*$^{+/-}$ rats. Next, I assessed the distance covered by decoded trajectories classified as replay events, though here results were comparable between genotypes (**Figure 5.6E**; p=0.7; Student's t-test).

In contrast to the results of ***5.3.3.*** the previous analysis suggests increased replay in *Cacna1c*$^{+/-}$ rats however the strength of this replay was very low in both genotypes. This analysis concerned sleep following a familiar track session and as such these results may reflect a reduced demand for memory consolidation. To assess replay when learning may be more likely to have occurred, I next characterised replay during the post-sleep session following the novel orientation linear track session (**Figure 5.7**).

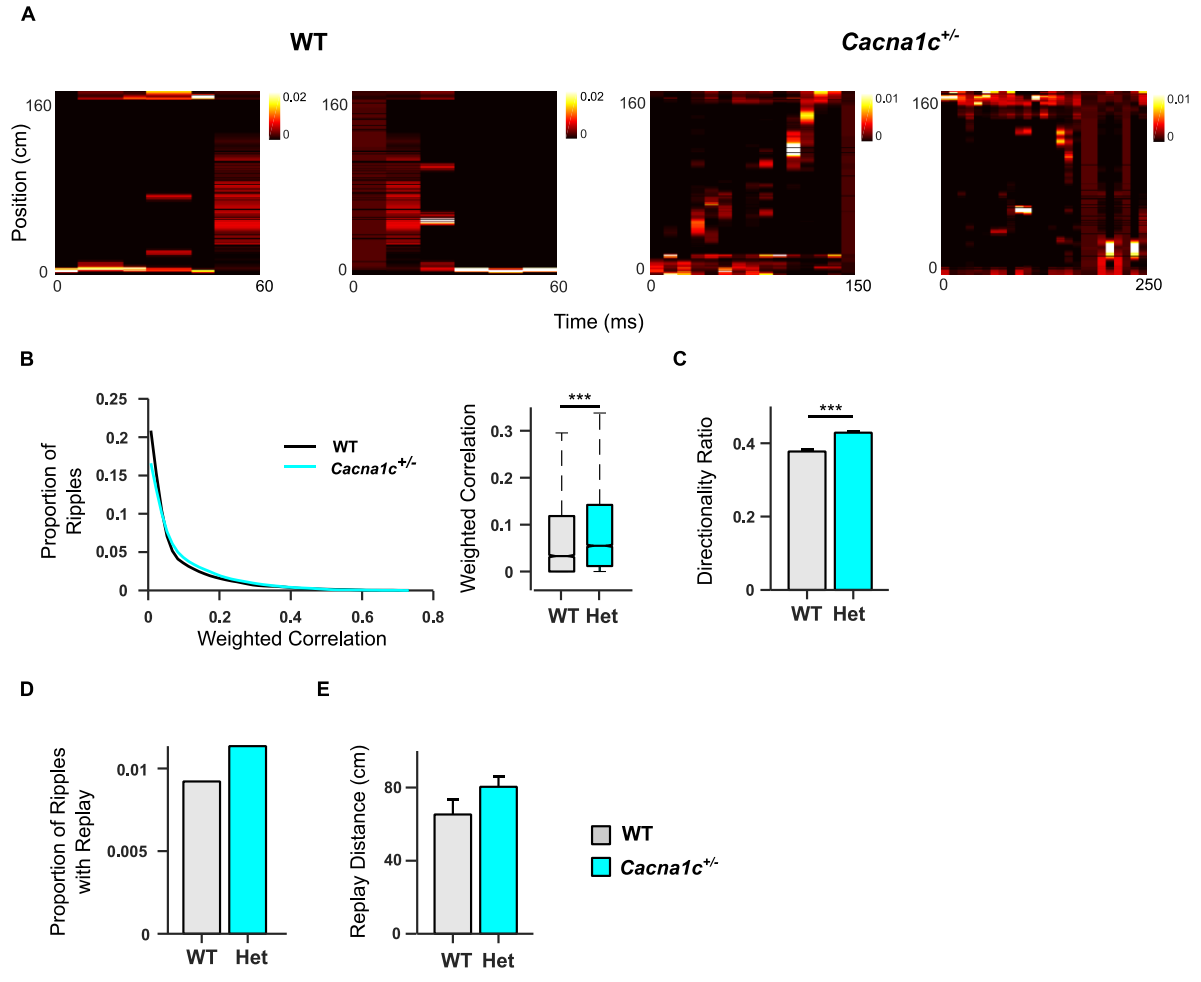

***Figure 5.7* | Replay of run trajectories during sleep following the novel track run session**
(A) Example posterior probability matrices depicting decoded position during each 10ms bin of a ripple window, shown for WTs (*left*) and *Cacna1c*$^{+/-}$ rats (*right*).
(B) Weighted correlation scores of posterior probability matrices. (Left) Distribution of weighted correlation scores across all decoded ripple events. (Right) Median weighted correlation across all ripple events. *Cacna1c*$^{+/-}$ rats showed a significant increase in weighted correlation compared to WTs (Median±Upper/Lower quartiles, ***p<0.001; Wilcoxon Rank-Sum Test).
(C) Directionality of replay defined as ratio between weighted correlation in the left→right and right→left direction. *Cacna1c*$^{+/-}$ rats displayed an increase in replay directionality (Mean±SEM, ***p<0.001; Student's t-test).
(D) Proportion of ripple events exhibiting significant replay (p>0.05; χ^2 test).
(E) Mean distance covered by replay trajectories of significant replay events. (mean±SEM; p>0.05; Student's t-test)
(WT: n=2519 ripple events; Cacna1c$^{+/-}$*: n=5024 ripple events. WT in black, Cacna1c*$^{+/-}$ *in cyan)*

Weighted correlation values were again left-skewed, indicating a low tendency towards replaying run trajectories, though the weighted correlation values were higher again in *Cacna1c*$^{+/-}$ rats than WTs (**Figure 5.7B**; p=3.02x10^{-58}; Wilcoxon rank-sum test). In contrast to the familiar track however, the proportion of candidate events meeting the criteria for replay was not different between genotypes (**Figure 5.7D**; p=0.198; χ^2 Test). A comparison of replay properties this time revealed an increase in the directionality of weighted correlations (**Figure 5.7B**; p=1.27x10^{-14}; Student's t-test) though both genotypes showed values below 0.5 indicating a tendency towards bidirectional replay. Finally the distance covered by replay event trajectories was similarly comparable between genotypes (**Figure 5.7E**; p=0.244; Student's t-test).

Taken together, analysis of replay following the familiar and novel linear track revealed an increased tendency towards the replay of wake trajectories in *Cacna1c*$^{+/-}$ rats than in WTs.

Table 6. Summary of findings reported in Chapter 5.

Test	Session	Effect	Statistical significance
Sharp-wave ripple properties	Pre-sleep (Familiar linear track)	Comparable frequency, amplitude, length and density	p>0.05
	Post-sleep (Familiar linear track)	Comparable frequency, amplitude, length and density	p>0.05
Sharp-wave ripple single unit activity	Pre-sleep (Familiar linear track)	Increased spikes fired per ripple and increased proportion of ripple events cells active in *Cacna1c*$^{+/-}$	p<0.05, p<0.001
	Post-sleep (Familiar linear track)	Increased spikes fired per ripple and increased proportion of ripple events cells active in *Cacna1c*$^{+/-}$	p<0.05, p<0.001
Sharp-wave ripple pairwise activity	Pre-sleep (Familiar linear track)	Increased proportion of significantly correlated cell-pairs during sharp-wave ripples in *Cacna1c*$^{+/-}$	p<0.001

		Reduced peak cell-pair correlation magnitude during sharp-wave ripples in *Cacna1c*$^{+/-}$	p<0.001
		Comparable lack of correlation between peak cross-correlation time-lag and place-cell distance	p>0.05
		Reduced variance in peak cross-correlation time-lags in *Cacna1c*$^{+/-}$	p<0.001
	Post-sleep (Familiar linear track)	Increased proportion of significantly correlated cell-pairs during sharp-wave ripples in *Cacna1c*$^{+/-}$	p<0.001
		Reduced peak cell-pair correlation magnitude during sharp-wave ripples in *Cacna1c*$^{+/-}$	p<0.001
		Loss of correlation between peak cross-correlation time-lag and place-field distance in *Cacna1c*$^{+/-}$	p<0.001
		Reduced variance in peak cross-correlation time-lags in *Cacna1c*$^{+/-}$	p<0.001
Bayesian decoding	Post-sleep (Familiar linear track)	Increased weighted correlation, reduced bidirectionality ratio of replay trajectories and increased proportion of ripples with replay in *Cacna1c*$^{+/-}$	p<0.001, p<0.001, p<0.05
		Comparable replay trajectory distance	p>0.05
	Post-sleep (Linear track in novel-orientation)	Increased weighted correlation and bidirectionality of replay trajectories in *Cacna1c*$^{+/-}$	p<0.001, p<0.001
		Comparable proportion of ripples with replay and replay distance	p>0.05

5.4. Discussion

5.4.1. Key Findings

Analysis of hippocampal LFP during sleep and rest revealed normal SPW-R oscillations in *Cacna1c*$^{+/-}$ rats however analysis of spiking activity revealed an elevated participation of *Cacna1c*$^{+/-}$ pyramidal cells in these oscillations. Additionally analysis of network activity during SPW-R events showed that *Cacna1c*$^{+/-}$ rats displayed a significant increase in the proportion of cross-correlated cells during ripples yet the magnitude of these correlations was significantly reduced. Additionally a loss of relationship between the timing of correlated firing and place-field proximity was observed in *Cacna1c*$^{+/-}$ rats. Finally to better understand the functional relevance of the alterations in spiking activity during ripples I looked for evidence of replay.

While neither genotype revealed strong evidence for replay under these conditions, this analysis revealed potential enhancement of replay in *Cacna1c*$^{+/-}$ rats compared to WTs.

5.4.2. Sharp-Wave Ripple Properties

All ripple properties assessed here were shown to be normal in *Cacna1c*$^{+/-}$ rats. This was surprising in many respects, given that a) altered SPW-R properties are observed in other genetic models of psychiatric disease (Suh et al., 2013, Altimus et al., 2015) and b) in vitro evidence points to an important role of LTCCs in SPW-R generation (Chiovini et al., 2014). What this in vitro evidence means in vivo is less clear. As discussed in ***5.1***, SPW-R alterations are observed in rats after nifedipine administration yet this effect shows a peculiar age dependency (Kouvaros et al., 2015). The results presented here however, would point to a limited dependence of SPW-R generation on LTCCs.

Alternatively, one might expect an indirect ripple effect to be observed. *Cacna1c* is associated with impaired Schaffer-collateral plasticity (Moosmang et al., 2005, Tigaret et al., 2020) and, given the importance of this process in SPW-R generation (Schlingloff et al., 2014), such a deficit here might be expected to affect ripple properties. There is some evidence to suggest this is the case – one study found that reducing CA3 output to CA1 led to a reduction in ripple frequency (Nakashiba et al., 2009) however this involved reducing input altogether rather than plasticity specifically. LTP induction in vitro can lead to the emergence of SPW-R - like oscillations (Behrens et al., 2005). Whether such a phenomenon occurs in vivo is unclear but SPW-R occurrence appears to increase following learning and such a phenomenon is blocked by NMDA receptor antagonists (Girardeau et al., 2014). However the role of Schaffer-collateral plasticity specifically here is unknown. Certainly these oscillations are very important in the induction of this form of plasticity (Sadowski et al., 2016), but whether this has any role in the generation of SPW-R's is yet to be elucidated. The evidence presented here, though indirectly, would suggest not.

5.4.3. Spiking Activity During Sharp-Wave Ripples

Analysis of spiking activity in relation to SPW-Rs revealed a significant increase in *Cacna1c*$^{+/-}$ rats, both in the spikes emitted per ripple event and the proportion of ripple events cells were active in. This would suggest an increased excitability of pyramidal cells in *Cacna1c*$^{+/-}$ rats during SPW-Rs. The normal mean firing rate profiles in *Cacna1c*$^{+/-}$ rats (see Chapter 3) do not point to an enhancement in their basal excitability levels, however an alternative mechanism may underlie the SPW-R effects.

This enhanced excitability is ostensibly surprising, given the reduction to Schaffer-collateral plasticity observed in *Cacna1c*$^{+/-}$ rats. However research on the importance of this

pathway to CA1 spiking activity during SPW-Rs is conflicting. Computational modelling work reveals that CA1 spiking during SPW-Rs is driven predominantly by CA3 inputs (Taxidis et al., 2012), yet intracellular recordings in vivo have revealed that CA1 membrane potentials do not depend on input to CA1 during ripple events (Hulse et al., 2016), indicating that deficits to CA3 input should have limited bearing on spiking during ripples.

This does not however explain the *elevated* spike participation during SPW-Rs. The action of inhibitory interneurons may have an important role here. The firing of action potentials during ripples is tightly controlled by concurrent shunting inhibition (Csicsvari et al., 1999, English et al., 2014) and both excitation and inhibition are observed to increase (Csicsvari et al., 1999). Given the important role of LTCCs in dendritic spiking underlying PV interneuron activity during SPW-Rs (Chiovini et al., 2014), a loss of LTCCs here could have a disinhibiting effect, leading to an elevation in the excitability of CA1 pyramidal cells. Furthermore the role of LTCCs in the maturation of PV interneurons (Jiang and Swann, 2005) could lead to impairments that alter the EI balance maintained by these interneurons during SPW-Rs thus altering the intrinsic excitability of pyramidal cells during these events. These results also fit with other literature on ripples in psychiatric disease. As mentioned in ***5.1***, calcineurin knockout animals, an animal model of SCZ, also display strikingly similar ripple-associated firing alterations (Suh et al., 2013). Incidentally the calciuneurin-KO animal model also gives rise to deficits in latent inhibition (Miyakawa et al., 2003) as seen in *Cacna1c*$^{+/-}$ rats (Tigaret et al., 2020). This SPW-R firing alteration could therefore represent an important underlying mechanism in the development of certain SCZ-related symptoms.

5.4.4. Network Activity During Ripples

SPW-R's highly synchronize populations of cells in the hippocampus (Ylinen et al., 1995). On this basis I next set out to assess whether the changes in the excitability of cells during SPW-Rs corresponded to any changes in the synchronous activity of these neurons. This analysis revealed very significant reductions in the peak correlations of cell-pairs in *Cacna1c*$^{+/-}$ rats compared to WTs. This result was somewhat paradoxical given the enhanced participation of spikes in ripple events though this effect may have underlain the concurrent increase in the proportion of correlated cell pairs observed in *Cacna1c*$^{+/-}$ rats.

The role of CA3-CA1 input may have some role in the reduction of cross correlation magnitudes here. Reducing CA3-CA1 input in mice has previously been observed to reduce cross correlations between cell pairs in CA1 during SPW-Rs (Nakashiba et al., 2009). This may relate to the plasticity this pathway undergoes during ripples (Sadowski et al., 2016). As such, a loss of plasticity in *Cacna1c*$^{+/-}$ rats may have given rise to reduced connectivity between cells. This result also does not necessarily contradict the concurrent increase in the proportion of correlated cell pairs observed in *Cacna1c*$^{+/-}$ rats. Across the duration of sleep,

pyramidal cell and interneuron excitability reduces, possibly as part of the homeostatic downscaling effects of sleep. This effect also however co-occurs with an increase in correlated firing between cell-pairs and increased activation during ripples of these cells (Grosmark et al., 2012) - possibly a result of plasticity. As such while the majority of cells reduce their activity, the behaviourally relevant cell pairs continue firing during ripples (Kudrimoti et al., 1999, O'Neill et al., 2006). If this process is disrupted though, perhaps through interneuron dysregulation, the firing of cells across the board could still remain high during SPW-Rs. This could feasibly lead to a greater number of weakly correlated cells showing activation during ripple events. This effect is REM sleep-dependent (Grosmark et al., 2012) and thus future research into the REM sleep effects of *Cacna1c* heterozygosity would be warranted.

I next considered the behavioural relevance of such ripple-associated firing patterns and this revealed a loss of spike-timing dependence on place-field proximity between cell pairs. This result is consistent with that observed in the calcineurin knockout mice (Suh et al., 2013), lending further weight to the possibility that ripple-associated firing deficits may reflect a psychiatric-disease relevant pattern of dysfunction. In the calcineurin knockout mice study the authors posit that this loss of place-field distance spike-timing correlation reflects a deficit in replay, yet subsequent replay analysis in my own data did not appear to support this conclusion (see ***5.3.4***). Furthermore the correlation observed in WTs, though significant, was very weak (R^2=0.03). This apparent discrepancy may reflect the reactivation of experience unrelated to the linear track and previous research has revealed a role for replay in the activation of remote experiences in addition to recent experience (Karlsson and Frank, 2009, Gupta et al., 2010). Importantly however the rigidity of spike-timing in *Cacna1c*$^{+/-}$ rats, with most cross-correlations centred around zero, would indicate a tendency for cells to fire at once rather than exhibiting a sequential pattern of activation. As sequential activation is essential for the formation of a 'cognitive map' (Levy, 1996), a lack of variability in spike-timing may affect sleep-dependent memory consolidation.

5.4.5. Hippocampal Replay

In contrast to the cross-correlation analysis, Bayesian decoding of spatial location during ripples following runs on the familiar track revealed an enhancement rather than a deficit in replay in *Cacna1c*$^{+/-}$ rats compared to WTs. This was observed both by an increased proportion of ripple events fulfilling the criteria for replay and an increased weighted correlation of all ripple events. Importantly the weighted correlation values here were low. The fairly liberal threshold of 0.4 still resulted in less than 1% of all ripples being classified as containing replay. Here I hypothesized that the familiar track session did not have a high enough demand for learning and so also applied this replay detection to the sleep period following runs on the

rotated track. This however produced fairly similar results: the degree of replay was low in both genotypes, but a modest increase was observed in *Cacna1c*$^{+/-}$ rats.

Replay detection importantly is contingent upon the number of cells recorded (Foster, 2017). Consequently the cell count here may have restricted the ability to detect high numbers of replay, yet the similar effects observed after both sessions gives more merit to the possibility replay is enhanced in *Cacna1c*$^{+/-}$ rats. What mechanism could give rise to such an effect? There are a couple of possible contenders. Firstly the place-field size increases observed in Chapter 3 might increase the overlap of place-fields. This wouldn't increase replay per se, but it would increase the probability that cells re-fire together (Wilson and McNaughton, 1994) and therefore the probability of detecting replay. This may also at least partially explain the tendency for cross-correlations in the *Cacna1c*$^{+/-}$ rats to concentrate around zero lag. This would imply that replay isn't increased, just that more cells are involved in a replay event, an interpretation that would fit with both the elevated spike count during ripples and the increased proportion of correlated cells. Alternatively the effects on plasticity may have a role here. In human participants replay appears strongest for the least well remembered items (Schapiro et al., 2018). A deficit in plasticity would result in memories being weaker across the board which could correspond to an increase in replay to account for this. Whether a similar effect is observed in rodents is unknown, though replay has been observed to be higher for events an animal experienced less (Gupta et al., 2010).

If replay is enhanced in *Cacna1c*$^{+/-}$ rats, this result would run counter to what was observed in the calcineurin-KO mouse, where the increased spike participation in ripples corresponded to a loss of replay (Suh et al., 2013), suggesting *reduced* replay underlies psychiatric disease symptoms. An alternative hypothesis however proposes that elevated replay may underlie rumination that could give rise to symptoms of depression and anxiety (Heller and Bagot, 2020), though the evidence for such a viewpoint is currently very limited. Alternatively excessive replay could give rise to conflicting memory traces. In a context-dependent discrimination task, hippocampal activation of the incorrect context can lead to errors in the current one (Bulkin et al., 2016), presumably due to the conflict between representations. High levels of replay, enhanced cellular activation during SPW-Rs and overlapping place-fields could all increase the crossover between hippocampal representations which as a result could lead to cognitive deficits. Latent inhibition relies on balancing two conflicting associations – the deficits observed in *Cacna1c*$^{+/-}$ rats could partially result from some of the hippocampal deficits discussed here.

5.4.6. Conclusion

The results presented in this chapter highlight some important sleep/rest-dependent electrophysiological deficits. *Cacna1c*$^{+/-}$ rats display normal SPW-R's yet their cellular

activation during these events is enhanced. Importantly this is an effect also seen in another animal model of psychiatric disease. This lends weight to the possibility that this is a mechanism underlying certain symptoms of these disorders.

A closer inspection of cellular activation during SPW-R's revealed a higher proportion of correlated cell pairs yet a reduced firing correlation within each pair. Increased SPW-R activation may have given rise to the elevated proportion of correlated cell-pairs, yet plasticity deficits may have reduced their relative correlated firing magnitude. Presumably these effects would give rise to deficits in sleep-dependent memory consolidation. The analysis here suggested that replay, a potential mechanism underlying memory consolidation was enhanced, though how this relates to memory consolidation and by extension the cognitive deficits associated with *CACNA1C* remains to be determined.

A limitation to this analysis is that its focus was constrained to the hippocampus. Sleep-dependent memory consolidation unites the hippocampus with the cortex through the activity of spindles and slow-waves. A future study making use of cortical recordings may provide further insight into how these SPW-R related deficits fit in with the broader picture of sleep-dependent memory consolidation. This process is widely implicated in psychiatric disease and the research presented here only gives further credit to the importance of this line of enquiry.

6

Chapter 6

Susceptibility to Ketamine Administration in *Cacna1c* Heterozygous Rats: A 'Two-Hit' Model of Psychiatric Risk

6.1. Introduction

6.1.1. Interacting Biological Pathways in Psychiatric Disease

The polygenic nature of psychiatric disorders (Purcell et al., 2009, Purcell et al., 2014, Schizophrenia Working Group of the Psychiatric Genomics Consortium, 2014) renders it highly likely that in individual sufferers, multiple biological pathways are disrupted via the diverse effects of multiple risk gene variants (Purcell et al., 2014). In addition genetic risk cannot solely explain liability to psychiatric disease (Sullivan et al., 2003, Sullivan et al., 2012) with environmental risk factors playing a significant role also (Byrne et al., 2004, Allardyce and Boydell, 2006, Varese et al., 2012). Childhood trauma for example, a risk factor for psychiatric illness (Read et al., 2005, Carr et al., 2013), causes similar alterations in hippocampal size (Picken and Tarrier, 2011, Samplin et al., 2013) to what is observed in SCZ patients (Lawrie and Abukmeil, 1998, Nelson et al., 1998), indicating that genetic and environmental risk factors may converge on similar biological pathways.

The 'Two-Hit' model of SCZ hypothesizes that genetic risk generates a vulnerability to later environmental insult to confer susceptibility to SCZ (Bayer et al., 1999, Maynard et al., 2001). Experimental work does indeed point to a gene environment interaction in psychiatric risk (van Os et al., 2008, Wermter et al., 2010, Assary et al., 2018) though it appears that many risk factors interact across multiple stages of development (Pantelis et al., 2003b, Pantelis et al., 2005, Howes et al., 2017) leading some to propose instead a 'Multi-Hit' model of psychiatric risk (Davis et al., 2016). Under this model individual genetic risk factors may

leave biological pathways more susceptible to further insult from other factors across an individual's lifetime. *CACNA1C* gene variants thus likely confer vulnerability to psychiatric risk in combination both with additional risk gene variants and environmental insult to perturb normal brain function.

Up to this point I have considered the role of LTCCs in hippocampal function, yet calcium signalling represents only one component of psychiatric disease relevant biological dysfunction identified through genetic studies. The post-synaptic density and in particular NMDA receptor related genes have also been heavily implicated in the genetic risk for disorders such as SCZ and BPD (Doornbos et al., 2009, Kirov et al., 2012, Fromer et al., 2014) and additionally NMDA receptors and LTCCs appear to have a cooperative relationship in hippocampal function, particularly with regards to CA1 synaptic signalling (Grover and Teyler, 1990, Coussens et al., 1997, Freir and Herron, 2003, Kouvaros et al., 2015, Papatheodoropoulos and Kouvaros, 2016, Sachser et al., 2016).

In this chapter I introduce a 'second-hit' to *Cacna1c* heterozygotes via ketamine administration so as to combine NMDA receptor blockade with reduced LTCC expression. I hypothesize that convergent LTCC/NMDA receptor signalling in addition to the role for LTCCs in PV interneuron function will result in a heightened response to this 'second-hit', both in terms of locomotive and network activity, in *Cacna1c*$^{+/-}$ rats compared to WTs.

6.1.2. NMDA Receptor Dysfunction in Psychiatric Disorders

In the 1950s, phencyclidine (PCP), a non-competitive NMDA receptor antagonist, was brought to the attention of SCZ researchers due to the apparent similarity of the drug's effects with symptoms of SCZ (Luby et al., 1959, Meyer et al., 1959, Rosenbaum et al., 1959). Studies since then have revealed that non-competitive NMDA receptor blockade, through the use of antagonists such as ketamine and PCP, reliably mimics positive, negative, and cognitive symptoms of SCZ in healthy patients (Krystal et al., 1994, Adler et al., 1999, Umbricht et al., 2002, Krystal et al., 2005a) leading to these drugs to be referred to as psychotomimetics (Stodieck, 1983, Krystal et al., 1994). This is in contrast with previous psychotomimetic compounds such as amphetamine – thought to recapitulate the dopaminergic effects of SCZ (Lieberman et al., 1987) – which give rise to positive symptoms but not cognitive symptoms (Angrist and Gershon, 1970, Angrist et al., 1974, Krystal et al., 2005b) leading to a move from a predominantly dopamine-focused view of SCZ to one that now encompasses the role of glutamate also (Howes et al., 2015).

Work in SCZ patients also highlights the importance of glutamatergic signalling in this disorder, particularly with respect to NMDA receptors. PET scans making use of an NDMA receptor specific tracer, demonstrate a reduced level of NMDA binding in the hippocampus of medication-free SCZ patients (Pilowsky et al., 2006). Additionally in the prefrontal cortex of

SCZ patients, alterations in mRNA levels of different NMDA subunits are observed (Akbarian et al., 1996, Catts et al., 2016) and similar alterations are also observed in hippocampal tissue samples from SCZ patients (Law and Deakin, 2001, Stan et al., 2015). Some of these studies are ambiguous as to the direction of the effects on NMDA receptors, however if hypofunction is assumed to the cause then one would expect that additional hypofunction through the use of NMDA receptor antagonists could further exacerbate symptoms. Indeed that does appear to the case with ketamine administration to SCZ patients worsening both their positive and cognitive symptoms (Lahti et al., 1995, Malhotra et al., 1997).

6.1.3. NMDA Receptor Antagonism as an Animal Model of Psychosis

In rodents, administration of NMDA receptor antagonists gives rise to a range of cognitive impairments (Nabeshima et al., 1986, Noda et al., 2001, Abdul-Monim et al., 2003) possibly reflecting cognitive deficits in SCZ including impairments in novel object recognition (Asif-Malik et al., 2017) and spatial and non-spatial working memory (Pitsikas et al., 2008). Deficits in pre-pulse inhibition (PPI), a potential biomarker of sensorimotor gating deficits in SCZ (Mena et al., 2016), are also observed following administration of these compounds (Mansbach and Geyer, 1989, Depoortere et al., 1999, Martinez et al., 2000). PCP gives rise to social withdrawal which may reflect negative symptom domains (Sams-Dodd, 1995). Finally one of the most pronounced behavioural effects of these drugs is hyperlocomotion (Sturgeon et al., 1979, Irifune et al., 1991, Irifune et al., 1995, Jentsch et al., 1998, Chatterjee et al., 2011). Though not directly comparable to human SCZ symptoms, this effect appears to result from excessive dopamine as evidenced by inhibition through subsequent administration of dopamine receptor antagonists (Irifune et al., 1991, Jentsch et al., 1998) in addition to research demonstrating an elevation in dopamine release following NMDA receptor antagonist administration (Hernandez et al., 1988, Miller and Abercrombie, 1996, Schmidt and Fadayel, 1996), suggesting that NMDA receptor antagonism in rodents may also model dopamine dysfunction in rodents. NMDA receptor antagonism as a rodent animal model accordingly possesses both construct validity and face validity for SCZ.

As in SCZ patients, administration of NMDA receptor antagonists to animal models of SCZ can exacerbate the effects, as observed through increased levels of hyperlocomotion (Phillips et al., 2012b, Ji et al., 2013, Didriksen et al., 2017, Nielsen et al., 2017). Additionally effects such as PPI deficits are observed in the Df(h22q11)/+ mouse model, a genetic model mirroring the 22q11.2 deletion in humans (Morrow et al., 2018), but only when in combination with NDMA receptor antagonists (Didriksen et al., 2017), highlighting the importance of biological interventions in combination, rather than in isolation to produce psychiatric disease symptoms.

It is unknown whether the effects observed in the aforementioned studies are the result of these model's effects on NDMA receptor function. In the case of the Sp4 hypomorphic mouse model, though the gene in question here is not involved in NMDA receptor encoding, it appears to indirectly affect the expression of NMDA (Zhou et al., 2010). This would imply that the NMDA receptor antagonist-mediated exacerbation of hyperlocomotion in this model (Ji et al., 2013), is the result of a combined hypoglutamatergic effect. Alternatively, the Df(h1q21)/+ mouse models the human 1q21.1 human microdeletion, and this gene is thought to affect dopamine receptor expression (Grandy et al., 1992). The effects relating to PCP here were attributed to dopamine signalling (Nielsen et al., 2017) and as such the enhancing effects of NMDA receptor antagonism may result from multiple interacting biological pathways. In this chapter I will assess whether reduced LTCC expression is enhanced by NMDA receptor hypofunction by assessing locomotory effects in *Cacna1c*$^{+/-}$ rats following administration of ketamine. This could be regarded as an intervention in two distinct pathways however LTCCs and NMDA receptors also appear to have a highly co-operative relationship as we shall explore next.

6.1.4. LTCCs & NMDA Receptors

As previously reported, LTCCs play an important role in Schaffer-collateral plasticity (Grover and Teyler, 1990, Moosmang et al., 2005, Nanou et al., 2016, Tigaret et al., 2020). The deficits observed here are often reported to be NMDA receptor independent (Grover and Teyler, 1990, Tigaret et al., 2020), though only in regards to certain stimulation patterns. LTP brought upon by a tetanus stimulus for example remains intact with NMDA receptor antagonism, however switching to low frequency stimulation moves to a dependence on NMDA receptors for LTP (Grover and Teyler, 1990). Additionally high-frequency stimulation dependent LTP is impaired following administration of either LTCC or NMDA receptor antagonists (Freir and Herron, 2003, Papatheodoropoulos and Kouvaros, 2016) highlighting the importance of both channels in combination – an effect also observed in vivo (Freir and Herron, 2003). Which of these stimulation protocols is most biologically relevant is disputed (Albensi et al., 2007) however these experiments highlight the importance both of NMDA receptors and LTCCs in CA3-CA1 synaptic signalling.

The cooperative importance of LTCCs and NMDA receptors extends beyond the hippocampus. In the lateral amygdala for example, LTP can be inhibited with both LTCC and NMDA receptor antagonism, again depending on the stimulation protocol. In vivo this corresponds to behavioural deficits with both forms of antagonism blocking long-term contextual fear memories (Bauer et al., 2002), highlighting the role of both receptor types in signalling here.

LTD is also an important component of synaptic signalling. In the CA1, glucocorticoid-mediated LTD can occur, however this is reliant both on LTCCs and NMDA receptors. LTD may enable the forgetting of previously acquired memories (Tsumoto, 1993) and in vivo, forgetting of an object-in-place memory shows contingency both on NMDA receptors and LTCCs (Sachser et al., 2016).

One mechanism by which these channels may act in concert is through calcium influx. NMDA receptors in addition to glutamate are highly permeable to calcium (Ascher and Nowak, 1988) and use of MK-801, another non-competitive NMDA receptor antagonist, leads to a reduction in intracellular calcium in mouse hippocampal neurons (Yuzaki et al., 1990). This influx is essential to NMDA receptor-mediated Schaffer-collateral plasticity (Lynch et al., 1983). This effect may result from the downstream signalling cascades initiated by such calcium influx and indeed at a molecular level NMDA receptors and LTCCs appear to activate convergent downstream pathways. In particular both channels have been reported to regulate activation of the transcription factor CREB (Hardingham et al., 1999, Hardingham et al., 2002), through the activation of both the MAPK/erk signalling pathway (Hardingham et al., 2001) and the calmodulin-kinase pathway (Dolmetsch et al., 2001, Wheeler et al., 2008) and this gene transcription may have an important role in plasticity (Winder et al., 1999, Patterson et al., 2010). In forebrain-specific *Cacna1c* knockout animals, reduced activation of this pathway was observed, and this corresponded to an impairment in Schaffer-collateral plasticity (Moosmang et al., 2005). In combination with reduced LTCC expression through *Cacna1c* heterozygosity, NMDA receptor antagonism would be expected to further exacerbate the loss of calcium influx which would be likely to further impair Schaffer-collateral signalling.

In this chapter I will investigate the in vivo effects of such signalling deficits by observing changes to network activity, though first it is worth considering the effects of NMDA receptor antagonism on network activity in isolation.

6.1.5. Oscillatory Effects of NMDA Receptor Antagonism

One of the most striking effects of NMDA receptor antagonist administration is the change in gamma frequency oscillatory activity. Administration in rats gives rise to increases in cortical gamma power observed through EEG (Pinault, 2008). Additionally in the hippocampus, gamma power increases are observed following NMDA receptor antagonism (Ma and Leung, 2000) and these effects are seen both in the CA1 and DG (Kittelberger et al., 2012). These effects are not constrained to rodents either, with similar effects observed in cortical gamma in humans (Shaw et al., 2015), monkeys (Herrero et al., 2013) and sheep (Nicol and Morton, 2020) indicating a conserved cellular mechanism across species.

The enhanced gamma power implies an increased degree of excitation which appears paradoxical at first, given that these compounds block synaptic transmission rather than

facilitate it. This may relate to the effects here on interneurons. Modulation of inputs to CA1 pyramidal cells shows that NMDA receptor antagonism has a stronger effect on IPSPs resulting from recurrent inhibitory inputs than on EPSPs from Schaffer-collateral input (Grunze et al., 1996). This suggests that NMDA receptor antagonists exert a disinhibiting effect through their activity at NMDA receptors on interneurons. Similarly in cortical pyramidal cells, a reduction in IPSPs was observed following MK-801 administration (Li et al., 2002) and in vivo this same compound exerted a stronger effect on interneuron firing than on pyramidal cells (Homayoun and Moghaddam, 2007). The disinhibiting effects of these drugs may relate to their mechanism of action. These drugs are open-channel blockers and as such rely on use-dependence to overcome the Mg^{2+} block on NMDA receptors (MacDonald et al., 1987, Huettner and Bean, 1988). As interneuron populations such as PV interneurons typically have higher firing rates (Connors and Gutnick, 1990, Mizuseki and Buzsáki, 2013), channels of these cells may be blocked more readily giving rise to the disinhibiting effects observed.

As mentioned in Chapter 3, some limited research highlights the importance of LTCCs to PV interneuron function. For example, their maturation is dependent on LTCCs with antagonists supressing their growth in cell cultures (Jiang and Swann, 2005). Additionally PV interneuron-pyramidal cell synapses in the hippocampus are regulated by the activity of LTCCs (Horn and Nicoll, 2018) and calcium currents into PV-interneurons depend primarily on Cav1 channels (Rendón-Ochoa et al., 2018), though the exact subtype here was not specified. Combining NMDA receptor antagonism with reduced LTCC expression would therefore be expected to exacerbate the PV interneuronal effects giving rise to enhanced gamma activity.

In addition to the power of gamma oscillations, PAC deficits are also observed after administration of NMDA receptor antagonists. Theta-fast gamma coupling in the CA1 has been observed to increase following a low dose of ketamine (Caixeta et al., 2013) with concurrent reductions observed for theta-slow gamma coupling (Michaels et al., 2018). This effect appears to be regional with the DG displaying reduced theta-gamma coupling following administration of MK-801 (Kalweit et al., 2017). Notably the deficit observed for theta-slow gamma coupling matches that described in Chapter 3 in *Cacna1c*$^{+/-}$ rats. In this chapter I will test whether the PAC deficits associated with *Cacna1c* heterozygosity are further impaired when introducing ketamine. Additionally, though no effects on gamma power during free exploration were observed in *Cacna1c*$^{+/-}$ rats, I will assess whether NMDA receptor antagonism gives rise to similar gamma power changes in *Cacna1c*$^{+/-}$ rats as WTs which may shed light on the importance of both channels in network activity in the hippocampus.

6.1.6. Chapter Aims

Cacna1c heterozygosity may recapitulate certain biological components of psychiatric disorders, as does NMDA receptor antagonism. Here I will observe their effects in combination by assessing locomotory behaviour after administration of a sub-anaesthetic dose of ketamine to *Cacna1c*$^{+/-}$ rats. Additionally LTCCs and NMDA receptors operate in concert both in the hippocampus and in other brain regions. Here I will assess the effects of dysfunction in both regions together by observing gamma activity in the hippocampus following ketamine administration. Finally I will characterise oscillatory coupling by assessing theta – slow gamma and theta fast gamma PAC.

6.2. Methods

6.2.1. Animals

Table 7. Summary table of number of animals used.

Treatment	Number of Recording Days	Number of Sessions	Genotype	Number of animals
Vehicle	1	1	WT	6
			Cacna1c$^{+/-}$	5
Drug	1	1	WT	6
			Cacna1c$^{+/-}$	5

6 *Cacna1c* heterozygous rats and 5 WTs were used in these ketamine experiments. In 2 animals (1 *Cacna1c*$^{+/-}$ rat and 1 WT) data from vehicle sessions are missing as their microdrives fell off before recordings could be taken. Additional recordings were undertaken in one further *Cacna1c*$^{+/-}$ rat (in addition to the 6 reported here), however this data was excluded as an outlier due to the lack of hyperlocomotion and loss of observed gamma power changes.

6.2.2. Behavioural Protocol

The behavioural protocol used is described in **Figure 6.1**. Animals were placed into the open-field (see ***3.2*** for further details) for approximately 20 minutes while concurrently recording local field potentials and animal position. Animals then received an intraperitoneal injection of S(+)-ketamine (Sigma) dissolved in 0.9% saline at 16mg/ml to deliver a dose of 16mg/kg or a

vehicle injection of 0.9% saline at an equivalent volume. Following injection, animals were placed back into the open-field and recorded for an additional 60 minutes.

All animals (excluding the 2 who only received the drug) were subject to the above protocol twice: once for a ketamine injection and once for a vehicle injection. The order in which they received both injections was varied and counterbalanced across genotypes, as was the time of day of the injection such that a comparable number of WTs and *Cacna1c*$^{+/-}$ rats received each drug-vehicle ordering at each time of day (morning or afternoon).

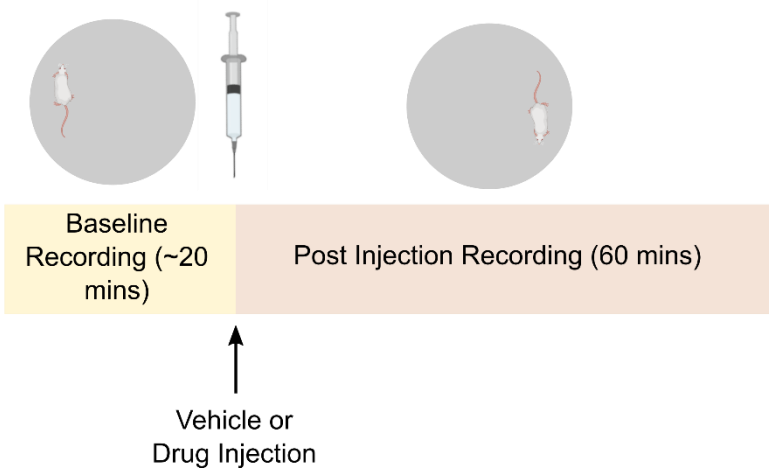

***Figure 6.1* | Behavioural protocol** Schematic depicting behavioural protocol for Ketamine and Vehicle Sessions.

6.2.3. Data Analysis

6.2.3.1. Locomotor Activity Analysis

Position data across the whole recording period was divided into 5-minute bins. Within each bin the linear velocity at each timepoint was calculated and smoothed with a gaussian smoothing filter to limit the effects of small movements. The mean velocity within each bin was then calculated to gain an estimate of peak velocity across all bins and time taken to reach peak velocity. The total track area covered was estimated as the sum of the mean velocity values in all bins multiplied by the total length of the recording.

6.2.3.2. Spectral Analysis

Power spectral analysis was carried out as described in ***3.2***. Power spectrograms were computed with Chronux using 500ms windows and a 10ms overlap with a time-bandwidth product of 3 and 5 tapers. Time-bandpower spectra were computed by dividing the recording

period into 5-minute bins and computing the power at slow-gamma (25-55Hz) and fast-gamma (60-140Hz) using parameters as described previously.

6.2.3.3. Phase-Amplitude Coupling

PAC was computed as described in ***3.2***. Analysis here was restricted to the 40-minute period following injection for the mean comodulograms and the time-course comodulograms were computed in 10-minute bins across the full duration of the recording period.

6.2.4. Statistical Analysis

When comparing mean values between genotypes in both sessions a two-way ANOVA was used. To compare effects across time (eg. time-bandpower analysis) a two-way ANOVA with repeated measures was used.

6.3. Results

6.3.1. Locomotor Activity

To assess the behavioural response to ketamine administration, I characterised locomotive activity in 5-minute windows prior to and following drug treatment (ketamine or vehicle) by measuring the animal's running speed (**Figure 6.2**). Consistent with previous studies, ketamine administration produced a robust increase in running speed in the time windows following injection in both genotypes (**Figure 6.2A**).

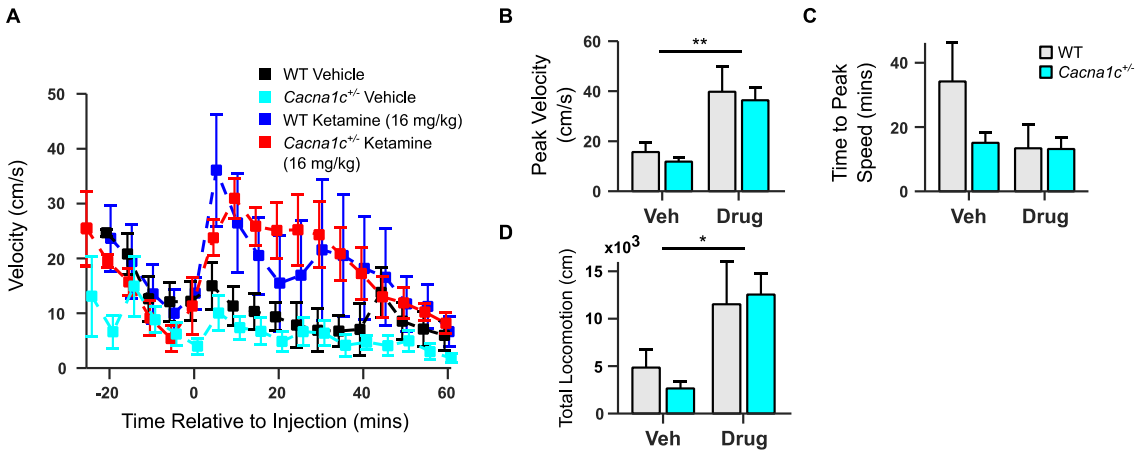

***Figure 6.2* | Locomotory behaviour following ketamine administration**
(A) Mean running speed (cm/s) in 5-minute bins prior to and following injection of either ketamine (16mg/kg) or vehicle. *(Vehicle: WT in black, Cacna1c$^{+/-}$ in cyan; Drug: WT in blue, Cacna1c$^{+/-}$ in red)*

(B) Mean peak running speed in vehicle and ketamine (drug) sessions. Analysis revealed a significant effect of drug treatment on peak running speed though no effect of genotype (Treatment effect: $p<0.01$, Genotype effect: $p>0.05$; Two-way ANOVA).
(C) Time taken post-injection to reach peak running speed. Analysis here did not reveal an effect of drug treatment or genotype ($p>0.05$, Two-way ANOVA).
(D) Total locomotion across full recording period. Analysis here revealed a significant treatment effect ($p<0.05$) though no effect of genotype ($p>0.05$; Two-way ANOVA).
(All data presented as mean±SEM; WT: n=6 animals, Cacna1c$^{+/-}$: n=6 animals. WT in black, Cacna1c$^{+/-}$ in cyan)

To quantify genotype differences in hyperlocomotion I first assessed peak running speeds across the duration of the recording following drug treatment. This analysis showed a significant effect of drug treatment (**Figure 6.2B**; $F_{1,16}$=14.1, p=0.002; Two-way ANOVA) though no effect of genotype ($F_{1,16}$=0.67, p=0.43; Two-way ANOVA). Analysis of total locomotion also showed a similar pattern of results (**Figure 6.2C**; Drug Treatment: $F_{1,18}$=9.7, p=0.006; Genotype: $F_{1,18}$=0.28, p=0.603; Two-way ANOVA). I next assessed whether the time-course of the drug effects in either genotype varied by quantifying the time taken to reach peak locomotion (**Figure 6.2C**). This analysis however did not reveal an effect of drug treatment or of genotype (Drug Treatment: $F_{1,16}$=3.6, p=0.08; Genotype: $F_{1,16}$=2.1, p=0.165; Two-way ANOVA).

Together this analysis reveals similar behavioural effects as described by locomotion in both genotypes.

6.3.2. Oscillatory Activity

NMDA receptor antagonists produce prominent alterations in gamma activity throughout the brain (Ma and Leung, 2000, Pinault, 2008, Kittelberger et al., 2012, Herrero et al., 2013, Shaw et al., 2015, Nicol and Morton, 2020). This was evident in the hippocampal LFP of both genotypes (**Figure 6.3**). To gain more insight into the frequency-specific effects I produced time-frequency spectrograms for each genotype prior to and following each drug treatment (**Figure 6.4**). These clearly showed gamma activity in the range of (~30-~100Hz) following injection of ketamine that was not present following the vehicle injection.

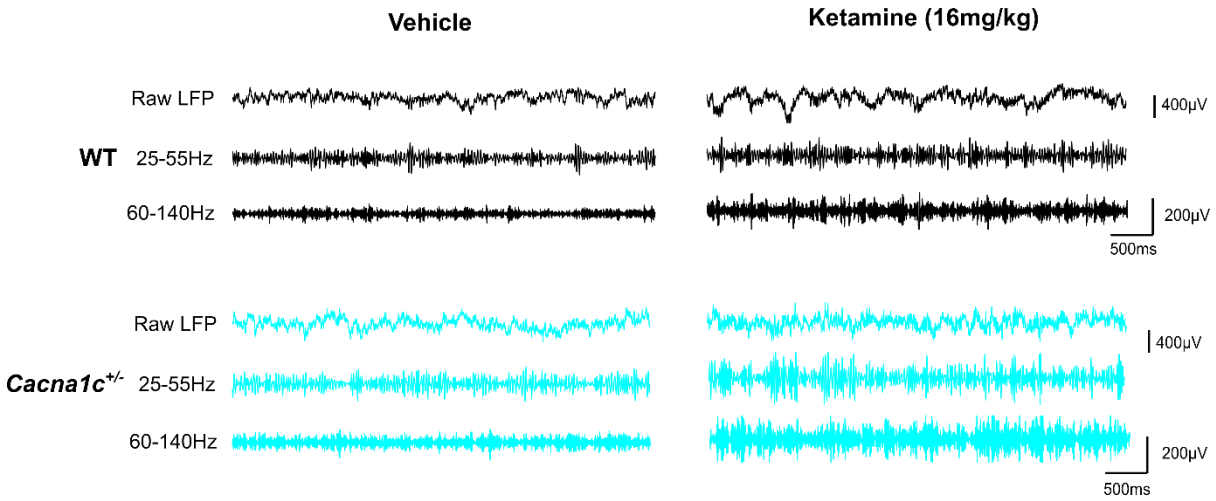

***Figure 6.3* | Representative raw LFP**
Example raw hippocampal LFP traces taken in a 5s window during the vehicle session (left) and ketamine session (right) from one animal in each genotype. All traces taken from a comparable time-point in each session. Top trace in each show broadband LFP (0.1-475Hz). Middle traces show LFP filtered at slow-gamma frequency (25-55Hz) and bottom traces show LFP filtered at fast-gamma frequency (60-140Hz). (Note the increased amplitude of both gamma frequency filtered traces in each genotype in the ketamine session compared to the vehicle session)

To quantify these effects and assess whether genotype differences were present, in addition to teasing apart the slow and fast gamma specific effects, I next observed gamma power changes within 5-minute time-windows prior to and following drug treatment (**Figure 6.5**). Both genotypes showed a clear increase in slow (**Figure 6.5A**) and fast gamma (**Figure 6.5C**) expressed as a percentage change from pre-injection baseline. Analysis of the time course of these effects revealed a significant drug treatment x time interaction ($p<0.05$; Two-way ANOVA with repeated measures) but no genotype or genotype interaction effects ($p>0.05$; Two-way ANOVA with repeated measures).

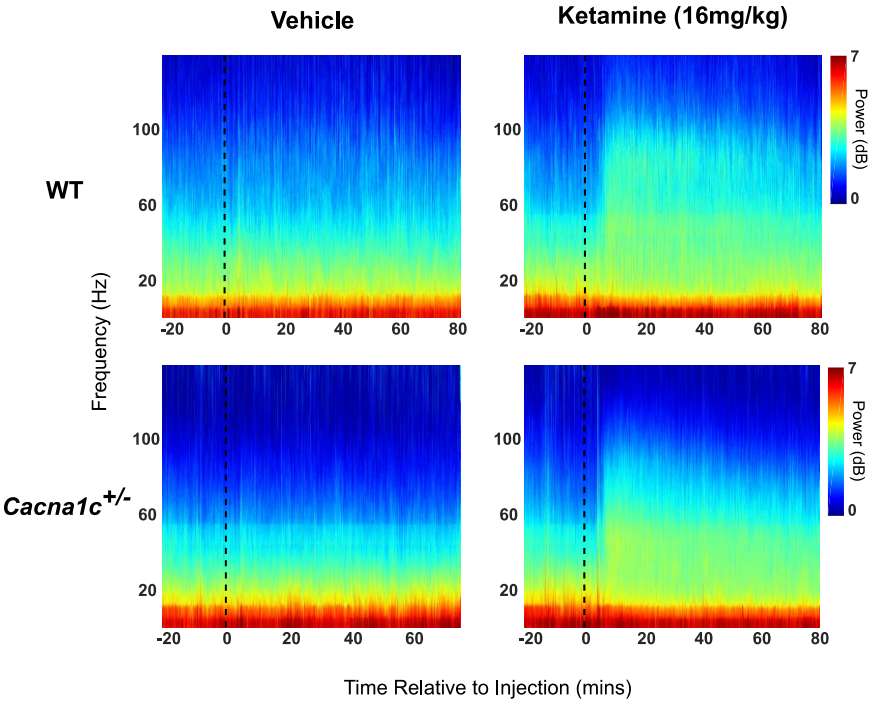

***Figure 6.4* | Mean power spectrograms**
Mean power spectrograms showing log power vs. time for each drug treatment session in each genotype. Time relative to injection shown on the x-axis and frequency (1-140Hz) on the y-axis. Colour depicts the log power at each frequency band. Dotted black line indicates the time of injection.
(WT: n=5 animals, Cacna1c$^{+/-}$: n=6 animals)

In the time-course plots, slow-gamma power appeared to show a greater change from baseline in *Cacna1c*$^{+/-}$ rats than in WTs. To further quantify this I assessed peak gamma power at both frequency bands following drug treatment (**Figure 6.5C,D**). This analysis while showing an effect of drug treatment as expected ($p<0.001$,$p<0.05$; Two-way ANOVA) did not reveal any genotype or genotype interaction effects ($p>0.05$; Two-way ANOVA).

In summary this analysis revealed comparable degrees of gamma power increase in both the slow and fast frequency ranges in both genotypes.

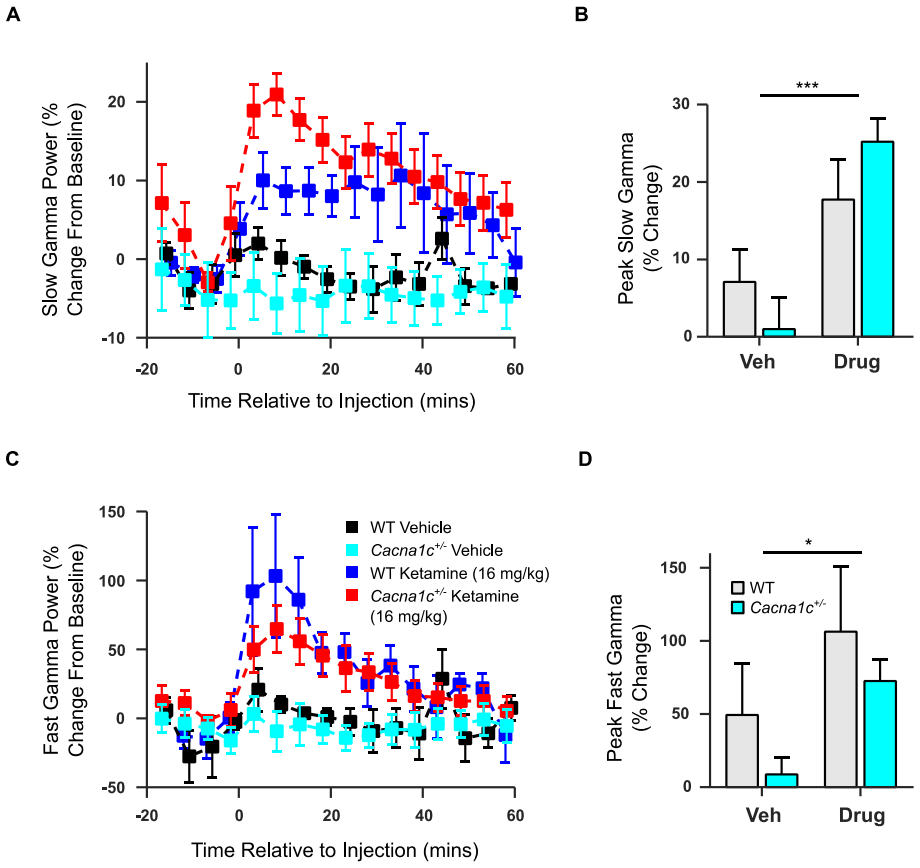

***Figure 6.5* | Gamma power variations across time**
(A,C) Mean gamma power variations relative to pre-injection baseline within 5-minute bins prior to and following drug treatment shown for **(A)** slow-gamma (25-55Hz) and **(C)** fast-gamma (60-140Hz) ($p>0.05$, Two-way ANOVA; Vehicle: WT in black, Cacna1c$^{+/-}$ in cyan; Drug: WT in blue, Cacna1c$^{+/-}$ in red).
(B,D) Peak Gamma Power change relative to baseline shown for both drug treatments in both genotypes. Analysis of both peak **(B)** slow-gamma and **(D)** fast-gamma power changes revealed a significant effect of drug treatment ($*p<0.05$) but no effect of genotype ($p>0.05$, Two-way ANOVA).
(All data presented as mean±SEM; WT: n=5 animals, Cacna1c$^{+/-}$: n=6 animals. WT in black, Cacna1c$^{+/-}$ in cyan)

6.3.3. Phase-Amplitude Coupling

While the changes in the power of individual gamma bands were comparable between genotypes following drug treatment, I next assessed whether the coupling of these to theta was impaired by characterising PAC in the 40 minutes following drug treatment.

PAC comodulograms (**Figure 6.6**) revealed clear patterns of theta-slow gamma and theta-fast gamma coupling in the WTs in both drug treatment conditions. On the other hand *Cacna1c*$^{+/-}$ rats appeared to show very little coupling of either gamma frequency band to theta in either condition. In the slow-gamma frequency range, this coupling did not appear to differ either for genotype ($F_{1,16}$=2.3, p=0.146; Two-way ANOVA) or for drug treatment ($F_{1,16}$=0.3, p=0.58; Two-way ANOVA). Theta – fast gamma coupling on the other hand did show a

genotype effect ($F_{1,16}$=6.7, p=0.02; Two-way ANOVA) but drug treatment did not appear to have an effect here ($F_{1,16}$=0.02, p=0.89).

In summary, this analysis might point to a deficit in theta-fast gamma PAC in *Cacna1c*$^{+/-}$ rats however theta-gamma coupling does not appear to be affected by ketamine administration at this dosage.

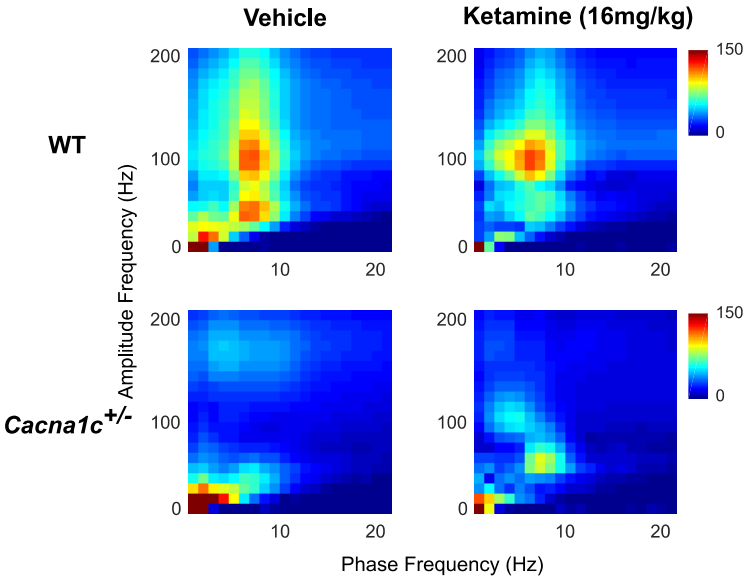

***Figure 6.6* | Phase-amplitude coupling following ketamine administration**
(A) Mean phase-amplitude coupling comodulograms taken from the 40-minute period following ketamine or vehicle injection. Phase frequencies (1-20Hz) shown on the x-axis and amplitude frequencies (1-200Hz) shown on the y-axis. Colour depicts the modulation index.
(WT: n=5 animals, Cacna1c$^{+/-}$: n=6 animals)

Though a drug effect was not observed when quantifying PAC across the 40-minute post injection period, prior research reveals a strong time-dependence of hippocampal PAC on ketamine administration with a peak around 10 minutes after administration (Caixeta et al., 2013).

To assess the time-course of coupling changes here I next quantified PAC within 10-minute bins prior to and following drug treatment (**Figure 6.7**). To quantify the variation of PAC with time, I computed mean theta-slow gamma and theta-fast gamma modulation indices at every time-point (**Figure 6.7B**). This analysis did not reveal a drug treatment x time interaction (p>0.05, Two-way ANOVA with repeated measures) effect nor a genotype x time interaction effect (p>0.05, Two-way ANOVA with repeated measures) for either slow or fast-gamma indicating no effect of drug treatment on coupling of theta to either of these bands in either genotype.

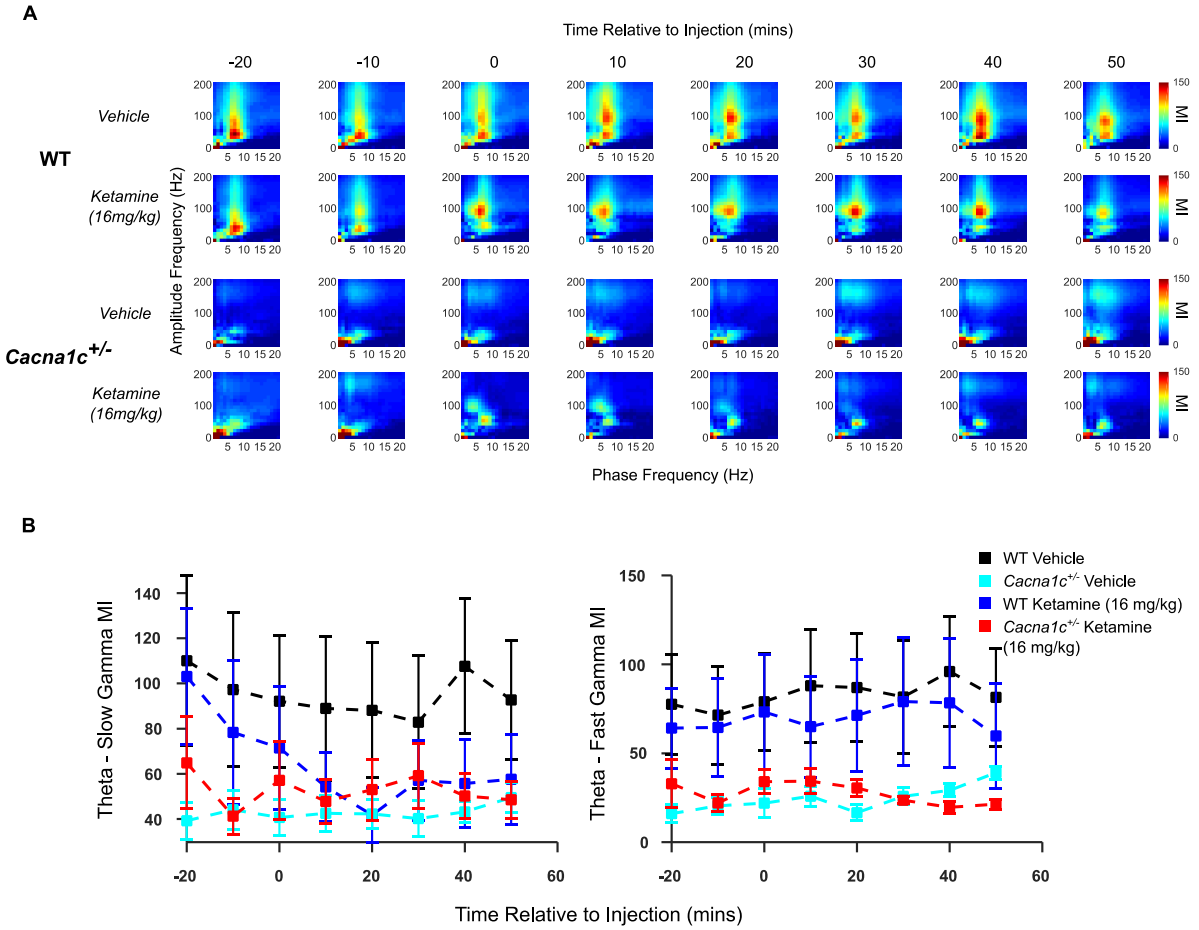

***Figure 6.7* | Time-course of phase-amplitude coupling changes following ketamine administration**

(A) Mean phase-amplitude coupling comodulograms taken in 10-minute bins prior to and following drug treatment. Time axis shown above all plots with phase frequencies (1-20Hz) on the x-axis and amplitude frequencies (1-200Hz) on the y-axis. Colour depicts modulation index.

(B) Mean modulation index values within 10-minute bins prior to and following drug treatment shown for slow-gamma (25-55Hz) (*left*) and fast-gamma (60-140Hz) (*right*). No significant genotype x time or drug treatment x time interaction was observed ($p>0.05$, Two-way ANOVA with repeated measures). (*Data presented as mean±SEM; WT: n=5 animals, Cacna1c$^{+/-}$: n=6 animals; Vehicle: WT in black, Cacna1c$^{+/-}$ in cyan; Drug: WT in blue, Cacna1c$^{+/-}$ in red)*

In summary, this analysis might point to a deficit in theta-fast gamma PAC in *Cacna1c*$^{+/-}$ rats, however theta-gamma coupling does not appear to be affected by ketamine administration at this dosage.

6.4. Discussion

6.4.1. Key Findings

In this chapter I administered 16mg/kg of ketamine to *Cacna1c*$^{+/-}$ rats and WTs to assess the behavioural and electrophysiological responses to NMDA receptor antagonism, testing the hypothesis that a combination of reduced *Cacna1c* expression may alter behavioural and/or neurophysiological responsivity to ketamine.

Administration of ketamine gave rise to transient increases in locomotion that did not show any dependence on genotype. Additionally ketamine caused a significant increase in hippocampal slow and fast gamma power which again did not differ between genotypes. Finally an analysis of PAC did not reveal an effect of ketamine here though *Cacna1c*$^{+/-}$ rats did show an impairment in theta – fast gamma coupling.

6.4.2. Effects on Locomotion

Administration of NMDA receptor antagonists gives rise to increased dopamine levels both in rodents (Hondo et al., 1994, Balla et al., 2001, Kokkinou et al., 2018) and humans (Vollenweider et al., 2000). This increased dopamine may underlie effects on hyperlocomotion as dopamine receptor antagonists in combination with NMDA receptor antagonism diminish the hyperlocomotive effects (Irifune et al., 1991, Irifune et al., 1995). Some hyperlocomotive behaviour has been shown to remain even with dopamine antagonism in place (Chartoff et al., 2005), but the effect is diminished pointing to a prominent role for dopamine in this effect. Though it differs depending on the compound, ketamine's effect on dopamine presumably is the result of its high affinity for dopamine receptors in addition to NMDA receptors (Kapur and Seeman, 2001).

Here I showed that ketamine did indeed induce the expected hyperlocomotive response however this did not vary with genotype. Given the dopamine-dependence of this effect, understanding the role of LTCCs in dopamine signalling will help make sense of these results. LTCCs do appear to have an important role in dopaminergic signalling. In striatal dopamine neurons, D1 agonists enhance the responses of NDMA receptors in these neurons, but this effect appears to depend on LTCCs as observed by the diminishing of this effect with nifedipine (Liu et al., 2004). Additionally D1 receptor signalling cascades involved in synaptic plasticity are also inhibited by nifedipine (Surmeier et al., 1995). These effects may alter the firing properties of dopaminergic neurons. In the ventral tegmental area (VTA) burst firing of neurons here is modulated by Cav1.2 though this effect is primarily mediated by Cav1.3 (Liu et al., 2014).

These results would imply an enhancing effect of LTCCs on dopaminergic activity and thus *Cacna1c* heterozygosity would be expected to diminish this effect leading to a reduction in dopaminergic activity. This might be expected to manifest as a reduction in the hyperlocomotive effects of ketamine, however this was not observed here implying that a loss of LTCC signalling did not alter dopaminergic activity. Importantly, LTCCs, as in the hippocampus, appear to act in concert with NMDA receptors. As mentioned, their effect in striatal neurons appears to be a regulation of the NMDA receptor response (Liu et al., 2004), and additionally another study demonstrated alterations in the phosphorylation of CREB in D1 receptors following nifedipine administration, though this effect was mediated through glutamate (Eaton et al., 2004). Without the activity on NMDA receptors, LTCCs may not be capable of exerting effects on dopaminergic signalling, hence the comparable degree of locomotion between WTs and *Cacna1c*$^{+/-}$ rats.

One potential caveat with this interpretation is that it assumes that without NMDA receptor antagonism, LTCC-mediated dopaminergic activity affects locomotive activity. However in Chapter 3 locomotion was assessed in *Cacna1c*$^{+/-}$ rats during exposure to the open-field and was observed to be comparable to WTs. This would imply that dopamine signalling, at least as it pertains to locomotion, was in fact intact in *Cacna1c*$^{+/-}$ rats indicating a limited reliance on LTCCs for this form of dopaminergic signalling.

6.4.3. Gamma Rhythms

The lack of alteration of ketamine-induced hyperlocomotion in either genotype should not necessarily have any bearing on the gamma effects. While it is certainly true that gamma has links to running speed, and this was explored in detail in Chapter 3, the effects of NMDA receptor antagonism on hyperlocomotion and on gamma power have been previously shown to be dissociated from the gamma power effects (Hakami et al., 2009). That being said, both slow and fast gamma, despite showing the expected increase in power following ketamine administration, like the hyperlocomotive effects, did not differ between genotypes.

As mentioned in ***6.1***, the changes in gamma power observed with NMDA receptor antagonism are likely the results of their effects on interneurons (Grunze et al., 1996, Li et al., 2002, Homayoun and Moghaddam, 2007). In particular PV interneurons appear to regulate the activity of gamma (Bartos et al., 2002, Bartos et al., 2007, Sohal et al., 2009). Prior research into the MAM animal model of SCZ, revealed an attenuated gamma power increase following ketamine administration in MAM animals in certain cortical regions, and this corresponded to a PV interneuron reduction (Phillips et al., 2012b). This would imply that any alterations to the effects of ketamine on gamma frequency alterations depend on PV interneuron activity. As mentioned in ***6.1***, there is some research highlighting a role for LTCC in PV interneuron function, yet despite the role, analysis of slow and fast gamma rhythms in

Chapter 3 revealed intact oscillatory activity in *Cacna1c*$^{+/-}$ rats. This would point to normal PV interneuron function in *Cacna1c*$^{+/-}$ rats which makes the lack of alteration in ketamine-induced gamma power increase unsurprising. However this result is somewhat in contrast to the aforementioned studies into LTCCs and PV interneurons. To better understand this finding research characterising PV interneuron levels within different hippocampal subfields is required as a more direct assessment of the effects of LTCCs here.

6.4.4. Phase-Amplitude Coupling

PAC, despite a deficit in *Cacna1c*$^{+/-}$ rats, did not appear to show a ketamine-mediated effect. This was surprising given that it contrasts with previous literature showing PAC effects following NMDA receptor antagonist administration (Caixeta et al., 2013, Kalweit et al., 2017, Michaels et al., 2018) and coupling here relies on PV interneurons (Wulff et al., 2009) so would be expected to alter with NMDA receptor antagonism. Two of these studies also assessed PAC in the CA1 (while the other looked at the DG (Kalweit et al., 2017)) making these more comparable to the research undertaken here. In both CA1 papers, an increase was observed in theta – fast gamma PAC following ketamine administration. Both of these recordings were undertaken during free exploration but what differed to my analysis was the dose, with these two studies observing this effect after a dose of 25mg/kg (Caixeta et al., 2013) and 30mg/kg (Michaels et al., 2018) respectively. Importantly, the effect of ketamine on theta-fast gamma coupling is dose-dependent. Higher doses than this lead to a reduction in this coupling (Caixeta et al., 2013), yet it is unknown what the effect of a lower dose is. The results reported in this chapter would suggest that a 16mg/kg dose is not sufficient to disrupt theta-gamma coupling.

The loss of theta-fast gamma coupling in *Cacna1c*$^{+/-}$ rats, independent of the effects of ketamine was surprising, given that theta-fast gamma coupling was shown to be intact in Chapter 3. This effect was unlikely to be the result of behavioural differences given that locomotor behaviour was comparable between genotypes. One possibility is that this effect was the result of differing behavioural demands. In the linear track sessions where a theta-slow gamma deficit was observed, animals were running for a reward whereas here they did not. Place cells appear to alter their coding regime depending on whether the animal is approaching a reward or leaving a reward site, with retrospective and prospective coding mechanisms occurring respectively (Gupta et al., 2012, Bieri et al., 2014) and the prominence of specific gamma bands here appears to relate to these differing forms of coding (Bieri et al., 2014). It is unknown which coding regime is more prominent when animals are not running for a reward and as such the results here may not be directly comparable to those observed on the linear track. That being said, a fast-gamma coupling deficit here would imply an impairment

in perforant path input to the CA1 (Colgin et al., 2009), yet this appears to be intact *Cacna1c*$^{+/-}$ rats (Tigaret et al., 2020) and as such these results remain elusive.

Alternatively this shift to a fast-gamma PAC deficit might reflect tetrode positioning. As mentioned in ***6.2***, two animals lost microdrives between the drug and vehicle sessions and it is likely microdrive instability preceded this point. Additionally, though not quantified, a loss of single unit yield was observed in several other animals during these sessions compared to the single unit yield observed in the linear track and open-field sessions, indicating a shift in tetrode position, though it is less clear in which direction tetrodes shifted. Gamma band coupling to theta reflects differing inputs to the CA1 with slow-gamma reflecting Schaffer-collateral input which terminates at stratum radiatum and fast-gamma reflecting EC input, thought to terminate at stratum lacunosum (Belluscio et al., 2012). Some evidence also points towards a split within fast-gamma with coupling to ~80Hz highest within stratum lacunosum and higher gamma frequencies (~140Hz) coupled more strongly to theta within stratum oriens (Scheffer-Teixeira et al., 2012). Importantly however the layer-specific termination of different gamma sources results in a variation of PAC with electrode depth (Scheffer-Teixeira et al., 2012). This is highlighted in **Figure 6.8**. Here data was taken from a recording on the linear track in one WT animal. The sharp-wave polarity across different tetrodes was used as a measure of electrode depth relative to the CA1 pyramidal layer and PAC was computed for each tetrode. As one moves from the most to least superficial (left→right) tetrode, the spectral characteristics of the PAC comodulogram shifts, with theta fast-gamma PAC peaking prior to theta slow-gamma PAC. Consequently the shift from a slow-gamma to a fast-gamma PAC deficit may reflect a shift in tetrode depth rather than a change in PAC itself.

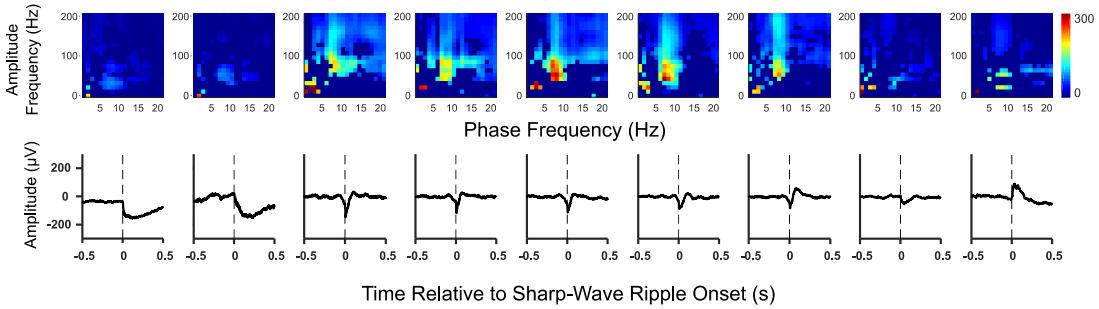

***Figure 6.8* | Phase-amplitude depth profile for an individual animal**
Phase-amplitude coupling comodulogram (top) vs sharp-wave ripple triggered average LFP (bottom) shown for 9 different tetrodes from one microdrive on an individual WT rat during the familiar linear track session. Sharp-wave ripple polarity was used as in indicator for depth relative to CA1 pyramidal cell layer and comodulogram-LFP pairs were arranged from most superficial to deepest from left to right respectively.

6.4.5. Conclusion

Both LTCC dysfunction and NMDA receptor dysfunction may recapitulate dysfunction underlying symptoms of psychiatric disorders. Here I assessed whether the combination of dysfunction at both of these receptors gives rise to altered deficits that are not present from either alone, with the aim both of understanding how biological pathways may interact in psychiatric disorders, and of uncovering the dual effects of both of these receptors on hippocampal network activity.

The analysis undertaken here revealed clear effects of ketamine on behaviour and oscillatory activity in the hippocampus though reduced LTCC function did not affect this. This suggests that the coordinated action of these receptors is more subtle than what can be observed at the network level. Additionally the role of both of these receptors in psychiatric disease may occur through distinct biological pathways or through pathways not characterised in the research here.

7

Chapter 7

General Discussion

7.1. Summary of Findings

The aim of this thesis was to investigate the consequences of *Cacna1c* heterozygosity for hippocampal function during free exploration and rest, in order to further understanding of the role of this gene, and calcium signalling more broadly, in conferring susceptibility to psychiatric risk.

- Chapter 3 revealed that *Cacna1c*$^{+/-}$ rats show experience-dependent alterations in place-field size and the spatial information content of CA1 place cells.
- Additionally, theta and gamma rhythms, though normal in terms of power, were impaired in their coupling during runs on a linear track in a novel orientation. The modulation of theta power by running speed was also impaired in *Cacna1c*$^{+/-}$ rats.
- In Chapter 4, robust circadian activity was observed in *Cacna1c*$^{+/-}$ rats indicating intact sleep rhythms.
- Chapter 5 revealed intact oscillatory activity in CA1 LFP during sleep/rest, yet the modulation of spiking activity was impaired, with increased spiking observed during SPW-Rs in *Cacna1c*$^{+/-}$ rats.
- This enhanced spiking activity corresponded to an enhancement of cells exhibiting cross-correlated activity during SPW-Rs yet the magnitude of cross-correlated activity between place-cell pairs was significantly impaired in *Cacna1c*$^{+/-}$ rats.
- Finally, Chapter 5 revealed normal responses to systemic ketamine administration in *Cacna1c*$^{+/-}$ rats.

In order to assay hippocampal function across multiple anatomical and temporal scales, I considered the activity both of individual hippocampal neurons via single unit recordings, and

their collective action through the use of LFP recordings. Both lines of analysis, as reported above, revealed impairments associated with *Cacna1c* heterozygosity.

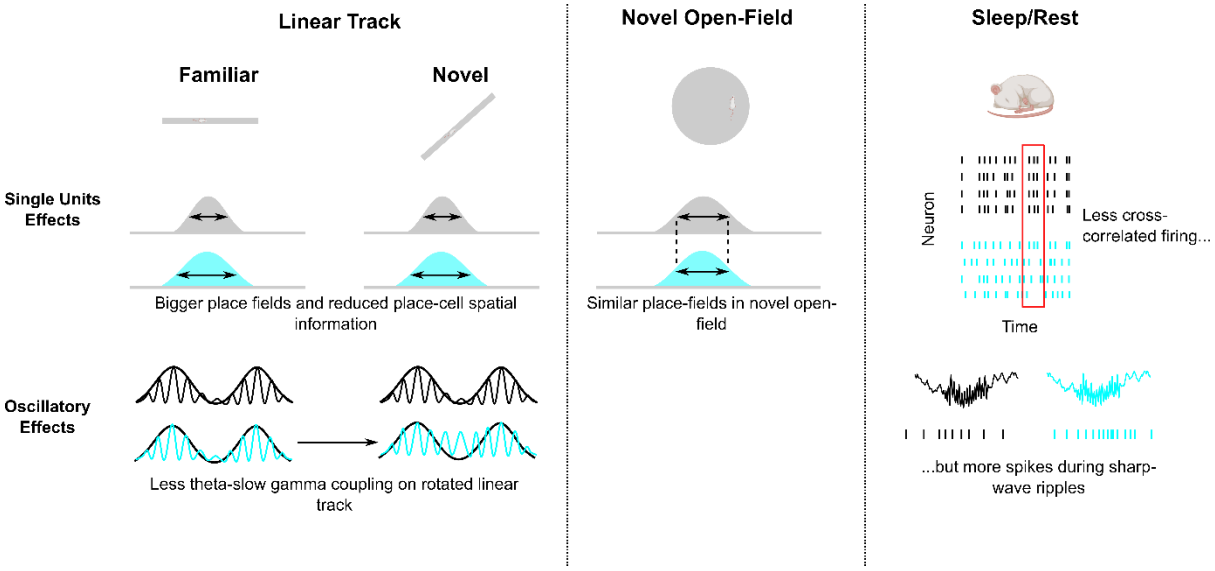

***Figure 7.1* | Graphical summary of principal findings**
Schematic detailing effects of *Cacna1c*$^{+/-}$ heterozygosity (cyan) on neurophysiology during exploration of a linear track (*left*), novel open-field (*centre*) and during sleep/rest (*right*). *(WTs in black/grey)*

7.1.1. Altered Place-Cell Properties During Wake and Rest

To characterise the effects of *Cacna1c* reduced gene dosage on the physiology of individual hippocampal neurons, I quantified place-cell properties during free exploration of a range of environments and during rest prior to and following these sessions. Previous research has indicated a role for synaptic plasticity in modulating certain place-field properties such as place-field size and place-cell spatial information (McHugh et al., 1996, Cacucci et al., 2007). In the *Cacna1c*$^{+/-}$ rats, both of these measures showed alterations on the linear track, which may in part have been the result of the impairments to Schaffer-collateral plasticity previously reported with reduced *Cacna1c* gene dosage in rodent models (Moosmang et al., 2005, Tigaret et al., 2020). Despite these subtle changes to the properties of place-fields in the familiar environments, the capacity to form place-fields was not impaired as evidenced by the comparable place-field properties in the novel open-field and the comparable number of place-fields per place-cell in all environments. In this regard it is interesting to note that other psychiatric disease gene manipulations have clear effects on Schaffer-collateral plasticity (Zeng et al., 2001) yet also harbour limited place-field alterations (Suh et al., 2013), implying that CA3-CA1 plasticity is not essential to the mechanisms governing place-field formation.

What is the role of plasticity at CA3 input to CA1 here? One possibility is that this plasticity serves to recruit cells into assemblies. For example, a calcium imaging study characterised concurrent activation of CA1 cells and observed the involvement of Schaffer-collateral plasticity. (Yuan et al., 2011). These authors showed that Schaffer-collateral

plasticity could both increase the size of cell assemblies, that is incorporate more neurons into the ensemble, and merge apparently distinct ensembles This is in agreement with an NMDAR1 study of plasticity in relation to place-field size, mentioned above, where mice lacking functional NMDA receptors in CA1 place cells displayed a loss of cross correlated activity between cell pairs (McHugh et al., 1996). Calcium imaging during exploration and sleep in *Cacna1c*$^{+/-}$ rats may enable a more direct quantification of ensemble activity in future research.

In my own analysis, though cross-correlated activity was not altered during exploration, striking deficits in the magnitude of cross-correlated firing were observed between place-cell pairs during SPW-R's in the *Cacna1c*$^{+/-}$ rats. Despite this loss of cross-correlated firing during SPW-R's, *Cacna1c*$^{+/-}$ rats exhibited an increase in both the activation and participation of individual CA1 cells during these epochs, an effect also observed in the calcineurin genetic model of psychiatric risk (Suh et al., 2013). This result might appear paradoxical at first. One might assume that increased cellular activation during SPW-Rs would give rise to greater coactivation, and indeed the proportion of place-cell pairs for which cross-correlated firing was above-chance did show a significant increase in the *Cacna1c*$^{+/-}$ rats. Yet concurrent activation on a ~500ms timescale does not equate to concurrent activation at a higher-resolution <200ms timescale; instead, these results imply that in *Cacna1c*$^{+/-}$ rats, place cells are both more active in general, but less precisely coactive during SPW-Rs. This would fit with a model in which both inhibition and plasticity are reduced. Such effects are observed in psychotomimetic animal models of SCZ – administration of these compounds give rise to disinhibition of CA1 pyramidal cells (Ma and Leung, 2000, Kittelberger et al., 2012), while Schaffer-collateral plasticity is also impaired (Stringer et al., 1984, Duan et al., 2013) - indicating this pattern of dysfunction as potentially pertinent to psychiatric disease. Though direct support of this model in *Cacna1c*$^{+/-}$ rats is lacking - little support was garnered for the presence of dysfunctional inhibition on the basis of oscillatory activity as I shall review shortly - these results highlight a potential future line of enquiry. Cav1.2 channels also have an important role in neuronal excitability (Kratzer et al., 2013, Moore and Murphy, 2020) and though such an alteration in excitability wasn't immediately clear from the analysis of ISIs and burst firing in Chapter 3, altered cellular excitability as a result of reduced calcium currents could provide some explanation for the alterations to firing properties during SPW-Rs. A thorough investigation of EI balance and underlying circuit alterations in relation to *Cacna1c* heterozygosity may provide more evidence to investigate these proposed models further.

7.1.2. Oscillatory Activity and Alterations in Phase-Amplitude Coupling

In psychiatric disorders, oscillatory deficits are consistently observed at the cortical level (Cho et al., 2006, Haenschel et al., 2009, Uhlhaas and Singer, 2010, Sun et al., 2013) and rhythmic

disturbance in the brain is commonly touted as a potential underlying cause of psychiatric dysfunction (Uhlhaas and Singer, 2010, Williams and Boksa, 2010, McNally and McCarley, 2016, Hunt et al., 2017). I hypothesized that *Cacna1c* heterozygosity may give rise to oscillatory impairments in the hippocampus on the basis of prior work demonstrating the importance of LTCCs in the formation of synchronous cell networks in culture (Plumbly et al., 2019). In contrast, oscillatory activity during both active exploration and rest appeared normal, as evidenced by the comparable amplitude and frequency of theta, slow and fast gamma, and ripples in *Cacna1c*$^{+/-}$ rats. On the other hand under certain experimental conditions, deficits in theta-gamma coupling were observed.

Oscillations of different frequencies rely on the activity of different inputs and populations of interneurons. Faster gamma oscillations for example require the activity of fast-spiking interneurons. This is evidenced by optogenetic studies which demonstrate that PV interneuron manipulation can drive gamma rhythms in vivo (Cardin et al., 2009, Sohal et al., 2009). Similarly, ripples oscillations rely on fast-spiking interneurons and indeed optogenetic analysis here reveals the importance both of PV and somatostatin interneurons in ripple generation (Stark et al., 2014). The slower frequency of theta oscillations may rely on interneurons whose activation occurs over a slower timescale. OLM interneurons appear to fire at theta frequency (Gloveli et al., 2005) and disruption of interneuronal firing within the stratum oriens, where these interneurons are typically found, gives rise to a loss of theta frequency (Gillies et al., 2002), highlighting a potential role for this interneuron subtype in theta oscillations.

LTCCs and Cav1.2 in particular play a key role in the maturation of PV interneurons (Jiang and Swann, 2005). On this basis one might assume a disruption to faster oscillations in *Cacna1c*$^{+/-}$ rats would be observed, though no such alteration was detected. Yet recordings in vivo reveal that the hippocampus may be more robust to genetic perturbations to specific interneuron subtypes than optogenetic studies would otherwise indicate. In mice with a gene deletion in a PV interneuron subunit, gamma rhythms remain intact. Yet in this study theta rhythms showed a reduction in amplitude and theta-gamma coupling was impaired. One important facet of this study was that though a loss of theta would be expected to impair theta-gamma coupling, the deficit in coupling observed here went beyond what could be accounted for by the loss of theta (Wulff et al., 2009). Given the alterations to theta-gamma coupling in *Cacna1c*$^{+/-}$ rats, it is possible that if an alteration to PV interneurons was only very modest, theta-gamma coupling might still be affected while leaving theta intact. A more direct assessment of the density and physiology of hippocampal interneuron subtypes in *Cacna1c*$^{+/-}$ rats is necessary to understand whether these also contribute to the alterations to theta-gamma coupling observed during runs on the novel track. Moreover, the most recent SCZ GWAS highlighted several risk loci for genes involved in GABAergic signalling (Ripke et al.,

2020) indicating a crucial role for interneurons in susceptibility to psychiatric risk. Understanding the association between calcium channel dysfunction and interneuronal deficits may be important in broadening our understanding of the role of inhibition in psychiatric risk.

7.1.3. Negative Findings

The aforementioned lack of impairment observed to oscillatory activity was ostensibly surprising. Effects have been reported throughout this thesis where no such deficit was observed in *Cacna1c*$^{+/-}$ rats despite good prior reasoning to believe L-type calcium channel dysfunction might give rise to alterations, such as the phase-locking of pyramidal cells to theta and gamma oscillations, where previous research indicates a reliance on Schaffer-collateral plasticity (Kitanishi et al., 2015). Additionally, despite showing a modest experience-dependent alteration in certain place-cell properties, place-field formation was not impaired in *Cacna1c*$^{+/-}$, nor were any changes seen in the number of place-fields exhibited per place-cell despite the reliance of place-field formation on dendritic spiking (Sheffield and Dombeck, 2015, Sheffield et al., 2017) for which L-type calcium channels have an important role (Golding et al., 2002).

One potential explanation for these negative findings that has not yet been discussed, is the role of compensatory mechanisms in the nervous system. Within the brain there appear to be a wealth of methods by which the nervous system seeks to stabilize neuronal activity in response to alterations to synaptic activity, potentially as a method to resist destabilization of neuronal networks (Turrigiano and Nelson, 2000, Yin and Yuan, 2014). These include alterations to the equilibrium potential of ventral spiny neurons following excitatory block (Chub and O'Donovan, 1998), regulation of the conductance of individual neurons (Golowasch et al., 1999), and structural changes, such as an increase in the number of dendritic spines on hippocampal CA1 pyramidal cells following blockade of synaptic transmission (Kirov and Harris, 2000). Additionally rhythmic activity may be under homeostatic regulation. In the lobster ganglion, neuromodulatory input regulates the rhythmic motor output of networks of neurons, yet following blockade of this neuromodulatory input, neuronal rhythmicity gradually returns (Thoby-Brisson and Simmers, 1998), indicating that even the network activity of neurons is under tight homeostatic control.

Gene expression also appears to be under homeostatic control. In Drosophila, increased transcription is observed for genes on X chromosomes in males so as to compensate for the change in gene dosage that results from a smaller Y chromosome (Lucchesi and Kuroda, 2015), and similar effects have been observed in mammals (Brockdorff and Turner, 2015). Furthermore, genetic compensation is observed in response to gene

knockout (El-Brolosy and Stainier, 2017). For example knockout of a ribosome gene in mice, causes upregulation of a normally inhibited paralogue gene (O'Leary et al., 2013).

Given the wealth of evidence supporting a role for homeostatic responses to both genetic alterations and synaptic changes that might result from such genetic changes, it is likely that in *Cacna1c*$^{+/-}$ rats, adaptations exist so as to account for the loss of calcium influx. Indeed that does appear to be the case. Research in thalamo-amygdala synapses indicates that knockdown of *Cacna1c* prompts an incorporation of calcium permeable AMPA receptors into the post-synaptic density (Langwieser et al., 2010). It is unknown whether such an effect exists in CA1 synapses, though it is clear that calcium channels are essential to normal brain function as homozygous knockout of *Cacna1c* is embryonically lethal and thus without such compensatory mechanisms, one would expect heterozygous knockout to be considerably more deleterious. Restoration of the intrinsic excitability of CA1 pyramidal cells, whether through alterations to the strength of individual synapses or through structural changes, such as increasing the number of dendritic spines may explain why place-cell formation was not impaired. Additionally mechanisms to compensate for alterations to network activity may at least in part explain why oscillatory activity appeared largely intact.

7.1.4. Behavioural Relevance of Electrophysiological Findings

The functional and behavioural relevance of the hippocampal neurophysiological deficits reported here require further analysis. A reduction in the cross-correlated activity of place-cell pairs during SPW-Rs might indicate an impairment to hippocampal 'replay', though the results of subsequent 'replay' analysis in Chapter 5 were conflicting. Given the important role of SPW-R's in sleep-dependent memory consolidation (Girardeau et al., 2009, Ramadan et al., 2009, Ego-Stengel and Wilson, 2010) in addition to the well-established evidence of sleep-dependent memory consolidation impairments in relation to psychiatric disease (Dresler et al., 2011, Wamsley et al., 2012, Genzel et al., 2015, Baran et al., 2018) it seems plausible that the SPW-R associated impairments in *Cacna1c*$^{+/-}$ rats may reflect a deficit here. Indeed, place-field alterations were observed only following experience, indicating that these may have emerged as a result of dysfunctional memory consolidation during sleep, yet the behavioural protocol used here did not place any explicit spatial memory demands on the rats used in these studies, given that all recordings were undertaken during free exploration. As such, on the basis of the evidence provided in this thesis, it is not possible to say whether the deficits observed at a hippocampal neurophysiological level are reflective of a broader impairment in spatial memory consolidation.

On the other hand, it is possible that these neurophysiological deficits may have some bearing on prior work demonstrating cognitive impairments in relation to *CACNA1C* as reviewed in Chapter 1. One such impairment is that of latent inhibition, where it has been

shown that *Cacna1c*$^{+/-}$ rats fail to inhibit subsequent fear responses following an extended pre-exposure to a 'neutral' environment (Tigaret et al., 2020). Latent inhibition relies upon the formation of context-associations which may require the formation of cell assemblies (Liu et al., 2012), linking back to some of the previously discussed links between assembly formation and correlated CA1 activity. A loss of cross-correlated activity in *Cacna1c*$^{+/-}$ rats might reflect a reduced ability to form cell assemblies, potentially giving rise to deficits here. Computational modelling also reveals an important role for feedforward inhibition in latent inhibition. Here, prior formed context-associations engage feedforward inhibition to 'gate' irrelevant stimuli (Insel et al., 2018). On this basis a latent inhibition deficit in *Cacna1c*$^{+/-}$ rats could emerge as a result of a deficit to inhibition, though equally a failure to form sufficiently strong initial context associations may prevent the engagement of adequate feedforward inhibition to prevent subsequent contextual fear associations from being formed. The research presented here, though not sufficient to conclusively support either view, provides some remit for the interrogation of cellular activation during latent inhibition to elucidate this further.

In summary the research presented in this thesis provides clear evidence of deficits to spiking activity during SPW-Rs in addition to impairments to place-cell properties following experience and alterations to oscillatory coupling under certain conditions in *Cacna1c*$^{+/-}$ rats. These deficits to hippocampal neurophysiology may in turn underlie the cognitive impairments previously identified in relation to *Cacna1c* reduced gene dosage. Though these findings may have important implications for our understanding of *CACNA1C*, and its role in psychiatric disease, this work was not without its limitations, which one must bear in mind in any interpretation of the data.

7.2. Limitations & Future Directions

7.2.1. Statistical Limitations

Throughout this thesis, due to the inherent difficulties associated with carrying out electrophysiological recordings in vivo, in addition to ethical concerns regarding the use of large numbers of animals, the sample size was relatively low. A lower sample size increases the likelihood that a reported effect is false even if statistical analysis reveals such an effect to be statistically significant (Button et al., 2013). Though for many of the larger effects reported in this thesis the lower sample size may still have been adequate, without a comprehensive power analysis this cannot be said for certain. In future work, where possible, performing power analysis prior to carrying out experiments may be an effective remedy to the potential pitfalls of a low sample size.

In addition to the potential sample size limitations, another statistical limitation of the analyses presented in this thesis was the use of cell numbers as the sample n for much of the analysis presented in chapters 3 and 5. This practice, despite its common usage in the field (Lazic et al., 2018), violates the assumption of independence among experimental units, and as such may lead to incorrect conclusions regarding whether or not one can reject the null hypothesis (Lazic, 2010). One potential solution to this problem in the future would be to make use of mixed effects models (Lazic, 2010, Zimmerman et al., 2021). Mixed effects models contain both fixed and random effects and thus allow one to represent the hierarchical structure inherent in the data, where fixed effects may be used to represent the variable of interest and random effects to represent variation between individual animals.

7.2.2. Regional Specificity

All electrophysiological research presented here concerned the CA1 region of the dorsal hippocampus. Though there was good motivation to focus on this brain region as discussed in Chapter 1, to do so solely came at the expense of other important brain regions of interest.

7.2.2.1. Hippocampal Specificity

Within the hippocampus I restricted focus to the CA1 subregion and this in part was motivated by research demonstrating plasticity impairments within CA1 (Moosmang et al., 2005, Tigaret et al., 2020). Yet *Cacna1c* expression has been found in all major hippocampal subregions (Sykes et al., 2018) indicating that there may be utility in expanding the analyses to encompass the CA3 and DG in order to more effectively parse the relative contributions to hippocampal function and dysfunction from each subregion in *Cacna1c*$^{+/-}$ rats. Current source density might be an effective method by which one could perform such analysis. Using multielectrode silicon probes one could simultaneously record LFP from multiple hippocampal layers (Csicsvari et al., 2003) and in turn could infer sources and sinks of LFP activity and more accurately estimate the flow of oscillatory activity (Brankack et al., 1993) within the hippocampus. This approach may be of particular value in furthering our understanding of the PAC deficits reported in this thesis.

More broadly, the focus of this research was restricted to the dorsal hippocampus, yet the function of the hippocampus varies across the dorsoventral axis with lesion studies revealing a role for the dorsal hippocampus in spatial learning (Moser et al., 1995, Moser and Moser, 1998) while the ventral hippocampus, through its connectivity with regions involved in emotional processing such as the amygdala, appears to play a more significant role in emotional learning (Swanson and Cowan, 1977, Groenewegen et al., 1987). This is further evidenced by impairments to emotional learning observed after NMDA receptor antagonist

administration to the ventral hippocampus (Zhang et al., 2001). Within both animals and human participants harbouring *CACNA1C* variants, deficits in emotional processing have been reported (Dao et al., 2010, Dedic et al., 2018), potentially implicating ventral hippocampal dysfunction here. Moreover, in a *Cacna1c* forebrain conditional knockout mouse model, deficits in adult neurogenesis have been observed across the dorsoventral axis (Lee et al., 2016) and neurogenesis within the ventral hippocampus in particular, is reported to play a role in emotional processing (Jayatissa et al., 2006, Anacker et al., 2018). Deficits here may consequently have an important mechanistic link to emotional symptoms in psychiatric disease. By considering only the dorsal hippocampus, this research was biased towards an interrogation of cognitive symptoms rather than emotional symptoms in relation to *Cacna1c*.

Finally, all neurophysiological recordings in this thesis were from the right hippocampus, yet *CACNA1C* appears to exert bilateral effects on the hippocampus. This has been observed in human participants harbouring the risk variant of the rs1006737 SNP, whereby reduced bilateral hippocampal coupling was observed during a memory recall task (Erk et al., 2010). In contrast, elevated bilateral activation of the hippocampus has also been observed in carriers of the same risk SNP though in this instance during an emotional processing task (Bigos et al., 2010), again pointing to a potential effect of *CACNA1C* on ventral hippocampal function. By focusing only on the right hippocampus, the research presented in this thesis fails to account for dysfunction lateralized to the left hemisphere in addition to hemispheric interactions. In order to more rigorously characterise the effects of *CACNA1C* on hippocampal function, future research might make use of bilateral hippocampal electrophysiology which, combined with the use of recordings across multiple hippocampal cell layers and recordings from the ventral hippocampus, could signify a more holistic approach to characterising the impact of *Cacna1c* heterozygosity on hippocampal function. This would complement the recordings undertaken at a localised level of analysis in the current work, with recordings focused on the hippocampus at a more global level of analysis.

7.2.2.2. Prefrontal Cortex

Much of the motivation for focus on the hippocampus in this research concerned the expression profile of *Cacna1c* in the hippocampus in conjunction with the evidence of hippocampus-dependent behavioural deficits in humans and animals harbouring *CACNA1C* variants. On this basis a similar case could be made to also consider the prefrontal cortex (PFC). *Cacna1c* expression is observed across the medial, ventral, and lateral PFC (Sykes et al., 2018) and PFC alterations in BDNF expression, a downstream signalling molecule of LTCCs, have been linked to reversal learning deficits in *Cacna1c*$^{+/-}$ rats and human risk allele carriers alike (Sykes et al., 2019). Though research focusing solely on the prefrontal cortex would be of interest per se, combined electrophysiological recordings from both the

hippocampus and PFC may prove of greater utility. Spatial learning for example depends on connectivity between the PFC and hippocampus (Floresco et al., 1997) and at a cellular and network level, these regions show coherent LFP at theta frequency during working memory that corresponds to phase-locking of units in both regions to this coherent rhythmic activity (Jones and Wilson, 2005b). Such coupling may have pertinence to psychiatric risk. In the Df(16)A$^{+/-}$ genetic mouse model of SCZ, neuronal synchrony between these two brain regions is impaired (Sigurdsson et al., 2010) and altered coupling is also observed in human risk allele carriers (Esslinger et al., 2009, Cousijn et al., 2015). Additionally, in a neurodevelopmental model of SCZ, a loss of spindle-ripple coupling is observed between the hippocampus and PFC (Phillips et al., 2012a). Given the SPW-R-associated firing alterations observed in *Cacna1c*$^{+/-}$ rats it would be useful to understand what effect this has downstream of the hippocampus. Simultaneous recordings from both the PFC and hippocampus could resolve this question by quantifying spindle associated firing in the PFC alongside hippocampus ripple-associated firing activity. In addition, recordings during wake may shed further light on the role of PFC-hippocampus synchrony in relation to psychiatric disease and in particular how this pertains to LTCC expression.

7.2.3. Behavioural Limitations

Despite finding evidence of hippocampal deficits in relation to *Cacna1c* heterozygosity as indicated earlier, the functional relevance of these effects remains uncertain given that the behavioural tasks in which they were recorded provided limited scope to quantify cognitive function. In particular, this research could have benefitted from a behavioural task in which the animals' learning could have been directly quantified in order to more effectively link deficits in hippocampal function to overt cognitive impairment. A range of tasks have been devised to assess spatial learning; two of the most well established are the Morris-water maze (Morris, 1981) and the radial arm maze (Olton and Samuelson, 1976). Both of these tasks display reliance on the hippocampus (Morris et al., 1982, Winocur, 1982) though in assessing place learning the Morris-water maze might be more suitable given that some evidence indicates the learning of associations between corridors and reward in the radial-arm maze may engage associative rather than spatial learning (Hodges, 1996). On the other hand, there are significant feasibility/practical implications in the use of a water-based maze with sensitive electrophysiological equipment. Alternatively, another commonly used cognitive behavioural task is the spatial alternation task, typically performed using some variation of a T-maze. Performance here also relies on the hippocampus (McHugh et al., 2008), though this task appears to probe spatial working memory (Olton et al., 1979), rather than simply spatial

learning. This behavioural task also depends on hippocampal-prefrontal connectivity (Floresco et al., 1997) and has been used frequently to assess coupling between these structures (Jones and Wilson, 2005a, Jones and Wilson, 2005b). As such it may be of particular utility in future research seeking to assess the impact of *Cacna1c* heterozygosity on hippocampal-prefrontal activity as was posited as a potential future avenue of research earlier.

Another limitation of the experimental design in this thesis concerned the place-cell remapping analysis reported in Chapter 3. Here I sought to quantify how place-cells remapped in both genotypes by rotating the linear track 45°. Though this engendered some degree of both rate and global remapping, the mixed responses across cell populations indicate that this intervention did not impart full novelty onto hippocampal representations. Alternative approaches to instigating place-cell remapping have included manipulations to the external walls of an environment (Muller and Kubie, 1987, Kentros et al., 1998), though this is less straightforward on a relatively open raised linear-track, and use of an L-shaped track (Dragoi and Tonegawa, 2013). In the latter approach familiar runs are undertaken on one arm of the track, with a barrier blocking the animals from exploring the orthogonal arm. In the novel run session the barrier is subsequently removed enabling the exploration of this second arm. Both arms here are of a comparable length, enabling more direct comparisons to be made between place-cell representations on each arm than would otherwise be possible if exposing animals to an entirely altered environment. This approach in the future may have more utility in gaining an understanding of how *Cacna1c* heterozygosity impacts on the flexibility of hippocampal representations across distinct yet similar environments.

Novel place-cell properties were additionally characterised through the use of a novel open-field and many place-cell deficits appeared to depend on the familiarity of the environment indicating that place cell deficits in relation to *Cacna1c* heterozygosity manifest only after repeated exposures to an environment. This could have been quantified more rigorously had recordings been undertaken over several days as has been the approach of other studies (Cacucci et al., 2007) reporting similar place-cell deficits. This approach would enable study of both place-field formation upon first exposure to the environment, and the subsequent refinement of place-fields over the following days of recordings, purportedly impaired in *Cacna1c*$^{+/-}$ rats. Importantly, such an approach would rely on the use of a rat strain for which exploration during the first exposure to an environment does not markedly differ from exploration as the environment becomes more familiar (Piazza et al., 1989, Stead et al., 2006), as appeared to be the case for the rat strain used in this research.

7.2.4. Limitations of the Animal Model

How relevant is *Cacna1c* heterozygosity to human genetic variation in *CACNA1C*? As discussed in Chapter 1, research into the expression profile of *CACNA1C* in individuals

harbouring risk variants is conflicting with both elevated (Bigos et al., 2010, Yoshimizu et al., 2015) and reduced (Gershon et al., 2014, Roussos et al., 2014, Eckart et al., 2016, Jaffe et al., 2020) expression profiles reported. Yet in the hippocampus it appears that a reduction in expression stemming from heterozygosity might recapitulate the reduced *CACNA1C* expression observed in relation to SCZ (Jaffe et al., 2020), providing the rationale for the approach taken here. Importantly though, this was observed only within the DG and the exact expression changes found within CA1 are unknown. Furthermore the 50% reduction presumed to arise as a result of heterozygous knockout in vivo (Sykes et al., 2019), may not match the effect size of *CACNA1C* variation on gene expression in patient populations.

Whether or not *Cacna1c* heterozygosity reliably models genetic variation in *CACNA1C* in the human population, the more direct relevance to psychiatric risk is less clear. The odds ratio of rs1006737 for example is low (like most risk SNPs) – at 1.77 (Bigos et al., 2010). As such modelling this dysfunction in animals, though useful for understanding the role of this gene in brain function, is likely only to have small effects on psychiatric relevant brain function and dysfunction. Use of a rare high impact mutation such as 22q11.2 (Marshall et al., 2017) might have a greater impact on hippocampal function in animals in a psychiatric disease-relevant manner. That being said, rare mutations by definition are less common and thus dysfunction associated with these variants may not be representative of brain dysfunction more typically associated with psychiatric disease.

Another potential limitation of the animal model used throughout this research was the use of all-male rats. Numerous studies report sex specific effects in relation to *Cacna1c* genetic variation (Dao et al., 2010, Strohmaier et al., 2013, Braun et al., 2018). For example in heterozygous mice, elevated anxiety levels restricted to female mice have been reported, and this same study reported sex-specific associations with mood disorders (increased risk in female participants) for several *CACNA1C* SNPs (Dao et al., 2010). Likewise sex-specific genetic associations have been found for risk SNP rs1006737 and various psychiatric relevant endophenotypes such as emotional lability in female participants and resilience in male participants (Strohmaier et al., 2013). For *Cacna1c* animal research to have utility in furthering our understanding of human psychiatric risk, future research should make use of animals of both sexes to account for these sex-specific effects on brain function.

Finally, genetic risk does not solely explain the liability to risk for any psychiatric disorder (Polderman et al., 2015) with environmental influence playing a significant role also. Gene x environment interactions have been previously reported in relation to *CACNA1C*. In a study of *Cacna1c* forebrain knockout-mice, increased susceptibility to chronic stress was reported. Additionally, this study also reported a significant interaction with adverse life events in conferring risk for psychiatric disease in human carriers of *CACNA1C* risk alleles (Dedic et al., 2018). Combining genetic models with behavioural protocols such as chronic stress may

be an effective method by which to model psychiatric risk, and the associated effects on brain function, in future research.

7.2.5. Role of Neurodevelopment

Several psychiatric disorders for which *CACNA1C* genetic variants are associated are classed as neurodevelopmental disorders; disorders for which their aetiology is, at least in part, the result of disruption to development of the nervous system (Rutter, 1995, Thapar et al., 2017). This includes disorders known to emerge during childhood such as ASD and ADHD (Doernberg and Hollander, 2016), but evidence also supports a role for disrupted neurodevelopment in SCZ (Gupta and Kulhara, 2010, Owen et al., 2011), which is further supported by evidence of a shared genetic architecture between these disorders (Owen and O'Donovan, 2017).

Given the association of *CACNA1C* with ASD and SCZ it is reasonable to hypothesize that gene variants may disrupt neurodevelopment and indeed several lines of evidence suggest this is the case. Studies of neuron development reveal an important role for CaM kinases, a downstream signalling target of LTCCs, in a variety of processes involved in neuron development such as neuronal morphogenesis and spine formation (Gomez and Spitzer, 1999, Yamagata et al., 2009, Takemoto-Kimura et al., 2010, Horigane et al., 2016). The calcium signal responsible for triggering this signalling cascade appears to be LTCC-dependent. In a study which made use of a calcium indicator in developing cortical neurons, a loss of regenerative calcium transients was observed following pharmacological inhibition of LTCCs. Additionally, genetic knockout of LTCCs impaired neurite growth and neuronal migration (Kamijo et al., 2018), highlighting the important role of calcium channel mediated signalling in the developing nervous system. Further evidence for a role of *CACNA1C* in neurodevelopment comes from study of Timothy Syndrome, the disorder caused by a mutation in *CACNA1C*. This disorder is associated with a range of traits typically associated with neurodevelopmental disorders such as ASD and intellectual disability, in addition to a range of facial features often observed in other known neurodevelopmental conditions (Splawski et al., 2004). Furthermore, study of iPSC-derived neurons from individuals with Timothy Syndrome reveals abnormal neuronal differentiation and dendritic retraction (Paşca et al., 2011, Krey et al., 2013).

In both rodents and humans, the spatial component of episodic memory develops during early childhood and this development is impaired in neurodevelopmental disorders (Ainge and Langston, 2012, Mastrogiuseppe et al., 2019). It is thus plausible that the *Cacna1c* associated hippocampal deficits reported in adulthood in this thesis, may have arisen as a result of disrupted neurodevelopment earlier in development. To further interrogate this, a series of recordings taken over the course of development in heterozygous *Cacna1c* rats, or

a series of targeted *Cacna1c* knockdowns at different points in development, would elucidate the extent to which hippocampal deficits observed during adulthood emerge as a result of disrupted nervous system development.

7.2.6. Rescue Experiments

The next stage in any psychiatric research, following identification of brain dysfunction associated with psychiatric risk, is to identify treatments and interventions which reverse this dysfunction. Preliminary evidence supports the role of neurotrophin receptor activation in rescuing the synaptic plasticity and behavioural deficits associated with *Cacna1c* heterozygosity. Here, LM22B-10 an activator of the TrkB/TrkC neurotrophin receptor was used in an attempt to counteract effects of reduced LTCC expression on downstream signalling, in particular the MAPK signalling pathway (Tigaret et al., 2020). Likewise, in a forebrain-specific *Cacna1c* knockout mouse model, targeting of another downstream signalling molecule, in this instance eIF2α, with an inhibitor (ISRIB) rescued associated social deficits and elevated anxiety behaviour (Kabir et al., 2017a). In future research it would be informative to assess whether either of these compounds have any effects on the hippocampal deficits identified in this thesis.

Additionally, in human participants LTCC antagonists have previously been trialled and used, though to limited levels of success, in the treatment of a range of psychiatric symptoms (Grebb et al., 1986, Schwartz et al., 1997, Hollister and Trevino, 1999, Cipriani et al., 2016) and there is an ongoing clinical trial to investigate the role of nicardipine on a battery of psychiatric symptoms (Atkinson et al., 2019). Use of these compounds presumably targets instances in which an increase in expression of calcium channel genes is observed in relation to psychiatric disease (Bigos et al., 2010, Yoshimizu et al., 2015), in order to reverse deficits associated with elevated calcium channel expression. Such interventions are unlikely to have utility in the hippocampus of *Cacna1c*$^{+/-}$ rats where a further reduction in LTCC function might be expected to exacerbate deficits identified here. In contrast, use of an LTCC activator might be considered as a mechanism to enhance the activity of LTCCs that remain in heterozygous animals to try and counteract the effects of reduced gene expression in the hippocampus.

In summary the research presented in this thesis provides preliminary evidence of dysfunction in the hippocampus of *Cacna1c*$^{+/-}$ rats, yet at both a neurophysiological level and a behavioural level, this research had a restricted focus. The next steps will now be to expand this focus, both to capture the activity of additional brain regions and to characterise associated behavioural dysfunction that can be directly linked to deficits in neurophysiology. Furthermore it would be valuable to capture brain activity across multiple temporal scales in order to identify the changes in neurophysiology that occur both over the course of day or weeks of recording,

but also more broadly, over the course of an animal's lifetime. Finally, understanding how identified brain dysfunction can be reversed will be invaluable in identifying potential novel therapeutic targets for psychiatric treatment.

7.3. Conclusion

Insights from genetic studies into psychiatric disorders have identified important pathways in the pathophysiology of psychiatric risk. I investigated *CACNA1C* to understand how calcium channel dysfunction may underlie psychiatric disease related brain dysfunction. Prior research has implicated *Cacna1c* heterozygosity in plasticity and behavioural deficits in the hippocampus while imaging work reveals changes in hippocampal structure and activation during tasks in carriers of risk associated *CACNA1C* SNPs.

This thesis sought to address the question of how synaptic deficits might manifest at the single unit and neuronal network level in order to better understand how genetic variation in this gene might confer psychiatric risk. Here I showed that *Cacna1c* reduced gene dosage alters single unit properties within the dorsal hippocampus during free exploration and rest. Analysis of single unit properties revealed experience-dependent alterations in place-field size and spatial information during linear track exploration, whilst during rest, place-cells were both more active and less coactive in the *Cacna1c*$^{+/-}$ rats. Meanwhile analysis of oscillatory activity revealed a loss of theta-gamma coupling under certain experimental conditions.

These patterns of dysfunction have important implications for hippocampus-mediated cognition and have opened up new avenues of research to investigate this further. Continued *CACNA1C* research will help elucidate the role of calcium channel signalling in psychiatric risk and in turn, this may identify new targets for interventions in order to mitigate psychiatric symptoms that our current treatments fail to address.

Bibliography

Abbott, A. 2011. Novartis to shut brain research facility. *Nature,* 480**,** 161-2.

Abdul-Monim, Z., Reynolds, G. P. & Neill, J. C. 2003. The atypical antipsychotic ziprasidone, but not haloperidol, improves phencyclidine-induced cognitive deficits in a reversal learning task in the rat. *J Psychopharmacol,* 17**,** 57-65.

Addis, L., Virdee, J. K., Vidler, L. R., Collier, D. A., Pal, D. K. & Ursu, D. 2017. Epilepsy-associated GRIN2A mutations reduce NMDA receptor trafficking and agonist potency - molecular profiling and functional rescue. *Sci Rep,* 7**,** 66.

Adler, C. M., Malhotra, A. K., Elman, I., Goldberg, T., Egan, M., Pickar, D. & Breier, A. 1999. Comparison of ketamine-induced thought disorder in healthy volunteers and thought disorder in schizophrenia. *Am J Psychiatry,* 156**,** 1646-9.

Aguirre, G. K., Detre, J. A., Alsop, D. C. & D'esposito, M. 1996. The parahippocampus subserves topographical learning in man. *Cereb Cortex,* 6**,** 823-9.

Ahmed, O. J. & Mehta, M. R. 2012. Running speed alters the frequency of hippocampal gamma oscillations. *J Neurosci,* 32**,** 7373-83.

Ainge, J. A. & Langston, R. F. 2012. Ontogeny of neural circuits underlying spatial memory in the rat. *Front Neural Circuits,* 6**,** 8.

Akbarian, S., Sucher, N. J., Bradley, D., Tafazzoli, A., Trinh, D., Hetrick, W. P., . . . Jones, E. G. 1996. Selective alterations in gene expression for NMDA receptor subunits in prefrontal cortex of schizophrenics. *J Neurosci,* 16**,** 19-30.

Albensi, B. C., Oliver, D. R., Toupin, J. & Odero, G. 2007. Electrical stimulation protocols for hippocampal synaptic plasticity and neuronal hyper-excitability: are they effective or relevant? *Exp Neurol,* 204**,** 1-13.

Allardyce, J. & Boydell, J. 2006. Review: the wider social environment and schizophrenia. *Schizophr Bull,* 32**,** 592-8.

Alme, C. B., Miao, C., Jezek, K., Treves, A., Moser, E. I. & Moser, M. B. 2014. Place cells in the hippocampus: eleven maps for eleven rooms. *Proc Natl Acad Sci U S A,* 111**,** 18428-35.

Altimus, C., Harrold, J., Jaaro-Peled, H., Sawa, A. & Foster, D. J. 2015. Disordered ripples are a common feature of genetically distinct mouse models relevant to schizophrenia. *Mol Neuropsychiatry,* 1**,** 52-59.

Anacker, C., Luna, V. M., Stevens, G. S., Millette, A., Shores, R., Jimenez, J. C., . . . Hen, R. 2018. Hippocampal neurogenesis confers stress resilience by inhibiting the ventral dentate gyrus. *Nature,* 559**,** 98-102.

Anderzhanova, E., Kirmeier, T. & Wotjak, C. T. 2017. Animal models in psychiatric research: The RDoC system as a new framework for endophenotype-oriented translational neuroscience. *Neurobiol Stress,* 7**,** 47-56.

Andreasen, M. & Lambert, J. D. 1995. Regenerative properties of pyramidal cell dendrites in area CA1 of the rat hippocampus. *J Physiol,* 483 (Pt 2)**,** 421-41.

Angrist, B., Sathananthan, G., Wilk, S. & Gershon, S. 1974. Amphetamine psychosis: behavioral and biochemical aspects. *J Psychiatr Res,* 11**,** 13-23.

Angrist, B. M. & Gershon, S. 1970. The phenomenology of experimentally induced amphetamine psychosis--preliminary observations. *Biol Psychiatry,* 2**,** 95-107.

Ascher, P. & Nowak, L. 1988. The role of divalent cations in the N-methyl-D-aspartate responses of mouse central neurones in culture. *J Physiol,* 399**,** 247-66.

Asif-Malik, A., Dautan, D., Young, A. M. J. & Gerdjikov, T. V. 2017. Altered cortico-striatal crosstalk underlies object recognition memory deficits in the sub-chronic phencyclidine model of schizophrenia. *Brain Struct Funct,* 222**,** 3179-3190.

Assary, E., Vincent, J. P., Keers, R. & Pluess, M. 2018. Gene-environment interaction and psychiatric disorders: Review and future directions. *Semin Cell Dev Biol,* 77**,** 133-143.

Association, A. P. 2013. *Diagnostic and statistical manual of mental disorders (5th edition).* Washington, DC.

Atkinson, L. Z., Colbourne, L., Smith, A., Harmer, C. H., Nobre, A. C., Rendell, J., . . . Harrison, P. J. 2019. The Oxford study of Calcium channel Antagonism, Cognition, Mood instability and Sleep (OxCaMS): study protocol for a randomised controlled, experimental medicine study. *Trials,* 20**,** 120.

Austin, M. P., Mitchell, P. & Goodwin, G. M. 2001. Cognitive deficits in depression: possible implications for functional neuropathology. *Br J Psychiatry,* 178**,** 200-6.

Axmacher, N., Henseler, M. M., Jensen, O., Weinreich, I., Elger, C. E. & Fell, J. 2010. Cross-frequency coupling supports multi-item working memory in the human hippocampus. *Proc Natl Acad Sci U S A,* 107**,** 3228-33.

Babadi, B. & Brown, E. N. 2014. A review of multitaper spectral analysis. *IEEE Trans Biomed Eng,* 61**,** 1555-64.

Bader, P. L., Faizi, M., Kim, L. H., Owen, S. F., Tadross, M. R., Alfa, R. W., . . . Shamloo, M. 2011. Mouse model of Timothy syndrome recapitulates triad of autistic traits. *Proc Natl Acad Sci U S A,* 108**,** 15432-7.

Bähner, F., Demanuele, C., Schweiger, J., Gerchen, M. F., Zamoscik, V., Ueltzhöffer, K., . . . Meyer-Lindenberg, A. 2015. Hippocampal-dorsolateral prefrontal coupling as a species-conserved cognitive mechanism: a human translational imaging study. *Neuropsychopharmacology,* 40**,** 1674-81.

Balla, A., Koneru, R., Smiley, J., Sershen, H. & Javitt, D. C. 2001. Continuous phencyclidine treatment induces schizophrenia-like hyperreactivity of striatal dopamine release. *Neuropsychopharmacology,* 25**,** 157-64.

Baran, B., Correll, D., Vuper, T. C., Morgan, A., Durrant, S. J., Manoach, D. S. & Stickgold, R. 2018. Spared and impaired sleep-dependent memory consolidation in schizophrenia. *Schizophr Res,* 199**,** 83-89.

Barr, M. S., Rajji, T. K., Zomorrodi, R., Radhu, N., George, T. P., Blumberger, D. M. & Daskalakis, Z. J. 2017. Impaired theta-gamma coupling during working memory performance in schizophrenia. *Schizophr Res,* 189**,** 104-110.

Barry, C., Ginzberg, L. L., O'keefe, J. & Burgess, N. 2012. Grid cell firing patterns signal environmental novelty by expansion. *Proc Natl Acad Sci U S A,* 109**,** 17687-92.

Bartos, M., Vida, I., Frotscher, M., Meyer, A., Monyer, H., Geiger, J. R. & Jonas, P. 2002. Fast synaptic inhibition promotes synchronized gamma oscillations in hippocampal interneuron networks. *Proc Natl Acad Sci U S A,* 99**,** 13222-7.

Bartos, M., Vida, I. & Jonas, P. 2007. Synaptic mechanisms of synchronized gamma oscillations in inhibitory interneuron networks. *Nat Rev Neurosci,* 8**,** 45-56.

Bartsch, U., Simpkin, A. J., Demanuele, C., Wamsley, E., Marston, H. M. & Jones, M. W. 2019. Distributed slow-wave dynamics during sleep predict memory consolidation and its impairment in schizophrenia. *NPJ Schizophr,* 5**,** 18.

Bauer, E. P., Schafe, G. E. & Ledoux, J. E. 2002. NMDA receptors and L-type voltage-gated calcium channels contribute to long-term potentiation and different components of fear memory formation in the lateral amygdala. *J Neurosci,* 22**,** 5239-49.

Baumgärtel, K. & Mansuy, I. M. 2012. Neural functions of calcineurin in synaptic plasticity and memory. *Learn Mem,* 19**,** 375-84.

Bavley, C. C., Fischer, D. K., Rizzo, B. K. & Rajadhyaksha, A. M. 2017. Cav1.2 channels mediate persistent chronic stress-induced behavioral deficits that are associated with prefrontal

cortex activation of the p25/Cdk5-glucocorticoid receptor pathway. *Neurobiol Stress,* 7**,** 27-37.

Bayer, T. A., Falkai, P. & Maier, W. 1999. Genetic and non-genetic vulnerability factors in schizophrenia: the basis of the "two hit hypothesis". *J Psychiatr Res,* 33**,** 543-8.

Behrens, C. J., Van Den Boom, L. P., De Hoz, L., Friedman, A. & Heinemann, U. 2005. Induction of sharp wave-ripple complexes in vitro and reorganization of hippocampal networks. *Nat Neurosci,* 8**,** 1560-7.

Belluscio, M. A., Mizuseki, K., Schmidt, R., Kempter, R. & Buzsáki, G. 2012. Cross-frequency phase-phase coupling between θ and γ oscillations in the hippocampus. *J Neurosci,* 32**,** 423-35.

Bender, F., Gorbati, M., Cadavieco, M. C., Denisova, N., Gao, X., Holman, C., . . . Ponomarenko, A. 2015. Theta oscillations regulate the speed of locomotion via a hippocampus to lateral septum pathway. *Nat Commun,* 6**,** 8521.

Bergen, S. E., Ploner, A., Howrigan, D., O'donovan, M. C., Smoller, J. W., Sullivan, P. F., . . . Consortium, C. a. G. a. T. S. W. G. O. T. P. G. 2019. Joint Contributions of Rare Copy Number Variants and Common SNPs to Risk for Schizophrenia. *Am J Psychiatry,* 176**,** 29-35.

Berton, O. & Nestler, E. J. 2006. New approaches to antidepressant drug discovery: beyond monoamines. *Nat Rev Neurosci,* 7**,** 137-51.

Besedovsky, L., Lange, T. & Born, J. 2012. Sleep and immune function. *Pflugers Arch,* 463**,** 121-37.

Bieri, K. W., Bobbitt, K. N. & Colgin, L. L. 2014. Slow and fast γ rhythms coordinate different spatial coding modes in hippocampal place cells. *Neuron,* 82**,** 670-81.

Bigos, K. L., Mattay, V. S., Callicott, J. H., Straub, R. E., Vakkalanka, R., Kolachana, B., . . . Weinberger, D. R. 2010. Genetic variation in CACNA1C affects brain circuitries related to mental illness. *Arch Gen Psychiatry,* 67**,** 939-45.

Bikbaev, A. & Manahan-Vaughan, D. 2008. Relationship of hippocampal theta and gamma oscillations to potentiation of synaptic transmission. *Front Neurosci,* 2**,** 56-63.

Bittner, K. C., Grienberger, C., Vaidya, S. P., Milstein, A. D., Macklin, J. J., Suh, J., . . . Magee, J. C. 2015. Conjunctive input processing drives feature selectivity in hippocampal CA1 neurons. *Nat Neurosci,* 18**,** 1133-42.

Blackwood, D. H., Fordyce, A., Walker, M. T., St Clair, D. M., Porteous, D. J. & Muir, W. J. 2001. Schizophrenia and affective disorders--cosegregation with a translocation at chromosome 1q42 that directly disrupts brain-expressed genes: clinical and P300 findings in a family. *Am J Hum Genet,* 69**,** 428-33.

Bland, B. H. 1986. The physiology and pharmacology of hippocampal formation theta rhythms. *Prog Neurobiol,* 26**,** 1-54.

Bliss, T. V. & Collingridge, G. L. 1993. A synaptic model of memory: long-term potentiation in the hippocampus. *Nature,* 361**,** 31-9.

Bliss, T. V. & Lomo, T. 1973. Long-lasting potentiation of synaptic transmission in the dentate area of the anaesthetized rabbit following stimulation of the perforant path. *J Physiol,* 232**,** 331-56.

Blum, S., Moore, A. N., Adams, F. & Dash, P. K. 1999. A mitogen-activated protein kinase cascade in the CA1/CA2 subfield of the dorsal hippocampus is essential for long-term spatial memory. *J Neurosci,* 19**,** 3535-44.

Bogerts, B., Ashtari, M., Degreef, G., Alvir, J. M., Bilder, R. M. & Lieberman, J. A. 1990. Reduced temporal limbic structure volumes on magnetic resonance images in first episode schizophrenia. *Psychiatry Res,* 35**,** 1-13.

Bostock, E., Muller, R. U. & Kubie, J. L. 1991. Experience-dependent modifications of hippocampal place cell firing. *Hippocampus,* 1**,** 193-205.

Bragin, A., Jandó, G., Nádasdy, Z., Hetke, J., Wise, K. & Buzsáki, G. 1995. Gamma (40-100 Hz) oscillation in the hippocampus of the behaving rat. *J Neurosci,* 15**,** 47-60.

Brambilla, P., Barale, F., Caverzasi, E. & Soares, J. C. 2002. Anatomical MRI findings in mood and anxiety disorders. *Epidemiol Psichiatr Soc,* 11**,** 88-99.

Brankack, J., Stewart, M. & Fox, S. E. 1993. Current source density analysis of the hippocampal theta rhythm: associated sustained potentials and candidate synaptic generators. *Brain Res,* 615**,** 310-27.

Braun, M. D., Kisko, T. M., Vecchia, D. D., Andreatini, R., Schwarting, R. K. W. & Wöhr, M. 2018. Sex-specific effects of Cacna1c haploinsufficiency on object recognition, spatial memory, and reversal learning capabilities in rats. *Neurobiol Learn Mem,* 155**,** 543-555.

Bremer, T., Man, A., Kask, K. & Diamond, C. 2006. CACNA1C polymorphisms are associated with the efficacy of calcium channel blockers in the treatment of hypertension. *Pharmacogenomics,* 7**,** 271-9.

Bremner, J. D., Narayan, M., Anderson, E. R., Staib, L. H., Miller, H. L. & Charney, D. S. 2000. Hippocampal volume reduction in major depression. *Am J Psychiatry,* 157**,** 115-8.

Brockdorff, N. & Turner, B. M. 2015. Dosage compensation in mammals. *Cold Spring Harb Perspect Biol,* 7**,** a019406.

Brown, A. S. & Derkits, E. J. 2010. Prenatal infection and schizophrenia: a review of epidemiologic and translational studies. *Am J Psychiatry,* 167**,** 261-80.

Brown, L. A., Hasan, S., Foster, R. G. & Peirson, S. N. 2016. COMPASS: Continuous Open Mouse Phenotyping of Activity and Sleep Status. *Wellcome Open Res,* 1**,** 2.

Buchsbaum, M. S. & Haier, R. J. 1978. Biological homogeneity, symptom heterogeneity, and the diagnosis of schizophrenia. *Schizophr Bull,* 4**,** 473-5.

Buckley, P. F., Miller, B. J., Lehrer, D. S. & Castle, D. J. 2009. Psychiatric comorbidities and schizophrenia. *Schizophr Bull,* 35**,** 383-402.

Bulkin, D. A., Law, L. M. & Smith, D. M. 2016. Placing memories in context: Hippocampal representations promote retrieval of appropriate memories. *Hippocampus,* 26**,** 958-71.

Burgess, N., Maguire, E. A. & O'keefe, J. 2002. The human hippocampus and spatial and episodic memory. *Neuron,* 35**,** 625-41.

Burmeister, M., Mcinnis, M. G. & Zöllner, S. 2008. Psychiatric genetics: progress amid controversy. *Nat Rev Genet,* 9**,** 527-40.

Burnashev, N. & Szepetowski, P. 2015. NMDA receptor subunit mutations in neurodevelopmental disorders. *Curr Opin Pharmacol,* 20**,** 73-82.

Button, K. S., Ioannidis, J. P., Mokrysz, C., Nosek, B. A., Flint, J., Robinson, E. S. & Munafo, M. R. 2013. Power failure: why small sample size undermines the reliability of neuroscience. *Nat Rev Neurosci,* 14**,** 365-76.

Buzsáki, G. 1989. Two-stage model of memory trace formation: A role for "noisy" brain states. Neuroscience.

Buzsáki, G. 2002. Theta oscillations in the hippocampus. *Neuron,* 33**,** 325-40.

Buzsáki, G. 2015. Hippocampal sharp wave-ripple: A cognitive biomarker for episodic memory and planning. *Hippocampus,* 25**,** 1073-188.

Buzsáki, G., Leung, L. W. & Vanderwolf, C. H. 1983. Cellular bases of hippocampal EEG in the behaving rat. *Brain Res,* 287**,** 139-71.

Buzsáki, G. & Moser, E. I. 2013. Memory, navigation and theta rhythm in the hippocampal-entorhinal system. *Nat Neurosci,* 16**,** 130-8.

Buzsáki, G. & Wang, X. J. 2012. Mechanisms of gamma oscillations. *Annu Rev Neurosci,* 35**,** 203-25.

Byrne, E. M., Gehrman, P. R., Medland, S. E., Nyholt, D. R., Heath, A. C., Madden, P. A., . . . Consortium, C. 2013. A genome-wide association study of sleep habits and insomnia. *Am J Med Genet B Neuropsychiatr Genet,* 162B**,** 439-51.

Byrne, M., Agerbo, E., Eaton, W. W. & Mortensen, P. B. 2004. Parental socio-economic status and risk of first admission with schizophrenia- a Danish national register based study. *Soc Psychiatry Psychiatr Epidemiol,* 39**,** 87-96.

Cacucci, F., Wills, T. J., Lever, C., Giese, K. P. & O'keefe, J. 2007. Experience-dependent increase in CA1 place cell spatial information, but not spatial reproducibility, is dependent on the

autophosphorylation of the alpha-isoform of the calcium/calmodulin-dependent protein kinase II. *J Neurosci,* 27**,** 7854-9.
Caixeta, F. V., Cornélio, A. M., Scheffer-Teixeira, R., Ribeiro, S. & Tort, A. B. 2013. Ketamine alters oscillatory coupling in the hippocampus. *Sci Rep,* 3**,** 2348.
Canolty, R. T., Edwards, E., Dalal, S. S., Soltani, M., Nagarajan, S. S., Kirsch, H. E., . . . Knight, R. T. 2006. High gamma power is phase-locked to theta oscillations in human neocortex. *Science,* 313**,** 1626-8.
Caplan, J. B., Madsen, J. R., Schulze-Bonhage, A., Aschenbrenner-Scheibe, R., Newman, E. L. & Kahana, M. J. 2003. Human theta oscillations related to sensorimotor integration and spatial learning. *J Neurosci,* 23**,** 4726-36.
Cardin, J. A., Carlén, M., Meletis, K., Knoblich, U., Zhang, F., Deisseroth, K., . . . Moore, C. I. 2009. Driving fast-spiking cells induces gamma rhythm and controls sensory responses. *Nature,* 459**,** 663-7.
Cardno, A. G. & Owen, M. J. 2014. Genetic relationships between schizophrenia, bipolar disorder, and schizoaffective disorder. *Schizophr Bull,* 40**,** 504-15.
Carr, C. P., Martins, C. M., Stingel, A. M., Lemgruber, V. B. & Juruena, M. F. 2013. The role of early life stress in adult psychiatric disorders: a systematic review according to childhood trauma subtypes. *J Nerv Ment Dis,* 201**,** 1007-20.
Carroll, L. S. & Owen, M. J. 2009. Genetic overlap between autism, schizophrenia and bipolar disorder. *Genome Med,* 1**,** 102.
Casamassima, F., Huang, J., Fava, M., Sachs, G. S., Smoller, J. W., Cassano, G. B., . . . Perlis, R. H. 2010. Phenotypic effects of a bipolar liability gene among individuals with major depressive disorder. *Am J Med Genet B Neuropsychiatr Genet,* 153B**,** 303-9.
Caspi, A., Houts, R. M., Belsky, D. W., Goldman-Mellor, S. J., Harrington, H., Israel, S., . . . Moffitt, T. E. 2014. The p Factor: One General Psychopathology Factor in the Structure of Psychiatric Disorders? *Clin Psychol Sci,* 2**,** 119-137.
Catterall, W. A., Striessnig, J., Snutch, T. P., Perez-Reyes, E. & Pharmacology, I. U. O. 2003. International Union of Pharmacology. XL. Compendium of voltage-gated ion channels: calcium channels. *Pharmacol Rev,* 55**,** 579-81.
Catts, V. S., Lai, Y. L., Weickert, C. S., Weickert, T. W. & Catts, S. V. 2016. A quantitative review of the postmortem evidence for decreased cortical N-methyl-D-aspartate receptor expression levels in schizophrenia: How can we link molecular abnormalities to mismatch negativity deficits? *Biol Psychol,* 116**,** 57-67.
Charpak, S., Paré, D. & Llinás, R. 1995. The entorhinal cortex entrains fast CA1 hippocampal oscillations in the anaesthetized guinea-pig: role of the monosynaptic component of the perforant path. *Eur J Neurosci,* 7**,** 1548-57.
Chartoff, E. H., Heusner, C. L. & Palmiter, R. D. 2005. Dopamine is not required for the hyperlocomotor response to NMDA receptor antagonists. *Neuropsychopharmacology,* 30**,** 1324-33.
Chatterjee, M., Ganguly, S., Srivastava, M. & Palit, G. 2011. Effect of 'chronic' versus 'acute' ketamine administration and its 'withdrawal' effect on behavioural alterations in mice: implications for experimental psychosis. *Behav Brain Res,* 216**,** 247-54.
Chen, Z., Resnik, E., Mcfarland, J. M., Sakmann, B. & Mehta, M. R. 2011. Speed controls the amplitude and timing of the hippocampal gamma rhythm. *PLoS One,* 6**,** e21408.
Chiovini, B., Turi, G. F., Katona, G., Kaszás, A., Pálfi, D., Maák, P., . . . Rózsa, B. 2014. Dendritic spikes induce ripples in parvalbumin interneurons during hippocampal sharp waves. *Neuron,* 82**,** 908-24.
Cho, R. Y., Konecky, R. O. & Carter, C. S. 2006. Impairments in frontal cortical gamma synchrony and cognitive control in schizophrenia. *Proc Natl Acad Sci U S A,* 103**,** 19878-83.

Chub, N. & O'donovan, M. J. 1998. Blockade and recovery of spontaneous rhythmic activity after application of neurotransmitter antagonists to spinal networks of the chick embryo. *J Neurosci,* 18**,** 294-306.

Cipriani, A., Saunders, K., Attenburrow, M. J., Stefaniak, J., Panchal, P., Stockton, S., . . . Harrison, P. J. 2016. A systematic review of calcium channel antagonists in bipolar disorder and some considerations for their future development. *Mol Psychiatry,* 21**,** 1324-32.

Clapcote, S. J., Lipina, T. V., Millar, J. K., Mackie, S., Christie, S., Ogawa, F., . . . Roder, J. C. 2007. Behavioral phenotypes of Disc1 missense mutations in mice. *Neuron,* 54**,** 387-402.

Clark, R. E. & Squire, L. R. 2013. Similarity in form and function of the hippocampus in rodents, monkeys, and humans. *Proc Natl Acad Sci U S A,* 110 Suppl 2**,** 10365-70.

Clemens, Z., Mölle, M., Eross, L., Barsi, P., Halász, P. & Born, J. 2007. Temporal coupling of parahippocampal ripples, sleep spindles and slow oscillations in humans. *Brain,* 130**,** 2868-78.

Cloues, R. K. & Sather, W. A. 2003. Afterhyperpolarization regulates firing rate in neurons of the suprachiasmatic nucleus. *J Neurosci,* 23**,** 1593-604.

Cohen, N. J. & Eichenbaum, H. 1993. *Memory, amnesia, and the hippocampal system* . Cambridge, Mass, MIT Press.

Colgin, L. L., Denninger, T., Fyhn, M., Hafting, T., Bonnevie, T., Jensen, O., . . . Moser, E. I. 2009. Frequency of gamma oscillations routes flow of information in the hippocampus. *Nature,* 462**,** 353-7.

Collingridge, G. L., Kehl, S. J. & Mclennan, H. 1983. Excitatory amino acids in synaptic transmission in the Schaffer collateral-commissural pathway of the rat hippocampus. *J Physiol,* 334**,** 33-46.

Connors, B. W. & Gutnick, M. J. 1990. Intrinsic firing patterns of diverse neocortical neurons. *Trends Neurosci,* 13**,** 99-104.

Contreras, D., Destexhe, A., Sejnowski, T. J. & Steriade, M. 1996. Control of spatiotemporal coherence of a thalamic oscillation by corticothalamic feedback. *Science,* 274**,** 771-4.

Cornwell, B. R., Arkin, N., Overstreet, C., Carver, F. W. & Grillon, C. 2012. Distinct contributions of human hippocampal theta to spatial cognition and anxiety. *Hippocampus,* 22**,** 1848-59.

Cosgrove, D., Mothersill, O., Kendall, K., Konte, B., Harold, D., Giegling, I., . . . Consortium, W. T. C. C. 2017. Cognitive Characterization of Schizophrenia Risk Variants Involved in Synaptic Transmission: Evidence of CACNA1C's Role in Working Memory. *Neuropsychopharmacology,* 42**,** 2612-2622.

Cousijn, H., Tunbridge, E. M., Rolinski, M., Wallis, G., Colclough, G. L., Woolrich, M. W., . . . Harrison, P. J. 2015. Modulation of hippocampal theta and hippocampal-prefrontal cortex function by a schizophrenia risk gene. *Hum Brain Mapp,* 36**,** 2387-95.

Coussens, C. M., Kerr, D. S. & Abraham, W. C. 1997. Glucocorticoid receptor activation lowers the threshold for NMDA-receptor-dependent homosynaptic long-term depression in the hippocampus through activation of voltage-dependent calcium channels. *J Neurophysiol,* 78**,** 1-9.

Coyle, J. T. 2012. NMDA receptor and schizophrenia: a brief history. *Schizophr Bull,* 38**,** 920-6.

Craddock, N. & Owen, M. J. 2005. The beginning of the end for the Kraepelinian dichotomy. *Br J Psychiatry,* 186**,** 364-6.

Cross-Disorder Group of the Psychiatric Genomics Consortium 2013. Identification of risk loci with shared effects on five major psychiatric disorders: a genome-wide analysis. *Lancet,* 381**,** 1371-9.

Cryan, J. F., Mombereau, C. & Vassout, A. 2005. The tail suspension test as a model for assessing antidepressant activity: review of pharmacological and genetic studies in mice. *Neurosci Biobehav Rev,* 29**,** 571-625.

Csicsvari, J., Henze, D. A., Jamieson, B., Harris, K. D., Sirota, A., Barthó, P., . . . Buzsáki, G. 2003. Massively parallel recording of unit and local field potentials with silicon-based electrodes. *J Neurophysiol,* 90**,** 1314-23.

Csicsvari, J., Hirase, H., Czurkó, A., Mamiya, A. & Buzsáki, G. 1999. Fast network oscillations in the hippocampal CA1 region of the behaving rat. *J Neurosci,* 19**,** RC20.

Csicsvari, J., O'neill, J., Allen, K. & Senior, T. 2007. Place-selective firing contributes to the reverse-order reactivation of CA1 pyramidal cells during sharp waves in open-field exploration. *Eur J Neurosci,* 26**,** 704-16.

Cui, L., Sun, W., Yu, M., Li, N., Guo, L., Gu, H. & Zhou, Y. 2016. Disrupted-in-schizophrenia1 (DISC1) L100P mutation alters synaptic transmission and plasticity in the hippocampus and causes recognition memory deficits. *Mol Brain,* 9**,** 89.

Cuthbert, B. N. 2014. The RDoC framework: facilitating transition from ICD/DSM to dimensional approaches that integrate neuroscience and psychopathology. *World Psychiatry,* 13**,** 28-35.

Cuthbert, B. N. & Insel, T. R. 2013. Toward the future of psychiatric diagnosis: the seven pillars of RDoC. *BMC Med,* 11**,** 126.

D'agostino, A., Castelnovo, A., Cavallotti, S., Casetta, C., Marcatili, M., Gambini, O., . . . Sarasso, S. 2018. Sleep endophenotypes of schizophrenia: slow waves and sleep spindles in unaffected first-degree relatives. *NPJ Schizophr,* 4**,** 2.

Daban, C., Martinez-Aran, A., Torrent, C., Tabarés-Seisdedos, R., Balanzá-Martínez, V., Salazar-Fraile, J., . . . Vieta, E. 2006. Specificity of cognitive deficits in bipolar disorder versus schizophrenia. A systematic review. *Psychother Psychosom,* 75**,** 72-84.

Dao, D. T., Mahon, P. B., Cai, X., Kovacsics, C. E., Blackwell, R. A., Arad, M., . . . Consortium, B. G. S. B. 2010. Mood disorder susceptibility gene CACNA1C modifies mood-related behaviors in mice and interacts with sex to influence behavior in mice and diagnosis in humans. *Biol Psychiatry,* 68**,** 801-10.

Dashti, H. S., Jones, S. E., Wood, A. R., Lane, J. M., Van Hees, V. T., Wang, H., . . . Saxena, R. 2019. Genome-wide association study identifies genetic loci for self-reported habitual sleep duration supported by accelerometer-derived estimates. *Nat Commun,* 10**,** 1100.

Davidson, T. J., Kloosterman, F. & Wilson, M. A. 2009. Hippocampal replay of extended experience. *Neuron,* 63**,** 497-507.

Davis, J., Eyre, H., Jacka, F. N., Dodd, S., Dean, O., Mcewen, S., . . . Berk, M. 2016. A review of vulnerability and risks for schizophrenia: Beyond the two hit hypothesis. *Neurosci Biobehav Rev,* 65**,** 185-94.

Day, M., Olson, P. A., Platzer, J., Striessnig, J. & Surmeier, D. J. 2002. Stimulation of 5-HT(2) receptors in prefrontal pyramidal neurons inhibits Ca(v)1.2 L type Ca(2+) currents via a PLCbeta/IP3/calcineurin signaling cascade. *J Neurophysiol,* 87**,** 2490-504.

De Almeida, L., Idiart, M. & Lisman, J. E. 2009. A second function of gamma frequency oscillations: an E%-max winner-take-all mechanism selects which cells fire. *J Neurosci,* 29**,** 7497-503.

De La Rocha, J., Doiron, B., Shea-Brown, E., Josić, K. & Reyes, A. 2007. Correlation between neural spike trains increases with firing rate. *Nature,* 448**,** 802-6.

Dean, K. & Murray, R. M. 2005. Environmental risk factors for psychosis. *Dialogues Clin Neurosci,* 7**,** 69-80.

Dedic, N., Pöhlmann, M. L., Richter, J. S., Mehta, D., Czamara, D., Metzger, M. W., . . . Deussing, J. M. 2018. Cross-disorder risk gene CACNA1C differentially modulates susceptibility to psychiatric disorders during development and adulthood. *Mol Psychiatry,* 23**,** 533-543.

Degoulet, M., Stelly, C. E., Ahn, K. C. & Morikawa, H. 2016. L-type Ca^{2+} channel blockade with antihypertensive medication disrupts VTA synaptic plasticity and drug-associated contextual memory. *Mol Psychiatry,* 21**,** 394-402.

Depoortere, R., Perrault, G. & Sanger, D. J. 1999. Prepulse inhibition of the startle reflex in rats: effects of compounds acting at various sites on the NMDA receptor complex. *Behav Pharmacol,* 10**,** 51-62.

Diba, K. & Buzsáki, G. 2007. Forward and reverse hippocampal place-cell sequences during ripples. *Nat Neurosci,* 10**,** 1241-2.

Didriksen, M., Fejgin, K., Nilsson, S. R., Birknow, M. R., Grayton, H. M., Larsen, P. H., . . . Nielsen, J. 2017. Persistent gating deficit and increased sensitivity to NMDA receptor antagonism after puberty in a new mouse model of the human 22q11.2 microdeletion syndrome: a study in male mice. *J Psychiatry Neurosci,* 42**,** 48-58.

Doernberg, E. & Hollander, E. 2016. Neurodevelopmental Disorders (ASD and ADHD): DSM-5, ICD-10, and ICD-11. *CNS Spectr,* 21**,** 295-9.

Doherty, J. L. & Owen, M. J. 2014. Genomic insights into the overlap between psychiatric disorders: implications for research and clinical practice. *Genome Med,* 6**,** 29.

Dolmetsch, R. E., Pajvani, U., Fife, K., Spotts, J. M. & Greenberg, M. E. 2001. Signaling to the nucleus by an L-type calcium channel-calmodulin complex through the MAP kinase pathway. *Science,* 294**,** 333-9.

Dolphin, A. C. 2012. Calcium channel auxiliary α2δ and β subunits: trafficking and one step beyond. *Nat Rev Neurosci,* 13**,** 542-55.

Donaldson, Z. R. & Hen, R. 2015. From psychiatric disorders to animal models: a bidirectional and dimensional approach. *Biol Psychiatry,* 77**,** 15-21.

Doornbos, M., Sikkema-Raddatz, B., Ruijvenkamp, C. A., Dijkhuizen, T., Bijlsma, E. K., Gijsbers, A. C., . . . Van Ravenswaaij-Arts, C. M. 2009. Nine patients with a microdeletion 15q11.2 between breakpoints 1 and 2 of the Prader-Willi critical region, possibly associated with behavioural disturbances. *Eur J Med Genet,* 52**,** 108-15.

Dragoi, G. & Buzsáki, G. 2006. Temporal encoding of place sequences by hippocampal cell assemblies. *Neuron,* 50**,** 145-57.

Dragoi, G. & Tonegawa, S. 2013. Development of schemas revealed by prior experience and NMDA receptor knock-out. *Elife,* 2**,** e01326.

Dresler, M., Kluge, M., Pawlowski, M., Schüssler, P., Steiger, A. & Genzel, L. 2011. A double dissociation of memory impairments in major depression. *J Psychiatr Res,* 45**,** 1593-9.

Driessen, M., Herrmann, J., Stahl, K., Zwaan, M., Meier, S., Hill, A., . . . Petersen, D. 2000. Magnetic resonance imaging volumes of the hippocampus and the amygdala in women with borderline personality disorder and early traumatization. *Arch Gen Psychiatry,* 57**,** 1115-22.

Duan, T. T., Tan, J. W., Yuan, Q., Cao, J., Zhou, Q. X. & Xu, L. 2013. Acute ketamine induces hippocampal synaptic depression and spatial memory impairment through dopamine D1/D5 receptors. *Psychopharmacology (Berl),* 228**,** 451-61.

Ducharme, G., Lowe, G. C., Goutagny, R. & Williams, S. 2012. Early alterations in hippocampal circuitry and theta rhythm generation in a mouse model of prenatal infection: implications for schizophrenia. *PLoS One,* 7**,** e29754.

Eastman, C. I. & Burgess, H. J. 2009. How To Travel the World Without Jet lag. *Sleep Med Clin,* 4**,** 241-255.

Eaton, M. E., Macías, W., Youngs, R. M., Rajadhyaksha, A., Dudman, J. T. & Konradi, C. 2004. L-type Ca2+ channel blockers promote Ca2+ accumulation when dopamine receptors are activated in striatal neurons. *Brain Res Mol Brain Res,* 131**,** 65-72.

Eckart, N., Song, Q., Yang, R., Wang, R., Zhu, H., Mccallion, A. S. & Avramopoulos, D. 2016. Functional Characterization of Schizophrenia-Associated Variation in CACNA1C. *PLoS One,* 11**,** e0157086.

Ego-Stengel, V. & Wilson, M. A. 2010. Disruption of ripple-associated hippocampal activity during rest impairs spatial learning in the rat. *Hippocampus,* 20**,** 1-10.

Eichenbaum, H. 2004. Hippocampus: cognitive processes and neural representations that underlie declarative memory. *Neuron,* 44**,** 109-20.

Eichenbaum, H. 2017. The role of the hippocampus in navigation is memory. *J Neurophysiol,* 117**,** 1785-1796.

Eichenbaum, H. & Cohen, N. J. 2014. Can we reconcile the declarative memory and spatial navigation views on hippocampal function? *Neuron,* 83**,** 764-70.

Ekelund, J., Hovatta, I., Parker, A., Paunio, T., Varilo, T., Martin, R., . . . Peltonen, L. 2001. Chromosome 1 loci in Finnish schizophrenia families. *Hum Mol Genet,* 10**,** 1611-7.

Ekstrom, A. D., Kahana, M. J., Caplan, J. B., Fields, T. A., Isham, E. A., Newman, E. L. & Fried, I. 2003. Cellular networks underlying human spatial navigation. *Nature,* 425**,** 184-8.

El-Brolosy, M. A. & Stainier, D. Y. R. 2017. Genetic compensation: A phenomenon in search of mechanisms. *PLoS Genet,* 13**,** e1006780.

Elgar, M. A., Pagel, M. D. & Harvey, P. H. 1988. Sleep in Mammals. Animal Behaviour.

Emslie, G. J., Rush, A. J., Weinberg, W. A., Rintelmann, J. W. & Roffwarg, H. P. 1990. Children with major depression show reduced rapid eye movement latencies. *Arch Gen Psychiatry,* 47**,** 119-24.

English, D. F., Peyrache, A., Stark, E., Roux, L., Vallentin, D., Long, M. A. & Buzsáki, G. 2014. Excitation and inhibition compete to control spiking during hippocampal ripples: intracellular study in behaving mice. *J Neurosci,* 34**,** 16509-17.

Erk, S., Meyer-Lindenberg, A., Linden, D. E. J., Lancaster, T., Mohnke, S., Grimm, O., . . . Walter, H. 2014. Replication of brain function effects of a genome-wide supported psychiatric risk variant in the CACNA1C gene and new multi-locus effects. *Neuroimage,* 94**,** 147-154.

Erk, S., Meyer-Lindenberg, A., Schnell, K., Opitz Von Boberfeld, C., Esslinger, C., Kirsch, P., . . . Walter, H. 2010. Brain function in carriers of a genome-wide supported bipolar disorder variant. *Arch Gen Psychiatry,* 67**,** 803-11.

Eschenko, O., Ramadan, W., Mölle, M., Born, J. & Sara, S. J. 2008. Sustained increase in hippocampal sharp-wave ripple activity during slow-wave sleep after learning. *Learn Mem,* 15**,** 222-8.

Esslinger, C., Walter, H., Kirsch, P., Erk, S., Schnell, K., Arnold, C., . . . Meyer-Lindenberg, A. 2009. Neural mechanisms of a genome-wide supported psychosis variant. *Science,* 324**,** 605.

Fanselow, M. S. & Dong, H. W. 2010. Are the dorsal and ventral hippocampus functionally distinct structures? *Neuron,* 65**,** 7-19.

Farrell, M. S., Werge, T., Sklar, P., Owen, M. J., Ophoff, R. A., O'donovan, M. C., . . . Sullivan, P. F. 2015. Evaluating historical candidate genes for schizophrenia. *Mol Psychiatry,* 20**,** 555-62.

Fell, J., Ludowig, E., Staresina, B. P., Wagner, T., Kranz, T., Elger, C. E. & Axmacher, N. 2011. Medial temporal theta/alpha power enhancement precedes successful memory encoding: evidence based on intracranial EEG. *J Neurosci,* 31**,** 5392-7.

Ferreira, M. A., O'donovan, M. C., Meng, Y. A., Jones, I. R., Ruderfer, D. M., Jones, L., . . . Consortium, W. T. C. C. 2008. Collaborative genome-wide association analysis supports a role for ANK3 and CACNA1C in bipolar disorder. *Nat Genet,* 40**,** 1056-8.

Fischer, S., Nitschke, M. F., Melchert, U. H., Erdmann, C. & Born, J. 2005. Motor memory consolidation in sleep shapes more effective neuronal representations. *J Neurosci,* 25**,** 11248-55.

Flavell, S. W. & Greenberg, M. E. 2008. Signaling mechanisms linking neuronal activity to gene expression and plasticity of the nervous system. *Annu Rev Neurosci,* 31**,** 563-90.

Flint, J. & Munafò, M. R. 2007. The endophenotype concept in psychiatric genetics. *Psychol Med,* 37**,** 163-80.

Floresco, S. B., Seamans, J. K. & Phillips, A. G. 1997. Selective roles for hippocampal, prefrontal cortical, and ventral striatal circuits in radial-arm maze tasks with or without a delay. *J Neurosci,* 17**,** 1880-90.

Ford, J. M. & Mathalon, D. H. 2004. Electrophysiological evidence of corollary discharge dysfunction in schizophrenia during talking and thinking. *J Psychiatr Res,* 38**,** 37-46.

Ford, J. M., Mathalon, D. H., Heinks, T., Kalba, S., Faustman, W. O. & Roth, W. T. 2001. Neurophysiological evidence of corollary discharge dysfunction in schizophrenia. *Am J Psychiatry,* 158**,** 2069-71.

Foster, D. J. 2017. Replay Comes of Age. *Annu Rev Neurosci,* 40**,** 581-602.

Foster, D. J. & Wilson, M. A. 2006. Reverse replay of behavioural sequences in hippocampal place cells during the awake state. *Nature,* 440**,** 680-3.

Frank, L. M., Stanley, G. B. & Brown, E. N. 2004. Hippocampal plasticity across multiple days of exposure to novel environments. *J Neurosci,* 24**,** 7681-9.

Freir, D. B. & Herron, C. E. 2003. Inhibition of L-type voltage dependent calcium channels causes impairment of long-term potentiation in the hippocampal CA1 region in vivo. *Brain Res,* 967**,** 27-36.

Fromer, M., Pocklington, A. J., Kavanagh, D. H., Williams, H. J., Dwyer, S., Gormley, P., . . . O'donovan, M. C. 2014. De novo mutations in schizophrenia implicate synaptic networks. *Nature,* 506**,** 179-84.

Fuhrmann, F., Justus, D., Sosulina, L., Kaneko, H., Beutel, T., Friedrichs, D., . . . Remy, S. 2015. Locomotion, Theta Oscillations, and the Speed-Correlated Firing of Hippocampal Neurons Are Controlled by a Medial Septal Glutamatergic Circuit. *Neuron,* 86**,** 1253-64.

Furman, J. L., Sompol, P., Kraner, S. D., Pleiss, M. M., Putman, E. J., Dunkerson, J., . . . Norris, C. M. 2016. Blockade of Astrocytic Calcineurin/NFAT Signaling Helps to Normalize Hippocampal Synaptic Function and Plasticity in a Rat Model of Traumatic Brain Injury. *J Neurosci,* 36**,** 1502-15.

Fyhn, M., Molden, S., Witter, M. P., Moser, E. I. & Moser, M. B. 2004. Spatial representation in the entorhinal cortex. *Science,* 305**,** 1258-64.

Galambos, R. 1941. Cochlear Potentials from the Bat. *Science,* 93**,** 215.

Gao, X. M., Sakai, K., Roberts, R. C., Conley, R. R., Dean, B. & Tamminga, C. A. 2000. Ionotropic glutamate receptors and expression of N-methyl-D-aspartate receptor subunits in subregions of human hippocampus: effects of schizophrenia. *Am J Psychiatry,* 157**,** 1141-9.

García-Bea, A., Bermudez, I., Harrison, P. J. & Lane, T. A. 2017. A group II metabotropic glutamate receptor 3 (mGlu3, GRM3) isoform implicated in schizophrenia interacts with canonical mGlu3 and reduces ligand binding. *J Psychopharmacol,* 31**,** 1519-1526.

Gaugler, T., Klei, L., Sanders, S. J., Bodea, C. A., Goldberg, A. P., Lee, A. B., . . . Buxbaum, J. D. 2014. Most genetic risk for autism resides with common variation. *Nat Genet,* 46**,** 881-5.

Geisler, C., Robbe, D., Zugaro, M., Sirota, A. & Buzsáki, G. 2007. Hippocampal place cell assemblies are speed-controlled oscillators. *Proc Natl Acad Sci U S A,* 104**,** 8149-54.

Gejman, P. V., Sanders, A. R. & Duan, J. 2010. The role of genetics in the etiology of schizophrenia. *Psychiatr Clin North Am,* 33**,** 35-66.

Genovese, G., Fromer, M., Stahl, E. A., Ruderfer, D. M., Chambert, K., Landén, M., . . . Mccarroll, S. A. 2016. Increased burden of ultra-rare protein-altering variants among 4,877 individuals with schizophrenia. *Nat Neurosci,* 19**,** 1433-1441.

Genzel, L., Dresler, M., Cornu, M., Jäger, E., Konrad, B., Adamczyk, M., . . . Goya-Maldonado, R. 2015. Medial prefrontal-hippocampal connectivity and motor memory consolidation in depression and schizophrenia. *Biol Psychiatry,* 77**,** 177-86.

Gerber, D. J., Hall, D., Miyakawa, T., Demars, S., Gogos, J. A., Karayiorgou, M. & Tonegawa, S. 2003. Evidence for association of schizophrenia with genetic variation in the 8p21.3 gene, PPP3CC, encoding the calcineurin gamma subunit. *Proc Natl Acad Sci U S A,* 100**,** 8993-8.

Gershon, E. S., Grennan, K., Busnello, J., Badner, J. A., Ovsiew, F., Memon, S., . . . Liu, C. 2014. A rare mutation of CACNA1C in a patient with bipolar disorder, and decreased gene expression associated with a bipolar-associated common SNP of CACNA1C in brain. *Mol Psychiatry,* 19**,** 890-4.

Gerstein, G. L. 2004. Searching for significance in spatio-temporal firing patterns. *Acta Neurobiol Exp (Wars),* 64**,** 203-7.

Gevins, A. & Cutillo, B. 1993. Spatiotemporal dynamics of component processes in human working memory. *Electroencephalogr Clin Neurophysiol,* 87**,** 128-43.

Giese, K. P., Fedorov, N. B., Filipkowski, R. K. & Silva, A. J. 1998a. Autophosphorylation at Thr286 of the alpha calcium-calmodulin kinase II in LTP and learning. *Science,* 279**,** 870-3.

Giese, K. P., Storm, J. F., Reuter, D., Fedorov, N. B., Shao, L. R., Leicher, T., . . . Silva, A. J. 1998b. Reduced K+ channel inactivation, spike broadening, and after-hyperpolarization in Kvbeta1.1-deficient mice with impaired learning. *Learn Mem,* 5**,** 257-73.

Gillies, M. J., Traub, R. D., Lebeau, F. E., Davies, C. H., Gloveli, T., Buhl, E. H. & Whittington, M. A. 2002. A model of atropine-resistant theta oscillations in rat hippocampal area CA1. *J Physiol,* 543**,** 779-93.

Gilman, S. R., Iossifov, I., Levy, D., Ronemus, M., Wigler, M. & Vitkup, D. 2011. Rare de novo variants associated with autism implicate a large functional network of genes involved in formation and function of synapses. *Neuron,* 70**,** 898-907.

Girardeau, G., Benchenane, K., Wiener, S. I., Buzsáki, G. & Zugaro, M. B. 2009. Selective suppression of hippocampal ripples impairs spatial memory. *Nat Neurosci,* 12**,** 1222-3.

Girardeau, G., Cei, A. & Zugaro, M. 2014. Learning-induced plasticity regulates hippocampal sharp wave-ripple drive. *J Neurosci,* 34**,** 5176-83.

Gloveli, T., Dugladze, T., Saha, S., Monyer, H., Heinemann, U., Traub, R. D., . . . Buhl, E. H. 2005. Differential involvement of oriens/pyramidale interneurones in hippocampal network oscillations in vitro. *J Physiol,* 562**,** 131-47.

Goldberg, D. 2011. The heterogeneity of "major depression". *World Psychiatry,* 10**,** 226-8.

Golding, N. L., Kath, W. L. & Spruston, N. 2001. Dichotomy of action-potential backpropagation in CA1 pyramidal neuron dendrites. *J Neurophysiol,* 86**,** 2998-3010.

Golding, N. L., Staff, N. P. & Spruston, N. 2002. Dendritic spikes as a mechanism for cooperative long-term potentiation. *Nature,* 418**,** 326-31.

Golowasch, J., Casey, M., Abbott, L. F. & Marder, E. 1999. Network stability from activity-dependent regulation of neuronal conductances. *Neural Comput,* 11**,** 1079-96.

Gomez, T. M. & Spitzer, N. C. 1999. In vivo regulation of axon extension and pathfinding by growth-cone calcium transients. *Nature,* 397**,** 350-5.

Gonçalves, B. S., Cavalcanti, P. R., Tavares, G. R., Campos, T. F. & Araujo, J. F. 2014. Nonparametric methods in actigraphy: An update. *Sleep Sci,* 7**,** 158-64.

Gonzalez, S., Xu, C., Ramirez, M., Zavala, J., Armas, R., Contreras, S. A., . . . Escamilla, M. 2013. Suggestive evidence for association between L-type voltage-gated calcium channel (CACNA1C) gene haplotypes and bipolar disorder in Latinos: a family-based association study. *Bipolar Disord,* 15**,** 206-14.

Gottesman, I. I. & Shields, J. 1973. Genetic theorizing and schizophrenia. *Br J Psychiatry,* 122**,** 15-30.

Gould, T. D. & Gottesman, I. I. 2006. Psychiatric endophenotypes and the development of valid animal models. *Genes Brain Behav,* 5**,** 113-9.

Goutagny, R., Jackson, J. & Williams, S. 2009. Self-generated theta oscillations in the hippocampus. *Nat Neurosci,* 12**,** 1491-3.

Grandy, D. K., Allen, L. J., Zhang, Y., Magenis, R. E. & Civelli, O. 1992. Chromosomal localization of three human D5 dopamine receptor genes. *Genomics,* 13**,** 968-73.

Grastyan, E., Lissak, K., Madarasz, I. & Donhoffer, H. 1959. Hippocampal electrical activity during the development of conditioned reflexes. *Electroencephalogr Clin Neurophysiol,* 11**,** 409-30.

Grebb, J. A., Shelton, R. C., Taylor, E. H. & Bigelow, L. B. 1986. A negative, double-blind, placebo-controlled, clinical trial of verapamil in chronic schizophrenia. *Biol Psychiatry,* 21**,** 691-4.

Green, E. K., Grozeva, D., Jones, I., Jones, L., Kirov, G., Caesar, S., . . . Consortium, W. T. C. C. 2010. The bipolar disorder risk allele at CACNA1C also confers risk of recurrent major depression and of schizophrenia. *Mol Psychiatry,* 15**,** 1016-22.

Green, E. K., Hamshere, M., Forty, L., Gordon-Smith, K., Fraser, C., Russell, E., . . . Wtccc 2013. Replication of bipolar disorder susceptibility alleles and identification of two novel genome-wide significant associations in a new bipolar disorder case-control sample. *Mol Psychiatry,* 18**,** 1302-7.

Grent-'T-Jong, T., Rivolta, D., Sauer, A., Grube, M., Singer, W., Wibral, M. & Uhlhaas, P. J. 2016. MEG-measured visually induced gamma-band oscillations in chronic schizophrenia: Evidence for

impaired generation of rhythmic activity in ventral stream regions. *Schizophr Res,* 176**,** 177-185.

Groenewegen, H. J., Vermeulen-Van Der Zee, E., Te Kortschot, A. & Witter, M. P. 1987. Organization of the projections from the subiculum to the ventral striatum in the rat. A study using anterograde transport of Phaseolus vulgaris leucoagglutinin. *Neuroscience,* 23**,** 103-20.

Grosmark, A. D., Mizuseki, K., Pastalkova, E., Diba, K. & Buzsáki, G. 2012. REM sleep reorganizes hippocampal excitability. *Neuron,* 75**,** 1001-7.

Grover, L. M. & Teyler, T. J. 1990. Two components of long-term potentiation induced by different patterns of afferent activation. *Nature,* 347**,** 477-9.

Grunze, H. C., Rainnie, D. G., Hasselmo, M. E., Barkai, E., Hearn, E. F., Mccarley, R. W. & Greene, R. W. 1996. NMDA-dependent modulation of CA1 local circuit inhibition. *J Neurosci,* 16**,** 2034-43.

Gu, N., Vervaeke, K. & Storm, J. F. 2007. BK potassium channels facilitate high-frequency firing and cause early spike frequency adaptation in rat CA1 hippocampal pyramidal cells. *J Physiol,* 580**,** 859-82.

Guan, F., Zhang, B., Yan, T., Li, L., Liu, F., Li, T., . . . Li, S. 2014. MIR137 gene and target gene CACNA1C of miR-137 contribute to schizophrenia susceptibility in Han Chinese. *Schizophr Res,* 152**,** 97-104.

Gupta, A. S., Van Der Meer, M. A., Touretzky, D. S. & Redish, A. D. 2010. Hippocampal replay is not a simple function of experience. *Neuron,* 65**,** 695-705.

Gupta, A. S., Van Der Meer, M. A., Touretzky, D. S. & Redish, A. D. 2012. Segmentation of spatial experience by hippocampal θ sequences. *Nat Neurosci,* 15**,** 1032-9.

Gupta, S. & Kulhara, P. 2010. What is schizophrenia: A neurodevelopmental or neurodegenerative disorder or a combination of both? A critical analysis. *Indian J Psychiatry,* 52**,** 21-7.

Haenschel, C., Bittner, R. A., Waltz, J., Haertling, F., Wibral, M., Singer, W., . . . Rodriguez, E. 2009. Cortical oscillatory activity is critical for working memory as revealed by deficits in early-onset schizophrenia. *J Neurosci,* 29**,** 9481-9.

Hafting, T., Fyhn, M., Molden, S., Moser, M. B. & Moser, E. I. 2005. Microstructure of a spatial map in the entorhinal cortex. *Nature,* 436**,** 801-6.

Hakami, T., Jones, N. C., Tolmacheva, E. A., Gaudias, J., Chaumont, J., Salzberg, M., . . . Pinault, D. 2009. NMDA receptor hypofunction leads to generalized and persistent aberrant gamma oscillations independent of hyperlocomotion and the state of consciousness. *PLoS One,* 4**,** e6755.

Han, D., Xue, X., Yan, Y. & Li, G. 2019. Dysfunctional Cav1.2 channel in Timothy syndrome, from cell to bedside. *Exp Biol Med (Maywood),* 244**,** 960-971.

Hansen, A. K., Nedergaard, S. & Andreasen, M. 2014. Intrinsic Ca2+-dependent theta oscillations in apical dendrites of hippocampal CA1 pyramidal cells in vitro. *J Neurophysiol,* 112**,** 631-43.

Hardingham, G. E., Arnold, F. J. & Bading, H. 2001. A calcium microdomain near NMDA receptors: on switch for ERK-dependent synapse-to-nucleus communication. *Nat Neurosci,* 4**,** 565-6.

Hardingham, G. E., Chawla, S., Cruzalegui, F. H. & Bading, H. 1999. Control of recruitment and transcription-activating function of CBP determines gene regulation by NMDA receptors and L-type calcium channels. *Neuron,* 22**,** 789-98.

Hardingham, G. E., Fukunaga, Y. & Bading, H. 2002. Extrasynaptic NMDARs oppose synaptic NMDARs by triggering CREB shut-off and cell death pathways. *Nat Neurosci,* 5**,** 405-14.

Harrison, P. J. 2015. Recent genetic findings in schizophrenia and their therapeutic relevance. *J Psychopharmacol,* 29**,** 85-96.

Harvey, A. G., Talbot, L. S. & Gershon, A. 2009a. Sleep Disturbance in Bipolar Disorder Across the Lifespan. *Clin Psychol (New York),* 16**,** 256-277.

Harvey, C. D., Collman, F., Dombeck, D. A. & Tank, D. W. 2009b. Intracellular dynamics of hippocampal place cells during virtual navigation. *Nature,* 461**,** 941-6.

Hashimoto, R., Numakawa, T., Ohnishi, T., Kumamaru, E., Yagasaki, Y., Ishimoto, T., . . . Kunugi, H. 2006. Impact of the DISC1 Ser704Cys polymorphism on risk for major depression, brain morphology and ERK signaling. *Hum Mol Genet,* 15**,** 3024-33.

Hastings, M. 1998. The brain, circadian rhythms, and clock genes. *BMJ,* 317**,** 1704-7.

Hastings, M. H. 1997. Central clocking. *Trends Neurosci,* 20**,** 459-64.

Hayashi-Takagi, A., Takaki, M., Graziane, N., Seshadri, S., Murdoch, H., Dunlop, A. J., . . . Sawa, A. 2010. Disrupted-in-Schizophrenia 1 (DISC1) regulates spines of the glutamate synapse via Rac1. *Nat Neurosci,* 13**,** 327-32.

He, K., An, Z., Wang, Q., Li, T., Li, Z., Chen, J., . . . Shi, Y. 2014. CACNA1C, schizophrenia and major depressive disorder in the Han Chinese population. *Br J Psychiatry,* 204**,** 36-9.

Heckers, S., Rauch, S. L., Goff, D., Savage, C. R., Schacter, D. L., Fischman, A. J. & Alpert, N. M. 1998. Impaired recruitment of the hippocampus during conscious recollection in schizophrenia. *Nat Neurosci,* 1**,** 318-23.

Heinrichs, R. W. & Zakzanis, K. K. 1998. Neurocognitive deficit in schizophrenia: a quantitative review of the evidence. *Neuropsychology,* 12**,** 426-45.

Heller, A. S. & Bagot, R. C. 2020. Is Hippocampal Replay a Mechanism for Anxiety and Depression? *JAMA Psychiatry*.

Hennah, W., Thomson, P., Peltonen, L. & Porteous, D. 2006. Genes and schizophrenia: beyond schizophrenia: the role of DISC1 in major mental illness. *Schizophr Bull,* 32**,** 409-16.

Hernandez, L., Auerbach, S. & Hoebel, B. G. 1988. Phencyclidine (PCP) injected in the nucleus accumbens increases extracellular dopamine and serotonin as measured by microdialysis. Life Sciences.

Herrero, J. L., Gieselmann, M. A., Sanayei, M. & Thiele, A. 2013. Attention-induced variance and noise correlation reduction in macaque V1 is mediated by NMDA receptors. *Neuron,* 78**,** 729-39.

Herring, B. E. & Nicoll, R. A. 2016. Long-Term Potentiation: From CaMKII to AMPA Receptor Trafficking. *Annu Rev Physiol,* 78**,** 351-65.

Herz, M. I. & Melville, C. 1980. Relapse in schizophrenia. *Am J Psychiatry,* 137**,** 801-5.

Heston, L. L. 1966. Psychiatric disorders in foster home reared children of schizophrenic mothers. *Br J Psychiatry,* 112**,** 819-25.

Hettema, J. M., Neale, M. C. & Kendler, K. S. 2001. A review and meta-analysis of the genetic epidemiology of anxiety disorders. *Am J Psychiatry,* 158**,** 1568-78.

Heyes, S., Pratt, W. S., Rees, E., Dahimene, S., Ferron, L., Owen, M. J. & Dolphin, A. C. 2015. Genetic disruption of voltage-gated calcium channels in psychiatric and neurological disorders. *Prog Neurobiol,* 134**,** 36-54.

Hodges, H. 1996. Maze procedures: the radial-arm and water maze compared. *Brain Res Cogn Brain Res,* 3**,** 167-81.

Hodgkinson, C. A., Goldman, D., Jaeger, J., Persaud, S., Kane, J. M., Lipsky, R. H. & Malhotra, A. K. 2004. Disrupted in schizophrenia 1 (DISC1): association with schizophrenia, schizoaffective disorder, and bipolar disorder. *Am J Hum Genet,* 75**,** 862-72.

Hollister, L. E. & Trevino, E. S. 1999. Calcium channel blockers in psychiatric disorders: a review of the literature. *Can J Psychiatry,* 44**,** 658-64.

Hölscher, C., Anwyl, R. & Rowan, M. J. 1997. Stimulation on the positive phase of hippocampal theta rhythm induces long-term potentiation that can Be depotentiated by stimulation on the negative phase in area CA1 in vivo. *J Neurosci,* 17**,** 6470-7.

Holsheimer, J., Boer, J., Lopes Da Silva, F. H. & Van Rotterdam, A. 1982. The double dipole model of theta rhythm generation: simulation of laminar field potential profiles in dorsal hippocampus of the rat. *Brain Res,* 235**,** 31-50.

Holt, W. & Maren, S. 1999. Muscimol inactivation of the dorsal hippocampus impairs contextual retrieval of fear memory. *J Neurosci,* 19**,** 9054-62.

Homayoun, H. & Moghaddam, B. 2007. NMDA receptor hypofunction produces opposite effects on prefrontal cortex interneurons and pyramidal neurons. *J Neurosci,* 27**,** 11496-500.
Hondo, H., Yonezawa, Y., Nakahara, T., Nakamura, K., Hirano, M., Uchimura, H. & Tashiro, N. 1994. Effect of phencyclidine on dopamine release in the rat prefrontal cortex; an in vivo microdialysis study. *Brain Res,* 633**,** 337-42.
Hori, H., Yamamoto, N., Fujii, T., Teraishi, T., Sasayama, D., Matsuo, J., . . . Kunugi, H. 2012. Effects of the CACNA1C risk allele on neurocognition in patients with schizophrenia and healthy individuals. *Sci Rep,* 2**,** 634.
Horigane, S., Ageta-Ishihara, N., Kamijo, S., Fujii, H., Okamura, M., Kinoshita, M., . . . Bito, H. 2016. Facilitation of axon outgrowth via a Wnt5a-CaMKK-CaMKIα pathway during neuronal polarization. *Mol Brain,* 9**,** 8.
Horn, M. E. & Nicoll, R. A. 2018. Somatostatin and parvalbumin inhibitory synapses onto hippocampal pyramidal neurons are regulated by distinct mechanisms. *Proc Natl Acad Sci U S A,* 115**,** 589-594.
Hovatta, I., Varilo, T., Suvisaari, J., Terwilliger, J. D., Ollikainen, V., Arajärvi, R., . . . Peltonen, L. 1999. A genomewide screen for schizophrenia genes in an isolated Finnish subpopulation, suggesting multiple susceptibility loci. *Am J Hum Genet,* 65**,** 1114-24.
Howes, O., Mccutcheon, R. & Stone, J. 2015. Glutamate and dopamine in schizophrenia: an update for the 21st century. *J Psychopharmacol,* 29**,** 97-115.
Howes, O. D., Mccutcheon, R., Owen, M. J. & Murray, R. M. 2017. The Role of Genes, Stress, and Dopamine in the Development of Schizophrenia. *Biol Psychiatry,* 81**,** 9-20.
Huber, R., Ghilardi, M. F., Massimini, M. & Tononi, G. 2004. Local sleep and learning. *Nature,* 430**,** 78-81.
Hudson, J. I., Lipinski, J. F., Frankenburg, F. R., Grochocinski, V. J. & Kupfer, D. J. 1988. Electroencephalographic sleep in mania. *Arch Gen Psychiatry,* 45**,** 267-73.
Huerta, P. T. & Lisman, J. E. 1996. Synaptic plasticity during the cholinergic theta-frequency oscillation in vitro. *Hippocampus,* 6**,** 58-61.
Huettner, J. E. & Bean, B. P. 1988. Block of N-methyl-D-aspartate-activated current by the anticonvulsant MK-801: selective binding to open channels. *Proc Natl Acad Sci U S A,* 85**,** 1307-11.
Hulse, B. K., Moreaux, L. C., Lubenov, E. V. & Siapas, A. G. 2016. Membrane Potential Dynamics of CA1 Pyramidal Neurons during Hippocampal Ripples in Awake Mice. *Neuron,* 89**,** 800-13.
Hunt, M. J., Kopell, N. J., Traub, R. D. & Whittington, M. A. 2017. Aberrant Network Activity in Schizophrenia. *Trends Neurosci,* 40**,** 371-382.
Hussaini, S. A., Kempadoo, K. A., Thuault, S. J., Siegelbaum, S. A. & Kandel, E. R. 2011. Increased size and stability of CA1 and CA3 place fields in HCN1 knockout mice. *Neuron,* 72**,** 643-53.
Hyman, S. E. 2013. Psychiatric drug development: diagnosing a crisis. *Cerebrum,* 2013**,** 5.
Insel, N., Guerguiev, J. & Richards, B. A. 2018. Irrelevance by inhibition: Learning, computation, and implications for schizophrenia. *PLoS Comput Biol,* 14**,** e1006315.
International Schizophrenia Consortium 2008. Rare chromosomal deletions and duplications increase risk of schizophrenia. *Nature,* 455**,** 237-41.
Irifune, M., Shimizu, T. & Nomoto, M. 1991. Ketamine-induced hyperlocomotion associated with alteration of presynaptic components of dopamine neurons in the nucleus accumbens of mice. *Pharmacol Biochem Behav,* 40**,** 399-407.
Irifune, M., Shimizu, T., Nomoto, M. & Fukuda, T. 1995. Involvement of N-methyl-D-aspartate (NMDA) receptors in noncompetitive NMDA receptor antagonist-induced hyperlocomotion in mice. *Pharmacol Biochem Behav,* 51**,** 291-6.
Ivorra, J. L., Rivero, O., Costas, J., Iniesta, R., Arrojo, M., Ramos-Ríos, R., . . . Sanjuán, J. 2014. Replication of previous genome-wide association studies of psychiatric diseases in a large schizophrenia case-control sample from Spain. *Schizophr Res,* 159**,** 107-13.

Jaaro-Peled, H., Hayashi-Takagi, A., Seshadri, S., Kamiya, A., Brandon, N. J. & Sawa, A. 2009. Neurodevelopmental mechanisms of schizophrenia: understanding disturbed postnatal brain maturation through neuregulin-1-ErbB4 and DISC1. *Trends Neurosci,* 32**,** 485-95.

Jackson, J. C., Johnson, A. & Redish, A. D. 2006. Hippocampal sharp waves and reactivation during awake states depend on repeated sequential experience. *J Neurosci,* 26**,** 12415-26.

Jaffe, A. E., Hoeppner, D. J., Saito, T., Blanpain, L., Ukaigwe, J., Burke, E. E., . . . Hyde, T. M. 2020. Profiling gene expression in the human dentate gyrus granule cell layer reveals insights into schizophrenia and its genetic risk. *Nat Neurosci,* 23**,** 510-519.

Jaffe, D. B., Wang, B. & Brenner, R. 2011. Shaping of action potentials by type I and type II large-conductance Ca^{2}+-activated K+ channels. *Neuroscience,* 192**,** 205-18.

Jamain, S., Quach, H., Betancur, C., Råstam, M., Colineaux, C., Gillberg, I. C., . . . Study, P. a. R. I. S. 2003. Mutations of the X-linked genes encoding neuroligins NLGN3 and NLGN4 are associated with autism. *Nat Genet,* 34**,** 27-9.

Jansen, P. R., Watanabe, K., Stringer, S., Skene, N., Bryois, J., Hammerschlag, A. R., . . . Team, A. R. 2019. Genome-wide analysis of insomnia in 1,331,010 individuals identifies new risk loci and functional pathways. *Nat Genet,* 51**,** 394-403.

Jayatissa, M. N., Bisgaard, C., Tingström, A., Papp, M. & Wiborg, O. 2006. Hippocampal cytogenesis correlates to escitalopram-mediated recovery in a chronic mild stress rat model of depression. *Neuropsychopharmacology,* 31**,** 2395-404.

Jensen, O. & Lisman, J. E. 2000. Position reconstruction from an ensemble of hippocampal place cells: contribution of theta phase coding. *J Neurophysiol,* 83**,** 2602-9.

Jentsch, J. D., Taylor, J. R. & Roth, R. H. 1998. Subchronic phencyclidine administration increases mesolimbic dopaminergic system responsivity and augments stress- and psychostimulant-induced hyperlocomotion. *Neuropsychopharmacology,* 19**,** 105-13.

Ji, B., Wang, X., Pinto-Duarte, A., Kim, M., Caldwell, S., Young, J. W., . . . Zhou, X. 2013. Prolonged Ketamine Effects in Sp4 Hypomorphic Mice: Mimicking Phenotypes of Schizophrenia. *PLoS One,* 8**,** e66327.

Jia, P., Kao, C. F., Kuo, P. H. & Zhao, Z. 2011. A comprehensive network and pathway analysis of candidate genes in major depressive disorder. *BMC Syst Biol,* 5 Suppl 3**,** S12.

Jiang, M. & Swann, J. W. 2005. A role for L-type calcium channels in the maturation of parvalbumin-containing hippocampal interneurons. *Neuroscience,* 135**,** 839-50.

Jiang, Y. H., Yuen, R. K., Jin, X., Wang, M., Chen, N., Wu, X., . . . Scherer, S. W. 2013. Detection of clinically relevant genetic variants in autism spectrum disorder by whole-genome sequencing. *Am J Hum Genet,* 93**,** 249-63.

Jones, M. W. & Wilson, M. A. 2005a. Phase precession of medial prefrontal cortical activity relative to the hippocampal theta rhythm. *Hippocampus,* 15**,** 867-73.

Jones, M. W. & Wilson, M. A. 2005b. Theta rhythms coordinate hippocampal-prefrontal interactions in a spatial memory task. *PLoS Biol,* 3**,** e402.

Jouvet, M. 1969. Biogenic amines and the states of sleep. *Science,* 163**,** 32-41.

Jung, D., Hwang, Y. J., Ryu, H., Kano, M., Sakimura, K. & Cho, J. 2016. Conditional Knockout of Cav2.1 Disrupts the Accuracy of Spatial Recognition of CA1 Place Cells and Spatial/Contextual Recognition Behavior. *Front Behav Neurosci,* 10**,** 214.

Kabir, Z. D., Che, A., Fischer, D. K., Rice, R. C., Rizzo, B. K., Byrne, M., . . . Rajadhyaksha, A. M. 2017a. Rescue of impaired sociability and anxiety-like behavior in adult cacna1c-deficient mice by pharmacologically targeting eIF2α. *Mol Psychiatry,* 22**,** 1096-1109.

Kabir, Z. D., Lee, A. S., Burgdorf, C. E., Fischer, D. K., Rajadhyaksha, A. M., Mok, E., . . . Duman, R. S. 2017b. Cacna1c in the Prefrontal Cortex Regulates Depression-Related Behaviors via REDD1. *Neuropsychopharmacology,* 42**,** 2032-2042.

Kabir, Z. D., Martínez-Rivera, A. & Rajadhyaksha, A. M. 2017c. From Gene to Behavior: L-Type Calcium Channel Mechanisms Underlying Neuropsychiatric Symptoms. *Neurotherapeutics,* 14**,** 588-613.

Kaefer, K., Malagon-Vina, H., Dickerson, D. D., O'neill, J., Trossbach, S. V., Korth, C. & Csicsvari, J. 2019. Disrupted-in-schizophrenia 1 overexpression disrupts hippocampal coding and oscillatory synchronization. *Hippocampus,* 29**,** 802-816.

Kalweit, A. N., Amanpour-Gharaei, B., Colitti-Klausnitzer, J. & Manahan-Vaughan, D. 2017. Changes in Neuronal Oscillations Accompany the Loss of Hippocampal LTP that Occurs in an Animal Model of Psychosis. *Front Behav Neurosci,* 11**,** 36.

Kamijo, S., Ishii, Y., Horigane, S. I., Suzuki, K., Ohkura, M., Nakai, J., . . . Bito, H. 2018. A Critical Neurodevelopmental Role for L-Type Voltage-Gated Calcium Channels in Neurite Extension and Radial Migration. *J Neurosci,* 38**,** 5551-5566.

Kamondi, A., Acsády, L., Wang, X. J. & Buzsáki, G. 1998. Theta oscillations in somata and dendrites of hippocampal pyramidal cells in vivo: activity-dependent phase-precession of action potentials. *Hippocampus,* 8**,** 244-61.

Kantojärvi, K., Liuhanen, J., Saarenpää-Heikkilä, O., Satomaa, A. L., Kylliäinen, A., Pölkki, P., . . . Paunio, T. 2017. Variants in calcium voltage-gated channel subunit Alpha1 C-gene (CACNA1C) are associated with sleep latency in infants. *PLoS One,* 12**,** e0180652.

Kapur, A., Yeckel, M. F., Gray, R. & Johnston, D. 1998. L-Type calcium channels are required for one form of hippocampal mossy fiber LTP. *J Neurophysiol,* 79**,** 2181-90.

Kapur, S. & Seeman, P. 2001. Ketamine has equal affinity for NMDA receptors and the high-affinity state of the dopamine D2 receptor. *Biol Psychiatry,* 49**,** 954-7.

Karayiorgou, M., Morris, M. A., Morrow, B., Shprintzen, R. J., Goldberg, R., Borrow, J., . . . Lasseter, V. K. 1995. Schizophrenia susceptibility associated with interstitial deletions of chromosome 22q11. *Proc Natl Acad Sci U S A,* 92**,** 7612-6.

Karlsson, M. P. & Frank, L. M. 2009. Awake replay of remote experiences in the hippocampus. *Nat Neurosci,* 12**,** 913-8.

Katz, G., Durst, R., Zislin, Y., Barel, Y. & Knobler, H. Y. 2001. Psychiatric aspects of jet lag: review and hypothesis. *Med Hypotheses,* 56**,** 20-3.

Keefe, R. S., Bilder, R. M., Davis, S. M., Harvey, P. D., Palmer, B. W., Gold, J. M., . . . Group, N. W. 2007. Neurocognitive effects of antipsychotic medications in patients with chronic schizophrenia in the CATIE Trial. *Arch Gen Psychiatry,* 64**,** 633-47.

Keene, A. C. & Duboue, E. R. 2018. The origins and evolution of sleep. *J Exp Biol,* 221.

Kendall, K. M., Rees, E., Bracher-Smith, M., Legge, S., Riglin, L., Zammit, S., . . . Walters, J. T. R. 2019. Association of Rare Copy Number Variants With Risk of Depression. *JAMA Psychiatry*.

Kendler, K. S. 2013. What psychiatric genetics has taught us about the nature of psychiatric illness and what is left to learn. *Mol Psychiatry,* 18**,** 1058-66.

Kendler, K. S., Prescott, C. A., Myers, J. & Neale, M. C. 2003. The structure of genetic and environmental risk factors for common psychiatric and substance use disorders in men and women. *Arch Gen Psychiatry,* 60**,** 929-37.

Kentros, C., Hargreaves, E., Hawkins, R. D., Kandel, E. R., Shapiro, M. & Muller, R. V. 1998. Abolition of long-term stability of new hippocampal place cell maps by NMDA receptor blockade. *Science,* 280**,** 2121-6.

Kessler, R. C., Aguilar-Gaxiola, S., Alonso, J., Chatterji, S., Lee, S., Ormel, J., . . . Wang, P. S. 2009. The global burden of mental disorders: an update from the WHO World Mental Health (WMH) surveys. *Epidemiol Psichiatr Soc,* 18**,** 23-33.

Kim, J. Y., Duan, X., Liu, C. Y., Jang, M. H., Guo, J. U., Pow-Anpongkul, N., . . . Ming, G. L. 2009. DISC1 regulates new neuron development in the adult brain via modulation of AKT-mTOR signaling through KIAA1212. *Neuron,* 63**,** 761-73.

Kirov, G., Pocklington, A. J., Holmans, P., Ivanov, D., Ikeda, M., Ruderfer, D., . . . Owen, M. J. 2012. De novo CNV analysis implicates specific abnormalities of postsynaptic signalling complexes in the pathogenesis of schizophrenia. *Mol Psychiatry,* 17**,** 142-53.

Kirov, G., Rees, E., Walters, J. T., Escott-Price, V., Georgieva, L., Richards, A. L., . . . Owen, M. J. 2014. The penetrance of copy number variations for schizophrenia and developmental delay. *Biol Psychiatry,* 75**,** 378-85.

Kirov, S. A. & Harris, K. M. 2000. Dendrites are more spiny on mature hippocampal neurons when synapses are inactivated. *Nat Neurosci,* 3**,** 409.

Kitanishi, T., Ujita, S., Fallahnezhad, M., Kitanishi, N., Ikegaya, Y. & Tashiro, A. 2015. Novelty-Induced Phase-Locked Firing to Slow Gamma Oscillations in the Hippocampus: Requirement of Synaptic Plasticity. *Neuron,* 86**,** 1265-76.

Kittelberger, K., Hur, E. E., Sazegar, S., Keshavan, V. & Kocsis, B. 2012. Comparison of the effects of acute and chronic administration of ketamine on hippocampal oscillations: relevance for the NMDA receptor hypofunction model of schizophrenia. *Brain Struct Funct,* 217**,** 395-409.

Kokkinou, M., Ashok, A. H. & Howes, O. D. 2018. The effects of ketamine on dopaminergic function: meta-analysis and review of the implications for neuropsychiatric disorders. *Mol Psychiatry,* 23**,** 59-69.

Korman, M., Doyon, J., Doljansky, J., Carrier, J., Dagan, Y. & Karni, A. 2007. Daytime sleep condenses the time course of motor memory consolidation. *Nat Neurosci,* 10**,** 1206-13.

Kouvaros, S., Kotzadimitriou, D. & Papatheodoropoulos, C. 2015. Hippocampal sharp waves and ripples: Effects of aging and modulation by NMDA receptors and L-type Ca2+ channels. *Neuroscience,* 298**,** 26-41.

Kratzer, S., Mattusch, C., Metzger, M. W., Dedic, N., Noll-Hussong, M., Kafitz, K. W., . . . Rammes, G. 2013. Activation of CRH receptor type 1 expressed on glutamatergic neurons increases excitability of CA1 pyramidal neurons by the modulation of voltage-gated ion channels. *Front Cell Neurosci,* 7**,** 91.

Krey, J. F., Paşca, S. P., Shcheglovitov, A., Yazawa, M., Schwemberger, R., Rasmusson, R. & Dolmetsch, R. E. 2013. Timothy syndrome is associated with activity-dependent dendritic retraction in rodent and human neurons. *Nat Neurosci,* 16**,** 201-9.

Krystal, J. H., Abi-Saab, W., Perry, E., D'souza, D. C., Liu, N., Gueorguieva, R., . . . Breier, A. 2005a. Preliminary evidence of attenuation of the disruptive effects of the NMDA glutamate receptor antagonist, ketamine, on working memory by pretreatment with the group II metabotropic glutamate receptor agonist, LY354740, in healthy human subjects. *Psychopharmacology (Berl),* 179**,** 303-9.

Krystal, J. H., Karper, L. P., Seibyl, J. P., Freeman, G. K., Delaney, R., Bremner, J. D., . . . Charney, D. S. 1994. Subanesthetic effects of the noncompetitive NMDA antagonist, ketamine, in humans. Psychotomimetic, perceptual, cognitive, and neuroendocrine responses. *Arch Gen Psychiatry,* 51**,** 199-214.

Krystal, J. H., Perry, E. B., Gueorguieva, R., Belger, A., Madonick, S. H., Abi-Dargham, A., . . . D'souza, D. C. 2005b. Comparative and interactive human psychopharmacologic effects of ketamine and amphetamine: implications for glutamatergic and dopaminergic model psychoses and cognitive function. *Arch Gen Psychiatry,* 62**,** 985-94.

Krystal, J. H. & State, M. W. 2014. Psychiatric disorders: diagnosis to therapy. *Cell,* 157**,** 201-14.

Kudrimoti, H. S., Barnes, C. A. & Mcnaughton, B. L. 1999. Reactivation of hippocampal cell assemblies: effects of behavioral state, experience, and EEG dynamics. *J Neurosci,* 19**,** 4090-101.

Kumar, D., Dedic, N., Flachskamm, C., Deussing, J. & Kimura, M. 2013. CAV1.2 calcium channel is involved in the circadian regulation of sleep. Sleep Medicine.

Kumar, D., Dedic, N., Flachskamm, C., Voulé, S., Deussing, J. M. & Kimura, M. 2015. Cacna1c (Cav1.2) Modulates Electroencephalographic Rhythm and Rapid Eye Movement Sleep Recovery. *Sleep,* 38**,** 1371-80.

Kupfer, D. J. & Foster, F. G. 1972. Interval between onset of sleep and rapid-eye-movement sleep as an indicator of depression. *Lancet,* 2**,** 684-6.

Lahey, B. B., Applegate, B., Hakes, J. K., Zald, D. H., Hariri, A. R. & Rathouz, P. J. 2012. Is there a general factor of prevalent psychopathology during adulthood? *J Abnorm Psychol,* 121**,** 971-7.

Lahl, O., Wispel, C., Willigens, B. & Pietrowsky, R. 2008. An ultra short episode of sleep is sufficient to promote declarative memory performance. *J Sleep Res,* 17**,** 3-10.

Lahti, A. C., Koffel, B., Laporte, D. & Tamminga, C. A. 1995. Subanesthetic doses of ketamine stimulate psychosis in schizophrenia. *Neuropsychopharmacology,* 13**,** 9-19.

Langwieser, N., Christel, C. J., Kleppisch, T., Hofmann, F., Wotjak, C. T. & Moosmang, S. 2010. Homeostatic switch in hebbian plasticity and fear learning after sustained loss of Cav1.2 calcium channels. *J Neurosci,* 30**,** 8367-75.

Latchoumane, C. V., Ngo, H. V., Born, J. & Shin, H. S. 2017. Thalamic Spindles Promote Memory Formation during Sleep through Triple Phase-Locking of Cortical, Thalamic, and Hippocampal Rhythms. *Neuron,* 95**,** 424-435.e6.

Law, A. J. & Deakin, J. F. 2001. Asymmetrical reductions of hippocampal NMDAR1 glutamate receptor mRNA in the psychoses. *Neuroreport,* 12**,** 2971-4.

Lawrie, S. M. & Abukmeil, S. S. 1998. Brain abnormality in schizophrenia. A systematic and quantitative review of volumetric magnetic resonance imaging studies. *Br J Psychiatry,* 172**,** 110-20.

Lawrie, S. M., Whalley, H., Kestelman, J. N., Abukmeil, S. S., Byrne, M., Hodges, A., . . . Johnstone, E. C. 1999. Magnetic resonance imaging of brain in people at high risk of developing schizophrenia. *Lancet,* 353**,** 30-3.

Lazic, S. E. 2010. The problem of pseudoreplication in neuroscientific studies: is it affecting your analysis? *BMC Neurosci,* 11**,** 5.

Lazic, S. E., Clarke-Williams, C. J. & Munafo, M. R. 2018. What exactly is 'N' in cell culture and animal experiments? *PLoS Biol,* 16**,** e2005282.

Lee, A. K. & Wilson, M. A. 2002. Memory of sequential experience in the hippocampus during slow wave sleep. *Neuron,* 36**,** 1183-94.

Lee, A. S., De Jesús-Cortés, H., Kabir, Z. D., Knobbe, W., Orr, M., Burgdorf, C., . . . Pieper, A. A. 2016. The Neuropsychiatric Disease-Associated Gene cacna1c Mediates Survival of Young Hippocampal Neurons. *eNeuro,* 3.

Lee, A. S., Gonzales, K. L., Lee, A., Moosmang, S., Hofmann, F., Pieper, A. A. & Rajadhyaksha, A. M. 2012. Selective genetic deletion of cacna1c in the mouse prefrontal cortex. *Mol Psychiatry,* 17**,** 1051.

Lee, H., Simpson, G. V., Logothetis, N. K. & Rainer, G. 2005. Phase locking of single neuron activity to theta oscillations during working memory in monkey extrastriate visual cortex. *Neuron,* 45**,** 147-56.

Lee, I., Rao, G. & Knierim, J. J. 2004. A double dissociation between hippocampal subfields: differential time course of CA3 and CA1 place cells for processing changed environments. *Neuron,* 42**,** 803-15.

Lee, S. H., Ripke, S., Neale, B. M., Faraone, S. V., Purcell, S. M., Perlis, R. H., . . . (Iibdgc), I. I. B. D. G. C. 2013. Genetic relationship between five psychiatric disorders estimated from genome-wide SNPs. *Nat Genet,* 45**,** 984-94.

Leitch, B., Szostek, A., Lin, R. & Shevtsova, O. 2009. Subcellular distribution of L-type calcium channel subtypes in rat hippocampal neurons. *Neuroscience,* 164**,** 641-57.

Lenck-Santini, P. P. & Holmes, G. L. 2008. Altered phase precession and compression of temporal sequences by place cells in epileptic rats. *J Neurosci,* 28**,** 5053-62.

Lencz, T. & Malhotra, A. K. 2015. Targeting the schizophrenia genome: a fast track strategy from GWAS to clinic. *Mol Psychiatry,* 20**,** 820-6.

Lenzenweger, M. F. 2013. Endophenotype, intermediate phenotype, biomarker: definitions, concept comparisons, clarifications. *Depress Anxiety,* 30**,** 185-9.

Leproult, R. & Van Cauter, E. 2010. Role of sleep and sleep loss in hormonal release and metabolism. *Endocr Dev,* 17**,** 11-21.

Lett, T. A., Zai, C. C., Tiwari, A. K., Shaikh, S. A., Likhodi, O., Kennedy, J. L. & Müller, D. J. 2011. ANK3, CACNA1C and ZNF804A gene variants in bipolar disorders and psychosis subphenotype. *World J Biol Psychiatry,* 12**,** 392-7.

Leung, L. S. & Ma, J. 2018. Medial septum modulates hippocampal gamma activity and prepulse inhibition in an N-methyl-d-aspartate receptor antagonist model of schizophrenia. *Schizophr Res,* 198**,** 36-44.

Leung, L. W. & Borst, J. G. 1987. Electrical activity of the cingulate cortex. I. Generating mechanisms and relations to behavior. *Brain Res,* 407**,** 68-80.

Leung, L. W., Lopes Da Silva, F. H. & Wadman, W. J. 1982. Spectral characteristics of the hippocampal EEG in the freely moving rat. *Electroencephalogr Clin Neurophysiol,* 54**,** 203-19.

Leutgeb, S., Leutgeb, J. K., Barnes, C. A., Moser, E. I., Mcnaughton, B. L. & Moser, M. B. 2005. Independent codes for spatial and episodic memory in hippocampal neuronal ensembles. *Science,* 309**,** 619-23.

Lever, C., Burton, S., Jeewajee, A., Wills, T. J., Cacucci, F., Burgess, N. & O'keefe, J. 2010. Environmental novelty elicits a later theta phase of firing in CA1 but not subiculum. *Hippocampus,* 20**,** 229-34.

Levinson, D. F., Shi, J., Wang, K., Oh, S., Riley, B., Pulver, A. E., . . . Consortium, S. P. G. 2012. Genome-wide association study of multiplex schizophrenia pedigrees. *Am J Psychiatry,* 169**,** 963-73.

Levy, W. B. 1996. A sequence predicting CA3 is a flexible associator that learns and uses context to solve hippocampal-like tasks. *Hippocampus,* 6**,** 579-90.

Li, B., Tadross, M. R. & Tsien, R. W. 2016. Sequential ionic and conformational signaling by calcium channels drives neuronal gene expression. *Science,* 351**,** 863-7.

Li, H., Pink, M. D., Murphy, J. G., Stein, A., Dell'acqua, M. L. & Hogan, P. G. 2012a. Balanced interactions of calcineurin with AKAP79 regulate Ca2+-calcineurin-NFAT signaling. *Nat Struct Mol Biol,* 19**,** 337-45.

Li, J., Zhao, L., You, Y., Lu, T., Jia, M., Yu, H., . . . Wang, L. 2015. Schizophrenia Related Variants in CACNA1C also Confer Risk of Autism. *PLoS One,* 10**,** e0133247.

Li, J. Y., Kuo, T. B., Hsieh, I. T. & Yang, C. C. 2012b. Changes in hippocampal theta rhythm and their correlations with speed during different phases of voluntary wheel running in rats. *Neuroscience,* 213**,** 54-61.

Li, Q., Clark, S., Lewis, D. V. & Wilson, W. A. 2002. NMDA receptor antagonists disinhibit rat posterior cingulate and retrosplenial cortices: a potential mechanism of neurotoxicity. *J Neurosci,* 22**,** 3070-80.

Lichtenstein, P., Carlström, E., Råstam, M., Gillberg, C. & Anckarsäter, H. 2010. The genetics of autism spectrum disorders and related neuropsychiatric disorders in childhood. *Am J Psychiatry,* 167**,** 1357-63.

Lieberman, J. A., Girgis, R. R., Brucato, G., Moore, H., Provenzano, F., Kegeles, L., . . . Small, S. A. 2018. Hippocampal dysfunction in the pathophysiology of schizophrenia: a selective review and hypothesis for early detection and intervention. *Mol Psychiatry,* 23**,** 1764-1772.

Lieberman, J. A., Kane, J. M. & Alvir, J. 1987. Provocative tests with psychostimulant drugs in schizophrenia. *Psychopharmacology (Berl),* 91**,** 415-33.

Lindsay, E. A., Botta, A., Jurecic, V., Carattini-Rivera, S., Cheah, Y. C., Rosenblatt, H. M., . . . Baldini, A. 1999. Congenital heart disease in mice deficient for the DiGeorge syndrome region. *Nature,* 401**,** 379-83.

Lisman, J. E. & Jensen, O. 2013. The θ-γ neural code. *Neuron,* 77**,** 1002-16.

Liu, J. C., Defazio, R. A., Espinosa-Jeffrey, A., Cepeda, C., De Vellis, J. & Levine, M. S. 2004. Calcium modulates dopamine potentiation of N-methyl-D-aspartate responses: electrophysiological and imaging evidence. *J Neurosci Res,* 76**,** 315-22.

Liu, X., Ramirez, S., Pang, P. T., Puryear, C. B., Govindarajan, A., Deisseroth, K. & Tonegawa, S. 2012. Optogenetic stimulation of a hippocampal engram activates fear memory recall. *Nature,* 484**,** 381-5.

Liu, Y., Blackwood, D. H., Caesar, S., De Geus, E. J., Farmer, A., Ferreira, M. A., . . . Consortium, W. T. C.-C. 2011. Meta-analysis of genome-wide association data of bipolar disorder and major depressive disorder. *Mol Psychiatry,* 16**,** 2-4.

Liu, Y., Harding, M., Pittman, A., Dore, J., Striessnig, J., Rajadhyaksha, A. & Chen, X. 2014. Cav1.2 and Cav1.3 L-type calcium channels regulate dopaminergic firing activity in the mouse ventral tegmental area. *J Neurophysiol,* 112**,** 1119-30.

Lodge, D. J. 2013. The MAM rodent model of schizophrenia. *Curr Protoc Neurosci,* Chapter 9**,** Unit9.43.

Losonczy, A. & Magee, J. C. 2006. Integrative properties of radial oblique dendrites in hippocampal CA1 pyramidal neurons. *Neuron,* 50**,** 291-307.

Lu, X. & Bilkey, D. K. 2010. The velocity-related firing property of hippocampal place cells is dependent on self-movement. *Hippocampus,* 20**,** 573-83.

Lubenov, E. V. & Siapas, A. G. 2009. Hippocampal theta oscillations are travelling waves. *Nature,* 459**,** 534-9.

Luby, E. D., Cohen, B. D., Rosenbaum, G., Gottlieb, J. S. & Kelley, R. 1959. Study of a new schizophrenomimetic drug; sernyl. *AMA Arch Neurol Psychiatry,* 81**,** 363-9.

Lucchesi, J. C. & Kuroda, M. I. 2015. Dosage compensation in Drosophila. *Cold Spring Harb Perspect Biol,* 7.

Lunsford-Avery, J. R., Orr, J. M., Gupta, T., Pelletier-Baldelli, A., Dean, D. J., Smith Watts, A. K., . . . Mittal, V. A. 2013. Sleep dysfunction and thalamic abnormalities in adolescents at ultra high-risk for psychosis. *Schizophr Res,* 151**,** 148-53.

Luxenberger, H. 1928. Vorläufiger Bericht über psychiatrische Serienuntersuchungen an Zwillingen. Zeitschrift für die gesamte Neurologie und Psychiatrie.

Lynch, G., Larson, J., Kelso, S., Barrionuevo, G. & Schottler, F. 1983. Intracellular injections of EGTA block induction of hippocampal long-term potentiation. *Nature,* 305**,** 719-21.

Ma, D., Salyakina, D., Jaworski, J. M., Konidari, I., Whitehead, P. L., Andersen, A. N., . . . Pericak-Vance, M. A. 2009. A genome-wide association study of autism reveals a common novel risk locus at 5p14.1. *Ann Hum Genet,* 73**,** 263-73.

Ma, J. & Leung, L. S. 2000. Relation between hippocampal gamma waves and behavioral disturbances induced by phencyclidine and methamphetamine. *Behav Brain Res,* 111**,** 1-11.

Macdermott, A. B., Mayer, M. L., Westbrook, G. L., Smith, S. J. & Barker, J. L. 1986. NMDA-receptor activation increases cytoplasmic calcium concentration in cultured spinal cord neurones. *Nature,* 321**,** 519-22.

Macdonald, J. F., Miljkovic, Z. & Pennefather, P. 1987. Use-dependent block of excitatory amino acid currents in cultured neurons by ketamine. *J Neurophysiol,* 58**,** 251-66.

Magee, J. C. 2001. Dendritic mechanisms of phase precession in hippocampal CA1 pyramidal neurons. *J Neurophysiol,* 86**,** 528-32.

Magee, J. C. & Johnston, D. 1997. A synaptically controlled, associative signal for Hebbian plasticity in hippocampal neurons. *Science,* 275**,** 209-13.

Maguire, E. A., Burgess, N., Donnett, J. G., Frackowiak, R. S., Frith, C. D. & O'keefe, J. 1998. Knowing where and getting there: a human navigation network. *Science,* 280**,** 921-4.

Maier, W. 2008. Common risk genes for affective and schizophrenic psychoses. *Eur Arch Psychiatry Clin Neurosci,* 258 Suppl 2**,** 37-40.

Maingret, N., Girardeau, G., Todorova, R., Goutierre, M. & Zugaro, M. 2016. Hippocampo-cortical coupling mediates memory consolidation during sleep. *Nat Neurosci,* 19**,** 959-64.

Malenka, R. C. & Nicoll, R. A. 1999. Long-term potentiation--a decade of progress? *Science,* 285**,** 1870-4.

Malhotra, A. K., Adler, C. M., Kennison, S. D., Elman, I., Pickar, D. & Breier, A. 1997. Clozapine blunts N-methyl-D-aspartate antagonist-induced psychosis: a study with ketamine. *Biol Psychiatry,* 42**,** 664-8.

Malhotra, D. & Sebat, J. 2012. CNVs: harbingers of a rare variant revolution in psychiatric genetics. *Cell,* 148**,** 1223-41.

Mallas, E., Carletti, F., Chaddock, C. A., Shergill, S., Woolley, J., Picchioni, M. M., . . . Prata, D. P. 2017. The impact of CACNA1C gene, and its epistasis with ZNF804A, on white matter microstructure in health, schizophrenia and bipolar disorder. *Genes Brain Behav,* 16**,** 479-488.

Mangoni, M. E., Couette, B., Bourinet, E., Platzer, J., Reimer, D., Striessnig, J. & Nargeot, J. 2003. Functional role of L-type Cav1.3 Ca2+ channels in cardiac pacemaker activity. *Proc Natl Acad Sci U S A,* 100**,** 5543-8.

Manoach, D. S., Pan, J. Q., Purcell, S. M. & Stickgold, R. 2016. Reduced Sleep Spindles in Schizophrenia: A Treatable Endophenotype That Links Risk Genes to Impaired Cognition? *Biol Psychiatry,* 80**,** 599-608.

Manoach, D. S. & Stickgold, R. 2019. Abnormal Sleep Spindles, Memory Consolidation, and Schizophrenia. *Annu Rev Clin Psychol,* 15**,** 451-479.

Mansbach, R. S. & Geyer, M. A. 1989. Effects of phencyclidine and phencyclidine biologs on sensorimotor gating in the rat. *Neuropsychopharmacology,* 2**,** 299-308.

Marshall, C. R., Howrigan, D. P., Merico, D., Thiruvahindrapuram, B., Wu, W., Greer, D. S., . . . Consortium, C. a. S. W. G. O. T. P. G. 2017. Contribution of copy number variants to schizophrenia from a genome-wide study of 41,321 subjects. *Nat Genet,* 49**,** 27-35.

Marshall, L., Helgadóttir, H., Mölle, M. & Born, J. 2006. Boosting slow oscillations during sleep potentiates memory. *Nature,* 444**,** 610-3.

Marshall, W. H., Woolsey, C. N. & Bard, P. 1937. Cortical Representation of Tactile Sensibility as Inidicated by Cortical Potentials. *Science,* 85**,** 388-90.

Martin, S. J. & Clark, R. E. 2007. The rodent hippocampus and spatial memory: from synapses to systems. *Cell Mol Life Sci,* 64**,** 401-31.

Martinez, Z. A., Halim, N. D., Oostwegel, J. L., Geyer, M. A. & Swerdlow, N. R. 2000. Ontogeny of phencyclidine and apomorphine-induced startle gating deficits in rats. *Pharmacol Biochem Behav,* 65**,** 449-57.

Massimini, M., Huber, R., Ferrarelli, F., Hill, S. & Tononi, G. 2004. The sleep slow oscillation as a traveling wave. *J Neurosci,* 24**,** 6862-70.

Mastrogiuseppe, M., Bertelsen, N., Bedeschi, M. F. & Lee, S. A. 2019. The spatiotemporal organization of episodic memory and its disruption in a neurodevelopmental disorder. *Sci Rep,* 9**,** 18447.

Mathalon, D. H. & Ford, J. M. 2008. Corollary discharge dysfunction in schizophrenia: evidence for an elemental deficit. *Clin EEG Neurosci,* 39**,** 82-6.

Maynard, T. M., Sikich, L., Lieberman, J. A. & Lamantia, A. S. 2001. Neural development, cell-cell signaling, and the "two-hit" hypothesis of schizophrenia. *Schizophr Bull,* 27**,** 457-76.

Mccall, C. & Mccall, W. V. 2012. Comparison of actigraphy with polysomnography and sleep logs in depressed insomniacs. *J Sleep Res,* 21**,** 122-7.

Mccarroll, S. A. & Hyman, S. E. 2013. Progress in the genetics of polygenic brain disorders: significant new challenges for neurobiology. *Neuron,* 80**,** 578-87.

Mccarthy, M. J., Le Roux, M. J., Wei, H., Beesley, S., Kelsoe, J. R. & Welsh, D. K. 2016. Calcium channel genes associated with bipolar disorder modulate lithium's amplification of circadian rhythms. *Neuropharmacology,* 101**,** 439-48.

Mcdonald, C. & Murray, R. M. 2000. Early and late environmental risk factors for schizophrenia. *Brain Res Brain Res Rev,* 31**,** 130-7.

Mchugh, S. B., Niewoehner, B., Rawlins, J. N. & Bannerman, D. M. 2008. Dorsal hippocampal N-methyl-D-aspartate receptors underlie spatial working memory performance during non-matching to place testing on the T-maze. *Behav Brain Res,* 186**,** 41-7.

Mchugh, T. J., Blum, K. I., Tsien, J. Z., Tonegawa, S. & Wilson, M. A. 1996. Impaired hippocampal representation of space in CA1-specific NMDAR1 knockout mice. *Cell,* 87**,** 1339-49.

Mcnally, J. M. & Mccarley, R. W. 2016. Gamma band oscillations: a key to understanding schizophrenia symptoms and neural circuit abnormalities. *Curr Opin Psychiatry,* 29**,** 202-10.

Mehta, M. R., Quirk, M. C. & Wilson, M. A. 2000. Experience-dependent asymmetric shape of hippocampal receptive fields. *Neuron,* 25**,** 707-15.

Mena, A., Ruiz-Salas, J. C., Puentes, A., Dorado, I., Ruiz-Veguilla, M. & De La Casa, L. G. 2016. Reduced Prepulse Inhibition as a Biomarker of Schizophrenia. *Front Behav Neurosci,* 10**,** 202.

Mesbah-Oskui, L., Georgiou, J. & Roder, J. C. 2015. Hippocampal place cell and inhibitory neuron activity in disrupted-in-schizophrenia-1 mutant mice: implications for working memory deficits. *NPJ Schizophr,* 1**,** 15011.

Meyer, J. S., Greifenstein, F. & Devault, M. 1959. A new drug causing symptoms of sensory deprivation.: Journal of Nervous and Mental Disease.

Michaels, T. I., Long, L. L., Stevenson, I. H., Chrobak, J. J. & Chen, C. A. 2018. Effects of chronic ketamine on hippocampal cross-frequency coupling: implications for schizophrenia pathophysiology. *Eur J Neurosci,* 48**,** 2903-2914.

Millan, M. J., Agid, Y., Brüne, M., Bullmore, E. T., Carter, C. S., Clayton, N. S., . . . Young, L. J. 2012. Cognitive dysfunction in psychiatric disorders: characteristics, causes and the quest for improved therapy. *Nat Rev Drug Discov,* 11**,** 141-68.

Miller, D. W. & Abercrombie, E. D. 1996. Effects of MK-801 on spontaneous and amphetamine-stimulated dopamine release in striatum measured with in vivo microdialysis in awake rats. *Brain Res Bull,* 40**,** 57-62.

Mishara, A. L. & Goldberg, T. E. 2004. A meta-analysis and critical review of the effects of conventional neuroleptic treatment on cognition in schizophrenia: opening a closed book. *Biol Psychiatry,* 55**,** 1013-22.

Mitchell, S. J. & Ranck, J. B. 1980. Generation of theta rhythm in medial entorhinal cortex of freely moving rats. *Brain Res,* 189**,** 49-66.

Mitra, P. & Bokil, H. 2008. *Observed brain dynamics,* New York ; Oxford, Oxford University Press.

Mitzdorf, U. 1985. Current source-density method and application in cat cerebral cortex: investigation of evoked potentials and EEG phenomena. *Physiol Rev,* 65**,** 37-100.

Miyakawa, T., Leiter, L. M., Gerber, D. J., Gainetdinov, R. R., Sotnikova, T. D., Zeng, H., . . . Tonegawa, S. 2003. Conditional calcineurin knockout mice exhibit multiple abnormal behaviors related to schizophrenia. *Proc Natl Acad Sci U S A,* 100**,** 8987-92.

Mizuseki, K. & Buzsáki, G. 2013. Preconfigured, skewed distribution of firing rates in the hippocampus and entorhinal cortex. *Cell Rep,* 4**,** 1010-21.

Modi, B., Pimpinella, D., Pazienti, A., Zacchi, P., Cherubini, E. & Griguoli, M. 2019. Possible Implication of the CA2 Hippocampal Circuit in Social Cognition Deficits Observed in the Neuroligin 3 Knock-Out Mouse, a Non-Syndromic Animal Model of Autism. *Front Psychiatry,* 10**,** 513.

Molina, V., Reig, S., Pascau, J., Sanz, J., Sarramea, F., Gispert, J. D., . . . Desco, M. 2003. Anatomical and functional cerebral variables associated with basal symptoms but not risperidone response in minimally treated schizophrenia. *Psychiatry Res,* 124**,** 163-75.

Moon, A. L., Haan, N., Wilkinson, L. S., Thomas, K. L. & Hall, J. 2018. CACNA1C: Association With Psychiatric Disorders, Behavior, and Neurogenesis. *Schizophr Bull,* 44**,** 958-965.

Moore, S. J. & Murphy, G. G. 2020. The role of L-type calcium channels in neuronal excitability and aging. *Neurobiol Learn Mem,* 173**,** 107230.

Moosmang, S., Haider, N., Klugbauer, N., Adelsberger, H., Langwieser, N., Müller, J., . . . Kleppisch, T. 2005. Role of hippocampal Cav1.2 Ca2+ channels in NMDA receptor-independent synaptic plasticity and spatial memory. *J Neurosci,* 25**,** 9883-92.

Morris, R. G., Anderson, E., Lynch, G. S. & Baudry, M. 1986. Selective impairment of learning and blockade of long-term potentiation by an N-methyl-D-aspartate receptor antagonist, AP5. *Nature,* 319**,** 774-6.

Morris, R. G., Garrud, P., Rawlins, J. N. & O'keefe, J. 1982. Place navigation impaired in rats with hippocampal lesions. *Nature,* 297**,** 681-3.

Morris, R. G. M. 1981. Spatial localization does not require the presence of local cues. Learning and Motivation.

Morrison, R. S. & Dempsey, E. W. 1941. A Study of Thalamocortical Relations. The American Journal of Physiology.

Morrow, B. E., Mcdonald-Mcginn, D. M., Emanuel, B. S., Vermeesch, J. R. & Scambler, P. J. 2018. Molecular genetics of 22q11.2 deletion syndrome. *Am J Med Genet A,* 176**,** 2070-2081.

Moscovitch, M., Cabeza, R., Winocur, G. & Nadel, L. 2016. Episodic Memory and Beyond: The Hippocampus and Neocortex in Transformation. *Annu Rev Psychol,* 67**,** 105-34.

Moser, M. B. & Moser, E. I. 1998. Functional differentiation in the hippocampus. *Hippocampus,* 8**,** 608-19.

Moser, M. B., Moser, E. I., Forrest, E., Andersen, P. & Morris, R. G. 1995. Spatial learning with a minislab in the dorsal hippocampus. *Proc Natl Acad Sci U S A,* 92**,** 9697-701.

Muehlroth, B. E., Sander, M. C., Fandakova, Y., Grandy, T. H., Rasch, B., Shing, Y. L. & Werkle-Bergner, M. 2019. Precise Slow Oscillation-Spindle Coupling Promotes Memory Consolidation in Younger and Older Adults. *Sci Rep,* 9**,** 1940.

Muller, R. U. & Kubie, J. L. 1987. The effects of changes in the environment on the spatial firing of hippocampal complex-spike cells. *J Neurosci,* 7**,** 1951-68.

Muller, R. U., Kubie, J. L., Bostock, E. M., Taube, J. S. & Quirk, G. J. 1991. Spatial firing correlates of neurons in the hippocampal formation of freely moving rats. Brain and space: Oxford University Press.

Murphy, J. G., Sanderson, J. L., Gorski, J. A., Scott, J. D., Catterall, W. A., Sather, W. A. & Dell'acqua, M. L. 2014. AKAP-anchored PKA maintains neuronal L-type calcium channel activity and NFAT transcriptional signaling. *Cell Rep,* 7**,** 1577-1588.

Nabeshima, T., Kozawa, T., Furukawa, H. & Kameyama, T. 1986. Phencyclidine-induced retrograde amnesia in mice. *Psychopharmacology (Berl),* 89**,** 334-7.

Nahm, S. S., Farnell, Y. Z., Griffith, W. & Earnest, D. J. 2005. Circadian regulation and function of voltage-dependent calcium channels in the suprachiasmatic nucleus. *J Neurosci,* 25**,** 9304-8.

Nakashiba, T., Buhl, D. L., Mchugh, T. J. & Tonegawa, S. 2009. Hippocampal CA3 output is crucial for ripple-associated reactivation and consolidation of memory. *Neuron,* 62**,** 781-7.

Nanou, E. & Catterall, W. A. 2018. Calcium Channels, Synaptic Plasticity, and Neuropsychiatric Disease. *Neuron,* 98**,** 466-481.

Nanou, E., Sullivan, J. M., Scheuer, T. & Catterall, W. A. 2016. Calcium sensor regulation of the CaV2.1 Ca2+ channel contributes to short-term synaptic plasticity in hippocampal neurons. *Proc Natl Acad Sci U S A,* 113**,** 1062-7.

Napoli, I., Mercaldo, V., Boyl, P. P., Eleuteri, B., Zalfa, F., De Rubeis, S., . . . Bagni, C. 2008. The fragile X syndrome protein represses activity-dependent translation through CYFIP1, a new 4E-BP. *Cell,* 134**,** 1042-54.

Nelson, M. D., Saykin, A. J., Flashman, L. A. & Riordan, H. J. 1998. Hippocampal volume reduction in schizophrenia as assessed by magnetic resonance imaging: a meta-analytic study. *Arch Gen Psychiatry,* 55**,** 433-40.

Nestler, E. J. & Hyman, S. E. 2010. Animal models of neuropsychiatric disorders. *Nat Neurosci,* 13**,** 1161-9.

Network and Pathway Analysis Subgroup of Psychiatric Genomics Consortium 2015. Psychiatric genome-wide association study analyses implicate neuronal, immune and histone pathways. *Nat Neurosci,* 18**,** 199-209.

Nicol, A. U. & Morton, A. J. 2020. Characteristic patterns of EEG oscillations in sheep (Ovis aries) induced by ketamine may explain the psychotropic effects seen in humans. *Sci Rep,* 10**,** 9440.

Nicoll, R. A. 2017. A Brief History of Long-Term Potentiation. *Neuron,* 93**,** 281-290.

Nielsen, J., Fejgin, K., Sotty, F., Nielsen, V., Mørk, A., Christoffersen, C. T., . . . Didriksen, M. 2017. A mouse model of the schizophrenia-associated 1q21.1 microdeletion syndrome exhibits altered mesolimbic dopamine transmission. *Transl Psychiatry,* 7**,** 1261.

Niknazar, M., Krishnan, G. P., Bazhenov, M. & Mednick, S. C. 2015. Coupling of Thalamocortical Sleep Oscillations Are Important for Memory Consolidation in Humans. *PLoS One,* 10**,** e0144720.

Nishida, M., Pearsall, J., Buckner, R. L. & Walker, M. P. 2009. REM sleep, prefrontal theta, and the consolidation of human emotional memory. *Cereb Cortex,* 19**,** 1158-66.

Nishida, M. & Walker, M. P. 2007. Daytime naps, motor memory consolidation and regionally specific sleep spindles. *PLoS One,* 2**,** e341.

Noda, A., Noda, Y., Kamei, H., Ichihara, K., Mamiya, T., Nagai, T., . . . Nabeshima, T. 2001. Phencyclidine impairs latent learning in mice: interaction between glutamatergic systems and sigma(1) receptors. *Neuropsychopharmacology,* 24**,** 451-60.

Nofzinger, E. A., Thase, M. E., Reynolds, C. F., Himmelhoch, J. M., Mallinger, A., Houck, P. & Kupfer, D. J. 1991. Hypersomnia in bipolar depression: a comparison with narcolepsy using the multiple sleep latency test. *Am J Psychiatry,* 148**,** 1177-81.

Noguchi, T., Leise, T. L., Kingsbury, N. J., Diemer, T., Wang, L. L., Henson, M. A. & Welsh, D. K. 2017. Calcium Circadian Rhythmicity in the Suprachiasmatic Nucleus: Cell Autonomy and Network Modulation. *eNeuro,* 4.

Nurnberger, J. I., Koller, D. L., Jung, J., Edenberg, H. J., Foroud, T., Guella, I., . . . Group, P. G. C. B. 2014. Identification of pathways for bipolar disorder: a meta-analysis. *JAMA Psychiatry,* 71**,** 657-64.

Nyegaard, M., Demontis, D., Foldager, L., Hedemand, A., Flint, T. J., Sørensen, K. M., . . . Børglum, A. D. 2010. CACNA1C (rs1006737) is associated with schizophrenia. *Mol Psychiatry,* 15**,** 119-21.

O'keefe, J. 1976. Place units in the hippocampus of the freely moving rat. *Exp Neurol,* 51**,** 78-109.

O'keefe, J. & Dostrovsky, J. 1971. The hippocampus as a spatial map. Preliminary evidence from unit activity in the freely-moving rat. *Brain Res,* 34**,** 171-5.

O'keefe, J. & Nadel, L. 1978. *The hippocampus as a cognitive map*. Oxford: Clarendon Press.

O'keefe, J. & Recce, M. L. 1993. Phase relationship between hippocampal place units and the EEG theta rhythm. *Hippocampus,* 3**,** 317-30.

O'leary, M. N., Schreiber, K. H., Zhang, Y., Duc, A. C., Rao, S., Hale, J. S., . . . Kennedy, B. K. 2013. The ribosomal protein Rpl22 controls ribosome composition by directly repressing expression of its own paralog, Rpl22l1. *PLoS Genet,* 9**,** e1003708.

O'neill, J., Senior, T. & Csicsvari, J. 2006. Place-selective firing of CA1 pyramidal cells during sharp wave/ripple network patterns in exploratory behavior. *Neuron,* 49**,** 143-55.

Ognjanovski, N., Schaeffer, S., Wu, J., Mofakham, S., Maruyama, D., Zochowski, M. & Aton, S. J. 2017. Parvalbumin-expressing interneurons coordinate hippocampal network dynamics required for memory consolidation. *Nat Commun,* 8**,** 15039.

Olton, D. S., Becker, J. T. & Handelmann, G. E. 1979. Hippocampus, space, and memory. Behavioral and Brain Sciences.

Olton, D. S. & Samuelson, R. J. 1976. Remembrance of places passed: Spatial memory in rats. Journal of Experimental Psychology: Animal Behavior Processes.

Olton, D. S., Walker, J. A. & Gage, F. H. 1978. Hippocampal connections and spatial discrimination. *Brain Res,* 139**,** 295-308.

Onslow, A. C., Bogacz, R. & Jones, M. W. 2011. Quantifying phase-amplitude coupling in neuronal network oscillations. *Prog Biophys Mol Biol,* 105**,** 49-57.
Organization, W. H. 2020. International statistical classification of diseases and related health problems.
Orr, G., Rao, G., Houston, F. P., Mcnaughton, B. L. & Barnes, C. A. 2001. Hippocampal synaptic plasticity is modulated by theta rhythm in the fascia dentata of adult and aged freely behaving rats. *Hippocampus,* 11**,** 647-54.
Owen, M. J. 2014. New approaches to psychiatric diagnostic classification. *Neuron,* 84**,** 564-71.
Owen, M. J. & O'donovan, M. C. 2017. Schizophrenia and the neurodevelopmental continuum:evidence from genomics. *World Psychiatry,* 16**,** 227-235.
Owen, M. J., O'donovan, M. C., Thapar, A. & Craddock, N. 2011. Neurodevelopmental hypothesis of schizophrenia. *Br J Psychiatry,* 198**,** 173-5.
Pantelis, C., Velakoulis, D., Mcgorry, P. D., Wood, S. J., Suckling, J., Phillips, L. J., . . . Mcguire, P. K. 2003a. Neuroanatomical abnormalities before and after onset of psychosis: a cross-sectional and longitudinal MRI comparison. *Lancet,* 361**,** 281-8.
Pantelis, C., Yücel, M., Wood, S. J., Mcgorry, P. D. & Velakoulis, D. 2003b. Early and late neurodevelopmental disturbances in schizophrenia and their functional consequences. *Aust N Z J Psychiatry,* 37**,** 399-406.
Pantelis, C., Yücel, M., Wood, S. J., Velakoulis, D., Sun, D., Berger, G., . . . Mcgorry, P. D. 2005. Structural brain imaging evidence for multiple pathological processes at different stages of brain development in schizophrenia. *Schizophr Bull,* 31**,** 672-96.
Papatheodoropoulos, C. & Kouvaros, S. 2016. High-frequency stimulation-induced synaptic potentiation in dorsal and ventral CA1 hippocampal synapses: the involvement of NMDA receptors, mGluR5, and (L-type) voltage-gated calcium channels. *Learn Mem,* 23**,** 460-4.
Pardiñas, A. F., Holmans, P., Pocklington, A. J., Escott-Price, V., Ripke, S., Carrera, N., . . . Consortium, C. 2018. Common schizophrenia alleles are enriched in mutation-intolerant genes and in regions under strong background selection. *Nat Genet,* 50**,** 381-389.
Paré, D. & Collins, D. R. 2000. Neuronal correlates of fear in the lateral amygdala: multiple extracellular recordings in conscious cats. *J Neurosci,* 20**,** 2701-10.
Parsons, M. J., Lester, K. J., Barclay, N. L., Nolan, P. M., Eley, T. C. & Gregory, A. M. 2013. Replication of Genome-Wide Association Studies (GWAS) loci for sleep in the British G1219 cohort. *Am J Med Genet B Neuropsychiatr Genet,* 162B**,** 431-8.
Paşca, S. P., Portmann, T., Voineagu, I., Yazawa, M., Shcheglovitov, A., Paşca, A. M., . . . Dolmetsch, R. E. 2011. Using iPSC-derived neurons to uncover cellular phenotypes associated with Timothy syndrome. *Nat Med,* 17**,** 1657-62.
Pastalkova, E., Itskov, V., Amarasingham, A. & Buzsáki, G. 2008. Internally generated cell assembly sequences in the rat hippocampus. *Science,* 321**,** 1322-7.
Patterson, M. A., Szatmari, E. M. & Yasuda, R. 2010. AMPA receptors are exocytosed in stimulated spines and adjacent dendrites in a Ras-ERK-dependent manner during long-term potentiation. *Proc Natl Acad Sci U S A,* 107**,** 15951-6.
Paulus, F. M., Bedenbender, J., Krach, S., Pyka, M., Krug, A., Sommer, J., . . . Jansen, A. 2014. Association of rs1006737 in CACNA1C with alterations in prefrontal activation and fronto-hippocampal connectivity. *Hum Brain Mapp,* 35**,** 1190-200.
Payne, J. D., Stickgold, R., Swanberg, K. & Kensinger, E. A. 2008. Sleep preferentially enhances memory for emotional components of scenes. *Psychol Sci,* 19**,** 781-8.
Peigneux, P., Laureys, S., Fuchs, S., Collette, F., Perrin, F., Reggers, J., . . . Maquet, P. 2004. Are spatial memories strengthened in the human hippocampus during slow wave sleep? *Neuron,* 44**,** 535-45.
Penfield, W. & Milner, B. 1958. Memory deficit produced by bilateral lesions in the hippocampal zone. *AMA Arch Neurol Psychiatry,* 79**,** 475-97.

Penley, S. C., Hinman, J. R., Long, L. L., Markus, E. J., Escabí, M. A. & Chrobak, J. J. 2013. Novel space alters theta and gamma synchrony across the longitudinal axis of the hippocampus. *Front Syst Neurosci,* 7**,** 20.

Penttonen, M., Kamondi, A., Acsády, L. & Buzsáki, G. 1998. Gamma frequency oscillation in the hippocampus of the rat: intracellular analysis in vivo. *Eur J Neurosci,* 10**,** 718-28.

Perkel, D. J., Petrozzino, J. J., Nicoll, R. A. & Connor, J. A. 1993. The role of Ca2+ entry via synaptically activated NMDA receptors in the induction of long-term potentiation. *Neuron,* 11**,** 817-23.

Peterson, B. Z., Demaria, C. D., Adelman, J. P. & Yue, D. T. 1999. Calmodulin is the Ca2+ sensor for Ca2+ -dependent inactivation of L-type calcium channels. *Neuron,* 22**,** 549-58.

Phillips, K. G., Bartsch, U., Mccarthy, A. P., Edgar, D. M., Tricklebank, M. D., Wafford, K. A. & Jones, M. W. 2012a. Decoupling of sleep-dependent cortical and hippocampal interactions in a neurodevelopmental model of schizophrenia. *Neuron,* 76**,** 526-33.

Phillips, K. G., Cotel, M. C., Mccarthy, A. P., Edgar, D. M., Tricklebank, M., O'neill, M. J., . . . Wafford, K. A. 2012b. Differential effects of NMDA antagonists on high frequency and gamma EEG oscillations in a neurodevelopmental model of schizophrenia. *Neuropharmacology,* 62**,** 1359-70.

Phillips, K. G. & Uhlhaas, P. J. 2015. Neural oscillations as a translational tool in schizophrenia research: rationale, paradigms and challenges. *J Psychopharmacol,* 29**,** 155-68.

Piazza, P. V., Deminière, J. M., Le Moal, M. & Simon, H. 1989. Factors that predict individual vulnerability to amphetamine self-administration. *Science,* 245**,** 1511-3.

Picken, A. & Tarrier, N. 2011. Trauma and comorbid posttraumatic stress disorder in individuals with schizophrenia and substance abuse. *Compr Psychiatry,* 52**,** 490-7.

Pickenhain, L. & Klingberg, F. 1967. Hippocampal slow wave activity as a correlate of basic behavioral mechanisms in the rat. *Prog Brain Res,* 27**,** 218-27.

Pilowsky, L. S., Bressan, R. A., Stone, J. M., Erlandsson, K., Mulligan, R. S., Krystal, J. H. & Ell, P. J. 2006. First in vivo evidence of an NMDA receptor deficit in medication-free schizophrenic patients. *Mol Psychiatry,* 11**,** 118-9.

Pinault, D. 2008. N-methyl d-aspartate receptor antagonists ketamine and MK-801 induce wake-related aberrant gamma oscillations in the rat neocortex. *Biol Psychiatry,* 63**,** 730-5.

Pitsikas, N., Boultadakis, A. & Sakellaridis, N. 2008. Effects of sub-anesthetic doses of ketamine on rats' spatial and non-spatial recognition memory. *Neuroscience,* 154**,** 454-60.

Plana-Ripoll, O., Pedersen, C. B., Holtz, Y., Benros, M. E., Dalsgaard, S., De Jonge, P., . . . Mcgrath, J. J. 2019. Exploring Comorbidity Within Mental Disorders Among a Danish National Population. *JAMA Psychiatry,* 76**,** 259-270.

Platzer, J., Engel, J., Schrott-Fischer, A., Stephan, K., Bova, S., Chen, H., . . . Striessnig, J. 2000. Congenital deafness and sinoatrial node dysfunction in mice lacking class D L-type Ca2+ channels. *Cell,* 102**,** 89-97.

Plihal, W. & Born, J. 1997. Effects of early and late nocturnal sleep on declarative and procedural memory. *J Cogn Neurosci,* 9**,** 534-47.

Plumbly, W., Brandon, N., Deeb, T. Z., Hall, J. & Harwood, A. J. 2019. L-type voltage-gated calcium channel regulation of in vitro human cortical neuronal networks. *Sci Rep,* 9**,** 13810.

Polderman, T. J., Benyamin, B., De Leeuw, C. A., Sullivan, P. F., Van Bochoven, A., Visscher, P. M. & Posthuma, D. 2015. Meta-analysis of the heritability of human traits based on fifty years of twin studies. *Nat Genet,* 47**,** 702-9.

Purcell, S. M., Moran, J. L., Fromer, M., Ruderfer, D., Solovieff, N., Roussos, P., . . . Sklar, P. 2014. A polygenic burden of rare disruptive mutations in schizophrenia. *Nature,* 506**,** 185-90.

Purcell, S. M., Wray, N. R., Stone, J. L., Visscher, P. M., O'donovan, M. C., Sullivan, P. F., . . . Consortium, I. S. 2009. Common polygenic variation contributes to risk of schizophrenia and bipolar disorder. *Nature,* 460**,** 748-52.

Qian, H., Patriarchi, T., Price, J. L., Matt, L., Lee, B., Nieves-Cintrón, M., . . . Hell, J. W. 2017. Phosphorylation of Ser1928 mediates the enhanced activity of the L-type Ca2+ channel Cav1.2 by the β2-adrenergic receptor in neurons. *Sci Signal,* 10.

Raghavachari, S., Kahana, M. J., Rizzuto, D. S., Caplan, J. B., Kirschen, M. P., Bourgeois, B., . . . Lisman, J. E. 2001. Gating of human theta oscillations by a working memory task. *J Neurosci,* 21**,** 3175-83.

Ramachandraiah, C. T., Subramaniam, N. & Tancer, M. 2009. The story of antipsychotics: Past and present. *Indian J Psychiatry,* 51**,** 324-6.

Ramadan, W., Eschenko, O. & Sara, S. J. 2009. Hippocampal sharp wave/ripples during sleep for consolidation of associative memory. *PLoS One,* 4**,** e6697.

Read, J., Van Os, J., Morrison, A. P. & Ross, C. A. 2005. Childhood trauma, psychosis and schizophrenia: a literature review with theoretical and clinical implications. *Acta Psychiatr Scand,* 112**,** 330-50.

Rees, E., Walters, J. T., Georgieva, L., Isles, A. R., Chambert, K. D., Richards, A. L., . . . Kirov, G. 2014. Analysis of copy number variations at 15 schizophrenia-associated loci. *Br J Psychiatry,* 204**,** 108-14.

Rempel-Clower, N. L., Zola, S. M., Squire, L. R. & Amaral, D. G. 1996. Three cases of enduring memory impairment after bilateral damage limited to the hippocampal formation. *J Neurosci,* 16**,** 5233-55.

Rendón-Ochoa, E. A., Hernández-Flores, T., Avilés-Rosas, V. H., Cáceres-Chávez, V. A., Duhne, M., Laville, A., . . . Bargas, J. 2018. Calcium currents in striatal fast-spiking interneurons: dopaminergic modulation of Ca. *BMC Neurosci,* 19**,** 42.

Richard, G. R., Titiz, A., Tyler, A., Holmes, G. L., Scott, R. C. & Lenck-Santini, P. P. 2013. Speed modulation of hippocampal theta frequency correlates with spatial memory performance. *Hippocampus,* 23**,** 1269-79.

Ripke, S., Walters, J. T. & O'donovan, M. C. 2020. Mapping genomic loci prioritises genes and implicates synaptic biology in schizophrenia. *medRxiv***,** 2020.09.12.20192922.

Robbe, D. & Buzsáki, G. 2009. Alteration of theta timescale dynamics of hippocampal place cells by a cannabinoid is associated with memory impairment. *J Neurosci,* 29**,** 12597-605.

Rosenbaum, G., Cohen, B. D., Luby, E. D., Gottlieb, J. S. & Yelen, D. 1959. Comparison of sernyl with other drugs: simulation of schizophrenic performance with sernyl, LSD-25, and amobarbital (amytal) sodium; I. Attention, motor function, and proprioception. *AMA Arch Gen Psychiatry,* 1**,** 651-6.

Ross, R. S. & Eichenbaum, H. 2006. Dynamics of hippocampal and cortical activation during consolidation of a nonspatial memory. *J Neurosci,* 26**,** 4852-9.

Rotenberg, A., Mayford, M., Hawkins, R. D., Kandel, E. R. & Muller, R. U. 1996. Mice expressing activated CaMKII lack low frequency LTP and do not form stable place cells in the CA1 region of the hippocampus. Cell.

Rothschild, G., Eban, E. & Frank, L. M. 2017. A cortical-hippocampal-cortical loop of information processing during memory consolidation. *Nat Neurosci,* 20**,** 251-259.

Roussos, P., Mitchell, A. C., Voloudakis, G., Fullard, J. F., Pothula, V. M., Tsang, J., . . . Sklar, P. 2014. A role for noncoding variation in schizophrenia. *Cell Rep,* 9**,** 1417-29.

Royer, S., Sirota, A., Patel, J. & Buzsáki, G. 2010. Distinct representations and theta dynamics in dorsal and ventral hippocampus. *J Neurosci,* 30**,** 1777-87.

Ruderfer, D. M., Fanous, A. H., Ripke, S., Mcquillin, A., Amdur, R. L., Gejman, P. V., . . . Consortium, C.-D. W. G. O. T. P. G. 2014. Polygenic dissection of diagnosis and clinical dimensions of bipolar disorder and schizophrenia. *Mol Psychiatry,* 19**,** 1017-1024.

Rudin, E. 1916. Studien uber Vererbung und entstehung geistiger Storungen. I. Zur vererbung und neuentstehung der Dementia praecox. Monographien aus dem Gesamtgebiet der Neurologie und Psychiatrie: Springer.

Rutter, M. 1995. Relationships between mental disorders in childhood and adulthood. *Acta Psychiatr Scand,* 91**,** 73-85.

Sachser, R. M., Santana, F., Crestani, A. P., Lunardi, P., Pedraza, L. K., Quillfeldt, J. A., . . . Alvares, L. E. O. 2016. Forgetting of long-term memory requires activation of NMDA receptors, L-type voltage-dependent Ca2+ channels, and calcineurin. *Sci Rep,* 6**,** 22771.

Sadowski, J. H., Jones, M. W. & Mellor, J. R. 2011. Ripples make waves: binding structured activity and plasticity in hippocampal networks. *Neural Plast,* 2011**,** 960389.

Sadowski, J. H., Jones, M. W. & Mellor, J. R. 2016. Sharp-Wave Ripples Orchestrate the Induction of Synaptic Plasticity during Reactivation of Place Cell Firing Patterns in the Hippocampus. *Cell Rep,* 14**,** 1916-29.

Saini, S. M., Mancuso, S. G., Mostaid, M. S., Liu, C., Pantelis, C., Everall, I. P. & Bousman, C. A. 2017. Meta-analysis supports GWAS-implicated link between GRM3 and schizophrenia risk. *Transl Psychiatry,* 7**,** e1196.

Saitoh, T. & Schwartz, J. H. 1985. Phosphorylation-dependent subcellular translocation of a Ca2+/calmodulin-dependent protein kinase produces an autonomous enzyme in Aplysia neurons. *J Cell Biol,* 100**,** 835-42.

Samplin, E., Ikuta, T., Malhotra, A. K., Szeszko, P. R. & Derosse, P. 2013. Sex differences in resilience to childhood maltreatment: effects of trauma history on hippocampal volume, general cognition and subclinical psychosis in healthy adults. *J Psychiatr Res,* 47**,** 1174-9.

Sams-Dodd, F. 1995. Distinct effects of d-amphetamine and phencyclidine on the social behaviour of rats. *Behav Pharmacol,* 6**,** 55-65.

Sanders, A. R., Duan, J., Levinson, D. F., Shi, J., He, D., Hou, C., . . . Gejman, P. V. 2008. No significant association of 14 candidate genes with schizophrenia in a large European ancestry sample: implications for psychiatric genetics. *Am J Psychiatry,* 165**,** 497-506.

Sanders, S. J., Ercan-Sencicek, A. G., Hus, V., Luo, R., Murtha, M. T., Moreno-De-Luca, D., . . . State, M. W. 2011. Multiple recurrent de novo CNVs, including duplications of the 7q11.23 Williams syndrome region, are strongly associated with autism. *Neuron,* 70**,** 863-85.

Sartor, C. E., Grant, J. D., Lynskey, M. T., Mccutcheon, V. V., Waldron, M., Statham, D. J., . . . Nelson, E. C. 2012. Common heritable contributions to low-risk trauma, high-risk trauma, posttraumatic stress disorder, and major depression. *Arch Gen Psychiatry,* 69**,** 293-9.

Schapiro, A. C., Mcdevitt, E. A., Rogers, T. T., Mednick, S. C. & Norman, K. A. 2018. Human hippocampal replay during rest prioritizes weakly learned information and predicts memory performance. *Nat Commun,* 9**,** 3920.

Scheffer-Teixeira, R., Belchior, H., Caixeta, F. V., Souza, B. C., Ribeiro, S. & Tort, A. B. 2012. Theta phase modulates multiple layer-specific oscillations in the CA1 region. *Cereb Cortex,* 22**,** 2404-14.

Schiller, J., Schiller, Y. & Clapham, D. E. 1998. NMDA receptors amplify calcium influx into dendritic spines during associative pre- and postsynaptic activation. *Nat Neurosci,* 1**,** 114-8.

Schizophrenia Working Group of the Psychiatric Genomics Consortium 2014. Biological insights from 108 schizophrenia-associated genetic loci. *Nature,* 511**,** 421-7.

Schlingloff, D., Káli, S., Freund, T. F., Hájos, N. & Gulyás, A. I. 2014. Mechanisms of sharp wave initiation and ripple generation. *J Neurosci,* 34**,** 11385-98.

Schmahl, C. G., Vermetten, E., Elzinga, B. M. & Douglas Bremner, J. 2003. Magnetic resonance imaging of hippocampal and amygdala volume in women with childhood abuse and borderline personality disorder. *Psychiatry Res,* 122**,** 193-8.

Schmidt, C. J. & Fadayel, G. M. 1996. Regional effects of MK-801 on dopamine release: effects of competitive NMDA or 5-HT2A receptor blockade. *J Pharmacol Exp Ther,* 277**,** 1541-9.

Schmutz, I., Chavan, R., Ripperger, J. A., Maywood, E. S., Langwieser, N., Jurik, A., . . . Albrecht, U. 2014. A specific role for the REV-ERBα-controlled L-Type Voltage-Gated Calcium Channel CaV1.2 in resetting the circadian clock in the late night. *J Biol Rhythms,* 29**,** 288-98.

Schobel, S. A., Lewandowski, N. M., Corcoran, C. M., Moore, H., Brown, T., Malaspina, D. & Small, S. A. 2009. Differential targeting of the CA1 subfield of the hippocampal formation by schizophrenia and related psychotic disorders. *Arch Gen Psychiatry,* 66**,** 938-46.

Schwartz, B. L., Fay-Mccarthy, M., Kendrick, K., Rosse, R. B. & Deutsch, S. I. 1997. Effects of nifedipine, a calcium channel antagonist, on cognitive function in schizophrenic patients with tardive dyskinesia. *Clin Neuropharmacol,* 20**,** 364-70.

Scoville, W. B. & Milner, B. 2000. Loss of recent memory after bilateral hippocampal lesions. 1957. *J Neuropsychiatry Clin Neurosci,* 12**,** 103-13.

Sederberg, P. B., Schulze-Bonhage, A., Madsen, J. R., Bromfield, E. B., Mccarthy, D. C., Brandt, A., . . . Kahana, M. J. 2007. Hippocampal and neocortical gamma oscillations predict memory formation in humans. *Cereb Cortex,* 17**,** 1190-6.

Seeman, P. 2011. All roads to schizophrenia lead to dopamine supersensitivity and elevated dopamine D2(high) receptors. *CNS Neurosci Ther,* 17**,** 118-32.

Seibenhener, M. L. & Wooten, M. C. 2015. Use of the Open Field Maze to measure locomotor and anxiety-like behavior in mice. *J Vis Exp***,** e52434.

Seisenberger, C., Specht, V., Welling, A., Platzer, J., Pfeifer, A., Kühbandner, S., . . . Hofmann, F. 2000. Functional embryonic cardiomyocytes after disruption of the L-type alpha1C (Cav1.2) calcium channel gene in the mouse. *J Biol Chem,* 275**,** 39193-9.

Sellix, M. T., Evans, J. A., Leise, T. L., Castanon-Cervantes, O., Hill, D. D., Delisser, P., . . . Davidson, A. J. 2012. Aging differentially affects the re-entrainment response of central and peripheral circadian oscillators. *J Neurosci,* 32**,** 16193-202.

Selzam, S., Coleman, J. R. I., Caspi, A., Moffitt, T. E. & Plomin, R. 2018. A polygenic p factor for major psychiatric disorders. *Transl Psychiatry,* 8**,** 205.

Senior, T. J., Huxter, J. R., Allen, K., O'neill, J. & Csicsvari, J. 2008. Gamma oscillatory firing reveals distinct populations of pyramidal cells in the CA1 region of the hippocampus. *J Neurosci,* 28**,** 2274-86.

Shao, L. R., Halvorsrud, R., Borg-Graham, L. & Storm, J. F. 1999. The role of BK-type Ca2+-dependent K+ channels in spike broadening during repetitive firing in rat hippocampal pyramidal cells. *J Physiol,* 521 Pt 1**,** 135-46.

Sharma, P., Dikshit, R., Shah, N., Karia, S. & De Sousa, A. 2016. Excessive Daytime Sleepiness in Schizophrenia: A Naturalistic Clinical Study. *J Clin Diagn Res,* 10**,** VC06-VC08.

Shaw, A. D., Saxena, N., E Jackson, L., Hall, J. E., Singh, K. D. & Muthukumaraswamy, S. D. 2015. Ketamine amplifies induced gamma frequency oscillations in the human cerebral cortex. *Eur Neuropsychopharmacol,* 25**,** 1136-46.

Sheffield, M. E. & Dombeck, D. A. 2015. Calcium transient prevalence across the dendritic arbour predicts place field properties. *Nature,* 517**,** 200-4.

Sheffield, M. E. J., Adoff, M. D. & Dombeck, D. A. 2017. Increased Prevalence of Calcium Transients across the Dendritic Arbor during Place Field Formation. *Neuron,* 96**,** 490-504.e5.

Sheline, Y. I., Sanghavi, M., Mintun, M. A. & Gado, M. H. 1999. Depression duration but not age predicts hippocampal volume loss in medically healthy women with recurrent major depression. *J Neurosci,* 19**,** 5034-43.

Sheline, Y. I., Wang, P. W., Gado, M. H., Csernansky, J. G. & Vannier, M. W. 1996. Hippocampal atrophy in recurrent major depression. *Proc Natl Acad Sci U S A,* 93**,** 3908-13.

Shilyansky, C., Williams, L. M., Gyurak, A., Harris, A., Usherwood, T. & Etkin, A. 2016. Effect of antidepressant treatment on cognitive impairments associated with depression: a randomised longitudinal study. *Lancet Psychiatry,* 3**,** 425-35.

Shimada, M., Miyagawa, T., Kawashima, M., Tanaka, S., Honda, Y., Honda, M. & Tokunaga, K. 2010. An approach based on a genome-wide association study reveals candidate loci for narcolepsy. *Hum Genet,* 128**,** 433-41.

Shirvalkar, P. R., Rapp, P. R. & Shapiro, M. L. 2010. Bidirectional changes to hippocampal theta-gamma comodulation predict memory for recent spatial episodes. *Proc Natl Acad Sci U S A,* 107**,** 7054-9.

Siapas, A. G. & Wilson, M. A. 1998. Coordinated interactions between hippocampal ripples and cortical spindles during slow-wave sleep. *Neuron,* 21**,** 1123-8.

Sigurdsson, T., Stark, K. L., Karayiorgou, M., Gogos, J. A. & Gordon, J. A. 2010. Impaired hippocampal-prefrontal synchrony in a genetic mouse model of schizophrenia. *Nature,* 464**,** 763-7.

Singer, W. 1999. Neuronal synchrony: a versatile code for the definition of relations? *Neuron,* 24**,** 49-65, 111-25.

Singer, W. & Gray, C. M. 1995. Visual feature integration and the temporal correlation hypothesis. *Annu Rev Neurosci,* 18**,** 555-86.

Sirota, A. & Buzsáki, G. 2005. Interaction between neocortical and hippocampal networks via slow oscillations. *Thalamus Relat Syst,* 3**,** 245-259.

Skaggs, W. E., Mcnaughton, B. L. & Gothard, K. M. 1993. An Information-Theoretic Approach to Deciphering the Hippocampal Code. Advances in Neural Information Processing Systems 5 (NIPS 1992).

Skaggs, W. E., Mcnaughton, B. L., Wilson, M. A. & Barnes, C. A. 1996. Theta phase precession in hippocampal neuronal populations and the compression of temporal sequences. *Hippocampus,* 6**,** 149-72.

Smoller, J. W., Andreassen, O. A., Edenberg, H. J., Faraone, S. V., Glatt, S. J. & Kendler, K. S. 2019. Psychiatric genetics and the structure of psychopathology. *Mol Psychiatry,* 24**,** 409-420.

Soeiro-De-Souza, M. G., Lafer, B., Moreno, R. A., Nery, F. G., Chile, T., Chaim, K., . . . Vallada, H. 2017. The CACNA1C risk allele rs1006737 is associated with age-related prefrontal cortical thinning in bipolar I disorder. *Transl Psychiatry,* 7**,** e1086.

Sohal, V. S., Zhang, F., Yizhar, O. & Deisseroth, K. 2009. Parvalbumin neurons and gamma rhythms enhance cortical circuit performance. *Nature,* 459**,** 698-702.

Solé, B., Jiménez, E., Torrent, C., Reinares, M., Bonnin, C. D. M., Torres, I., . . . Vieta, E. 2017. Cognitive Impairment in Bipolar Disorder: Treatment and Prevention Strategies. *Int J Neuropsychopharmacol,* 20**,** 670-680.

Solovieff, N., Cotsapas, C., Lee, P. H., Purcell, S. M. & Smoller, J. W. 2013. Pleiotropy in complex traits: challenges and strategies. *Nat Rev Genet,* 14**,** 483-95.

Solstad, T., Moser, E. I. & Einevoll, G. T. 2006. From grid cells to place cells: a mathematical model. *Hippocampus,* 16**,** 1026-31.

Soltesz, I. & Deschênes, M. 1993. Low- and high-frequency membrane potential oscillations during theta activity in CA1 and CA3 pyramidal neurons of the rat hippocampus under ketamine-xylazine anesthesia. *J Neurophysiol,* 70**,** 97-116.

Splawski, I., Timothy, K. W., Sharpe, L. M., Decher, N., Kumar, P., Bloise, R., . . . Keating, M. T. 2004. Ca(V)1.2 calcium channel dysfunction causes a multisystem disorder including arrhythmia and autism. *Cell,* 119**,** 19-31.

Squire, L. R., Van Der Horst, A. S., Mcduff, S. G., Frascino, J. C., Hopkins, R. O. & Mauldin, K. N. 2010. Role of the hippocampus in remembering the past and imagining the future. *Proc Natl Acad Sci U S A,* 107**,** 19044-8.

St Clair, D., Blackwood, D., Muir, W., Carothers, A., Walker, M., Spowart, G., . . . Evans, H. J. 1990. Association within a family of a balanced autosomal translocation with major mental illness. *Lancet,* 336**,** 13-6.

Stahlberg, O., Soderstrom, H., Rastam, M. & Gillberg, C. 2004. Bipolar disorder, schizophrenia, and other psychotic disorders in adults with childhood onset AD/HD and/or autism spectrum disorders. *J Neural Transm (Vienna),* 111**,** 891-902.

Stan, A. D., Ghose, S., Zhao, C., Hulsey, K., Mihalakos, P., Yanagi, M., . . . Tamminga, C. A. 2015. Magnetic resonance spectroscopy and tissue protein concentrations together suggest lower glutamate signaling in dentate gyrus in schizophrenia. *Mol Psychiatry,* 20**,** 433-9.

Staresina, B. P., Bergmann, T. O., Bonnefond, M., Van Der Meij, R., Jensen, O., Deuker, L., . . . Fell, J. 2015. Hierarchical nesting of slow oscillations, spindles and ripples in the human hippocampus during sleep. *Nat Neurosci,* 18**,** 1679-1686.

Stark, E., Roux, L., Eichler, R., Senzai, Y., Royer, S. & Buzsáki, G. 2014. Pyramidal cell-interneuron interactions underlie hippocampal ripple oscillations. *Neuron,* 83**,** 467-480.

Stead, J. D., Clinton, S., Neal, C., Schneider, J., Jama, A., Miller, S., . . . Akil, H. 2006. Selective breeding for divergence in novelty-seeking traits: heritability and enrichment in spontaneous anxiety-related behaviors. *Behav Genet,* 36**,** 697-712.

Stefansson, H., Ophoff, R. A., Steinberg, S., Andreassen, O. A., Cichon, S., Rujescu, D., . . . (Group), G. R. a. O. I. P. 2009. Common variants conferring risk of schizophrenia. *Nature,* 460**,** 744-7.

Stefansson, H., Rujescu, D., Cichon, S., Pietiläinen, O. P., Ingason, A., Steinberg, S., . . . Group 2008. Large recurrent microdeletions associated with schizophrenia. *Nature,* 455**,** 232-6.

Stockmeier, C. A., Mahajan, G. J., Konick, L. C., Overholser, J. C., Jurjus, G. J., Meltzer, H. Y., . . . Rajkowska, G. 2004. Cellular changes in the postmortem hippocampus in major depression. *Biol Psychiatry,* 56**,** 640-50.

Stodieck, S. R. 1983. Phencyclidine (PCP): a psychotomimetic drug. Case report and review of literature. *Schweiz Med Wochenschr,* 113**,** 1396-402.

Storm, J. F. 1987. Action potential repolarization and a fast after-hyperpolarization in rat hippocampal pyramidal cells. *J Physiol,* 385**,** 733-59.

Stotz, S. C., Jarvis, S. E. & Zamponi, G. W. 2004. Functional roles of cytoplasmic loops and pore lining transmembrane helices in the voltage-dependent inactivation of HVA calcium channels. *J Physiol,* 554**,** 263-73.

Striessnig, J., Pinggera, A., Kaur, G., Bock, G. & Tuluc, P. 2014. L-type Ca2+ channels in heart and brain. *Wiley Interdiscip Rev Membr Transp Signal,* 3**,** 15-38.

Stringer, J. L., Hackett, J. T. & Guyenet, P. G. 1984. Long term potentiation blocked by phencyclidine and cyclazocine in vitro. *Eur J Pharmacol,* 98**,** 381-8.

Strohmaier, J., Amelang, M., Hothorn, L. A., Witt, S. H., Nieratschker, V., Gerhard, D., . . . Schulze, T. G. 2013. The psychiatric vulnerability gene CACNA1C and its sex-specific relationship with personality traits, resilience factors and depressive symptoms in the general population. *Mol Psychiatry,* 18**,** 607-13.

Stumpf , C. 1965. The Fast Component In The Electrical Activity Of Rabbit's Hippocampus. *Electroencephalogr Clin Neurophysiol,* 18**,** 477-86.

Stumpf, C., Petsche, H. & Gogolak, G. 1962. The significance of the rabbit's septum as a relay station between the midbrain and the hippocampus. II. The differential influence of drugs upon both the septal cell firing pattern and the hippocampus theta activity. *Electroencephalogr Clin Neurophysiol,* 14**,** 212-9.

Sturgeon, R. D., Fessler, R. G. & Meltzer, H. Y. 1979. Behavioral rating scales for assessing phencyclidine-induced locomotor activity, stereotyped behavior and ataxia in rats. *Eur J Pharmacol,* 59**,** 169-79.

Suh, J., Foster, D. J., Davoudi, H., Wilson, M. A. & Tonegawa, S. 2013. Impaired hippocampal ripple-associated replay in a mouse model of schizophrenia. *Neuron,* 80**,** 484-93.

Sullivan, P. F., Daly, M. J. & O'donovan, M. 2012. Genetic architectures of psychiatric disorders: the emerging picture and its implications. *Nat Rev Genet,* 13**,** 537-51.

Sullivan, P. F., Kendler, K. S. & Neale, M. C. 2003. Schizophrenia as a complex trait: evidence from a meta-analysis of twin studies. *Arch Gen Psychiatry,* 60**,** 1187-92.

Sullivan, P. F., Neale, M. C. & Kendler, K. S. 2000. Genetic epidemiology of major depression: review and meta-analysis. *Am J Psychiatry,* 157**,** 1552-62.

Sun, L., Castellanos, N., Grützner, C., Koethe, D., Rivolta, D., Wibral, M., . . . Uhlhaas, P. J. 2013. Evidence for dysregulated high-frequency oscillations during sensory processing in medication-naïve, first episode schizophrenia. *Schizophr Res,* 150**,** 519-25.

Surmeier, D. J., Bargas, J., Hemmings, H. C., Nairn, A. C. & Greengard, P. 1995. Modulation of calcium currents by a D1 dopaminergic protein kinase/phosphatase cascade in rat neostriatal neurons. *Neuron,* 14**,** 385-97.

Swanson, L. W. & Cowan, W. M. 1977. An autoradiographic study of the organization of the efferent connections of the hippocampal formation in the rat. *J Comp Neurol,* 172**,** 49-84.

Sykes, L., Clifton, N. E., Hall, J. & Thomas, K. L. 2018. Regulation of the Expression of the Psychiatric Risk Gene. *Mol Neuropsychiatry,* 4**,** 149-157.

Sykes, L., Haddon, J., Lancaster, T. M., Sykes, A., Azzouni, K., Ihssen, N., . . . Hall, J. 2019. Genetic Variation in the Psychiatric Risk Gene CACNA1C Modulates Reversal Learning Across Species. *Schizophr Bull,* 45**,** 1024-1032.

Tahmasian, M., Khazaie, H., Golshani, S. & Avis, K. T. 2013. Clinical application of actigraphy in psychotic disorders: a systematic review. *Curr Psychiatry Rep,* 15**,** 359.

Takata, A., Xu, B., Ionita-Laza, I., Roos, J. L., Gogos, J. A. & Karayiorgou, M. 2014. Loss-of-function variants in schizophrenia risk and SETD1A as a candidate susceptibility gene. *Neuron,* 82**,** 773-80.

Takemoto-Kimura, S., Suzuki, K., Kamijo, S., Ageta-Ishihara, N., Fujii, H., Okuno, H. & Bito, H. 2010. Differential roles for CaM kinases in mediating excitation-morphogenesis coupling during formation and maturation of neuronal circuits. *Eur J Neurosci,* 32**,** 224-30.

Tam, G. W., Van De Lagemaat, L. N., Redon, R., Strathdee, K. E., Croning, M. D., Malloy, M. P., . . . Grant, S. G. 2010. Confirmed rare copy number variants implicate novel genes in schizophrenia. *Biochem Soc Trans,* 38**,** 445-51.

Tamminga, C. A. 1998. Schizophrenia and glutamatergic transmission. *Crit Rev Neurobiol,* 12**,** 21-36.

Tansey, K. E., Owen, M. J. & O'donovan, M. C. 2015. Schizophrenia genetics: building the foundations of the future. *Schizophr Bull,* 41**,** 15-9.

Taxidis, J., Coombes, S., Mason, R. & Owen, M. R. 2012. Modeling sharp wave-ripple complexes through a CA3-CA1 network model with chemical synapses. *Hippocampus,* 22**,** 995-1017.

Temme, S. J., Bell, R. Z., Fisher, G. L. & Murphy, G. G. 2016. Deletion of the Mouse Homolog of. *eNeuro,* 3.

Terrazas, A., Krause, M., Lipa, P., Gothard, K. M., Barnes, C. A. & Mcnaughton, B. L. 2005. Self-motion and the hippocampal spatial metric. *J Neurosci,* 25**,** 8085-96.

Tesche, C. D. & Karhu, J. 2000. Theta oscillations index human hippocampal activation during a working memory task. *Proc Natl Acad Sci U S A,* 97**,** 919-24.

Thapar, A., Cooper, M. & Rutter, M. 2017. Neurodevelopmental disorders. *Lancet Psychiatry,* 4**,** 339-346.

Thase, M. E. 1999. Antidepressant treatment of the depressed patient with insomnia. *J Clin Psychiatry,* 60 Suppl 17**,** 28-31; discussion 46-8.

Thibault, O. & Landfield, P. W. 1996. Increase in single L-type calcium channels in hippocampal neurons during aging. *Science,* 272**,** 1017-20.

Thoby-Brisson, M. & Simmers, J. 1998. Neuromodulatory inputs maintain expression of a lobster motor pattern-generating network in a modulation-dependent state: evidence from long-term decentralization in vitro. *J Neurosci,* 18**,** 2212-25.

Thome, A., Marrone, D. F., Ellmore, T. M., Chawla, M. K., Lipa, P., Ramirez-Amaya, V., . . . Barnes, C. A. 2017. Evidence for an Evolutionarily Conserved Memory Coding Scheme in the Mammalian Hippocampus. *J Neurosci,* 37**,** 2795-2801.

Thompson, L. T. & Best, P. J. 1990. Long-term stability of the place-field activity of single units recorded from the dorsal hippocampus of freely behaving rats. *Brain Res,* 509**,** 299-308.

Tick, B., Bolton, P., Happé, F., Rutter, M. & Rijsdijk, F. 2016. Heritability of autism spectrum disorders: a meta-analysis of twin studies. *J Child Psychol Psychiatry,* 57**,** 585-95.

Tigaret, C. M., Olivo, V., Sadowski, J. H. L. P., Ashby, M. C. & Mellor, J. R. 2016. Coordinated activation of distinct Ca(2+) sources and metabotropic glutamate receptors encodes Hebbian synaptic plasticity. *Nat Commun,* 7**,** 10289.

Tigaret, C. M. L., Tzu-Ching E., Morrell, E., Sykes , L., O'donovan , M. C., Owen , M. J., Wilkinson , L. S., . . . Hall, J. 2020. Neurotrophin receptor activation rescues cognitive and synaptic abnormalities caused by mutation of the psychiatric risk gene *Cacna1c*. *bioRxiv*.

Tippens, A. L., Pare, J. F., Langwieser, N., Moosmang, S., Milner, T. A., Smith, Y. & Lee, A. 2008. Ultrastructural evidence for pre- and postsynaptic localization of Cav1.2 L-type Ca2+ channels in the rat hippocampus. *J Comp Neurol,* 506**,** 569-83.

Tolman , E. C. 1948. Cognitive maps in rats and men. *Psychol Rev,* 55**,** 189-208.

Tort, A. B., Kramer, M. A., Thorn, C., Gibson, D. J., Kubota, Y., Graybiel, A. M. & Kopell, N. J. 2008. Dynamic cross-frequency couplings of local field potential oscillations in rat striatum and hippocampus during performance of a T-maze task. *Proc Natl Acad Sci U S A,* 105**,** 20517-22.

Trivedi, J. K. 2006. Cognitive deficits in psychiatric disorders: Current status. *Indian J Psychiatry,* 48**,** 10-20.

Trossbach, S. V., Bader, V., Hecher, L., Pum, M. E., Masoud, S. T., Prikulis, I., . . . Korth, C. 2016. Misassembly of full-length Disrupted-in-Schizophrenia 1 protein is linked to altered dopamine homeostasis and behavioral deficits. *Mol Psychiatry,* 21**,** 1561-1572.

Tsuang, M. T., Lyons, M. J. & Faraone, S. V. 1990. Heterogeneity of schizophrenia. Conceptual models and analytic strategies. *Br J Psychiatry,* 156**,** 17-26.

Tsubokawa, H., Offermanns, S., Simon, M. & Kano, M. 2000. Calcium-dependent persistent facilitation of spike backpropagation in the CA1 pyramidal neurons. *J Neurosci,* 20**,** 4878-84.

Tsumoto, T. 1993. Long-term depression in cerebral cortex: a possible substrate of "forgetting" that should not be forgotten. *Neurosci Res,* 16**,** 263-70.

Tucker, M. A., Hirota, Y., Wamsley, E. J., Lau, H., Chaklader, A. & Fishbein, W. 2006. A daytime nap containing solely non-REM sleep enhances declarative but not procedural memory. *Neurobiol Learn Mem,* 86**,** 241-7.

Turrigiano, G. G. & Nelson, S. B. 2000. Hebb and homeostasis in neuronal plasticity. *Curr Opin Neurobiol,* 10**,** 358-64.

Uhlén, M., Fagerberg, L., Hallström, B. M., Lindskog, C., Oksvold, P., Mardinoglu, A., . . . Pontén, F. 2015. Proteomics. Tissue-based map of the human proteome. *Science,* 347**,** 1260419.

Uhlhaas, P. J. & Singer, W. 2010. Abnormal neural oscillations and synchrony in schizophrenia. *Nat Rev Neurosci,* 11**,** 100-13.

Umbricht, D., Koller, R., Vollenweider, F. X. & Schmid, L. 2002. Mismatch negativity predicts psychotic experiences induced by NMDA receptor antagonist in healthy volunteers. *Biol Psychiatry,* 51**,** 400-6.

Van Den Buuse, M. 2010. Modeling the positive symptoms of schizophrenia in genetically modified mice: pharmacology and methodology aspects. *Schizophr Bull,* 36**,** 246-70.

Van Os, J., Rutten, B. P. & Poulton, R. 2008. Gene-environment interactions in schizophrenia: review of epidemiological findings and future directions. *Schizophr Bull,* 34**,** 1066-82.

Van Vugt, M. K., Schulze-Bonhage, A., Litt, B., Brandt, A. & Kahana, M. J. 2010. Hippocampal gamma oscillations increase with memory load. *J Neurosci,* 30**,** 2694-9.

Vanderwolf, C. H. 1969. Hippocampal electrical activity and voluntary movement in the rat. *Electroencephalogr Clin Neurophysiol,* 26**,** 407-18.

Varela, F., Lachaux, J. P., Rodriguez, E. & Martinerie, J. 2001. The brainweb: phase synchronization and large-scale integration. *Nat Rev Neurosci,* 2**,** 229-39.

Varese, F., Smeets, F., Drukker, M., Lieverse, R., Lataster, T., Viechtbauer, W., . . . Bentall, R. P. 2012. Childhood adversities increase the risk of psychosis: a meta-analysis of patient-control, prospective- and cross-sectional cohort studies. *Schizophr Bull,* 38**,** 661-71.

Vertes, R. P. & Kocsis, B. 1997. Brainstem-diencephalo-septohippocampal systems controlling the theta rhythm of the hippocampus. *Neuroscience,* 81**,** 893-926.

Viswanathan, A. & Freeman, R. D. 2007. Neurometabolic coupling in cerebral cortex reflects synaptic more than spiking activity. *Nat Neurosci,* 10**,** 1308-12.

Vollenweider, F. X., Vontobel, P., Oye, I., Hell, D. & Leenders, K. L. 2000. Effects of (S)-ketamine on striatal dopamine: a [11C]raclopride PET study of a model psychosis in humans. *J Psychiatr Res,* 34**,** 35-43.

Walker, M. P., Brakefield, T., Seidman, J., Morgan, A., Hobson, J. A. & Stickgold, R. 2003. Sleep and the time course of motor skill learning. *Learn Mem,* 10**,** 275-84.

Waller, D. A., Hardy, B. W., Pole, R., Giles, D., Gullion, C. M., Rush, A. J. & Roffwarg, H. P. 1989. Sleep EEG in bulimic, depressed, and normal subjects. *Biol Psychiatry,* 25**,** 661-4.

Wamsley, E. J., Tucker, M. A., Shinn, A. K., Ono, K. E., Mckinley, S. K., Ely, A. V., . . . Manoach, D. S. 2012. Reduced sleep spindles and spindle coherence in schizophrenia: mechanisms of impaired memory consolidation? *Biol Psychiatry,* 71**,** 154-61.

Wardenaar, K. J. & De Jonge, P. 2013. Diagnostic heterogeneity in psychiatry: towards an empirical solution. *BMC Med,* 11**,** 201.

Weiner, I. 2001. Latent inhibition. *Curr Protoc Neurosci,* Chapter 8**,** Unit 8.13.

Weisskopf, M. G., Bauer, E. P. & Ledoux, J. E. 1999. L-type voltage-gated calcium channels mediate NMDA-independent associative long-term potentiation at thalamic input synapses to the amygdala. *J Neurosci,* 19**,** 10512-9.

Welsh, D. K., Logothetis, D. E., Meister, M. & Reppert, S. M. 1995. Individual neurons dissociated from rat suprachiasmatic nucleus express independently phased circadian firing rhythms. *Neuron,* 14**,** 697-706.

Wermter, A. K., Laucht, M., Schimmelmann, B. G., Banaschewski, T., Banaschweski, T., Sonuga-Barke, E. J., . . . Becker, K. 2010. From nature versus nurture, via nature and nurture, to gene x environment interaction in mental disorders. *Eur Child Adolesc Psychiatry,* 19**,** 199-210.

Wheeler, D. G., Barrett, C. F., Groth, R. D., Safa, P. & Tsien, R. W. 2008. CaMKII locally encodes L-type channel activity to signal to nuclear CREB in excitation-transcription coupling. *J Cell Biol,* 183**,** 849-63.

White, J. A., Mckinney, B. C., John, M. C., Powers, P. A., Kamp, T. J. & Murphy, G. G. 2008. Conditional forebrain deletion of the L-type calcium channel Ca V 1.2 disrupts remote spatial memories in mice. *Learn Mem,* 15**,** 1-5.

Whiteford, H. A., Degenhardt, L., Rehm, J., Baxter, A. J., Ferrari, A. J., Erskine, H. E., . . . Vos, T. 2013. Global burden of disease attributable to mental and substance use disorders: findings from the Global Burden of Disease Study 2010. *Lancet,* 382**,** 1575-86.

Wikenheiser, A. M. & Redish, A. D. 2013. The balance of forward and backward hippocampal sequences shifts across behavioral states. *Hippocampus,* 23**,** 22-9.

Williams, S. & Boksa, P. 2010. Gamma oscillations and schizophrenia. *J Psychiatry Neurosci,* 35**,** 75-7.

Wilson, M. A. & Mcnaughton, B. L. 1993. Dynamics of the hippocampal ensemble code for space. *Science,* 261**,** 1055-8.

Wilson, M. A. & Mcnaughton, B. L. 1994. Reactivation of hippocampal ensemble memories during sleep. *Science,* 265**,** 676-9.

Winder, D. G., Martin, K. C., Muzzio, I. A., Rohrer, D., Chruscinski, A., Kobilka, B. & Kandel, E. R. 1999. ERK plays a regulatory role in induction of LTP by theta frequency stimulation and its modulation by beta-adrenergic receptors. *Neuron,* 24**,** 715-26.

Winocur, G. 1982. Radial-arm-maze behavior by rats with dorsal hippocampal lesions: effect of cuing. *J Comp Physiol Psychol,* 96**,** 155-69.

Winson, J. 1978. Loss of hippocampal theta rhythm results in spatial memory deficit in the rat. *Science,* 201**,** 160-3.

Witting, W., Kwa, I. H., Eikelenboom, P., Mirmiran, M. & Swaab, D. F. 1990. Alterations in the circadian rest-activity rhythm in aging and Alzheimer's disease. *Biol Psychiatry,* 27**,** 563-72.

Workman, E. R., Niere, F. & Raab-Graham, K. F. 2013. mTORC1-dependent protein synthesis underlying rapid antidepressant effect requires GABABR signaling. *Neuropharmacology,* 73**,** 192-203.

Wray, N. R., Pergadia, M. L., Blackwood, D. H., Penninx, B. W., Gordon, S. D., Nyholt, D. R., . . . Sullivan, P. F. 2012. Genome-wide association study of major depressive disorder: new results, meta-analysis, and lessons learned. *Mol Psychiatry,* 17**,** 36-48.

Wright, I. C., Rabe-Hesketh, S., Woodruff, P. W., David, A. S., Murray, R. M. & Bullmore, E. T. 2000. Meta-analysis of regional brain volumes in schizophrenia. *Am J Psychiatry,* 157**,** 16-25.

Wu, X. & Foster, D. J. 2014. Hippocampal replay captures the unique topological structure of a novel environment. *J Neurosci,* 34**,** 6459-69.

Wulff, K., Dijk, D. J., Middleton, B., Foster, R. G. & Joyce, E. M. 2012. Sleep and circadian rhythm disruption in schizophrenia. *Br J Psychiatry,* 200**,** 308-16.

Wulff, P., Ponomarenko, A. A., Bartos, M., Korotkova, T. M., Fuchs, E. C., Bähner, F., . . . Monyer, H. 2009. Hippocampal theta rhythm and its coupling with gamma oscillations require fast inhibition onto parvalbumin-positive interneurons. *Proc Natl Acad Sci U S A,* 106**,** 3561-6.

Wurtz, R. H. & Sommer, M. A. 2004. Identifying corollary discharges for movement in the primate brain. *Prog Brain Res,* 144**,** 47-60.

Xu, B., Roos, J. L., Levy, S., Van Rensburg, E. J., Gogos, J. A. & Karayiorgou, M. 2008. Strong association of de novo copy number mutations with sporadic schizophrenia. *Nat Genet,* 40**,** 880-5.

Yamagata, Y., Kobayashi, S., Umeda, T., Inoue, A., Sakagami, H., Fukaya, M., . . . Okabe, S. 2009. Kinase-dead knock-in mouse reveals an essential role of kinase activity of Ca2+/calmodulin-dependent protein kinase IIalpha in dendritic spine enlargement, long-term potentiation, and learning. *J Neurosci,* 29**,** 7607-18.

Yartsev, M. M. 2010. Distinct or gradually changing spatial and nonspatial representations along the dorsoventral axis of the hippocampus. *J Neurosci,* 30**,** 7758-60.

Yasuda, H., Barth, A. L., Stellwagen, D. & Malenka, R. C. 2003. A developmental switch in the signaling cascades for LTP induction. *Nat Neurosci,* 6**,** 15-6.

Yin, J. & Yuan, Q. 2014. Structural homeostasis in the nervous system: a balancing act for wiring plasticity and stability. *Front Cell Neurosci,* 8**,** 439.

Ylinen, A., Bragin, A., Nádasdy, Z., Jandó, G., Szabó, I., Sik, A. & Buzsáki, G. 1995. Sharp wave-associated high-frequency oscillation (200 Hz) in the intact hippocampus: network and intracellular mechanisms. *J Neurosci,* 15**,** 30-46.

Yoshimizu, T., Pan, J. Q., Mungenast, A. E., Madison, J. M., Su, S., Ketterman, J., . . . Tsai, L. H. 2015. Functional implications of a psychiatric risk variant within CACNA1C in induced human neurons. *Mol Psychiatry,* 20**,** 162-9.

Young, C. K., Ruan, M. & Mcnaughton, N. 2020. Speed modulation of hippocampal theta frequency and power predicts water maze learning. bioRxiv.

Yuan, Q., Isaacson, J. S. & Scanziani, M. 2011. Linking neuronal ensembles by associative synaptic plasticity. *PLoS One,* 6**,** e20486.

Yuzaki, M., Miyawaki, A., Akita, K., Kudo, Y., Ogura, A., Ino, H. & Mikoshiba, K. 1990. Mode of blockade by MK-801 of N-methyl-D-aspartate-induced increase in intracellular Ca2+ in cultured mouse hippocampal neurons. *Brain Res,* 517**,** 51-6.

Zanini, M. A., Castro, J., Cunha, G. R., Asevedo, E., Pan, P. M., Bittencourt, L., . . . Brietzke, E. 2015. Abnormalities in sleep patterns in individuals at risk for psychosis and bipolar disorder. *Schizophr Res,* 169**,** 262-267.

Zaremba, J. D., Diamantopoulou, A., Danielson, N. B., Grosmark, A. D., Kaifosh, P. W., Bowler, J. C., . . . Losonczy, A. 2017. Impaired hippocampal place cell dynamics in a mouse model of the 22q11.2 deletion. *Nat Neurosci,* 20**,** 1612-1623.

Zeng, H., Chattarji, S., Barbarosie, M., Rondi-Reig, L., Philpot, B. D., Miyakawa, T., . . . Tonegawa, S. 2001. Forebrain-specific calcineurin knockout selectively impairs bidirectional synaptic plasticity and working/episodic-like memory. *Cell,* 107**,** 617-29.

Zhang, C. 2016. Genetic findings are challenging the symptom-based diagnostic classification system of mental disorders. *Shanghai Arch Psychiatry,* 28**,** 42-7.

Zhang, K., Ginzburg, I., Mcnaughton, B. L. & Sejnowski, T. J. 1998. Interpreting neuronal population activity by reconstruction: unified framework with application to hippocampal place cells. *J Neurophysiol,* 79**,** 1017-44.

Zhang, W. N., Bast, T. & Feldon, J. 2001. The ventral hippocampus and fear conditioning in rats: different anterograde amnesias of fear after infusion of N-methyl-D-aspartate or its noncompetitive antagonist MK-801 into the ventral hippocampus. *Behav Brain Res,* 126**,** 159-74.

Zheng, C., Bieri, K. W., Trettel, S. G. & Colgin, L. L. 2015. The relationship between gamma frequency and running speed differs for slow and fast gamma rhythms in freely behaving rats. *Hippocampus,* 25**,** 924-38.

Zheng, F., Zhang, Y., Xie, W., Li, W., Jin, C., Mi, W., . . . Yue, W. 2014. Further evidence for genetic association of CACNA1C and schizophrenia: new risk loci in a Han Chinese population and a meta-analysis. *Schizophr Res,* 152**,** 105-10.

Zhou, X., Nie, Z., Roberts, A., Zhang, D., Sebat, J., Malhotra, D., . . . Geyer, M. A. 2010. Reduced NMDAR1 expression in the Sp4 hypomorphic mouse may contribute to endophenotypes of human psychiatric disorders. *Hum Mol Genet,* 19**,** 3797-805.

Zimmerman, K. D., Espeland, M. A. & Langefeld, C. D. 2021. A practical solution to pseudoreplication bias in single-cell studies. *Nat Commun,* 12**,** 738.

Zola-Morgan, S., Squire, L. R. & Amaral, D. G. 1986. Human amnesia and the medial temporal region: enduring memory impairment following a bilateral lesion limited to field CA1 of the hippocampus. *J Neurosci,* 6**,** 2950-67.